Mechanisms of NPY Y_2 Receptor-Mediated Anxiogenesis in the Basolateral Amygdala

by

James Patrick Mackay

A thesis submitted in partial fulfillment of the requirements for the degree of

Doctor of Philosophy

Department of Pharmacology
University of Alberta

ABSTRACT

Mechanisms of NPY Y$_2$ Receptor-Mediated Anxiogenesis in the Basolateral Amygdala

PhD Thesis 2016, James Patrick Mackay

Department of Pharmacology, University of Alberta

Fear and anxiety are highly adaptive emotions that motivate species appropriate responses to threats: immediate and potential. Certain threats, such as ancestral predators, are highly predictable and can be recognized and addressed with innate (inherited) neural systems. This "genetic memory" underlies human phobias (ex. fear of snakes) and allows individuals to recognize and effectively respond to conserved dangers, regardless of previous encounters.

Unlearned fear systems, however, have clear limitations, the most fundamental being their inability to recognize every conceivable danger. Plastic threat appraisal systems overcome this limitation. The basolateral amygdala (BLA) is the principal brain site where learned associations between innocuous sensory cues and intrinsically aversive stimuli are formed (fear conditioning). Fear conditioning is though to model a key mechanism for identifying novel threats. Anxiety, a more sustained state of hyper-vigilance, is also mediated by the BLA and is most appropriate when threats are diffuse and not readily predicted by explicit cues.

In susceptible individuals, exposure to a severe unpredictable stressor can elicit a prolonged disordered anxiety state termed posttraumatic stress disorder (PTSD). Although protective to a degree, PTSD substantially impairs normal functioning and is profoundly unpleasant for the sufferer. An important factor thought to protect some individuals from the deleterious effects of traumatic stress is Neuropeptide Y (NPY). BLA NPY infusions are highly anxiolytic in rodents, while repeated infusions produce plastic changes culminating in a long lasting low-anxiety state.

Glutamatergic Principal neurons (PN) are the BLA's majority neuron type (85%) and mediate its output. The remaining 15% are a diverse group of GABA interneurons that tightly regulate PN activity. The output of a population PNs signals fear and anxiety. We previously showed that NPY inhibits BLA PNs via postsynaptic NPY Y_1 receptors (consistent with anxiolytic actions). Furthermore, Y_1 selective agonists mimic NPYs acute *in vivo* anxiolytic effects. Surprisingly, selective activation of BLA Y_2 receptors (Y_2-R) **increases** anxiety by an (until now) unknown mechanism. **The principal focus of this thesis is to mechanistically dissect Y_2-R functions in the BLA. A secondary aim is to determine if and how Y_2-Rs contribute to the overall anxiolytic actions of the full agonist NPY.**

Y_2-Rs are typically presynaptic and inhibit neurotransmitter release. We therefore, hypothesized Y_2-Rs disinhibit PNs by decreasing BLA interneuron GABA release. To test this, we used slice-patch electrophysiology in rat BLA-containing brain slices. Application of the selective Y_2-R agonist [ahx$^{5\text{-}24}$]NPY decreased the frequency of PN

miniature GABA$_A$ inhibitory postsynaptic currents (IPSC)s with no effect on amplitude (suggesting a presynaptic effect). Interestingly, in the absence of tetrodotoxin (TTX) [ahx$^{5\text{-}24}$]NPY increased the frequency of large amplitude fast kinetic sIPSCs, suggesting disinhibition of another interneuron type.

To determine the Y$_2$-R expressing interneuron type mediating the above effects, we used a mouse model engineered to express the TdTomato fluorophore under control of the Y$_2$-R gene promoter. Immunohistochemistry studies suggested Y$_2$-Rs are expressed exclusively on interneurons characterized by NPY and somatostatin (SOM) expression. SOM interneurons innervate PN dendrites and also target other interneuron types consistent with electrophysiology findings.

In addition to the above effects, [ahx$^{5\text{-}24}$]NPY increased PN excitability (indicated by a decrease in the depolarizing current required to elicit action potentials). These findings are consistent with the *in vivo* anxiogenic effects of selective Y$_2$-R agonists. Although [ahx$^{5\text{-}24}$]NPY only slightly depolarized most PNs, it substantially increased PN input resistance, indicating a net closure of ion channels. We hypothesized these effects were due to reduced tonic GABA$_A$-mediated inhibition. However voltage-clamp experiments indicated [ahx$^{5\text{-}24}$]NPY reduced a PN G-protein coupled inward rectifying K$^+$ conductance (GIRK). Subsequent experiments revealed this was due to reduced tonic GABA$_B$-R activation. Since PNs express postsynaptic GABA$_B$-Rs exclusively at their dendrites this effect is also consistent with actions on (Y$_2$-R expressing) NPY/SOM interneurons. Surprisingly, this Y$_2$-R action persisted in TTX, indicating it is largely

action potential-independent. Ultimately this finding reveals a highly novel consequence of action potential-independent neurotransmission.

NPY-mediated plasticity requires the Ca^{2+}-dependent phosphatase calcineurin (which mediates LTD-type learning and is expressed in dendrites). Dendritic $GABA_B$-GIRKs facilitate the Mg^{2+} block of NMDA receptors and dampen plasticity. Thus Y_2-Rs may function to disinhibit PN dendrites and facilitate Ca^{2+}-dependent, NPY-mediated plasticity. $[ahx^{5-24}]$NPY-mediated increases in PN calcium influx were revealed indirectly by an increase Ca^{2+} dependent slow after-hyperpolarization (sI_{AHP}) K^+ current in half of all responsive PNs.

PREFACE

This thesis is an original work by James Patrick Mackay. This work is part of a larger research project titled "Mechanisms underlying stress resilience" supported by the National Institutes of Health (NIH) (grant R01MH090297; Dr. Janice H. Urban, PI). This research received ethics approval from the University of Alberta Research Ethics Board, approval No. 056/02/08 (2008 – 2013) and AUP0000240 (2014 – 2016).

ACKNOWLEDGEMENTS

First and foremost I would like to thank my supervisor Dr. William F. Comers who has guided me throughout the course of my graduate studies. You pushed me hard to become the best scientist I could be, but always advocated for me when I needed someone in my corner. Under Dr. Colmers' tutelage (and during many vigorous debates over ion channels and dendritic calcium currents) I learned to more clearly articulate my ideas. Once I formulated a convincing argument Dr. Colmers often let me pursue my own ideas, which has been instrumental in my development as a scientist.

I would also like to thank my supervisory committee members: Dr. Janice Urban and Dr. Peter Smith. Thank you for your guidance over the years and the many reference letters you wrote on my behalf. I have enjoyed our conversations and hope to have many more at upcoming neuroscience meetings!

I have been very lucky to have shared my time at the Colmers lab with many wonderful graduate students and postdoctoral fellows, past and present. Dr. Trevor Hamilton taught me about back-propagating action potentials when I visited the lab in 2009. Since then Trevor has always been willing to meet and dispense valuable advice over a beer (sometimes several). Dr. Mellissa Chee taught me how to patch and has since become a great friend and mentor. Many long days of patching went by surprisingly quickly because I was hanging out with my dear friends Dr. Rebecca Mercer and Dr. Dirk

support during this journey. I know I would not be here today if not for you. You supported me no matter what career I pursued, as long as it made me happy, and for this I am truly grateful. I must say, however, that there were subtle pushes towards science and graduate studies in particular. My mother (a zoologist and piano teacher) started me thinking about evolutionary biology as early as the second grade. My father, a defense scientist, claims he spent his career playing with "really expensive" toys and always impressed on me the importance of enjoying your work even if you make a bit less money. Finally, my sister Frances, who completed a PhD in applied physics and math, suggested graduate school as a perfect fit for my personality (incidentally Frances is now in law school ☺).

Last, but most certainty not least, I would like to thank my beautiful and very patient partner Dr. Jelena Kolic. Beyond providing moral support, Jelena also helped with proof reading and editing this document. I could not have completed this thesis without your continual love and support. I would say that you will always have my heart, but this would be unbefitting since the heart is a mere muscular pump incorrectly ascribed the seat of the human soul. Instead you will always have my brain.

I hope to stay in touch with the many great friends and mentors I have met on this graduate school journey. Make sure to come visit us in Vancouver!

ABBREVIATIONS

°C	degree Celsius
5HT3	5-hydroxytryptamine
ACSF	artificial cerebrospinal fluid
AHP	afterhyperpolarization
$ahx^{5-24}NPY$	$[6\text{-aminohexanoic}^{5-24}]NPY$
AMPA	α-amino-3-hydroxy-5-methyl-4-isoxazolepropionic acid
ANOVA	analysis of variance
ATP	adenosine triphosphate
Ba	basal amygdala
BLA	basolateral amygdala
Bm	basal medial amygdala
BNST	bed nucleus of the stria terminalus
CA1	region I of hippocampus proper
CAMKII	calcium calmodulin dependent kinase type II
cAMP	cyclic adenosine monophosphate
CB	calbindin
CCK	cholecystikinin
CeA	central amygdala
CeL	lateral central amygdala
CeM	medial central amygdala
CGE	ganglionic eminence
CGP 46381	(3-Aminopropyl)(cyclohexylmethyl)phosphinic acid
CGP 52432	3-[[(3,4-Dichlorophenyl)methyl]amino]propyl]diethoxymethyl)phosphinic acid
CNS	central nervous system
CPSP	compound postsynaptic potentials
CR	calretinin
CRF	corticotropin releasing factor
CS	conditioned stimulus
CS_1	innocuous sensory cue with a shock
CS_2	innocuous sensory cue with a reward
CSF	cerebral spinal fluid
DIC	infrared-differential contrast optics
EGTA	ethylene glycol tetraacetic acid
EPM	elevated plus maze
F7P34NPY	[Phe7,Pro34]NPY
GABA	gamma-aminobutyric acid
GAD	generalized anxiety disorder
GIRK	G-protein coupled inward rectifying K^+ current
GPCR	G-protein coupled receptors
HCN	hyperpolarization activated cyclic nucleotide gated channel
HEPES	4-(2-hydroxyethyl)-1-piperazineethanesulfonic acid
Hz	hertz

I	current
icv	intracerebroventricular
IEI	inter-event interval
I_h	hyperpolarization activated cyclic nucleotide gated mixed cation conductance
I_{IR}	inwardly rectifying current
IL	infralimbic
IN	interneurons
IPSC	inhibitory postsynaptic current
IPSC	inhibitory postsynaptic current
IsAHP	slow afterhyperpolarizing K+ conductance
ITC	intercalated cell masses
L	liter
LA	lateral amygdala
LTD	long-term depression
LTP	long-term potentiation
mAHP	medium afterhyperpolarization
MGE	medial ganglionic eminence
min	minute
mIPSC	miniature inhibitory postsynaptic currents
ml	milliliter
mM	millimolar
mOsm	milliosmoles
mPFC	medial prefrontal cortex
ms	millisecond
mV	millivolt
MΩ	megaohm
NAc	nucleus accumbens
NCG	neurogliaform cells
NK1	Neurokinin 1
nM	nanonmolar
NMDA	N-Methyl-D-aspartate
NPY	neuropeptide Y
pA	picoamps
PBS	phosphate buffered saline
PKA	protein kinase A
PKC	protein kinase C
PL	prelimbic
pM	picomolar
PN	principal neurons
PP	pancreatic polypeptide
PTSD	post-traumatic stress disorder
PV^+	parvalbumin
PYY	peptide YY
R	resistance
RPM	resting membrane potential

s	second
sAHP	slow afterhyperpolarization
SCH 23390	R)-(+)-7-Chloro-8-hydroxy-3-methyl-1-phenyl-2,3,4,5-tetrahydro-1H-3-benzazepine hydrochloride
SEM	standard error of mean
SI	social interaction
SOM	somatostatin
SSRI	selective serotonin reuptake inhibitor
TdTomato	tandem tomato fluorescent protein
TTX	tetrodotoxin
UCL 2077	N-Trityl-3-pyridinemethanamine
US	unconditioned stimulus
V	voltage
VFTD	venus flytrap domain
VGCC	voltage gated Ca^{2+} channels
VIP	vasoactive intestinal peptide
Y_2-Tom	TdTomato fluorophore under expression control of the Y_2 receptor gene promoter
μg	microgram
μl	microliter
μM	micromolar

LIST OF FIGURES

TABLE OF CONTENTS

SUMMARY, GENERAL DISCUSSION AND FUTURE DIRECTIONS 225

Chapter 1

Introduction

1.1 OVERVIEW OF THE AMYGDALA AND ITS CENTRAL ROLE IN EMOTIONAL REGULATION

1.1a Emotion and its conserved circuitry

There is no universally accepted scientific definition of emotion, although many schemes have been proposed (LeDoux, 2012a; Weisfeld and Goetz, 2013). In general, emotions are viewed as biological drives, which motivate adaptive, and often species-specific behavior (LeDoux, 2012a). Emotions are evoked in response to salient triggers, which encompass both internal physiology and external sensory stimuli (Weisfeld and Goetz, 2013). For example, hunger and pain, both reflecting internal physiology, may be viewed as emotions evoked by food deprivation or tissue damage. Conversely, the presence of a predator, an external stimulus, will elicit the emotion fear.

An affective component also characterizes emotions, and differentiates consequent behaviors from simpler reflexive responses. In this context, affect is either of a positive or negative valence (but not neutral); that is, emotions are either pleasant or aversive (Russell and Barrett, 1999). Individuals will typically attempt to avoid or remove themselves from elicitors of negative emotions. Conversely, elicitors of positive emotions are appetitive. Emotional valence thus drives positive and negative reinforcement, as first described by B F Skinner (1938) the father of operant conditioning (Skinner, 1938).

Charles Darwin, in his then revolutionary work *Expression of Emotions in Man and Animals* (1872), first proposed that many aspects of human emotionality are shared amongst other animals. The limbic system concept, later formalized by Paul McLean (1949), proposed a structural framework for such phylogenetic conservation (MacLean, 1949). The amygdala was initially implicated as a critical component of this network by

Klüver and Bucy (1939), who described a behavioral syndrome resulting from bilateral temporal lobectomy in rhesus monkeys (Klüver and Bucy, 1997). Klüver and Bucy's procedure produced a profound reduction in fear (amongst other effects) but was not amygdala specific, later more specific ablation studies were required to clarify the role of the amygdala in fear-based behaviors.

Weiskrance (1956) selectively removed the amygdala in monkeys and reported a profound "taming" of animals following surgery, observing that lesioned animals no longer displayed fear towards humans. Additionally, animals with amygdala lesions were slower in learning a fear-based avoidance task and would often consume species inappropriate foods (Weiskrantz, 1956). Deficits in fear-related processing have since been described in human patients with amygdala damage (Adolphs et al., 1995; Feinstein et al., 2011), as well as in multiple other species (King, 1958). Through these and other reports, a prominent role has emerged for the amygdala in the detection of threats, and subsequent coordination of appropriate responses. Such a role is intimately tied to an organism's evolutionary fitness. Thus, and perhaps unsurprisingly, the amygdala is highly conserved. As such, most (if not all) vertebrates express brain structures homologous to the amygdala (Lanuza et al., 1998; Janak and Tye, 2015).

The limbic system has become increasingly ill-defined, to the extent that many contemporary neuroscientists now dispute its existence, as reviewed by (LeDoux, 2012b). Nonetheless, comparative biology suggests that certain conserved vertebrate brain structures, including the amygdala, drive fundamental behaviors critical to survival and reproduction (Pabba, 2013). In the case of lower vertebrates, such systems are largely sufficient for more stereotyped behavioral motifs. However, higher mammals (including

humans) show exquisitely flexible behavioral repertoires. Such complexity seemingly results via interactions between these conserved circuits and the more recently elaborated structures, such as the neocortex. Conservation of basic emotions motivates the study of the rodent amygdala and its regulation of relatively simple, emotion-based behaviors. Understanding such circuitry can thus inform our understanding of more complex human behaviors sharing a similar emotional basis.

1.1b The Amygdala

The amygdala, named after the Greek word for almond, is a diverse collection of brain nuclei located deep within each bilateral anterior medial temporal lobe **(Figure 1A)**. The almond-shaped structure originally described by Burdach in the early 19th century is now called the basolateral amygdala (BLA). The amygdala has since been extended to encompass multiple heterogeneous brain structures (collectively 13 nuclei) (Sah et al., 2003). These nuclei are grouped based on dense interconnections, and a common link to emotional regulation. The cortex-like BLA, and the striatum-like central Amygdala (CeA), will be discussed in greater detail below.

Additional amygdala structures include a group of laminar cortical nuclei, the medial amygdala (Keshavarzi et al., 2014) and the amygdala-hippocampal area (Pitkänen et al., 1997). The intercalated cell masses (ITC), a small but important group of interconnected GABA interneurons situated between the BLA and CeA, also bears mentioning. The ITCs appear to gate excitatory transmission from the BLA to the CeA via feed-forward inhibition (Marowsky et al., 2005). For comprehensive reviews of amygdala anatomy see the following (Sah et al., 2003; Duvarci and Paré, 2014).

1.1c The Basolateral Amygdala (BLA)

The BLA is located medial to the overlying neocortex and lateral to the CeA and striatum. Two fiber bundles, the external capsule and the longitudinal association bundle, form the BLA's respective lateral and medial borders and facilitate its identification in coronal brain slices **(Figure 1B)**.

Far greater neuronal input is received by the BLA than is reciprocated. The BLA is thus considered an important integrative node, and is also the major entry point for sensory information to the amygdala (LeDoux et al., 1990). The embryological origins of the BLA closely resemble those of the hippocampus and neocortex. As such, the BLA contains similar neuron types (although it lacks the laminar organization of the aforementioned structures). Complex projection neurons with spiny dendrites, called principal neurons (PN), are the predominant BLA neuron type (80%) (McDonald, 1984). These neurons use glutamate as their neurotransmitter and typically show pyramidal neuron morphology (McDonald, 1996). The remaining 20% of BLA neurons are spine-sparse GABA interneurons (INs), which exert inhibitory control over local circuits (McDonald et al., 2002). However, barring one known exception, INs do not project out of the BLA (McDonald, 2012). Both these main cell types will be discussed in greater detail in section 1.4.

The BLA actually comprises three densely interconnected nuclei: the lateral amygdala (LA), basal amygdala (Ba), and the basal medial amygdala (BM) nuclei (also termed basal accessory) **(Figure 1B)**. Due to a lack of clear anatomical boundaries, physiological studies often do not differentiate the Ba and BM, and thus collectively referred to these nuclei as the basal amygdala (BA). An alternate nomenclature

collectively refers to the Ba and Bm as the BLA excluding the LA, which is emphasized as a distinct entity. For the purpose of this thesis I will adhere to the former terminology and define the Basolateral complex as inclusive of the LA.

1.1d The Lateral Amygdala (LA)

Of the three BLA nuclei, sensory information most prominently innervates the LA (LeDoux et al., 1990). Consistent with this, learned associations between innate sensory cues and intrinsically noxious (painful) stimuli are principally formed in the LA. This process, called fear conditioning (discussed further in section 1.2b), is blocked by LA lesions (Nader et al., 2001). Sensory information of all modalities reaches the LA and, in rodents, can be divided into two main input paths: relatively less processed sensory inputs received from thalamic projections, and highly processed sensory inputs from the association cortices (Romanski and LeDoux, 1992). The LA, which is located dorsal to the Ba, has been studied more than the other BLA nuclei, owing to this preferential sensory innervation. However, the LA does not directly project to the medial central amygdala (CeM) (LeDoux, 2000), which is thought to be the major amygdala output center (discussed below). A major route for information to reach the CeM from the LA is thus via the BA (Pitkänen et al., 1997; Amano et al., 2010), to which the LA sends strong excitatory projections (Smith and Pare, 1994; Pitkänen et al., 1997). Information flow from the LA to the BA appears largely unidirectional as the BA only lightly projects back to the LA (Pitkänen et al., 1997).

Neuronal morphology, electrophysiology and organization appear strikingly similar throughout the BLA however, some differences between the LA and BA nuclei have been noted. PNs in the LA are somewhat smaller than those in the BA, with average

soma diameters between 10-15 μM compared to 15-20 μM in the BA (McDonald, 1982; Millhouse and DeOlmos, 1983). LA PNs also appear to receive less synaptic GABA inhibition and have smaller tonic $GABA_A$ currents than their counterparts in the BA (Marowsky et al., 2012). Particularly relevant to this thesis, different pharmacological responses to the anxiolytic neuromodulator, neuropeptide Y (NPY) have been described between PNs in the LA and BA. In the LA, NPY inhibits half of all PNs by activating a G-protein coupled inward rectifying K^+ conductance (GIRK) via actions on NPY Y_1 receptors (Sosulina et al., 2008). However, NPY does not potentiate GIRK currents in the BA; instead it hyperpolarizes half of all PNs by decreasing a tonic hyperpolarization activated cyclic nucleotide-gated mixed cation conductance (I_h) also via Y_1 receptors (Giesbrecht et al., 2010). Additional effects of NPY in the BA will be outlined in the results sections.

1.1e The Basal Amygdala (BA)

A principal focus of this thesis has been patch clamp electrophysiological studies of BA PNs. The BA includes two nuclei: the Ba, which is ventral to the LA and the BM, which is ventral to the Ba **(Figure 1B)**.

The BA receives multi-modal sensory inputs from the thalamus and association cortices, but to a lesser extent than does the LA, (Sah et al., 2003). The BA, is however, strongly innervated by the LA, and in turn projects to the CeM (the amygdala's main autonomic output center). A highly simplified amygdala circuit thus posits the LA as the entry point for sensory information; this information is further processed by the BA and finally relayed to the CeM **(Figure 2)**.

However, the BA is more than a passive relay between the LA and CeM. Like in the LA, many BM and Ba PNs respond with increased firing to previously fear conditioned sensory cues (Amano et al., 2011). Such increased activity is presumably due to excitatory LA input. However, PNs of the Ba (but not those of other nuclei) show persistently increased activity for upward of a minute after sensation of a fear-eliciting cue, suggesting these neurons extend and perhaps modulate some signals received from the LA (Amano et al., 2011).

The BA has also recently been ascribed an important role in the extinction of conditioned fear, an active learning process (discussed further in section 1.2c). Fear extinction requires NMDA receptor-dependent plasticity in the BA and can be blocked by pharmacological inactivation of either (or both) BA nuclei (Herry et al., 2008; Amano et al., 2011).

Consistent with its role in fear extinction, the BA communicates strongly with the medial prefrontal cortex (mPFC) and the hippocampus (Orsini et al., 2011). These structures appear to integrate contextual information, which can contain safety signals. Such information may allow the mPFC and hippocampus to update the amygdala on changing threat-related contingencies. The involvement of the BA in fear extinction is particularly relevant to this thesis, as this learned process is potentiated by NPY (Gutman et al., 2008). In addition to the CeA, the BA also sends largely unidirectional projections to other striatal structures, including the bed nucleus of the stria terminalus (BNST) and the nucleus accumbens (NAc). Projections to the BNST are thought to facilitate anxiety behaviors compared to CeA projections, which mediate fear (Walker et al., 2009). NAc projections are involved in reward processing (Stefanik and Kalivas, 2013).

1.1f The Central Amygdala (CeA)

The CeA is a striatum-like structure of sub-pallium origin. As such, its predominant neuron type is medium spiny projection neurons, which use GABA as their neurotransmitter (Sun and Cassell, 1993). The CeA contains two main constituent nuclei: the Lateral Central Amygdala (CeL) and the Medial Central Amygdala (CeM). The CeM is considered the amygdala's main output nucleus for fear responses (LeDoux et al., 1988; Nader et al., 2001). Indeed much of the autonomic and behavioral effects of fear are coordinated via projections from the CeM to other brain areas including: the periaqueductal gray matter, brainstem nuclei (including the ventral medulla and nucleus tractus solitarius) and hypothalamic areas (including the lateral hypothalamus and paraventricular nucleus) (LeDoux et al., 1988; Keifer et al., 2015). Consistent with this, CeM-specific lesions block the expression of conditioned fear (Nader et al., 2001). The CeL in turn, sends inhibitory projections to the CeM (Haubensak et al., 2010). These projections appear to tonically inhibit the CeM, as selective CeL inactivation actually increases fear behaviors (Ciocchi et al., 2010). However, the CeL is not a monolithic neuronal population, rather distinct populations of projection neurons have been characterized with opposing circuit roles. Following fear conditioning (discussed further in section 1.2b) one CeL population, termed Fear-On neurons, responds to a fear eliciting stimuli with increased firing. A separate CeL population, termed Fear-Off neurons, respond to the fear provoking stimuli with the opposite activity pattern (decreased firing) (Ciocchi et al., 2010; Haubensak et al., 2010). Fear-Off neurons, but not Fear-On neurons, express the protein kinase C δ isoform (PKCδ) (Ciocchi et al., 2010), while Fear-On neurons selectively express the neuropeptide somatostatin (SOM) (Li et al.,

2013). Fear-On and Fear-Off neurons mutually inhibit each other and both populations send inhibitory projections to the CeM (Ciocchi et al., 2010; Li et al., 2013); however, Fear-Off neurons inhibit the CeM to a far greater extent than do the Fear-On neurons (Li et al., 2013).

As mentioned above, the BA nuclei (but not the LA) project to the CeM. However, the LA sends excitatory projections directly to CeL which target both its Fear-On and Fear-Off neuronal populations (Krettek and Price, 1978; Li et al., 2013). Fear conditioning strengthens LA inputs onto SOM^+ (Fear-On) neurons, while decreasing the strength of LA inputs onto SOM^- (Fear-Off) neurons (Li et al., 2013). This circuitry thus provides another route for conditioned fear associations, formed in the LA, to activate the CeM and elicit fear behaviors. Specifically the increased excitatory drive from the LA onto Fear-On neurons in concert with decreased excitatory drive onto Fear-Off neurons, shifts activity in favor of the Fear-On circuit. This shift ultimately increases the activity of CeM neurons via disinhibition, since the SOM^- (Fear-Off) neurons (which normally tonically inhibit the CeM) are themselves inhibited via the increased activity of the SOM^+ (Fear-On) neurons (Li et al., 2013). This circuit may compensate for lesions to the BA and in part explain contradictory experimental findings. Specifically, expression of conditioned fear is blocked by post-training BA lesions, whereas pre-training BA lesions do not prevent subsequent fear conditioning or its expression (Nader et al., 2001; Anglada-Figueroa and Quirk, 2005).

The CeA, and particularly the CeL nucleus, is structurally complex and like the BLA-complex is a site of fear-related plasticity. As such, the view of the CeA as a passive amygdala output, although conceptually useful, is an oversimplification. Many of

the intricacies of the CeA circuit are beyond the scope of this thesis but have recently been reviewed by (Keifer et al., 2015).

1.2 FEAR AND ANXIETY

1.2a Fear vs. Anxiety

The terms fear and anxiety are often used interchangeably, but they represent distinct emotional states, and thus merit definition. Fear is defined as an apprehensive state, which occurs in response to concrete and imminent threats. Fear coordinates defensive behaviors such as fight or flight. Fear is phasic: it is elicited rapidly and terminated quickly upon removal of the inciting stimulus (Davis et al., 2010). Anxiety in contrast, involves a sustained state of heightened arousal in which a subject is preoccupied by potential (but not explicit) threats. Anxiety is more of a "future oriented state", and is believed to involve perceptions of unpredictable dangers and a loss of control (Barlow, 2000).

1.2b Conditioned Fear

Fear conditioning is a form of classical conditioning first documented by Pavlov in 1927. This paradigm involves delivering an innocuous sensory cue, termed the conditioned stimulus (CS) in close temporal proximity to an intrinsically unpleasant, unconditioned stimulus (US). In rodent models the CS is typically a tone or light, while a mildly painful foot shock is typically used as the US. After repeated pairings, the CS takes on the aversive qualities of the US, and will elicit fear behavior when presented in the absence of the US (Davis, 1997). Importantly, the US elicits species-specific defensive behaviors, which can be measured (eg., freezing in rodents). Fear conditioning is arguably the most robust known learning model and is also readily applied in human studies (Sehlmeyer et al., 2009).

Conditioned fear likely evolved to supplement innate (unlearned) fear, which members of a given species show towards predictable threats. For instance all macaque monkeys innately fear snakes regardless of previous encounters (Mineka and Ohman, 2002). Importantly, lesions to specific amygdala nuclei block both innate (Blanchard and Blanchard, 1972) and conditioned fear (Campeau and Davis, 1995; Nader et al., 2001) revealing the amygdala's central role in fear-based behaviors.

The primary neural correlate to fear conditioning, appears to be a Hebbian form of long-term potentiation (LTP), which occurs at synapses conveying sensory information onto LA PNs (Rogan et al., 1997). In this model, aversive (US coding) synapses are of sufficient strength to elicit PN firing, while CS synapses are not, prior to conditioning. US-evoked PN firing depolarizes dendrites via back propagating action potentials. This action removes the Mg^{2+} block of synaptic NMDA receptors and activates voltage-gated Ca^{2+} channels (VGCC) allowing coincidently received sensory inputs (CS) to be strengthened via increased Ca^{2+} entry (Blair et al., 2001). LA LTP and its behavioral correlate (conditioned fear) requires the calcium calmodulin-dependent kinase Type II (CaMKII), which initiates a signaling cascade culminating in increased synaptic strength (Rodrigues et al., 2004).

1.2c Extinction of Conditioned Fear

Following fear conditioning, repeated presentations of the CS (in the absence of the US) leads to a gradual decoupling of the CS-US association, and to a reduction in CS-elicited fear. It is generally accepted that this process, termed fear extinction, is not an unlearning of the CS-US association, but instead involves the formation of a new, fear suppressing memory, [reviewed in (Myers and Davis, 2002)]. Several lines of evidence

support post-extinction persistence of the fear memory. First, conditioned fear can be reinstated, by exposing the subject to the US in the absence of the CS. Second, the conditioned fear memory often spontaneously re-emerges with time. Third, fear extinction is highly context-dependent. Thus, when conditioning and extinction are performed in separate experimental contexts, re-exposure to the conditioning context rescues conditioned fear. It appears that contextual safety signals can thus specifically signal conditions under which the CS does not predict the US and fear is thus inappropriate.

Fear extinction decreases the activity of LA PNs, which suggests facilitation of BLA inhibition (Quirk et al., 1995). Paradoxically, fear extinction depends on excitatory neurotransmission within the BA and requires NMDA-type glutamate receptors. BLA infusions of either NMDA receptor antagonists or the positive allosteric NMDA receptor modulator, D-cycloserine, inhibit or potentiate fear extinction, respectively (Falls et al., 1992; Walker et al., 2002). Inactivating BA nuclei with local GABA infusions also prevents fear extinction (Amano et al., 2010). Interestingly, Ca^{2+} entry via L-type voltage gated Ca^{2+} channels (VGCC) has also been implicated in extinction (Cain et al., 2002). Studies suggest roles for both CaMKII and the Ca^{2+}-dependent phosphatase, calcineurin, in fear extinction (Lin et al., 2003). Calcineurin and CaMKII are expressed in pyramidal neuron dendritic spines, where they mediate long-term depression (LTD) and LTP respectively (Baumgärtel and Mansuy, 2012; Lisman et al., 2012).

1.2d Calcineurin and CaMKII – The Ca^{2+} Dependence of Fear and its Extinction

Like CaMKII, the enzymatic activity of calcineurin requires cytosolic Ca^{2+}. LTP mediated by CaMKII, strengthens synapses via AMPA receptor insertion; conversely,

calcineurin-mediated LTD, removes AMPA receptors and depotentiates synapses (Lu et al., 2010; Baumgärtel and Mansuy, 2012). Thus, CaMKII and calcineurin (protein complexes with diametrically opposing molecular actions) are located in the same neuronal compartments, yet are both Ca^{2+} dependent. This seemingly paradoxical fact is resolved by a differential affinity for cytosolic Ca^{2+}. Calcineurin shows higher Ca^{2+} affinity than CaMKII; thus at lower dendritic Ca^{2+} concentrations calcineurin activity and LTD predominates, while higher Ca^{2+} concentrations preferentially recruit CaMKII and LTP (Mansuy, 2003).

1.2e Linking Fear to Anxiety

Like fear, anxiety is intimately linked to the amygdala, and is reliably elicited when BLA output is enhanced by pharmacological manipulation or electrical stimulation (Sajdyk and Shekhar, 1997a; 1997b). Although, fear is a simpler, better-understood emotional state, anxiety is of greater clinical interest. A great deal of effort has thus been directed towards relating aspects of conditioned fear to pathological anxiety.

1.2e(i) Post-Traumatic Stress Disorder:

One of the strongest links between fear and anxiety comes from post-traumatic stress disorder (PTSD), an anxiety disorder affecting a subset of individuals who experience or witness a severe (potentially life threatening) trauma. Patients with PTSD suffer from frequent re-experiencing of the eliciting trauma, including flashbacks and/or nightmares. Additionally, situations, people and places which remind patients of the precipitating event, are actively avoided. Finally, prominent symptoms of hyperarousal, including sleep disturbances, irritability and poor concentration characterize PTSD

(Sareen, 2014). Often PTSD is likened to a single, profound fear-conditioning episode, which then elicits a prolonged pathological state of anxiety.

The ability to perform fear conditioning in human subjects, including those with anxiety disorders, has permitted aspects of conditioned fear (its acquisition and extinction) to be correlated with pathological anxiety. Rodent fear conditioning in turn permits behavioral studies in conjunction with more invasive methods, which can speak to cause and effect. Three facets of conditioned fear have been linked to PTSD and, in some cases, other anxiety disorders. These include 1) increased generalization of conditioned fear, 2) deficient extinction and 3) contextual conditioning.

1.2e(ii) Generalization of Conditioned Fear

Stimulus generalization, first documented in the appetitive domain by Pavlov (1927), involves generalization of a conditioned behavior towards sensory stimuli other than the trained CS. Typically, generalization occurs towards stimuli qualitatively similar to the CS, and decreases with diminished perceptual similarity. For instance, sound frequencies near that of an auditory CS better elicit conditioned fear than dissimilar tones. Stimulus generalization can thus be described by a perceptual gradient centered on the CS, however, the width of such gradients vary considerably between individuals. Animal models indicate that greater generalization of conditioned fear will predict increased anxiety behavior (Laxmi et al., 2003). Furthermore, several human anxiety disorders including panic disorder (PD), generalized anxiety disorder (GAD) and post-traumatic stress disorder (PTSD) are associated with over-generalization of conditioned fear (Lissek et al., 2010; Lissek, 2012; Lissek et al., 2014).

1.2e(iii) Contextual Conditioning

In the classical fear-conditioning model, two distinct perceptual substrates may become predictive of the US: the CS (discussed above) and the experimental apparatus (termed experimental context). The CS predicts the US with high temporal certainty. The experimental context is also of predictive value, but can't specify the timing of US delivery, only that shocks will occur whilst in the apparatus. The degree to which a subject conditions to the CS vs. context will determine behaviors displayed in the conditioning apparatus. Successful CS-US pairings result in expression of fear behavior only at discrete times (when the CS is present). In contrast, greater contextual conditioning results in a persistent state of US expectancy, similar to anxiety (Laxmi et al., 2003). Inter-individual variability exists in the propensity toward contextual conditioning (Baas et al., 2008), while contextual conditioning is more prevalent amongst human subjects with PTSD (Grillon et al., 1998).

A related conditioning approach uses un-signaled shocks to ensure greater contextual associations. Using such an approach an equivalent number of shocks will elicit greater anxiety-like behavior compared to classical fear conditioning (Grillon and Davis, 1997). This underlies a recurrent principal of anxiety, perceived unpredictability in the face of threats.

1.2e(iv) Deficient Fear extinction

Deficits in the extinction of conditioned fear have consistently been observed in patients suffering from PTSD (Wessa and Flor, 2007; Jovanovic et al., 2010). A causal relationship between PTSD and deficient extinction is supported by findings of reduced extinction amongst first-degree relatives of PTSD patients, themselves not suffering from

the disorder. Furthermore, exposure based therapy, which is conceptually similar to fear extinction, is among the best evidenced treatment for PTSD (Sareen, 2014). Animal models have indicated that fear extinction is potentiated by several compounds with long-term anxiolytic actions including, fluoxetine (but not other SSRI antidepressants) as well as the anxiolytic neuromodulator NPY (Gutman et al., 2008; Gunduz-Cinar et al., 2015).

1.2f Behavioral measures and Anxiety

Several experimental approaches have been used both to elicit and measure specific aspects of human anxiety in rodents with many of these models emphasizing vague or unpredictable threat.

1.2f(i) Acoustic startle

When mammals, including humans, are exposed to an unexpected loud noise they show a defensive behavior, termed the acoustic startle reflex, first documented by (BROWN et al., 1951). Both fearfulness and anxiety enhance acoustic startle amplitude, which is readily measured both in rodents and humans (Grillon and Davis, 1997). Thus, acoustic startle is not purely a measure of anxiety, but rather a versatile probe for defense-based emotions. When used in conjunction with classical fear conditioning, acoustic startle enhancement (fear potentiated startle) is typically only observed (post-training) during the distinct time period when the subject is exposed to CS (Davis et al., 1989). However, contextual conditioning elicits sustained acoustic startle enhancement, indicative of an anxiety-like state. Other anxiety-enhancing contextual manipulations, such as brightly lit areas (in rodents) or darkness (in the case of humans) also elicit sustained enhancement of acoustic startle (Grillon et al., 1997; Walker and Davis, 1997). Interestingly, anxiolytic drugs block the potentiating effects of anxiety on startle

amplitude but do not affect fear potentiated startle (de Jongh et al., 2002). Furthermore, the BNST mediates the effects of anxiety on startle amplitude (Gewirtz et al., 1998), while fear potentiation of startle occurs via CeA output (Campeau and Davis, 1995; Grillon, 2002). These data further suggest fear and anxiety are district behaviors mediated by overlapping but separate anatomical circuits.

1.2f(ii) The Elevated Plus Maze

The elevated plus maze (EPM), first described in 1955 by Montgomery et al. (MONTGOMERY, 1955), is an experimental protocol designed to measure the unconditioned state-anxiety of rodents (typically rats or mice). The EPM employs a plus sign-shaped apparatus, with two arms sheltered (or enclosed) and the other two exposed. The platform is elevated such that when exploring the open arms, rodents must contend with their natural aversion to heights. When placed in the EPM rodents may freely explore all four arms, although more time is virtually always spend in the enclosed arms.

The ethological principal underlying the EPM is a conflict between a rodent's natural desire to explore a novel environment and their innate fear of open spaces and heights. Lower states of anxiety will result in a greater desire to explore the novel context, which is inferred by either more entries, or more time spent in the open arms of the maze.

The EPM is one of the most simplistic and widely used measures of anxiety-like behavior in rodents and has been employed in thousands of peer-reviewed publications (Walf and Frye, 2007). Multiple lines of evidence support the validity of the EPM as an anxiety measure in rodents. For instance, anxiety-like behaviors, such as freezing and defecation, are increased in the open arms of the EPM (Pellow et al., 1985), while plasma

corticosterone levels are increased after open arm exposure (File et al., 1994). Treatment with known anxiogenic or anxiolytic drugs decrease, or increase, time spent in the open arms of the EPM, respectively (Pellow et al., 1985), confirming construct validity (Walf and Frye, 2007).

Theoretically, both the novelty and uncertainty of the EPM apparatus should be diminished with previous experience. The usefulness of the EPM test in measuring anxiety-like behavior in the same animal on multiple occasions has thus been disputed (Walf and Frye, 2007). Indeed, anxiety-like behavior is most clearly seen within the first five minutes of EPM exploration. Although it was initially reported that previous EPM testing did not bias the results of subsequent tests (Lister, 1987; File et al., 1990), more recent reports suggest decreased open arm activity upon a second EPM exposure (Bertoglio and Carobrez, 2000; 2002). The impact of repeated EPM testing may be lessened when the interval between tests is sufficiently long (~3 weeks) and when subsequent tests are conducted in different rooms (Adamec and Shallow, 2000; Adamec et al., 2005), thereby increasing context novelty.

1.2f(iii) Social Interaction

The social interaction (SI) test, first described by File et al. (File et al., 1976), is an assay of anxiety-like behavior used mainly in rats, but which has also been applied to mice and gerbils (de Angelis and File, 1979; Cheeta et al., 2001). The SI test pairs two unfamiliar conspecifics of the same sex (typically male) and measures the time the animals spend interacting socially (ie grooming, sniffing or following). Decreased anxiety is inferred when SI is increased, without increased motor activity; conversely, decreased SI reflects increased anxiety (File and Seth, 2003).

The SI test is inherently more complex than the EPM, as two animals are involved and one animal's behavior undoubtedly influences the other. For this reason both animals must be treated as a single experimental unit (or experimental n). Typically, either mean interactions between the pair are documented or, when only one animal receives a drug treatment, only interactions initiated by the treated animal (File and Seth, 2003).

Both familiarity of an animal with the experimental context and illumination levels influence SI. Low light and familiar contexts are least anxiogenic, eliciting greater SI. Conversely, anxiogenic experimental conditions (a brightly lit unfamiliar testing environment) reduce baseline SI. Intermediate anxiety levels are achieved with a combination of a low and high anxiety test variable. In general, effects of anxiogenic drugs are more readily observed under low anxiety test conditions and anxiolytic effects better detected under higher anxiety conditions; experimental designs may thus be adjusted accordingly (File and Seth, 2003).

Other behavioral measures of anxiety, such as freezing or defecation, are observed in association with decreased SI behavior (File and Seth, 2003). Furthermore, SI testing increases plasma corticosterone levels, with higher anxiety test conditions eliciting the greatest increases (File and Peet, 1980). These data suggest high face validity; that is decreased SI indeed appears to reflect an anxiety-like state. Numerous known anxiolytic compounds increase SI while; known anxiogenic drugs decrease SI (File et al., 1982), confirming the construct validity of the SI test. Relevant to this thesis, the acute behavioral effects of NPY, selective Y_1 and Y_2 receptor agonists and the type 2 corticotropin-releasing factor (CRF) receptor agonist Urocortin, have been measured with

the SI test (Sajdyk et al., 1999b; 2002b), as have the longer-term behavioral effects of repeated NPY and Urocortin treatments (Rainnie et al., 2004; Sajdyk et al., 2008).

Theoretically, the same animal can undergo SI testing on multiple occasions. However, when multiple tests are conducted, animals should be familiarized with the test apparatus prior to experimenting (File and Seth, 2003).

1.3 MODULATION OF FEAR AND ANXIETY BEHAVIOR BY NEUROPEPTIDE Y

1.3a Neuromodulation of BLA Circuitry

Numerous modulatory systems target the BLA, sculpting sensory integration and amygdala output. Serotonin, dopamine, norepinephrine and acetylcholine all have described actions in the BLA (DeBock et al., 2003; Zhu et al., 2005; Chu et al., 2012; Clinard et al., 2015). Thus, the neuromodulator balance within the BLA determines, at least in part, its output pattern and ultimately the individuals affective state.

In addition to small molecule transmitters, BLA activity is also modulated by multiple neuropeptides including Cholecystokinin (CCK), Corticotropin Releasing Factor (CRF), Neuropeptide Y (NPY) and Somatostatin (SOM) (Meis et al., 2005; Giesbrecht et al., 2010; Bowers and Ressler, 2015). Neuropeptides are 5-50 amino acid long peptides, typically cleaved from larger pre-prohormones and post-transcriptionally modified.

For numerous reasons, neuropeptides are ideally suited to evoke longer lasting, more widespread CNS action. Unlike the more classical transmitters such as acetylcholine, the amino acids or biogenic amines, neuropeptides have no specific reuptake systems, and are rendered ineffective by enzymatic cleavage, some more rapidly than others (McKelvy and Blumberg, 1986). Often released from extra-synaptic sites, neuropeptides can thus diffuse widely to reach distant targets via volume distribution. Neuropeptides often co-localize with classical neurotransmitters including GABA, and norepinephrine (van den Pol, 2003), in dense core granules. Classical transmitters are released efficiently by single presynaptic action potentials, while higher discharge frequencies (Gainer et al., 1986) or burst firing (Peng and Zucker, 1993; Muschol and Salzberg, 2000) are required to release

neuropeptides. Thus, periods of high circuit activity can elicit broad modulatory actions via neuropeptide release.

Central to this thesis are the actions of the ubiquitous neuropeptide NPY within the BLA. Therefore, NPY itself, its receptors and their common cellular actions will next be reviewed in greater detail.

1.3b Neuropeptide Y

Neuropeptide Y (NPY), whose name is derived from its tyrosine rich primary structure, is a 36-amino acid polypeptide, widely distributed throughout the mammalian central and peripheral nervous systems (Tatemoto et al., 1982; Adrian et al., 1983). NPY is often grouped with the structurally related Peptide YY (PYY) and Pancreatic polypeptide (PP), all three of which are C-terminally amidated and form (hairpin like) PP-fold containing tertiary structures (Kimmel et al., 1975; Tatemoto, 1982; Fuhlendorff et al., 1990). NPY has been isolated from numerous vertebrate species and shows high sequence homology across species, indicating its conserved evolution (Larhammar et al., 2001; Gehlert, 2004).

NPY is released from neuronal dense core granules during high frequency, repetitive action potential firing. This strong activity dependence is due to a greater requirement of presynaptic calcium entry for dense core granule release (compared to typical synaptic vesicles) (Muschol and Salzberg, 2000). NPY is not acted on by reuptake transporters and is generally only slowly degraded by local exopeptidases; consequently, extensive diffusion from its release site may facilitate longer-term, spatially widespread NPY effects.

In the peripheral nervous system NPY is expressed in sympathetic neurons and is co-localized and co-released with catecholamines (norepinephrine or dopamine) (Ekblad et al., 1984). In the CNS, NPY is considered the most abundant neuropeptide and is highly expressed in the hypothalamus, hippocampus, nucleus accumbens and the amygdala (Adrian et al., 1983). Given this wide spread expression, NPY unsurprisingly exerts diverse modulatory actions depending on its site of release. Relevant to this thesis, NPY has anxiolytic and antidepressant actions, exerted in brain areas including the amygdala, hippocampus and locus coeruleus (Kask et al., 1998; Sajdyk et al., 1999b; Smiałowska et al., 2007). Additionally, NPY modulates numerous other biological processes including (but not limited to) feeding and energy balance, learning, memory, and pain processing (Naveilhan et al., 2001; Chee and Colmers, 2008; Hamilton et al., 2010). NPY most often co-localizes with GABA in the CNS typically in local circuit interneurons (as is largely the case in the BLA). However, in brainstem nuclei including the locus coeruleus and the ventrolateral medulla oblongata, NPY co-localizes with norepinephrine (Everitt et al., 1984).

1.3c NPY Receptors

Five NPY receptor subtypes have been cloned, Y_1, Y_2, Y_4, Y_5 and y_6; all known NPY receptors are 7 transmembrane G-protein coupled receptors (GPCR) of the $G_{i/o}$ (pertussis toxin sensitive) type. As such, receptor activation reduces cyclic AMP (cAMP) accumulation by inhibiting adenylyl cyclase (Merten and Beck-Sickinger, 2006). NPY receptors also directly modulate Ca^{2+} and K^+ channels via membrane delimited direct channel interactions with G-protein $\beta\gamma$ subunits (McQuiston et al., 1996; Klenke et al., 2010). Like other GPCRs, NPY receptors may also signal through the β-arrestin pathway;

however the relevance of this signaling mode is unclear as G-protein or β-arrestin biased NPY agonists are only just emerging (Walther et al., 2011).

Although the y_6 receptor gene is present in numerous vertebrates including mice and humans, it is absent in rats, and functionally inactive in primates due to an ancestral frame shift mutation and is therefore denoted here with a lower case y. The Y_4 receptor shows high (pM) affinity for PP, but relatively low NPY and PYY affinity (nM range) (Bard et al., 1995) thus, the Y_4 receptor is considered a PP-preferring receptor.

The various NPY receptor types are relatively dissimilar, with an overall sequence homology of only 30-50% (Cabrele and Beck-Sickinger, 2000). The flexibility of the NPY peptide is thought to facilitate numerous energetically favorable conformations thus allowing actions at structurally dissimilar receptors. NPY peptide derivatives can achieve receptor specificity through conformational restrictions, which are achieved by amino acid substitution, truncation, and formation of cyclic analogous (Cabrele and Beck-Sickinger, 2000). The work outlined in the thesis has capitalized on several such receptor-specific NPY analogues.

1.3c(i) The Y_1 receptor

The Y_1 receptor is a 384 amino acid GPCR with high affinity for NPY and PYY and low affinity for PP (Cabrele and Beck-Sickinger, 2000). Y_1 receptors are highly expressed in hippocampal formation, amygdala, cortex, hypothalamic nuclei, the brainstem (Wolak et al., 2003) and in peripheral blood vessels (Wahlestedt et al., 1990). Numerous physiological processes are modulated by the Y_1 receptor including (amongst others) anxiety, feeding behavior (Kanatani et al., 2000), pain processing (Naveilhan et al., 2001), alcohol consumption and hormone secretion. Y_1 receptors are typically

postsynaptic although in some instances they may be presynaptic. N-terminally, truncated analogues of NPY and PYY show characteristically low Y_1 receptor affinity, while Pro^{34} substitution can enhance the Y_1 affinity of analogues (Krause et al., 1992). Y_1 receptors rapidly desensitize and internalize in the continued presence of agonists (Gicquiaux et al., 2002) likely via β-arrestin recruitment (Berglund et al., 2003).

1.3c(ii) The Y_2 receptor

The Y_2 receptor is a 381 amino acid GPCR that, like the Y_1 receptors, shows high NPY and PYY affinity but low PP affinity. Y_2 receptors are the most highly expressed NPY receptors in the brain and are typically expressed at presynaptic terminals where they inhibit neurotransmitter release (Michel et al., 1998). In contrast to Y_1 receptors, Pro^{34} substituted analogues show low Y_2 receptor affinity (Cabrele and Beck-Sickinger, 2000). However, C-terminally truncated analogues and the centrally truncated [ahx^{5-24}]NPY show high Y_2 receptor affinity (Walther et al., 2011). In many instances Y_2 receptors are expressed on NPY neurons, suggesting an auto-receptor function (King et al., 1999). However, Y_2 receptors frequently also act on neurons which do not express NPY, consistent with high receptor expression levels (Colmers and Bleakman, 1994). Y_2 receptors show low sequence homology with the Y_1 receptors (31%) (Cabrele and Beck-Sickinger, 2000).

1.3c(iii) The Y_5 receptor

Unlike the Y_1 and Y_2 receptor subtypes, NPY Y_5 receptors are largely restricted to CNS (Walther et al., 2011). Y_5 receptor mRNA is widely transcribed throughout the rat brain (Gerald et al., 1996; Parker and Herzog, 1999), however, autoradiography (Gerald

et al., 1996; Dumont et al., 1998; Parker and Herzog, 1999) and immunohistochemistry studies suggest Y_5 receptor proteins are actually relatively rare compared to Y_1 and Y_2 receptors (Morin and Gehlert, 2006). In the rat, Y_5 receptor expression is highest in the hippocampus, piriform cortex and supraoptic nucleus (Morin and Gehlert, 2006). Moderate Y_5 receptor expression is seen in the amygdala, lateral septum, hypothalamic nuclei (the arcuate and paraventricular nuclei), cerebellum and the locus coeruleus (Morin and Gehlert, 2006). Due to alternate splicing of the receptor gene, two Y_5 receptor isoforms are expressed which contain either 445 or 455 amino acids. However, both receptor isoforms appear to show similar pharmacological profiles (Rodriguez et al., 2003). Y_5 receptors show high affinity for both NPY and PYY and, like Y_1 receptors, bind Pro^{34}-containing analogues with high affinity (Walther et al., 2011). Highly Y_5 receptor selective NPY analogues can be generated by inserting a motif containing alanine at position 31 and the non-proteinogenic amino acid 2-aminoisobutyric acid (Aib) at position 32 (Cabrele et al., 2002). Prototypic Y_5 selective (Ala^{31}-Aib^{32}) containing analogues include [Ala^{31}-Aib^{32}]-pNPY and [cPP^{1-7}, $pNPY^{19-23}$, Ala^{31}, Aib^{32}, Gln^{34}]-hPP. A major functional difference between Y_1 and Y_5 receptors is the strikingly slow rate at which Y_5 receptors internalize in the continual presence of an agonist (Böhme et al., 2008). Indeed Y_5 receptors may not associate with β-arrestins (Walther et al., 2011) although conflicting reports exist (Berglund et al., 2003). Differences in kinetics amongst receptor types, along with their apparent differential expression at the level of tissues, cell types and sub-cellular domains likely facilitate NPY's diverse physiological actions.

1.3d NPY Modulates Fear and Anxiety – The Short and the Long-Term

1.3d(i) Correlative studies suggest NPY confers psychological resilience in humans

Amongst Canadians, the lifetime prevalence rate of PTSD has been estimated as 9.2%, with 2.4% of Canadians actively suffering from PTSD during a given month. This same study however, suggests the majority of Canadians (76.1%) have experienced at least one traumatic event, of sufficient severity, to potentially cause PTSD (Ameringen et al., 2015). These statistics highlight the apparent variability amongst individuals in susceptibility to trauma-induced psychopathology. Individuals who can withstand a substantial psychological trauma without suffering resultant psychiatric disorders (such as PTSD) are said to exhibit stress resilience. Variable NPY expression, presumably in key brain areas such as the amygdala and hippocampus, may be a key factor conferring stress resiliency amongst humans.

1.3d(ii) Plasma and CSF NPY levels are reduced in PTSD patients

Plasma NPY levels have been reported to be reduced in PTSD patients compared to healthy controls (Rasmusson et al., 2000). Interestingly, recovered combat veterans who previously experienced a PTSD episode, showed increased plasma NPY levels compared both to healthy veterans and those with active PTSD (Yehuda et al., 2006). These results suggest peripheral NPY levels parallel resiliency; however, it is unclear to what degree this reflects CNS levels. Direct microanalysis of specific brain structures is too invasive for human studies, however NPY levels in cerebral spinal fluid (CSF) have also been reported to be significantly lower in combat veterans with PTSD (Sah et al., 2009).

1.3d(iii) Genetic polymorphisms reducing NPY expression, may confer stress vulnerability:

Several genome-wide association studies suggest that genetic polymorphisms of the NPY system confer risk for human anxiety disorders. The Y_1 receptor gene-containing region (4q31-34), located on chromosome 4, has been identified as a risk locus for multiple anxiety disorders (Kaabi et al., 2006). Furthermore, Zhou et al. (2008) identified several haplotype polymorphisms which regulate NPY expression, including a single nucleotide polymorphism in the NPY promoter region (SNPrs16147), which accounted for greater than half the *in vivo* variability in expression. Individuals whose diplotype predicted lower NPY expression showed greater amygdala activation by emotionally charged stimuli and displayed higher trait anxiety in this study. Haplotype-predicted NPY expression was also correlated both with post mortem brain expression of NPY mRNA and plasma NPY levels (Zhou et al., 2008). These results suggest that plasma and CSF NPY measurements may indeed reflect global NPY levels (at least to some degree), and may thus correlate with brain expression.

1.3d(iv) NPY acutely reduces rodent anxiety behavior, via actions in the BLA

Heilig et al. (1989) initially demonstrated that intracerebroventricular (icv) NPY injection decreased anxiety behavior in rats, measured either with the EPM or the Vogel punished drinking conflict test (Heilig et al., 1989). Other studies corroborated NPYs anxiolytic actions with the SI test (Sajdyk et al., 1999b), and the light-dark compartment test (Pich et al., 1993). The amygdala was implicated in NPYs anxiolytic actions, by targeted injections that replicated its anxiolytic effects at a lower dose (10-fold) than in icv experiments (Heilig et al., 1993). Finally, more precise microinjections specifically implicated the BLA as the primary site of NPYs anxiolytic actions within the amygdala

(Sajdyk et al., 1999b). Although, this thesis focuses on the actions of NPY within the BLA, it is worth noting that other brain areas including the hippocampus (Smiałowska et al., 2007) and the locus coeruleus (Kask et al., 1998) have also been implicated in anxiolytic actions of NPY.

1.3d(v) NPY's anxiolytic actions are largely mediated by Y_1 receptors

Several lines of evidence suggest that NPY's anxiolytic effects are mediated largely via the Y_1 receptors, within the BLA and elsewhere. Intracerebroventricular administration of the selective Y_1 receptor agonist [D-His^{26}]NPY evoked a dose-dependent anxiolytic effect as seen with the EPM and open field tests (Sørensen et al., 2004). Furthermore, NPY's anxiolytic actions, measured with SI, are blocked by BLA infusion of the highly selective and nontoxic Y_1 receptor antagonist BIBO 3304 (Sajdyk et al., 1999b). Pharmacological studies have been complemented with antisense knockdown studies of the Y_1 receptor in the whole brain *in vivo*, after which NPY administration became anxiogenic (as opposed to anxiolytic), as measured with the EPM (Wahlestedt et al., 1993). This suggests that activation of other NPY receptors, in the absence of Y_1 receptor signaling, may actually increase anxiety.

1.3d(vi) Selective BLA Y_2 Receptor Activation Increases Anxiety Behavior

Interestingly, icv injection of the selective Y_2 receptor agonist NPY$_{13-36}$ increased EPM measured anxiety behavior (Nakajima et al., 1998). The BLA appears to mediate these anxiogenic effects, as direct BLA injection of C2-NPY (a selective Y_2 receptor agonist) is also anxiogenic as measured with SI (Sajdyk et al., 2002a). Furthermore, anxiolytic behavioral effects are observed when BLA Y_2 receptors are blocked with the selective antagonist BIIEO246 (Bacchi et al., 2006). These pharmacological studies have

been complimented by a study in adult mice in which BLA Y_2 receptors were selectively deleted, similarly resulting in decreased anxiety behavior as seen both with the EPM and light-dark tests (Tasan et al., 2010). Interestingly, the presence of Y_2 receptors in the central amygdala was anxiolytic in this study.

1.3d(vii) NPY Modulates Acquisition and Extinction of Conditioned Fear

Initial work indicated icv NPY injection decreased the acquisition of conditioned fear (via Y_1 and possibly Y_5 receptors) (Broqua et al., 1995). These effects were likely mediated (at least in part) via the BLA, as icv or BLA-targeted NPY injections both reduced conditioned fear expression (Gutman et al., 2008). Interestingly, these authors also found that BLA injections of the Y_1 antagonist BIBO 3304 had no effect on conditioned fear. However, as BIBO 3304 was not co-injected with NPY, it is unclear whether this indicates the requirement for other NPY receptors or simply resulted because conditioned fear was not damped by endogenous NPY (Gutman et al., 2008). Interestingly, NPY also potentiated extinction of conditioned fear; likely via Y_1 receptors, as BLA injections of BIBO 3304 blocked this effect (Gutman et al., 2008).

NPY also facilitates extinction of anxiety-like contextual fear conditioning (Gutman et al., 2008). Indeed, NPY may preferentially act on contextual fear, which is inhibited by lower icv doses of NPY than cued fear responses (Karlsson et al., 2005). Lach and de Lima (2013) found icv NPY injections reduced contextual fear expression during all phases of training (acquisition, consolidation and extinction). The Y_1 preferring agonist Leu^{31}Pro^{34}-NPY mimicked the effects of NPY on acquisition and consolidation. However, Leu^{31}Pro^{34}-NPY did not enhance extinction of contextual fear, suggesting contextual extinction requires other NPY receptors (Lach and de Lima, 2013).

Several germ-line knockout models have also been used to explore NPYs role in conditioned fear. Interestingly, although Y_1 receptor knockout mice showed slower extinction of conditioned fear, the acquisition and expression of conditioned fear were otherwise normal (Fendt et al., 2009; Verma et al., 2012). This was likely not due to developmental compensation, as conditioned fear expression was also unaffected in wild-type mice when one of two Y_1 agonists (Y-28 and Y-36) was injected after fear acquisition into BLA, nor were the effects of NPY blocked in wild-type animals by post-acquisition BIBO 3304 treatment. Furthermore, conditioned fear was similarly reduced by NPY injections both in Y_1 receptor knockout and wild-type animals (Fendt et al., 2009). In contrast NPY knockout mice show increased acquisition and expression of conditioned fear and are unable to achieve fear extinction (Verma et al., 2012). Generalization of conditioned fear was also more prominent in NPY knockout mice compared to wild-type. Increased generalization of conditioned fear was recapitulated in Y_2 receptor knockout mice; however, Y_2 knockout animals were otherwise normal. Interestingly, the phenotype of NPY knock out mice was only fully replicated with combined Y_1/Y_2 receptor knockout, suggesting synergy between Y_1 and Y_2 receptors in mediating the effects of NPY on conditioned fear (Verma et al., 2012).

In summary, it is clear NPY modulates multiple aspects of the fear conditioning process. Specifically, NPY inhibits the acquisition and expression of conditioned fear, while potentiating extinction of both cued and contextual fear. The BLA appears to at least partly mediate these NPY effects. However, there is a relative paucity of evidence implicating specific BLA NPY receptors in the various aspects of fear conditioning. There is a general consensus that BLA Y_1 receptors cannot account for all the effects of

local NPY injections but do play some role in NPYs fear-reducing actions. It is likely that both BLA Y_1 and Y_2 receptors are required to fully reproduce NPY's actions on conditioned fear and extinction. Future studies using targeted BLA injections of more specific pharmacological tools will be necessary to clarify the roles of specific NPY receptors within the BLA.

1.3d(viii) Repeated BLA Injections of NPY Elicit Long-Term "Stress Resilience"

Local BLA injections of NPY reduce anxiety-like behavior, while fear-conditioning studies suggest NPY modulates associative learning. Since NPY modulates fear-related plasticity within the BLA, similar plasticity mechanisms may also elicit longer-term changes in anxiety behavior. This hypothesis was first tested by Sajdyk et al. (2008), who found that repeated (five consecutive daily) NPY injections into the BLA produced a long lasting state of reduced anxiety in rats (Sajdyk et al., 2008). Following NPY injections, this reduced anxiety-like behavior was seen for up to eight weeks, measured as an increase in social interaction (SI). No effects were observed, however, when anxiety was measured with the elevated plus maze. Animals that received repeated NPY treatment were also resistant to the anxiogenic effects of acute restraint stress. Control animals showed increased anxiety for 90min following an episode of forced restraint (measured with SI), while identical restraint stress had no effect on SI at anytime point in NPY-treated animals (Sajdyk et al., 2008). Sajdyk et al. (2008) postulated that resistance to the anxiogenic effects of a "traumatic stressor" (restraint stress) seen in NPY treated rats, might model human stress resiliency. Interestingly, the longer-term (but not acute) behavioral effects of this repeated BLA NPY injection protocol were shown to depend on the calcium-dependent phosphatase calcineurin (Sajdyk et al., 2008).

Calcineurin co-localizes with NPY Y_1 receptors in BLA principal neurons (Leitermann et al., 2012) and mediates synaptic long-term depression (LTD) in pyramidal neurons (Zhou et al., 2004). In the BLA, fear extinction learning is at least partly mediated by calcineurin (Lin et al., 2003), suggesting that the longer-term anxiolytic effects of sub chronic NPY administration are mechanistically similar to fear extinction.

1.3d(ix) CRF Opposes the Actions of NPY Within the BLA

Corticotropin releasing factor (CRF) is a 41 amino acid neuropeptide highly expressed in multiple brain areas including the paraventricular nucleus of the hypothalamus (PVN), the central amygdala and the hindbrain (Merchenthaler et al., 1982). A model originally proposed by Heilig et al. (1994) suggests that the actions of CRF and NPY are intimately connected in the maintenance of emotional homeostasis. Specifically, emotional stress was proposed to cause release of CRF into the amygdala, thereby facilitating "fight or flight" type behavior; while subsequent NPY release dampens the effects of CRF and restores homeostasis (Heilig et al., 1994). CRF is indeed released into the amygdala during periods of high stress (Koob and Heinrichs, 1999) and appears to oppose the physiological and behavioral actions of NPY within the amygdala (Giesbrecht et al., 2010), and other brain areas including the hippocampus (Thorsell et al., 2000; Kagamiishi et al., 2003) and hypothalamus (Hastings et al., 2001). Additionally, local BLA injection of CRF receptor type 1 agonist Urocortin (Ucn) increases anxiety-like behavior measured with SI (Sajdyk et al., 1999a). Interestingly, when NPY is co-applied with CRF into the BLA, the anxiogenic effects of CRF are prevented (Sajdyk et al., 2006).

1.3d(x) Repeated BLA CRF Injections Elicit Longer-Term "Stress Vulnerability" via CaMKII

Interestingly, Rainnie et al. (2004) found that repeated BLA administration of a low Ucn dose (in rats), which on its own produced no acute anxiogenic effects, did produce a long lasting increase in anxiety-like behavior (measured with SI or EPM). The long-term effects of Ucn required CaMKII and NMDA receptors, suggesting an LTP-like form of Ca^{2+}-dependent plasticity (Rainnie et al., 2004).

The findings, in conjunction with those of Sajdyk et al. (2008) implicate Ca^{2+}-dependent processes in the persistent effects of both NPY and CRF. Furthermore, both CaMKII and calcineurin are located in dendritic spines of pyramidal neuron, making it an attractive idea that NPY and CRF may exert their long-term behavioral effects by actions on dendrites.

1.4 A CLOSER LOOK AT BLA CIRCUITRY

1.4a BLA Principal Neurons

Most BLA PNs show morphology similar to that of cortical pyramidal neurons. Specifically, PNs have a characteristic apical dendrite and two smaller basal dendrites, which emanate from vertices of a triangular soma **(Figure 3A)**. However, in contrast to their hippocampal and neocortical counterparts, BLA PNs have generally less pronounced apical dendrites. Additionally, some PNs show a more stellate morphology, while all PNs orient seemingly at random throughout the component BLA nuclei unlike in either the hippocampus or neocortex. BLA PNs are relatively large with soma diameters of ~20 μM and elaborate dendritic arbors (total dendritic lengths of ~6400 μM in adult rats) (Ryan et al., 2016). PNs exclusively express CaMKII, which is often used to differentiate them from local GABA interneurons (Rostkowski et al., 2009).

Dendrites of PNs are spine rich with distal dendrites showing the highest spine density (Ryan et al., 2016). These dendritic spines are the sites of excitatory glutamatergic synapses, both from extrinsic thalamic and cortical afferents as well as from other BLA PNs. Dendritic spines are also the predominant locus of synaptic plasticity. In contrast, the majority of inhibitory GABA inputs reach PNs at more proximal domains (soma and proximal dendrites) (Muller et al., 2006a).

PNs show relatively wide action potentials compared to most interneurons with spike halve widths of ~1.0 ms (Washburn and Moises, 1992a; Rainnie et al., 1993). When brought to threshold with depolarizing current, PNs typically fire action potential trains showing marked spike frequency adaptation with the first action potential often showing doublet or triplet bursts **(Figure 3B, C)**.

1.4b The Multi Faceted Amygdala - Valence Coding of Principal Neurons

Anxiety behaviors are reliably elicited when PN activity, and thus BLA output is non-specifically enhanced. The amygdala is therefore often ascribed the role of a "fear center." However, dating back to classical lesion studies, the amygdala has also been implicated in hedonic behaviors. Indeed, emerging evidence (discussed below) has confirmed the amygdala's role in reward-based emotion. Given however, that positive valence emotions motivate approach behavior, this poses the question: "How can the amygdala mediate both avoidance and approach?" It is becoming increasingly clear that the BLA encompasses multiple parallel circuits, which mediate these opposing emotional states. Uniformly exciting all PNs favors the BLAs anxiogenic output, however specific PN populations can elicit opposing behavior when selectively activated. Indeed, as with conditioned fear, associations between innocuous sensory stimuli and intrinsic rewards are mediated by synaptic plasticity within the BLA (Tye et al., 2008).

To better understand BLA circuitry (as it relates to fear and reward), several studies have combined classical conditioning with *in vivo* electrophysiology. In one such experiment (Paton et al., 2006), trained animals to associate an innocuous sensory cue (CS_1) with a shock, while a separate innocuous cue (CS_2) was paired with a reward. Following conditioning, two (largely non-overlapping) populations of BLA PNs were observed. One PN population increased its firing rates in response to the fear-predicting CS_1, while the other population fired in response to the reward-predicting CS_2. After initial learning was established the valence of the cues was switched, such that CS_1 predicted the reward and CS_2 the shock. Interestingly, upon learning this valence shift, the response patterns of PNs switched accordingly. PNs that responded to the CS_1, when

it predicted the reward, switched their response pattern towards the CS_2 after the valence shift was learnt. Similarly, a largely non-overlapping PN population responded to cues that predicted the aversive shock, apparently irrespective of the qualitative features of the cue, since this population responded to the CS_2 before the cues were valence shifted and the CS_1 after (Schoenbaum et al., 1998; Paton et al., 2006). These data, which have been independently confirmed in rats and non-human primates, suggest that BLA PNs code for the valence of a specific outcome (positive vs. negative) as opposed to the sensory features predicting the outcome.

Further supporting discrete populations of valence coding PNs, reward-coding PNs neurons have been shown to project to the nucleus accumbens (NAc), while fear-coding PNs target the CeM. This projection specificity has also allowed for population-selective optogenetic activation. Selectively activating reward neurons positively reinforces behaviors, while activation of fear neurons is a negative reinforcer (Namburi et al., 2015).

The functional heterogeneity amongst BLA PNs was further highlighted by Herry et al. (2008), who obtained single unit *in vivo* recordings from mouse BA neurons during acquisition and extinction of conditioned fear. During fear acquisition, 17% of BA PNs (termed fear neurons) responded to the CS with increased firing, while after extinction training these same neurons were inhibited by CS presentations. A separate 15% of BA PNs (termed extinction neurons) responded to the CS with the opposite firing pattern (inhibition during fear acquisition and increased CS elicited spiking during extinction). Although extinction neurons where restricted to the BA, they were intermingled in the BA with fear neurons. Fear and extinction neurons however, displayed different patterns

of afferent/efferent connectivity. Fear neurons received hippocampal input, whereas extinction neurons did not. Conversely, extinction neurons were reciprocally connected with the mPFC, while fear neurons projected to the medial prefrontal cortex (mPFC) but did not receive its afferent input (Herry et al., 2008). Although fear and extinction neurons both target the mPFC, extinction neurons project to the infralimbic (IL) mPFC while fear neurons targeted the prelimbic (PL) mPFC (Senn et al., 2014).

There are currently no known molecular markers for BLA fear neurons. However, a population of extinction neurons has been characterized by their expression of the cell surface protein Thy-1 (Jasnow et al., 2013). Thy-1 expressing PNs are far more numerous than the extinction neurons described by Herry et al. (2008) and project to the NAc (Porrero et al., 2010). This suggests overlap between extinction and reward coding PNs, which also target the NAc. Such overlap fits conceptually with Jerzy Konorski's (1967) concept of opposing motivational systems. In this context, extinction or the absence of fear is equivalent to safety and is thus appetitive, as it shifts behavior away from an aversive motivation toward an appetitive basis (Christianson et al., 2012). This concept also proposes mutual inhibition of fear and reward/extinction neurons, a theory yet to be confirmed, but shared by several prominent amygdala researchers (Janak and Tye, 2015). Such a circuit is appealing given the close proximity of fear and extinction neurons and thus the potential for rapid switches in motivational states. However, as both fear and extinction/reward neurons are glutamatergic, intervening feed-forward GABA interneurons would be required to complete this hypothetical circuit.

Ultimately, the intermingling of PNs coding for opposite emotional valences, provides challenges and opportunities for electrophysiologists who use the *ex-vivo* brain

slice preparation. As of yet, there are no objective morphological or electrophysiological parameters to differentiate fear, reward and extinction PNs in slice. Using the defined projections outlined above, PN valence can be identified by injecting retrograde tracers into appropriate brain regions, prior to slice preparation. Alternatively, transgenic models capitalizing on the selective expression Thy-1 by extinction neurons provide an appealing means of identifying these neurons. However, future studies will hopefully characterize further differences in the expression of other PN phenotypic markers, so as to facilitate functional identification *in vitro*. Such identifying markers have the potential to substantially expedite functional dissection of BLA circuits.

1.4c BLA Interneurons

Although local circuit GABA interneurons account for only a small proportion of the neurons within the BLA (15-20%), they show an imposing diversity of phenotypic markers, electrophysiological properties and morphological characteristics. The output of BLA PNs is disproportionately shaped by substantial inhibition from GABA interneurons. Thus, BLA PNs show strikingly low *in vivo* and *in vitro* firing rates despite extensive intrinsic and extrinsic excitatory innervation (Washburn and Moises, 1992b; Rosenkranz and Grace, 1999; Likhtik et al., 2006).

Different classification schemes have been proposed to contend with the high degree of BLA interneuron heterogeneity; these schemes generally focus on differential expression of Ca^{2+} binding proteins and neuropeptides, often in conjunction with electrophysiological properties. One popular scheme divides BLA interneurons into the following four distinct groups (Kemppainen and Pitkänen, 2000; McDonald and Betette, 2001; McDonald and Mascagni, 2001; 2002; Mascagni and McDonald, 2003).

1) Interneurons expressing the calcium binding protein parvalbumin (PV^+).

2) Interneurons expressing the neuropeptide Somatostatin (SOM^+).

3) Interneurons expressing the neuropeptide cholecystokinin (CCK) along with either the Ca^{2+} binding protein calretinin or vasoactive intestinal peptide (VIP).

4) Interneurons that express CCK but not calretinin or VIP.

Our understanding of the circuit roles subserved by these specific BLA interneuron subtypes is still in its infancy. However, BLA INs appear strikingly similar to better-studied IN types within the hippocampus and neocortex. Recent fate-mapping studies may explain such similarities; suggesting interneurons expressed throughout the telencephalon (including the BLA) can be assigned to one of three broad groups based on a shared lineage. These three groups include, PV^+-expressing interneurons, SOM expressing interneurons and interneurons which express the serotonin 5HT3a receptor (Rudy et al., 2011). Enormous functional diversity appears to be generated from these three canonical groups; for example up to 21 different interneuron types have been described in the well-studied hippocampal CA1 region alone (Somogyi and Klausberger, 2005; Klausberger and Somogyi, 2008; Klausberger, 2009). Despite such diversity common organizing principals appear conserved across brain regions. I will further discuss the PV^+ and SOM^+ interneurons as these groups are of great relevance to my thesis findings.

1.4c(i) PV^+ Interneurons

PV^+ INs, which also commonly express the Ca^{2+} binding protein calbindin (CB), are the single largest group of INs within the BLA (~40%) (McDonald and Mascagni, 2001; Rainnie et al., 2006). PV^+ INs show higher input resistance and fire faster action

potentials (spike half width ~0.5 ms) compared to PNs (Rainnie et al., 2006; Woodruff and Sah, 2007a). The ability to rapidly fire trains of action potential at frequencies >100 Hz has led PV[+] INs to be described as fast spiking (Rainnie et al., 2006).

As in other brain areas, BLA PV[+] INs function largely as basket and chandelier cells which target PNs at their soma/proximal dendrites, or axon initial segments respectively. Such proximal innervation suggests a prominent role in regulating PN output. Furthermore, a single PV[+] IN can target >50 postsynaptic PN allowing for diffuse inhibition. A largely feedback inhibitory function is inferred, as PV[+] INs receive their majority excitatory input (~ 90%) from PN collaterals. However, roles in local feed-forward circuits have also been proposed (Woodruff and Sah, 2007a).

Strong coupling between PV[+] INs, both by synaptic contacts and gap junctions, is thought to facilitate synchronized firing of PV[+] networks, and therefore precise synchronous inhibition of PNs. Thus, PV[+] INs may paradoxically facilitate integration of BLA output by synchronizing PN activity (Woodruff and Sah, 2007b). Furthermore, a depolarizing shift in the Cl^{-} reversal potential at the axon initial segment (Szabadics et al., 2006) may cause subpopulations of PV[+] INs to actually excite PNs. Woodruff et al. (2006) described a population of PV[+] INs capable of exciting postsynaptic PNs to threshold; interestingly, these cells displayed a characteristic hybrid chandelier-basket cell morphology (Woodruff et al., 2006).

Based on firing patterns and differential expression of postsynaptic currents, 2 or 4 distinct PV[+] IN subgroups have been proposed in the BLA (Rainnie et al., 2006; Woodruff and Sah, 2007a). The functional relevance of these subgroupings is supported

by paired PV[+] IN-IN recordings indicating preferential gap junction coupling amongst members of electrophysiology defined subgroups (Woodruff and Sah, 2007a).

Functional data indicates PV[+] INs also target SOM INs. In an important study by Wolff et al. (2014), single unit recording from genetically defined BLA IN populations were performed during *in vivo* fear conditioning. During CS presentation, PV[+] INs were activated which inhibited SOM INs, subsequently disinhibiting PN dendrites (Wolff et al., 2014).

1.4c(ii) SOM interneurons

SOM[+] interneurons account for ~11-18% of BLA interneurons and (like PV[+] INs) many express CB, but they do not express CR (McDonald and Mascagni, 2002; Wolff et al., 2014). Within the BLA, SOM[+] interneurons largely target PNs at smaller caliber (distal) dendrites and dendritic spines, while only sparsely innervating PN somata (Muller et al., 2006b; Wolff et al., 2014). This innervation pattern puts SOM[+] terminals in close proximity to the majority of excitatory glutamatergic PN inputs.

In the hippocampus, GABA events from SOM[+] interneurons show slow kinetics and are of low amplitude (measured from pyramidal neuron soma) suggesting significant dendritic filtering (Maccaferri et al., 2000). Assuming SOM[+] inputs are similarly attenuated in BLA PNs, activity of SOM[+] INs may not substantially impact PN output. However, SOM[+] terminals are ideally situated to dampen integration of excitatory inputs and inhibit LTP. Consistent with this, Wolff et al. (2014) found that optogenetic stimulation of BLA SOM[+] interneurons elicited PN IPSCs which, when appropriately timed, reduced the amplitude and increased the decay of EPSC evoked by stimulation of thalamic afferents (Wolff et al., 2014). Indeed, SOM[+] interneurons have been implicated

in such actions in other cortical circuits. Conversely, PNs express both $GABA_A$ and $GABA_B$ receptors at distal dendrites, while only $GABA_A$ receptors are expressed at more proximal PN domains (Washburn and Moises, 1992b; McDonald et al., 2004). As such, SOM^+ INs may elicit more sustained inhibitory actions by also activating metabotropic $GABA_B$ receptors.

In addition to distally innervating PNs, it appears SOM^+ INs also target other INs. McDonald et al. (2007), found that 5% of BLA SOM^+ synapses target PV^+ INs while, VIP expressing INs are targeted by SOM^+ synapses at a rate of 7.7% (Muller et al., 2006b). Since INs are far less numerous than PNs, these seemingly unimpressive numbers may be of great physiological relevance. Thus, SOM^+ synapses target PV^+ INs at a rate roughly scaled to their relative abundance; while VIP interneurons appear to be preferentially targeted. A given IN-IN input may well be of greater functional relevance than a corresponding IN-PN as INs have higher input resistance and have more depolarized resting potentials than PNs.

The pattern of afferent innervation received by BLA SOM^+ interneurons is unclear, however indirect evidence suggests they may receive cortical inputs and function in feed-forward circuits. A recent study by Unal et al. (2014) found CB expressing neurons received substantial input from the perirhinal and temporal cortices (Unal et al., 2014). In the BLA, both PV^+ and SOM^+ INs express CB however, a previous study suggested PV^+ neurons receive little cortical input. It can thus be inferred that cortical inputs targeted SOM^+, CB INs. However, more direct imaging studies will be required to definitively confirm such circuitry.

Interestingly, a small population of BLA SOM$^+$ neurons appears to be projection neurons. These neurons send long-range projections to the basal forebrain (BF), a major source of cholinergic innervation. These neurons were medium sized (15-20 μM) with three to four primary dendrites and expressed glutamic acid decarboxylase (GAD) suggesting they were GABAergic (McDonald, 2012). However, the functional implications of these GABAergic projection neurons are yet to be determined.

Particularly relevant to this thesis, approximately a third of all BLA SOM$^+$ interneurons co-express NPY, while virtually all NPY expressing neurons are SOM$^+$ positive (McDonald, 1989). These NPY$^+$/SOM$^+$ interneurons appear to be the only intrinsic source of NPY within the BLA, although other extrinsic sources of NPY have been described (Leitermann et al., 2016). It is unclear under what physiological conditions NPY is released from local INs, although presumably high neuronal activity is required. Virtually all NPY-expressing INs in the BLA co-express the NK1-type substance P receptor. NK1 expression appears restricted to NPY/SOM INs as it is not expressed with PV$^+$ or CR, which demarcate two large BLA IN populations. As such, substance P conjugated to the saporin toxin, has emerged as a relatively specific way to selectively ablate BLA NPY INs (Levita et al., 2003).

1.4c(iii) Neurogliaform Cells

NPY co-expression specifies an interesting subpopulation of SOM$^+$ INs termed neurogliaform cells (NGC). In the hippocampus and neocortex, NGCs rarely form distinct postsynaptic contacts. Rather, these IN's release GABA into the extra-synaptic space in a paracrine-like manner (Scanziani, 2000). NGCs exhibit dense local axonal clouds from which a single IN is speculated to release GABA equivalent to that of six

basket cells (Oláh et al., 2009). Such properties are ideal for recruiting $GABA_B$ receptors which pyramidal neuron express mainly at dendritic extra-synaptic sites. Indeed, most INs require synchronous activity, or multiple action potentials, to achieve synaptic GABA spill over, sufficient to recruit $GABA_B$ receptors (Scanziani, 2000). In comparison a single NGC action potential can substantially activate pyramidal neuron $GABA_B$ receptors (Oláh et al., 2009).

Histological studies have indicated that the BLA contains NGC-like INs (McDonald, 1984), while, Manko et al. (2012) found that many NPY expressing INs in mice show NGC-like electrophysiological properties (Mańko et al., 2012). These cells displayed lower input resistance (compared to other NPY/SOM^+ INs), showed significant firing rate spike frequency adaptation and fired broad action potentials. Paired PN-NGC recordings revealed NGC action potentials elicited slow $GABA_A$ mediated, inhibitory post synaptic currents (IPSC)s in PNs, which substantially recruited extra-synaptic receptors. The authors suggested that these slow NGC IPSCs did not involve $GABA_B$ receptors (unlike in other cortical circuits) (Mańko et al., 2012).

1.5 RELEVANT RECEPTORS CHANNELS AND CURRENTS IN BLA PRINCIPAL NEURONS

The bulk of the experimental work outlined in this thesis focuses on electrophysiological recordings from BLA PNs. I will therefore describe the electrical properties of BLA PNs specifically with reference to several important membrane ionic currents, their underlying ion channels and (where appropriate) regulating receptor systems.

1.5a GABA$_A$

As mentioned above, the low *in vitro* and *in vivo* excitability of BLA PNs appears to result largely from the high degree of resting GABA inhibition these neurons receive. As with most other cortical regions, ionotropic GABA$_A$ receptors are expressed in BLA PNs across all somatic-dendritic domains, and thus likely mediate a great deal of this GABA inhibition. GABA$_A$ receptors conduct Cl$^-$ ions when activated by GABA. In the adult CNS, these GABA$_A$ Cl$^-$ currents are largely inhibitory and reverse at ~ -70 mV. As, mature BLA PNs have relatively hyperpolarized resting membrane potentials, GABA$_A$ currents likely do not substantially hyperpolarize these neurons. However, GABA$_A$ receptor activation can also inhibit neurons by reducing their input resistance, thereby shunting other membrane currents, including those from excitatory synaptic inputs. Furthermore, as long as GABA$_A$ Cl$^-$ currents reverse at a potential substantially negative to action potential threshold, shunting predominates and GABA is inhibitory even if it is depolarizing at the neurons RMP. This is so since, once such a neuron is depolarized past the Cl$^-$ reversal potential, subsequent GABA$_A$ receptor activation will hyperpolarize the neuron away from the threshold (Fishell and Rudy, 2011).

GABA$_A$ channels are from the Cys loop family of ligand-gated channels (Miller and Smart, 2010), which also encompasses the nicotinic acetylcholine receptors (Corringer et al., 2000), serotonin 5HT$_3$ receptors (Thompson and Lummis, 2006) and the glycine receptor channels (Breitinger and Becker, 2002). GABA$_A$ receptors are pentomers formed from five of 19 potential subunit isoforms; six α subunits, three β subunits, three γ subunits, three ρ subunits and single ε, δ, θ and π subunits. Most GABA$_A$ receptors are composed of two α subunits, which alternate with two β subunits and a single γ subunit. The predominant GABA$_A$ receptor type in the CNS is thought to be the α$_1$/β$_2$/γ$_2$ receptor (Sigel and Steinmann, 2012). Each of the five subunits contributes to the channel pore, which is located at the center of the channel assembly. GABA binds to a site located at the interface between the α/β subunits, each GABA$_A$ receptor thus contains two GABA binding sites. Benzodiazepines, which exert their anxiolytic actions within the BLA, bind to a site located at the α/γ interface and are not intrinsic GABA$_A$ receptor agonists. Instead, benzodiazepines increase the channel open time when the channel has bound GABA at the agonist site (dramatically increasing macroscopic currents) (Sigel, 2002). Numerous other endogenous and exogenous compounds modulate GABA$_A$ receptors function, including neurosteroids, barbiturates, and ethanol (Lan and Gee, 1994; Wallner et al., 2003; Löscher and Rogawski, 2012). Picrotoxin, which directly blocks GABA$_A$ (and ionotropic glycine) receptor channels, and the competitive GABA antagonist bicuculline, are useful experimental tools for blocking GABA$_A$ currents.

In neuronal circuits GABA$_A$ receptors can mediate phasic, tonic or both types of inhibition. Phasic inhibition results from synaptic release of GABA, which acts on

GABA$_A$ receptors located at the postsynaptic specialization. Phasic inhibition is transient both because synaptic receptors desensitize and because GABA is rapidly removed from the synaptic cleft. Tonic GABA$_A$ inhibition, on the other hand, results when low ambient levels of GABA activate the higher affinity, extra-synaptic GABA$_A$ receptors. GABA reaches these extra-synaptic receptors when high synaptic levels overwhelm reuptake transporters, causing GABA to spill over into extra-synaptic spaces. Special interneuron types such as neurogliaform or Ivy cells also appear to release GABA directly to extra-synaptic sites.

BLA PNs receive both tonic and phasic GABA$_A$ inhibition **(Figure 4)**. In the BLA, phasic GABA$_A$ inhibition is mediated largely by α_2 subunit-containing receptors (Marowsky et al., 2004), which are also implicated in the anxiolytic but not sedating effects of benzodiazepines (Löw et al., 2000). Most extra-synaptic GABA$_A$ membrane current in the CNS is carried either by receptors that express the δ subunit (in place of γ), or by $\alpha5$ subunit-expressing receptors (Whissell et al., 2015). However, the BLA shows only modest expression of these GABA$_A$ receptor types (Pirker et al., 2000; Marowsky et al., 2012). It appears $\alpha3$-expressing receptors mediate much of the extra-synaptic GABA$_A$ mediated inhibition in the BA, although these receptors are less important in the LA (Marowsky et al., 2012).

1.5b GABA$_B$

Like the NPY receptors, GABA$_B$ receptors are pertussis toxin-sensitive $G_{i/o}$ GPCRs, which can couple to multiple downstream effectors. These metabotropic receptors are expressed by virtually all neurons and glial cells in the CNS (Gassmann and Bettler, 2012) and generally mediate more sustained GABA actions.

The GABA$_B$ receptors are type C, GPCRs characterized by a large, ligand-binding, extracellular Venus flytrap domain (VFTD). Functional receptors are obligate heterodimers of GABA$_{B1}$ and GABA$_{B2}$ subunits. Two GABA$_{B1}$ isoforms (GABA$_{B1a}$ and GABA$_{B1b}$) are known, while only one GABA$_{B2}$ subunit has been identified. Multiple allosteric GABA$_{B1}$-GABA$_{B2}$ interactions are necessary to couple GABA binding to G-protein activation. GABA appears to bind at the GABA$_{B1}$ subunit while GABA$_{B2}$ mediates G-protein activation (Marshall et al., 1999).

GABA$_B$ receptors modulate neuronal functions via multiple mechanisms and can be expressed at both presynaptic terminals and in postsynaptic compartments. Actions of GABA$_B$ receptors thus depend both on their local signaling environment and the cellular domain where they are expressed. Like other G$_{i/o}$ GPCRs, GABA$_B$ activation reduces cAMP levels via adenylyl cyclase inhibition. Furthermore, ion channels can be directly modulated by membrane-deliminated G-βγ subunit interactions, as is the case for G-protein coupled inward rectifying K$^+$ (GIRK) channels (Bettler et al., 2004).

Presynaptic GABA$_B$ receptors are expressed on both GABA (auto-receptor) and glutamate (hetero-receptor) terminals. In both cases, activation of these receptors reduces neurotransmitter release. As such, activation of presynaptic GABA$_B$ receptors can have complex effects on network activity. Activity-dependent neurotransmitter release is inhibited by direct G-βγ mediated inhibition of voltage-gated calcium channels, while both G-βγ and G-α$_{i/o}$ can also directly inhibit vesicular release, reducing miniature synaptic transmission (Bettler et al., 2004).

Postsynaptic GABA$_B$ receptors prototypically inhibit neurons via direct G-βγ mediated activation of GIRK channels. This increased K$^+$ conductance hyperpolarizes

membranes and shunts excitatory inputs. $GABA_B$ receptors have also been shown to activate two-pore domain TREK2 K^+ channels in the entorhinal cortex via inhibition of protein kinase A (Deng et al., 2009). In addition to activating K^+ channels, $GABA_B$ receptors directly inhibit voltage-gated Ca^{2+} channels also via G-βγ channel interactions (Chalifoux and Carter, 2011).

1.5b(i) Regulation of Dendritic Excitability by $GABA_B$ Receptors

Postsynaptic $GABA_B$ receptors are largely expressed in dendritic spines and shafts (Vigot et al., 2006). $GABA_{B1b}$ containing receptors are selectively expressed at dendritic spines where they closely associate with, and couple to GIRK channels (Kulik et al., 2006). Dendritic shafts express both $GABA_{B1b}$ and $GABA_{B1a}$ containing channels and couple to VGCC in addition to GIRKs (Pérez-Garci et al., 2013).

Postsynaptic $GABA_B$ receptors decrease dendritic Ca^{2+} influx via several mechanisms. Activated GIRK currents decrease dendritic Ca^{2+} spikes by inhibiting the back propagation of somatic action potentials (Leung and Peloquin, 2006). Furthermore, dendritic Ca^{2+} spikes are also damped by direct $GABA_B$-mediated inhibition of VGCCs (Chalifoux and Carter, 2011; Pérez-Garci et al., 2013). $GABA_B$-GIRK currents in dendritic spines facilitate the Mg^{2+} block of NMDA receptors by hyperpolarizing the postsynaptic membrane and thus reducing glutamate-mediated Ca^{2+} currents (Vigot et al., 2006). It has also recently been shown that $GABA_B$ receptors directly inhibit NMDA receptors via a PKA dependent mechanism (Chalifoux and Carter, 2010). Therefore, pyramidal cell $GABA_B$ receptor activation typically damps Ca^{2+}-dependent plasticity (Vigot et al., 2006).

1.5c G-Protein Coupled Inward Rectifying K$^+$ (GIRK) Channels

GIRK channels are members of the inward rectifying K$^+$ channel (Kir) family, which as their name implies, conduct K$^+$ more effectively in the intracellular direction. Inward K$^+$ currents are only seen under artificial conditions, as neurons are almost never physiologically hyperpolarized past the K$^+$ reversal potential. However, this inward rectification means Kir channels conduct outward K$^+$ currents more effectively at hyperpolarized membrane potentials. Conversely, currents through these channels become progressively less than that predicated by Ohms law, with membrane depolarization, and are negligible at highly depolarized potentials. Inward rectification results from the voltage-dependent block of channels by intracellular Mg^{2+} and polyamines (Yamada et al., 1998).

Functional Kir channels are tetramers formed from subunits containing only two trans-membrane domains. Thus Kir channels are simpler than most voltage gated K$^+$ channels and lack a true voltage-sensing domain. All Kir channels are blocked by extracellular Cs$^+$ and Ba^{2+} and require the membrane phospholipid, phoshatidylinosatol 4,5-bisphoshate (PIP2), for channel opening (Zhang et al., 1999). GIRK channels are activated by G$_{i/o}$ type GPCRs (including the GABA$_B$ and NPY receptors) via direct Gβγ-channel interaction (Huang et al., 1995; 1998). Four GIRK channel subunits (Kir3.1-3.4) have been identified, however Kir3.4 are not highly expressed in the brain (Wickman et al., 2000). The subunit composition of BLA GIRK channels is unknown; however heteromeric Kir3.1-Kir3.2 channels appear to be the predominant CNS GIRK channel type. SOM and NPY activate GIRK currents in the LA while GABA$_B$ mediated GIRK

currents have been documented in the BLA (Washburn and Moises, 1992b; Meis et al., 2005; Sosulina et al., 2008).

1.5d The H-current

The H-current (I_h) is a voltage-dependent, mixed cation conductance, carried by hyperpolarization-activated, cyclic nucleotide gated (HCN) channels. While HCN channels are related to voltage-gated K^+ channels, they are poorly K^+ selective, with K^+/Na^+ conductance ratios from 3:1 to 5:1. Thus (at RMP), I_h is depolarizing, as the driving force for Na^+ to enter neurons far exceeds the electro-chemical gradient driving K^+ out of the cell (ER= -20 mV to -40 mV) (Robinson and Siegelbaum, 2003). However, unlike virtually all other voltage-gated channels, I_h is activated by membrane hyperpolarization. Thus, when tonically active at RMP, I_h functions like a physiological voltage-clamp to limit hyperpolarization. These properties also lend I_h to involvement in membrane potential oscillations (Ehrlich et al., 2012) and pacemaker functions (Pape, 1996).

Four HCN channel subunits (HCN1-4) have been described; all are modulated by cyclic adenosine monophosphate (cAMP). Cyclic nucleotides shift the voltage activation of I_h to more depolarized potentials, allowing equivalent channel opening at more depolarized potentials. This property allows for potential modulation of I_h by signaling systems acting on cAMP. HCN4-type channels show the highest sensitivity, and HCN1 the least, to cyclic nucleotides. Differences in activation kinetics are also observed between channel types, with HCN1 showing the most rapid kinetics, and HCN4 the slowest. Similarly, HCN1 channels are activated at more depolarized membrane potentials while HCN4 channels activation requires the greatest hyperpolarization.

Most BLA PNs show a prominent I_h, with an appreciable component of this conductance active at the resting membrane potential. This tonic I_h causes PNs to rest more depolarized membrane potentials and decreases their input resistance and membrane time constant. Tonic I_h can thus have complex effects on neuronal excitability, causing neurons to rest closer to threshold (an excitatory effect) but also decreasing neuronal input resistance (an inhibitory effect). Pyramidal neurons in hippocampal CA1 and layer 5 of the neo-cortex show I_h channel gradients, with channel density lowest at the soma and highest at distal dendrites. In these neurons, dendritic I_h appears to be largely inhibitory, as it both attenuates excitatory inputs and decreases their summation (Magee, 1998; Anon, 2004). It is not clear if BLA PNs show a similar HCN channel distribution, however application of the nonselective I_h blocker ZD7288 excites BLA principal neurons and facilitates summation of evoked excitatory inputs (Park et al., 2007). Conversely, our lab has previously shown that NPY, via actions on Y_1 receptors, decreases I_h while also hyperpolarizing PNs and reducing their excitability (Giesbrecht et al., 2010). These results suggest that at least some of the I_h expressed by BLA PNs contributes to an increased basal excitability. All four HCN subunits are expressed in the BLA. However, PN I_h is not strongly modulated by the cell-permeable cAMP analogue db-cAMP nor does this compound block NPYs effects on I_h. These data suggest PNs predominantly express, the kinetically-rapid, relatively cAMP insensitive HCN1 channels. Additionally, immunohistochemical staining further suggests that PNs primarily express HCN1 protein (Giesbrecht et al., 2010).

1.6 RATIONALE AND GENERAL HYPOTHESIS

Behavioral data suggests that selective activation of the NPY Y_2 receptor in the rodent BLA increases anxiety-like behaviors (Sajdyk et al., 2002b), an action diametrically opposite to that of the (potently anxiolytic) full agonist NPY (Sajdyk et al., 1999b). When NPY is administered into the BLA (or released physiologically) it must activate all locally-expressed receptors, which in the BLA includes Y_1, Y_2 and Y_5 receptors. NPY is unambiguously anxiolytic in BLA. However the role that Y_2 receptor activation play in these anxiolytic effects is unclear. It remains to be determined whether BLA Y_2 receptors interact with Y_1 and Y_5 receptors in a manner that contributes to the overall anxiolytic effects of NPY, or whether they in fact mitigate the anxiolytic effects of the Y_1 and Y_5 receptors. The specific aims of this thesis were thus, as follows:

1) To explore the effects of selective NPY Y_2 receptor activation on the excitability and integrative properties of BLA PNs. Specifically, we sought to determine whether postsynaptic Y_2 receptors directly alter PN excitability, or whether synaptic inputs targeting PNs are modulated by presynaptic Y_2 receptors. This was undertaken in an attempt to identify potential cellular and circuit mechanisms via which selective Y_2 receptor activation elicits previously described anxiogenic behavioral effects.

2) To determine whether activation of BLA Y_2 receptors contributes to the overall anxiolytic effects of NPY when activated in concert with other BLA NPY receptor types (Y_1 and Y_5), and if such interactions do occur, to determine the mechanisms governing these effects.

1.6b General hypothesis

NPY Y_2 receptors are typically expressed on presynaptic terminals where they decrease neurotransmitter release (Colmers and Bleakman, 1994; Greber et al., 1994; Chen et al., 1997). Anxiety in turn, is elicited when BLA excitability is enhanced pharmacologically. Since selective Y_2 receptor activation is anxiogenic, such actions in the BLA should ultimately increase the activity of PNs coding for anxiety.

We therefore, hypothesized that Y_2 receptors are expressed on a population of local GABA interneurons. We propose that these interneurons normally gate anxiogenic BLA output by exerting a strong inhibitory GABA tone upon PNs. Activation of interneuron Y_2 receptors, which are likely on presynaptic terminals, reduces this tonic GABA, and disinhibits PNs. Once disinhibited, the anxiogenic output of BLA is increased, resulting in behavioral anxiety (Figure 5).

At the onset of this thesis work, it was not readily apparent how the actions of Y_2 receptors might interact with those of other NPY receptors within the BLA, or how such interactions might facilitate the overall (anxiolytic) effects of NPY. However, further insight was provided by initial experiments, which suggested that Y_2 receptor activation in the BLA increased Ca^{2+} entry, likely into PN dendrites. Since the long-term "stress resilient" effects of NPY require calcineurin (a Ca^{2+}-dependent phosphatase) this finding may link excitatory actions of the Y_2 receptor to calcineurin recruitment, and NPYs overall anxiolytic effects (Sajdyk et al., 2008). Calcineurin, expressed in BLA PNs, has also been implicated in the extinction of conditioned fear (Lin et al., 2003). However, no mechanism has been proposed to explain recruitment of calcineurin by NPY. Furthermore, all previously documented actions of NPY on BLA PNs are inhibitory, and

are thus inconsistent with influx of Ca^{2+} calcium into dendrites and calcineurin recruitment.

High dendritic $[Ca^{2+}]_i$ levels favor recruitment of the low Ca^{2+} affinity, Ca^{2+}-dependent kinase, CaMKII, whose actions oppose those of calcineurin. Activity of calcineurin, in turn, predominates at lower dendritic Ca^{2+} levels. It is thus possible that the inhibitory actions of NPY could reduce high basal dendritic Ca^{2+} levels, shifting CaMKII activity towards calcineurin. However, basal activation of CaMKII is unlikely, given that PNs are dominated by inhibitory signaling. Alternatively, NPY may simply up-regulate calcineurin expression, unrelated to electrical activity. However, disinhibition of principal neurons via Y_2 receptors provides the more parsimonious explanation. Sajdyk et al. (2008) proposed that the long-term anxiolytic effects of NPY are mediated by an LTD-like mechanism (Sajdyk et al., 2008).

I therefore hypothesize that NPY-mediated plasticity cannot occur in the BLA under basal conditions due to a high state of GABA-mediated PN inhibition. Activation of BLA Y_2 receptors removes this tonic GABA-mediated inhibition and places PNs in a state permissive to learning. Because selective Y_2 receptor activation disinhibits PNs, we propose that this action increases anxiogenic PN output. This increased PN activity accounts for the anxiogenic behavioral effects of selective Y_2 receptor activation.

Furthermore, I hypothesize that the inhibitory actions of other BLA NPY receptor types (Y_1 and Y_5), moderates the excitatory effects of selective Y_2 receptor activation. These effects decrease anxiogenic BLA output and in conjunction with Y_2

receptor-mediated dendritic disinhibition favor moderate dendritic Ca^{2+} levels. Thus, these actions ensure recruitment of calcineurin-mediated plasticity.

1.7 FIGURES

Figure 1: The Amygdala

Figure 1: The Amygdala
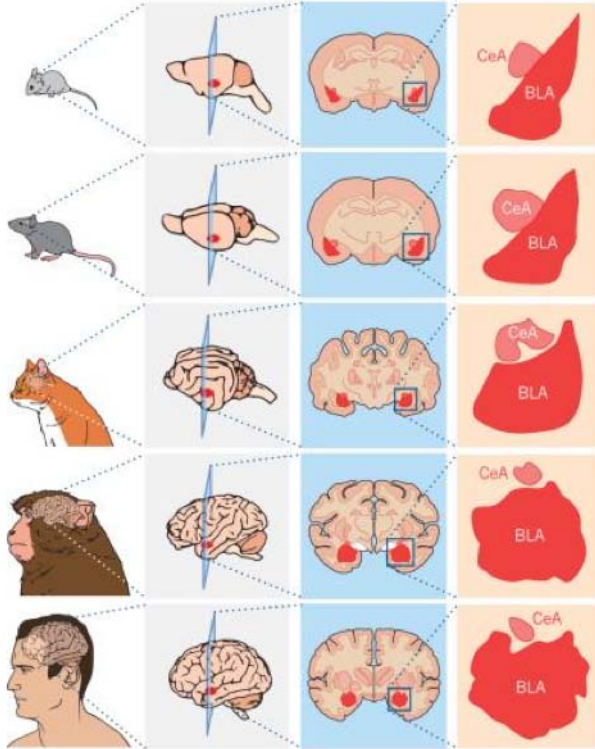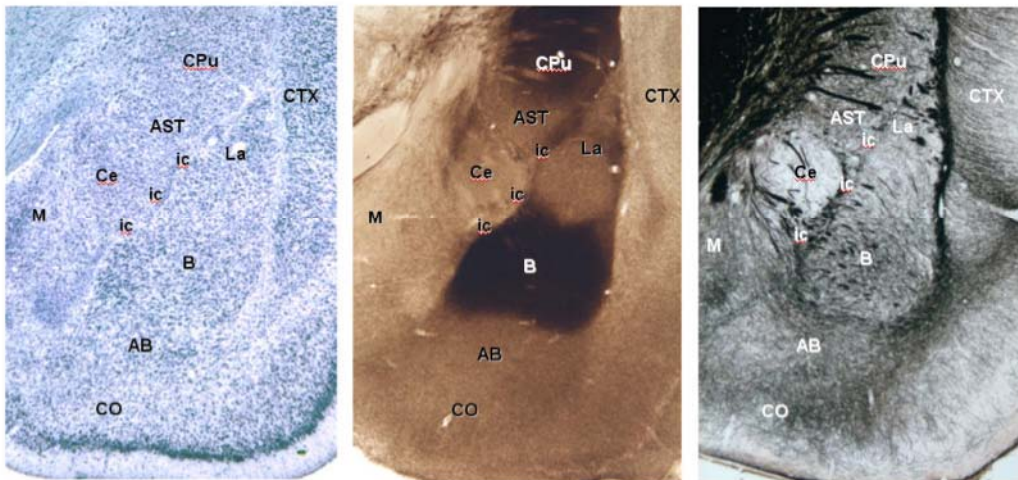
(A) Schematic showing the relative brain position of the amygdala in several mammals including: the mouse, rat, cat, non-human primates and man. Note that the BLA is increased in size relative to the CeM in higher mammals. Figure adapted from Janak et al. (2015) (Janak and Tye, 2015)

(B) Amygdala containing rat brain slices differentially stained as follows: Nissl stained for cell bodies (*left*), stained for acetylcholinesterase (*middle*) and silver fiber stained (*right*). Amygdala Abbreviations: La, lateral amygdala nucleus; B, basal amygdala nucleus; AB, basal medial (accessory) amygdala; Ce, central amygdala; ic, intercalated cell mass; M, medial amygdala; CO, cortical nuclei. Non-Amygdala Abbreviations: AST, amygdala striataltransition area; CTX, cortex; CPu, caudate putamen. Figure adapted from Ledoux et al. (2008) Scholarpedia.

Figure 2: Amygdala Circuits
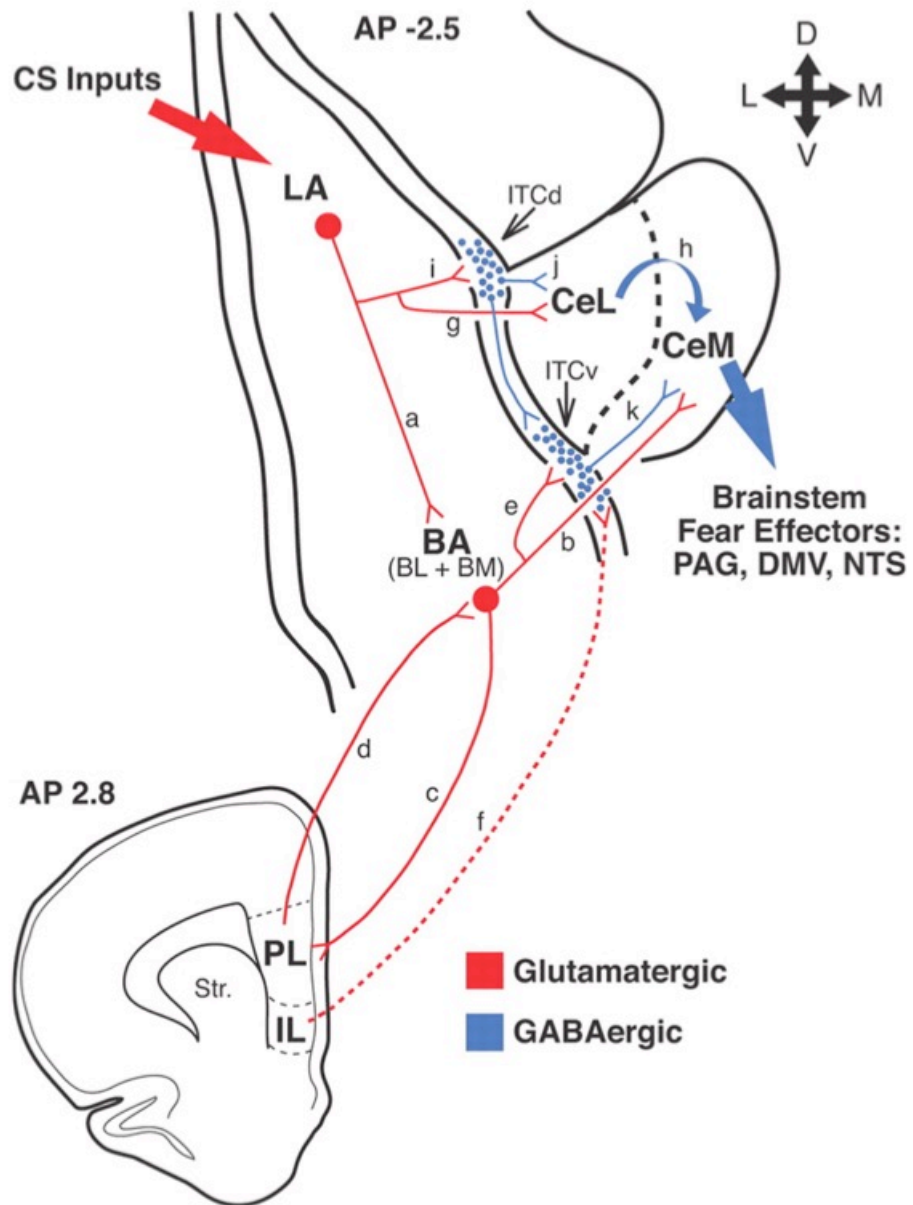
Figure 2: Amygdala Circuits

Information flow into and out of the amygdala: sensory inputs target the lateral amygdala (LA), which projects to the lateral central amygdala (CeL), the basal amygdala nuclei (BA) and the intercalated masses (ITC). The medial central amygdala (CeM) is the major output for fear signals. The CeM receives excitatory input from the BA and inhibitory input from the CeL. BA output is modulated by excitatory projections from the prelimbic (PL) and infralimbic (IL) medial prefrontal cortex areas. Figure adapted from Amano et al. (2011) (Amano et al., 2011).

Figure 3: BLA Principal Neurons

A
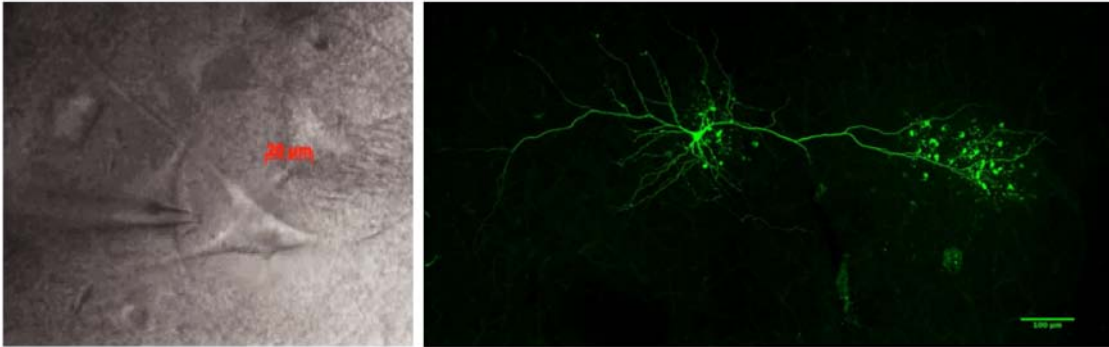
B
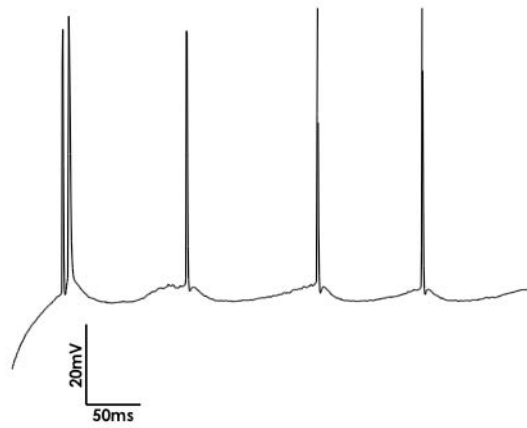
C
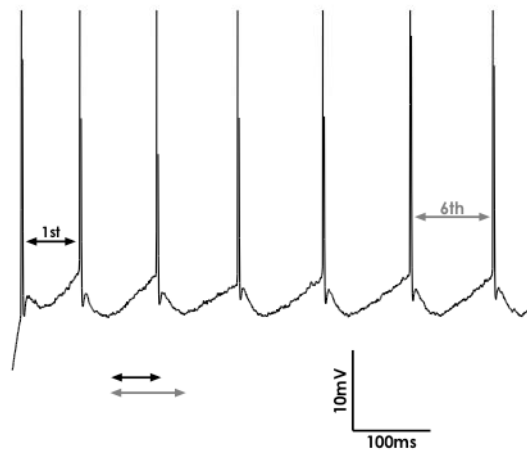
Figure 3: BLA Principal Neurons

(A) Differential interference contrast (DIC) image of a representative BLA PN under 60x magnification (*right*). Representative merged confocal Z-stack from a BLA containing brain slice. A representative fluorescent PN (green), loaded with neurobiotin via a patch pipette, is labeled with streptavidin ALEXA-488 (*left*).

(B) PN action potential trains elicited with a 800 ms depolarizing current step (250 pA). This PN shows a first action potential doublet spike burst, which is a common feature of many PNs.

(C) Action potential trains similarly evoked with a 800 ms depolarizing current step. This PN does not show a doublet burst but shows pronounced spike frequency adaptation of the action potential firing rate seen as an almost doubling of the 6th action potential inter-spike interval compared to the first.

Figure 4: Tonic vs. Phasic GABA$_A$
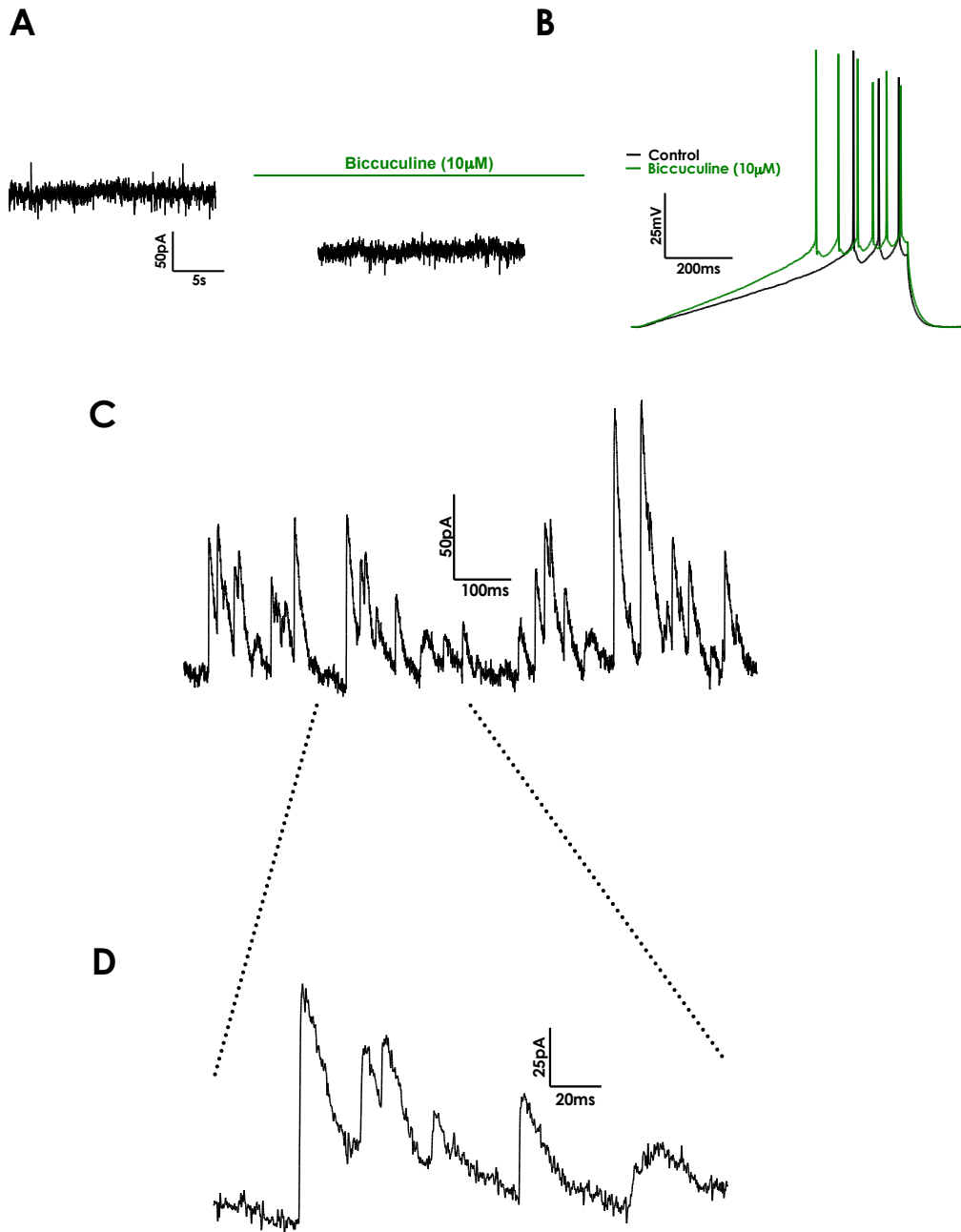
Figure 4: Tonic vs. Phasic GABA$_A$

(A) Voltage clamp recording from a BA PN held at -55 mV under control conditions and in the presence of biccuculine (10 μM). This PN shows substantial tonic GABA$_A$ inhibition, seen as a nearly 100 pA decrease in holding current in the presence of the GABA$_A$ antagonist.

(B) Current clamp ramps (at RMP) from the same PN under control conditions and in the presence of biccuculine (10 μM). PNs were excited by biccuculine, as less depolarizing current was needed to evoke PN action potentials in the presence of biccuculine (10 μM) indicating the inhibitory role of tonic GABA$_A$ currents.

(C and D) GABA$_A$ spontaneous inhibitory post synaptic currents (IPSCs) measured recorded from a representative BA PN in voltage clamp with intracellular Cs$^+$ at -14 mV. In contrast to tonic currents these IPSC are discrete currents mediated by synaptic receptors.

Figure 5: Hypothesis Summary
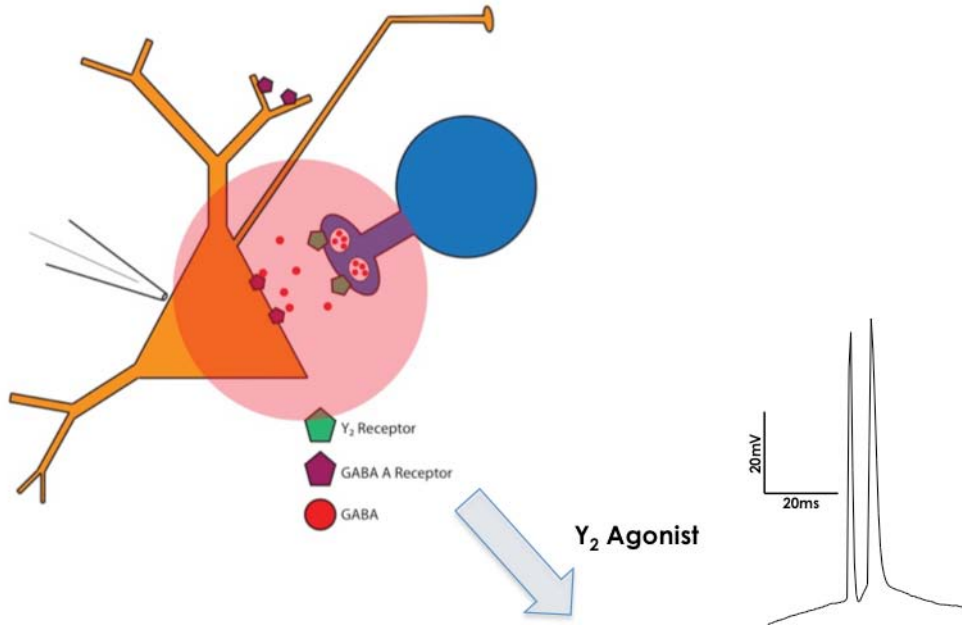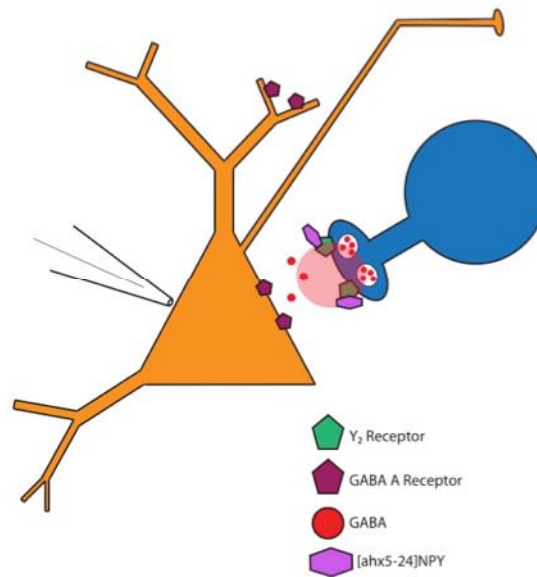
Figure 5: Hypothesis Summary

(A) Under basal conditions PNs are inhibited by GABAergic INs which express presynaptic NPY Y_2 receptors. Tonic GABA-mediated inhibition via these Y_2 expressing interneurons silences PNs.

(B) Activation of interneuron Y_2 receptors reduces GABA-mediated inhibition of PNs and increases their activity and anxiogenic output.

1.8 REFERENCES

Adamec R, Shallow T (2000) Effects of baseline anxiety on response to kindling of the right medial amygdala. Physiol Behav 70:67–80.

Adamec R, Shallow T, Burton P (2005) Anxiolytic and anxiogenic effects of kindling--role of baseline anxiety and anatomical location of the kindling electrode in response to kindling of the right and left basolateral amygdala. Behav Brain Res 159:73–88.

Adolphs R, Tranel D, Damasio H, Damasio AR (1995) Fear and the human amygdala. Journal of Neuroscience 15:5879–5891.

Adrian TE, Allen JM, Bloom SR, Ghatei MA, Rossor MN, Roberts GW, Crow TJ, Tatemoto K, Polak JM (1983) Neuropeptide Y distribution in human brain. Nature 306:584–586.

Amano T, Duvarci S, Popa D, Paré D (2011) The fear circuit revisited: contributions of the basal amygdala nuclei to conditioned fear. J Neurosci 31:15481–15489.

Amano T, Unal CT, Paré D (2010) Synaptic correlates of fear extinction in the amygdala. Nat Neurosci 13:489–494.

Ameringen MV, Simpson W, Patterson B, Turna J (2015) Internet screening for anxiety disorders: Treatment-seeking outcomes in a three-month follow-up study. Psychiatry Res 230:689–694.

Anglada-Figueroa D, Quirk GJ (2005) Lesions of the basal amygdala block expression of conditioned fear but not extinction. J Neurosci 25:9680–9685.

Anon (2004) Contribution of Ih and GABAB to Synaptically Induced Afterhyperpolarizations in CA1: A Brake on the NMDA Response. 92:2027–2039 Available at: http://jn.physiology.org/cgi/doi/10.1152/jn.00427.2004.

Baas JMP, van Ooijen L, Goudriaan A, Kenemans JL (2008) Failure to condition to a cue is associated with sustained contextual fear. Acta Psychol (Amst) 127:581–592.

Bacchi F, Mathé AA, Jiménez P, Stasi L, Arban R, Gerrard P, Caberlotto L (2006) Anxiolytic-like effect of the selective neuropeptide Y Y2 receptor antagonist BIIE0246 in the elevated plus-maze. Peptides 27:3202–3207.

Bard JA, Walker MW, Branchek TA, Weinshank RL (1995) Cloning and functional expression of a human Y4 subtype receptor for pancreatic polypeptide, neuropeptide Y, and peptide YY. J Biol Chem 270:26762–26765.

Barlow DH (2000) Unraveling the mysteries of anxiety and its disorders from the perspective of emotion theory. Am Psychol 55:1247–1263.

Baumgärtel K, Mansuy IM (2012) Neural functions of calcineurin in synaptic plasticity

and memory. Learn Mem 19:375–384.

Berglund MM, Schober DA, Statnick MA, McDonald PH, Gehlert DR (2003) The use of bioluminescence resonance energy transfer 2 to study neuropeptide Y receptor agonist-induced beta-arrestin 2 interaction. J Pharmacol Exp Ther 306:147–156.

Bertoglio LJ, Carobrez AP (2000) Previous maze experience required to increase open arms avoidance in rats submitted to the elevated plus-maze model of anxiety. Behav Brain Res 108:197–203.

Bertoglio LJ, Carobrez AP (2002) Behavioral profile of rats submitted to session 1-session 2 in the elevated plus-maze during diurnal/nocturnal phases and under different illumination conditions. Behav Brain Res 132:135–143.

Bettler B, Kaupmann K, Mosbacher J, Gassmann M (2004) Molecular structure and physiological functions of GABA(B) receptors. Physiological Reviews 84:835–867.

Blair HT, Schafe GE, Bauer EP, Rodrigues SM, LeDoux JE (2001) Synaptic plasticity in the lateral amygdala: a cellular hypothesis of fear conditioning. Learn Mem 8:229–242.

Blanchard DC, Blanchard RJ (1972) Innate and conditioned reactions to threat in rats with amygdaloid lesions. J Comp Physiol Psychol 81:281–290.

Bowers ME, Ressler KJ (2015) Interaction between the cholecystokinin and endogenous cannabinoid systems in cued fear expression and extinction retention. Neuropsychopharmacology 40:688–700.

Böhme I, Stichel J, Walther C, Mörl K, Beck-Sickinger AG (2008) Agonist induced receptor internalization of neuropeptide Y receptor subtypes depends on third intracellular loop and C-terminus. Cell Signal 20:1740–1749.

Breitinger H-G, Becker C-M (2002) The inhibitory glycine receptor-simple views of a complicated channel. Chembiochem 3:1042–1052.

Broqua P, Wettstein JG, Rocher MN, Gauthier-Martin B, Junien JL (1995) Behavioral effects of neuropeptide Y receptor agonists in the elevated plus-maze and fear-potentiated startle procedures. Behav Pharmacol 6:215–222.

BROWN JS, KALISH HI, FARBER IE (1951) Conditioned fear as revealed by magnitude of startle response to an auditory stimulus. J Exp Psychol 41:317–328.

Cabrele C, Beck-Sickinger AG (2000) Molecular characterization of the ligand-receptor interaction of the neuropeptide Y family. J Pept Sci 6:97–122.

Cabrele C, Wieland HA, Koglin N, Stidsen C, Beck-Sickinger AG (2002) Ala31-Aib32: identification of the key motif for high affinity and selectivity of neuropeptide Y at the Y5-receptor. Biochemistry 41:8043–8049.

Cain CK, Blouin AM, Barad M (2002) L-type voltage-gated calcium channels are required for extinction, but not for acquisition or expression, of conditional fear in mice. J Neurosci 22:9113–9121.

Campeau S, Davis M (1995) Involvement of the central nucleus and basolateral complex of the amygdala in fear conditioning measured with fear-potentiated startle in rats trained concurrently with auditory and visual conditioned stimuli. Journal of Neuroscience 15:2301–2311.

Chalifoux JR, Carter AG (2010) GABAB receptors modulate NMDA receptor calcium signals in dendritic spines. 66:101–113.

Chalifoux JR, Carter AG (2011) GABAB receptor modulation of voltage-sensitive calcium channels in spines and dendrites. J Neurosci 31:4221–4232.

Chee MJS, Colmers WF (2008) Y eat? Nutrition 24:869–877.

Cheeta S, Tucci S, Sandhu J, Williams AR, Rupniak NM, File SE (2001) Anxiolytic actions of the substance P (NK1) receptor antagonist L-760735 and the 5-HT1A agonist 8-OH-DPAT in the social interaction test in gerbils. Brain Research 915:170–175.

Chen X, DiMaggio DA, Han SP, Westfall TC (1997) Autoreceptor-induced inhibition of neuropeptide Y release from PC-12 cells is mediated by Y2 receptors. Am J Physiol 273:H1737–H1744.

Christianson JP, Fernando ABP, Kazama AM, Jovanovic T, Ostroff LE, Sangha S (2012) Inhibition of fear by learned safety signals: a mini-symposium review. J Neurosci 32:14118–14124.

Chu H-Y, Ito W, Li J, Morozov A (2012) Target-specific suppression of GABA release from parvalbumin interneurons in the basolateral amygdala by dopamine. J Neurosci 32:14815–14820.

Ciocchi S, Herry C, Grenier F, Wolff SBE, Letzkus JJ, Vlachos I, Ehrlich I, Sprengel R, Deisseroth K, Stadler MB, Müller C, LUthi A (2010) Encoding of conditioned fear in central amygdala inhibitory circuits. Nature 468:277–282.

Clinard CT, Bader LR, Sullivan MA, Cooper MA (2015) Activation of 5-HT2a receptors in the basolateral amygdala promotes defeat-induced anxiety and the acquisition of conditioned defeat in Syrian hamsters. Neuropharmacology 90:102–112.

Colmers WF, Bleakman D (1994) Effects of neuropeptide Y on the electrical properties of neurons. Trends Neurosci 17:373–379.

Corringer PJ, Le Novère N, Changeux JP (2000) Nicotinic receptors at the amino acid level. Annu Rev Pharmacol Toxicol 40:431–458.

Davis M (1997) Neurobiology of fear responses: the role of the amygdala. J Neuropsychiatry Clin Neurosci 9:382–402.

Davis M, Schlesinger LS, Sorenson CA (1989) Temporal specificity of fear conditioning: effects of different conditioned stimulus-unconditioned stimulus intervals on the fear-potentiated startle effect. J Exp Psychol Anim Behav Process 15:295–310.

Davis M, Walker DL, Miles L, Grillon C (2010) Phasic vs sustained fear in rats and humans: role of the extended amygdala in fear vs anxiety. Neuropsychopharmacology 35:105–135.

de Angelis L, File SE (1979) Acute and chronic effects of three benzodiazepines in the social interaction anxiety test in mice. Psychopharmacology (Berl) 64:127–129.

de Jongh R, Groenink L, van Der Gugten J, Olivier B (2002) The light-enhanced startle paradigm as a putative animal model for anxiety: effects of chlordiazepoxide, flesinoxan and fluvoxamine. Psychopharmacology (Berl) 159:176–180.

DeBock F, Kurz J, Azad SC, Parsons CG, Hapfelmeier G, Zieglgansberger W, Rammes G (2003) alpha2-Adrenoreceptor activation inhibits LTP and LTD in the basolateral amygdala: involvement of Gi/o-protein-mediated modulation of Ca2+-channels and inwardly rectifying K+-channels in LTD. Eur J Neurosci 17:1411–1424.

Deng P-Y, Xiao Z, Yang C, Rojanathammanee L, Grisanti L, Watt J, Geiger JD, Liu R, Porter JE, Lei S (2009) GABA(B) receptor activation inhibits neuronal excitability and spatial learning in the entorhinal cortex by activating TREK-2 K+ channels. 63:230–243.

Dumont Y, Jacques D, Bouchard P, Quirion R (1998) Species differences in the expression and distribution of the neuropeptide Y Y1, Y2, Y4, and Y5 receptors in rodents, guinea pig, and primates brains. J Comp Neurol 402:372–384.

Duvarci S, Paré D (2014) Amygdala microcircuits controlling learned fear. Neuron 82:966–980.

Ehrlich DE, Ryan SJ, Rainnie DG (2012) Postnatal development of electrophysiological properties of principal neurons in the rat basolateral amygdala. The Journal of Physiology 590:4819–4838.

Ekblad E, Edvinsson L, Wahlestedt C, Uddman R, Håkanson R, Sundler F (1984) Neuropeptide Y co-exists and co-operates with noradrenaline in perivascular nerve fibers. Regul Pept 8:225–235.

Everitt BJ, Hökfelt T, Terenius L, Tatemoto K, Mutt V, Goldstein M (1984) Differential co-existence of neuropeptide Y (NPY)-like immunoreactivity with catecholamines in the central nervous system of the rat. NSC 11:443–462.

Falls WA, Miserendino MJ, Davis M (1992) Extinction of fear-potentiated startle:

blockade by infusion of an NMDA antagonist into the amygdala. Journal of Neuroscience 12:854–863.

Feinstein JS, Adolphs R, Damasio A, Tranel D (2011) The human amygdala and the induction and experience of fear. Curr Biol 21:34–38.

Fendt M, Bürki H, Imobersteg S, Lingenhöhl K, McAllister KH, Orain D, Uzunov DP, Chaperon F (2009) Fear-reducing effects of intra-amygdala neuropeptide Y infusion in animal models of conditioned fear: an NPY Y1 receptor independent effect. Psychopharmacology (Berl) 206:291–301.

File SE, Hyde J, Pool M (1976) Effects of ethanol and chlordiazepoxide on social interaction in rats [proceedings]. Br J Pharmacol 58:465P.

File SE, Lister RG, Nutt DJ (1982) The anxiogenic action of benzodiazepine antagonists. Neuropharmacology 21:1033–1037.

File SE, Mabbutt PS, Hitchcott PK (1990) Characterisation of the phenomenon of "one-trial tolerance" to the anxiolytic effect of chlordiazepoxide in the elevated plus-maze. Psychopharmacology (Berl) 102:98–101.

File SE, Peet LA (1980) The sensitivity of the rat corticosterone response to environmental manipulations and to chronic chlordiazepoxide treatment. Physiol Behav 25:753–758.

File SE, Seth P (2003) A review of 25 years of the social interaction test. European Journal of Pharmacology 463:35–53.

File SE, Zangrossi H, Sanders FL, Mabbutt PS (1994) Raised corticosterone in the rat after exposure to the elevated plus-maze. Psychopharmacology (Berl) 113:543–546.

Fishell G, Rudy B (2011) Mechanisms of inhibition within the telencephalon: "where the wild things are". Annu Rev Neurosci 34:535–567.

Fuhlendorff J, Johansen NL, Melberg SG, Thøgersen H, Schwartz TW (1990) The antiparallel pancreatic polypeptide fold in the binding of neuropeptide Y to Y1 and Y2 receptors. J Biol Chem 265:11706–11712.

Gainer H, Wolfe SA, Obaid AL, Salzberg BM (1986) Action potentials and frequency-dependent secretion in the mouse neurohypophysis. Neuroendocrinology 43:557–563.

Gassmann M, Bettler B (2012) Regulation of neuronal GABA(B) receptor functions by subunit composition. Nat Rev Neurosci 13:380–394.

Gehlert DR (2004) Introduction to the reviews on neuropeptide Y. Neuropeptides 38:135–140.

Gerald C, Walker MW, Criscione L, Gustafson EL, Batzl-Hartmann C, Smith KE, Vaysse P, Durkin MM, Laz TM, Linemeyer DL, Schaffhauser AO, Whitebread S, Hofbauer KG, Taber RI, Branchek TA, Weinshank RL (1996) A receptor subtype involved in neuropeptide-Y-induced food intake. Nature 382:168–171.

Gewirtz JC, McNish KA, Davis M (1998) Lesions of the bed nucleus of the stria terminalis block sensitization of the acoustic startle reflex produced by repeated stress, but not fear-potentiated startle. Progress in Neuropsychopharmacology & Biological Psychiatry 22:625–648.

Gicquiaux H, Lecat S, Gaire M, Dieterlen A, Mély Y, Takeda K, Bucher B, Galzi J-L (2002) Rapid internalization and recycling of the human neuropeptide Y Y(1) receptor. J Biol Chem 277:6645–6655.

Giesbrecht CJ, Mackay JP, Silveira HB, Urban JH, Colmers WF (2010) Countervailing Modulation of Ih by Neuropeptide Y and Corticotrophin-Releasing Factor in Basolateral Amygdala As a Possible Mechanism for Their Effects on Stress-Related Behaviors. Journal of Neuroscience 30:16970–16982.

Greber S, Schwarzer C, Sperk G (1994) Neuropeptide Y inhibits potassium-stimulated glutamate release through Y2 receptors in rat hippocampal slices in vitro. Br J Pharmacol 113:737–740.

Grillon C (2002) Startle reactivity and anxiety disorders: aversive conditioning, context, and neurobiology. Biol Psychiatry 52:958–975.

Grillon C, Davis M (1997) Fear-potentiated startle conditioning in humans: explicit and contextual cue conditioning following paired versus unpaired training. Psychophysiology 34:451–458.

Grillon C, Morgan CA, Davis M, Southwick SM (1998) Effects of experimental context and explicit threat cues on acoustic startle in Vietnam veterans with posttraumatic stress disorder. Biol Psychiatry 44:1027–1036.

Grillon C, Pellowski M, Merikangas KR, Davis M (1997) Darkness facilitates the acoustic startle reflex in humans. Biol Psychiatry 42:453–460.

Gunduz-Cinar O, Flynn S, Brockway E, Kaugars K, Báldi R, Ramikie TS, Cinar R, Kunos G, Patel S, Holmes A (2015) Fluoxetine Facilitates Fear Extinction Through Amygdala Endocannabinoids. Neuropsychopharmacology.

Gutman AR, Yang Y, Ressler KJ, Davis M (2008) The Role of Neuropeptide Y in the Expression and Extinction of Fear-Potentiated Startle. Journal of Neuroscience 28:12682–12690.

Hamilton TJ, Wheatley BM, Sinclair DB, Bachmann M, Larkum ME, Colmers WF (2010) Dopamine modulates synaptic plasticity in dendrites of rat and human dentate granule cells. Proc Natl Acad Sci USA 107:18185–18190.

Hastings JA, McClure-Sharp JM, Morris MJ (2001) NPY Y1 receptors exert opposite effects on corticotropin releasing factor and noradrenaline overflow from the rat hypothalamus in vitro. Brain Research 890:32–37.

Haubensak W, Kunwar PS, Cai H, Ciocchi S, Wall NR, Ponnusamy R, Biag J, Dong H-W, Deisseroth K, Callaway EM, Fanselow MS, LUthi A, Anderson DJ (2010) Genetic dissection of an amygdala microcircuit that gates conditioned fear. Nature 468:270–276.

Heilig M, Koob GF, Ekman R, Britton KT (1994) Corticotropin-releasing factor and neuropeptide Y: role in emotional integration. Trends Neurosci 17:80–85.

Heilig M, McLeod S, Brot M, Heinrichs SC, Menzaghi F, Koob GF, Britton KT (1993) Anxiolytic-like action of neuropeptide Y: mediation by Y1 receptors in amygdala, and dissociation from food intake effects. Neuropsychopharmacology 8:357–363.

Heilig M, Söderpalm B, Engel JA, Widerlöv E (1989) Centrally administered neuropeptide Y (NPY) produces anxiolytic-like effects in animal anxiety models. Psychopharmacology (Berl) 98:524–529.

Herry C, Ciocchi S, Senn V, Demmou L, Müller C, LUthi A (2008) Switching on and off fear by distinct neuronal circuits. Nature 454:600–606.

Huang CL, Feng S, Hilgemann DW (1998) Direct activation of inward rectifier potassium channels by PIP2 and its stabilization by Gbetagamma. Nature 391:803–806.

Huang CL, Slesinger PA, Casey PJ, Jan YN, Jan LY (1995) Evidence that direct binding of G beta gamma to the GIRK1 G protein-gated inwardly rectifying K+ channel is important for channel activation. Neuron 15:1133–1143.

Janak PH, Tye KM (2015) From circuits to behaviour in the amygdala. Nature 517:284–292.

Jasnow AM, Ehrlich DE, Choi DC, Dabrowska J, Bowers ME, McCullough KM, Rainnie DG, Ressler KJ (2013) Thy1-expressing neurons in the basolateral amygdala may mediate fear inhibition. J Neurosci 33:10396–10404.

Jovanovic T, Norrholm SD, Blanding NQ, Davis M, Duncan E, Bradley B, Ressler KJ (2010) Impaired fear inhibition is a biomarker of PTSD but not depression. Depress Anxiety 27:244–251.

Kaabi B, Gelernter J, Woods SW, Goddard A, Page GP, Elston RC (2006) Genome scan for loci predisposing to anxiety disorders using a novel multivariate approach: strong evidence for a chromosome 4 risk locus. Am J Hum Genet 78:543–553.

Kagamiishi Y, Yamamoto T, Watanabe S (2003) Hippocampal serotonergic system is involved in anxiety-like behavior induced by corticotropin-releasing factor. Brain

Research 991:212–221.

Kanatani A, Mashiko S, Murai N, Sugimoto N, Ito J, Fukuroda T, Fukami T, Morin N, MacNeil DJ, Van der Ploeg LH, Saga Y, Nishimura S, Ihara M (2000) Role of the Y1 receptor in the regulation of neuropeptide Y-mediated feeding: comparison of wild-type, Y1 receptor-deficient, and Y5 receptor-deficient mice. Endocrinology 141:1011–1016.

Karlsson R-M, Holmes A, Heilig M, Crawley JN (2005) Anxiolytic-like actions of centrally-administered neuropeptide Y, but not galanin, in C57BL/6J mice. Pharmacol Biochem Behav 80:427–436.

Kask A, Rägo L, Harro J (1998) Anxiolytic-like effect of neuropeptide Y (NPY) and NPY13-36 microinjected into vicinity of locus coeruleus in rats. Brain Research 788:345–348.

Keifer OP, Hurt RC, Ressler KJ, Marvar PJ (2015) The Physiology of Fear: Reconceptualizing the Role of the Central Amygdala in Fear Learning. Physiology (Bethesda) 30:389–401.

Kemppainen S, Pitkänen A (2000) Distribution of parvalbumin, calretinin, and calbindin-D28k immunoreactivity in the rat amygdaloid complex and colocalization with γ-aminobutyric acid. J Comp Neurol.

Keshavarzi S, Sullivan RKP, Ianno DJ, Sah P (2014) Functional properties and projections of neurons in the medial amygdala. J Neurosci 34:8699–8715.

Kimmel JR, Hayden LJ, Pollock HG (1975) Isolation and characterization of a new pancreatic polypeptide hormone. J Biol Chem 250:9369–9376.

KING FA (1958) Effects of septal and amygdaloid lesions on emotional behavior and conditioned avoidance responses in the rat. J Nerv Ment Dis 126:57–63.

King PJ, Widdowson PS, Doods HN, Williams G (1999) Regulation of neuropeptide Y release by neuropeptide Y receptor ligands and calcium channel antagonists in hypothalamic slices. J Neurochem 73:641–646.

Klausberger T (2009) GABAergic interneurons targeting dendrites of pyramidal cells in the CA1 area of the hippocampus. Eur J Neurosci 30:947–957.

Klausberger T, Somogyi P (2008) Neuronal diversity and temporal dynamics: the unity of hippocampal circuit operations. Science 321:53–57.

Klenke U, Constantin S, Wray S (2010) Neuropeptide Y directly inhibits neuronal activity in a subpopulation of gonadotropin-releasing hormone-1 neurons via Y1 receptors. Endocrinology 151:2736–2746.

Klüver H, Bucy PC (1997) Preliminary analysis of functions of the temporal lobes in

monkeys. 1939. American Psychiatric Publishing.

Koob GF, Heinrichs SC (1999) A role for corticotropin releasing factor and urocortin in behavioral responses to stressors. Brain Research 848:141–152.

Krause J, Eva C, Seeburg PH, Sprengel R (1992) Neuropeptide Y1 subtype pharmacology of a recombinantly expressed neuropeptide receptor. Mol Pharmacol 41:817–821.

Krettek JE, Price JL (1978) A description of the amygdaloid complex in the rat and cat with observations on intra-amygdaloid axonal connections. J Comp Neurol 178:255–280.

Kulik A, Vida I, Fukazawa Y, Guetg N, Kasugai Y, Marker CL, Rigato F, Bettler B, Wickman K, Frotscher M, Shigemoto R (2006) Compartment-dependent colocalization of Kir3.2-containing K+ channels and GABAB receptors in hippocampal pyramidal cells. J Neurosci 26:4289–4297.

Lach G, de Lima TCM (2013) Role of NPY Y1 receptor on acquisition, consolidation and extinction on contextual fear conditioning: dissociation between anxiety, locomotion and non-emotional memory behavior. Neurobiol Learn Mem 103:26–33.

Lan NC, Gee KW (1994) Neuroactive steroid actions at the GABAA receptor. Horm Behav 28:537–544.

Lanuza E, Belekhova M, Martínez-Marcos A, Font C, Martínez-García F (1998) Identification of the reptilian basolateral amygdala: an anatomical investigation of the afferents to the posterior dorsal ventricular ridge of the lizard Podarcis hispanica. Eur J Neurosci 10:3517–3534.

Larhammar D, Wraith A, Berglund MM, Holmberg SK, Lundell I (2001) Origins of the many NPY-family receptors in mammals. Peptides 22:295–307.

Laxmi TR, Stork O, Pape H-C (2003) Generalisation of conditioned fear and its behavioural expression in mice. Behav Brain Res 145:89–98.

LeDoux J (2012a) Rethinking the emotional brain. 73:653–676.

LeDoux JE (2000) Emotion circuits in the brain. Annu Rev Neurosci 23:155–184.

LeDoux JE (2012b) Evolution of human emotion: a view through fear. Prog Brain Res 195:431–442.

LeDoux JE, Cicchetti P, Xagoraris A, Romanski LM (1990) The lateral amygdaloid nucleus: sensory interface of the amygdala in fear conditioning. Journal of Neuroscience 10:1062–1069.

LeDoux JE, Iwata J, Cicchetti P, Reis DJ (1988) Different projections of the central

amygdaloid nucleus mediate autonomic and behavioral correlates of conditioned fear. Journal of Neuroscience 8:2517–2529.

Leitermann RJ, Rostkowski AB, Urban JH (2016) Neuropeptide Y input to the rat basolateral amygdala complex and modulation by conditioned fear. J Comp Neurol:n/a–n/a.

Leitermann RJ, Sajdyk TJ, Urban JH (2012) Cell-specific expression of calcineurin immunoreactivity within the rat basolateral amygdala complex and colocalization with the neuropeptide Y Y1 receptor. J Chem Neuroanat 45:50–56.

Leung LS, Peloquin P (2006) GABA(B) receptors inhibit backpropagating dendritic spikes in hippocampal CA1 pyramidal cells in vivo. Hippocampus 16:388–407.

Levita L, Mania I, Gordon Rainnie D (2003) Subtypes of substance P receptor immunoreactive interneurons in the rat basolateral amygdala. Brain Research 981:41–51.

Li H, Penzo MA, Taniguchi H, Kopec CD, Huang ZJ, Li B (2013) Experience-dependent modification of a central amygdala fear circuit. Nat Neurosci 16:332–339.

Likhtik E, Pelletier JG, Popescu AT, Paré D (2006) Identification of basolateral amygdala projection cells and interneurons using extracellular recordings. Journal of Neurophysiology 96:3257–3265.

Lin C-H, Yeh S-H, Leu T-H, Chang W-C, Wang S-T, Gean P-W (2003) Identification of calcineurin as a key signal in the extinction of fear memory. J Neurosci 23:1574–1579.

Lisman J, Yasuda R, Raghavachari S (2012) Mechanisms of CaMKII action in long-term potentiation. Nat Rev Neurosci 13:169–182.

Lissek S (2012) Toward an account of clinical anxiety predicated on basic, neurally mapped mechanisms of Pavlovian fear-learning: the case for conditioned overgeneralization. 29:257–263.

Lissek S, Kaczkurkin AN, Rabin S, Geraci M, Pine DS, Grillon C (2014) Generalized anxiety disorder is associated with overgeneralization of classically conditioned fear. Biol Psychiatry 75:909–915.

Lissek S, Rabin S, Heller RE, Lukenbaugh D, Geraci M, Pine DS, Grillon C (2010) Overgeneralization of conditioned fear as a pathogenic marker of panic disorder. Am J Psychiatry 167:47–55.

Lister RG (1987) The use of a plus-maze to measure anxiety in the mouse. Psychopharmacology (Berl) 92:180–185.

Löscher W, Rogawski MA (2012) How theories evolved concerning the mechanism of

action of barbiturates. Epilepsia 53 Suppl 8:12–25.

Löw K, Crestani F, Keist R, Benke D, Brünig I, Benson JA, Fritschy JM, Rülicke T, Bluethmann H, Möhler H, Rudolph U (2000) Molecular and neuronal substrate for the selective attenuation of anxiety. Science 290:131–134.

Lu W, Isozaki K, Roche KW, Nicoll RA (2010) Synaptic targeting of AMPA receptors is regulated by a CaMKII site in the first intracellular loop of GluA1. Proc Natl Acad Sci USA 107:22266–22271.

Maccaferri G, Roberts JD, Szucs P, Cottingham CA, Somogyi P (2000) Cell surface domain specific postsynaptic currents evoked by identified GABAergic neurones in rat hippocampus in vitro. The Journal of Physiology 524 Pt 1:91–116.

MacLEAN PD (1949) Psychosomatic disease and the visceral brain; recent developments bearing on the Papez theory of emotion. Psychosom Med 11:338–353.

Magee JC (1998) Dendritic hyperpolarization-activated currents modify the integrative properties of hippocampal CA1 pyramidal neurons. Journal of Neuroscience 18:7613–7624.

Mansuy IM (2003) Calcineurin in memory and bidirectional plasticity. Biochem Biophys Res Commun 311:1195–1208.

Mańko M, Bienvenu TCM, Dalezios Y, Capogna M (2012) Neurogliaform cells of amygdala: a source of slow phasic inhibition in the basolateral complex. The Journal of Physiology 590:5611–5627.

Marowsky A, Fritschy J-M, Vogt KE (2004) Functional mapping of GABA A receptor subtypes in the amygdala. Eur J Neurosci 20:1281–1289.

Marowsky A, Rudolph U, Fritschy JM, Arand M (2012) Tonic Inhibition in Principal Cells of the Amygdala: A Central Role for 3 Subunit-Containing GABAA Receptors. Journal of Neuroscience 32:8611–8619.

Marowsky A, Yanagawa Y, Obata K, Vogt KE (2005) A specialized subclass of interneurons mediates dopaminergic facilitation of amygdala function. 48:1025–1037.

Marshall FH, Jones KA, Kaupmann K, Bettler B (1999) GABAB receptors - the first 7TM heterodimers. Trends Pharmacol Sci 20:396–399.

Mascagni F, McDonald AJ (2003) Immunohistochemical characterization of cholecystokinin containing neurons in the rat basolateral amygdala. Brain Research.

McDonald AJ (1982) Neurons of the lateral and basolateral amygdaloid nuclei: a Golgi study in the rat. J Comp Neurol 212:293–312.

McDonald AJ (1984) Neuronal organization of the lateral and basolateral amygdaloid nuclei in the rat. J Comp Neurol 222:589–606.

McDonald AJ (1989) Coexistence of somatostatin with neuropeptide Y, but not with cholecystokinin or vasoactive intestinal peptide, in neurons of the rat amygdala. Brain Research 500:37–45.

McDonald AJ (1996) Glutamate and aspartate immunoreactive neurons of the rat basolateral amygdala: colocalization of excitatory amino acids and projections to the limbic circuit. J Comp Neurol 365:367–379.

McDonald AJ (2012) Subpopulations of somatostatin-immunoreactive non-pyramidal neurons in the amygdala and adjacent external capsule project to the basal forebrain: evidence for the existence of GABAergic projection neurons in the cortical nuclei and basolateral nuclear complex. :1–16.

McDonald AJ, Betette RL (2001) Parvalbumin-containing neurons in the rat basolateral amygdala: morphology and co-localization of Calbindin-D(28k). NSC 102:413–425.

McDonald AJ, Mascagni F (2001) Colocalization of calcium-binding proteins and GABA in neurons of the rat basolateral amygdala. NSC 105:681–693.

McDonald AJ, Mascagni F (2002) Immunohistochemical characterization of somatostatin containing interneurons in the rat basolateral amygdala. Brain Research 943:237–244.

McDonald AJ, Mascagni F, Muller JF (2004) Immunocytochemical localization of GABABR1 receptor subunits in the basolateral amygdala. Brain Research 1018:147–158.

McDonald AJ, Muller JF, Mascagni F (2002) GABAergic innervation of alpha type II calcium/calmodulin-dependent protein kinase immunoreactive pyramidal neurons in the rat basolateral amygdala. J Comp Neurol 446:199–218.

McKelvy JF, Blumberg S (1986) Inactivation and metabolism of neuropeptides. Annu Rev Neurosci 9:415–434.

McQuiston AR, Petrozzino JJ, Connor JA, Colmers WF (1996) Neuropeptide Y1 receptors inhibit N-type calcium currents and reduce transient calcium increases in rat dentate granule cells. Journal of Neuroscience 16:1422–1429.

Meis S, Sosulina L, Schulz S, Höllt V, Pape H-C (2005) Mechanisms of somatostatin-evoked responses in neurons of the rat lateral amygdala. Eur J Neurosci 21:755–762.

Merchenthaler I, Vigh S, Petrusz P, Schally AV (1982) Immunocytochemical localization of corticotropin-releasing factor (CRF) in the rat brain. Am J Anat 165:385–396.

Merten N, Beck-Sickinger AG (2006) Molecular ligand-receptor interaction of the

NPY/PP peptide family. EXS:35–62.

Michel MC, Beck-Sickinger A, Cox H, Doods HN, Herzog H, Larhammar D, Quirion R, Schwartz T, Westfall T (1998) XVI. International Union of Pharmacology recommendations for the nomenclature of neuropeptide Y, peptide YY, and pancreatic polypeptide receptors. Pharmacol Rev 50:143–150.

Miller PS, Smart TG (2010) Binding, activation and modulation of Cys-loop receptors. Trends Pharmacol Sci 31:161–174.

Millhouse OE, DeOlmos J (1983) Neuronal configurations in lateral and basolateral amygdala. NSC 10:1269–1300.

Mineka S, Ohman A (2002) Phobias and preparedness: the selective, automatic, and encapsulated nature of fear. Biol Psychiatry 52:927–937.

MONTGOMERY KC (1955) The relation between fear induced by novel stimulation and exploratory behavior. J Comp Physiol Psychol 48:254–260.

Morin SM, Gehlert DR (2006) Distribution of NPY Y5-like immunoreactivity in the rat brain. J Mol Neurosci 29:109–114.

Muller JF, Mascagni F, McDonald AJ (2006a) Pyramidal cells of the rat basolateral amygdala: synaptology and innervation by parvalbumin-immunoreactive interneurons. J Comp Neurol 494:635–650.

Muller JF, Mascagni F, McDonald AJ (2006b) Postsynaptic targets of somatostatin-containing interneurons in the rat basolateral amygdala. J Comp Neurol 500:513–529.

Muschol M, Salzberg BM (2000) Dependence of transient and residual calcium dynamics on action-potential patterning during neuropeptide secretion. Journal of Neuroscience 20:6773–6780.

Myers KM, Davis M (2002) Behavioral and neural analysis of extinction. 36:567–584.

Nader K, Majidishad P, Amorapanth P, LeDoux JE (2001) Damage to the lateral and central, but not other, amygdaloid nuclei prevents the acquisition of auditory fear conditioning. Learn Mem 8:156–163.

Nakajima M, Inui A, Asakawa A, Momose K, Ueno N, Teranishi A, Baba S, Kasuga M (1998) Neuropeptide Y produces anxiety via Y2-type receptors. Peptides 19:359–363.

Namburi P, Beyeler A, Yorozu S, Calhoon GG, Halbert SA, Wichmann R, Holden SS, Mertens KL, Anahtar M, Felix-Ortiz AC, Wickersham IR, Gray JM, Tye KM (2015) A circuit mechanism for differentiating positive and negative associations. Nature 520:675–678.

Naveilhan P, Hassani H, Lucas G, Blakeman KH, Hao JX, Xu XJ, Wiesenfeld-Hallin Z, Thorén P, Ernfors P (2001) Reduced antinociception and plasma extravasation in mice lacking a neuropeptide Y receptor. Nature 409:513–517.

Oláh S, Füle M, Komlósi G, Varga C, Báldi R, Barzó P, Tamás G (2009) Regulation of cortical microcircuits by unitary GABA-mediated volume transmission. Nature 461:1278–1281.

Orsini CA, Kim JH, Knapska E, Maren S (2011) Hippocampal and prefrontal projections to the basal amygdala mediate contextual regulation of fear after extinction. J Neurosci 31:17269–17277.

Pabba M (2013) Evolutionary development of the amygdaloid complex. Front Neuroanat 7:27.

Pape HC (1996) Queer current and pacemaker: the hyperpolarization-activated cation current in neurons. Annu Rev Physiol 58:299–327.

Park K, Lee S, Kang SJ, Choi S, Shin KS (2007) Hyperpolarization-activated currents control the excitability of principal neurons in the basolateral amygdala. Biochem Biophys Res Commun 361:718–724.

Parker RM, Herzog H (1999) Regional distribution of Y-receptor subtype mRNAs in rat brain. Eur J Neurosci 11:1431–1448.

Paton JJ, Belova MA, Morrison SE, Salzman CD (2006) The primate amygdala represents the positive and negative value of visual stimuli during learning. Nature 439:865–870.

Pellow S, Chopin P, File SE, Briley M (1985) Validation of open:closed arm entries in an elevated plus-maze as a measure of anxiety in the rat. J Neurosci Methods 14:149–167.

Peng YY, Zucker RS (1993) Release of LHRH is linearly related to the time integral of presynaptic Ca2+ elevation above a threshold level in bullfrog sympathetic ganglia. Neuron 10:465–473.

Pérez-Garci E, Larkum ME, Nevian T (2013) Inhibition of dendritic Ca2+ spikes by GABAB receptors in cortical pyramidal neurons is mediated by a direct Gi/o-β-subunit interaction with Cav1 channels. The Journal of Physiology 591:1599–1612.

Pich EM, Agnati LF, Zini I, Marrama P, Carani C (1993) Neuropeptide Y produces anxiolytic effects in spontaneously hypertensive rats. Peptides 14:909–912.

Pirker S, Schwarzer C, Wieselthaler A, Sieghart W, Sperk G (2000) GABA(A) receptors: immunocytochemical distribution of 13 subunits in the adult rat brain. NSC 101:815–850.

Pitkänen A, Savander V, LeDoux JE (1997) Organization of intra-amygdaloid circuitries in the rat: an emerging framework for understanding functions of the amygdala. Trends Neurosci 20:517–523.

Porrero C, Rubio-Garrido P, Avendaño C, Clascá F (2010) Mapping of fluorescent protein-expressing neurons and axon pathways in adult and developing Thy1-eYFP-H transgenic mice. Brain Research 1345:59–72.

Quirk GJ, Repa C, LeDoux JE (1995) Fear conditioning enhances short-latency auditory responses of lateral amygdala neurons: parallel recordings in the freely behaving rat. 15:1029–1039.

Rainnie DG, Asprodini EK, Shinnick-Gallagher P (1993) Intracellular recordings from morphologically identified neurons of the basolateral amygdala. Journal of Neurophysiology 69:1350–1362.

Rainnie DG, Bergeron R, Sajdyk TJ, Patil M, Gehlert DR, Shekhar A (2004) Corticotrophin releasing factor-induced synaptic plasticity in the amygdala translates stress into emotional disorders. J Neurosci 24:3471–3479.

Rainnie DG, Mania I, Mascagni F, McDonald AJ (2006) Physiological and morphological characterization of parvalbumin-containing interneurons of the rat basolateral amygdala. J Comp Neurol 498:142–161.

Rasmusson AM, Hauger RL, Morgan CA, Bremner JD, Charney DS, Southwick SM (2000) Low baseline and yohimbine-stimulated plasma neuropeptide Y (NPY) levels in combat-related PTSD. Biol Psychiatry 47:526–539.

Robinson RB, Siegelbaum SA (2003) Hyperpolarization-activated cation currents: from molecules to physiological function. Annu Rev Physiol 65:453–480.

Rodrigues SM, Farb CR, Bauer EP, LeDoux JE, Schafe GE (2004) Pavlovian fear conditioning regulates Thr286 autophosphorylation of Ca2+/calmodulin-dependent protein kinase II at lateral amygdala synapses. J Neurosci 24:3281–3288.

Rodriguez M, Audinot V, Dromaint S, Macia C, Lamamy V, Beauverger P, Rique H, Imbert J, Nicolas JP, Boutin JA, Galizzi JP (2003) Molecular identification of the long isoform of the human neuropeptide Y Y5 receptor and pharmacological comparison with the short Y5 receptor isoform. Biochem J 369:667–673.

Rogan MT, Stäubli UV, LeDoux JE (1997) Fear conditioning induces associative long-term potentiation in the amygdala. Nature 390:604–607.

Romanski LM, LeDoux JE (1992) Equipotentiality of thalamo-amygdala and thalamo-cortico-amygdala circuits in auditory fear conditioning. Journal of Neuroscience 12:4501–4509.

Rosenkranz JA, Grace AA (1999) Modulation of basolateral amygdala neuronal firing

and afferent drive by dopamine receptor activation in vivo. J Neurosci 19:11027–11039.

Rostkowski AB, Teppen TL, Peterson DA, Urban JH (2009) Cell-specific expression of neuropeptide Y Y1 receptor immunoreactivity in the rat basolateral amygdala. J Comp Neurol 517:166–176.

Rudy B, Fishell G, Lee S, Hjerling-Leffler J (2011) Three groups of interneurons account for nearly 100% of neocortical GABAergic neurons. McBain CJ, Fishell G, eds. Dev Neurobiol 71:45–61.

Russell JA, Barrett LF (1999) Core affect, prototypical emotional episodes, and other things called emotion: dissecting the elephant. J Pers Soc Psychol 76:805–819.

Ryan SJ, Ehrlich DE, Rainnie DG (2016) Morphology and dendritic maturation of developing principal neurons in the rat basolateral amygdala. Brain Struct Funct 221:839–854.

Sah P, Faber ESL, Lopez De Armentia M, Power J (2003) The amygdaloid complex: anatomy and physiology. Physiological Reviews 83:803–834.

Sah R, Ekhator NN, Strawn JR, Sallee FR, Baker DG, Horn PS, Geracioti TD (2009) Low cerebrospinal fluid neuropeptide Y concentrations in posttraumatic stress disorder. Biol Psychiatry 66:705–707.

Sajdyk TJ, Fitz SD, Shekhar A (2006) The role of neuropeptide Y in the amygdala on corticotropin-releasing factor receptor-mediated behavioral stress responses in the rat. Stress 9:21–28.

Sajdyk TJ, Johnson PL, Leitermann RJ, Fitz SD, Dietrich A, Morin M, Gehlert DR, Urban JH, Shekhar A (2008) Neuropeptide Y in the Amygdala Induces Long-Term Resilience to Stress-Induced Reductions in Social Responses But Not Hypothalamic-Adrenal-Pituitary Axis Activity or Hyperthermia. Journal of Neuroscience 28:893–903.

Sajdyk TJ, Schober DA, Gehlert DR (2002a) Neuropeptide Y receptor subtypes in the basolateral nucleus of the amygdala modulate anxiogenic responses in rats. Neuropharmacology 43:1165–1172.

Sajdyk TJ, Schober DA, Gehlert DR, Shekhar A (1999a) Role of corticotropin-releasing factor and urocortin within the basolateral amygdala of rats in anxiety and panic responses. Behav Brain Res 100:207–215.

Sajdyk TJ, Schober DA, Smiley DL, Gehlert DR (2002b) Neuropeptide Y-Y2 receptors mediate anxiety in the amygdala. Pharmacol Biochem Behav 71:419–423.

Sajdyk TJ, Shekhar A (1997a) Excitatory amino acid receptor antagonists block the cardiovascular and anxiety responses elicited by gamma-aminobutyric acidA receptor

blockade in the basolateral amygdala of rats. J Pharmacol Exp Ther 283:969–977.

Sajdyk TJ, Shekhar A (1997b) Excitatory amino acid receptors in the basolateral amygdala regulate anxiety responses in the social interaction test. Brain Research 764:262–264.

Sajdyk TJ, Vandergriff MG, Gehlert DR (1999b) Amygdalar neuropeptide Y Y1 receptors mediate the anxiolytic-like actions of neuropeptide Y in the social interaction test. European Journal of Pharmacology 368:143–147.

Sareen J (2014) Posttraumatic stress disorder in adults: impact, comorbidity, risk factors, and treatment. Can J Psychiatry 59:460–467.

Scanziani M (2000) GABA spillover activates postsynaptic GABA(B) receptors to control rhythmic hippocampal activity. 25:673–681.

Schoenbaum G, Chiba AA, Gallagher M (1998) Orbitofrontal cortex and basolateral amygdala encode expected outcomes during learning. Nat Neurosci 1:155–159.

Sehlmeyer C, Schöning S, Zwitserlood P, Pfleiderer B, Kircher T, Arolt V, Konrad C (2009) Human fear conditioning and extinction in neuroimaging: a systematic review. Gendelman HE, ed. PLoS ONE 4:e5865.

Senn V, Wolff SBE, Herry C, Grenier F, Ehrlich I, Gründemann J, Fadok JP, Müller C, Letzkus JJ, LUthi A (2014) Long-range connectivity defines behavioral specificity of amygdala neurons. 81:428–437.

Sigel E (2002) Mapping of the benzodiazepine recognition site on GABA(A) receptors. Curr Top Med Chem 2:833–839.

Sigel E, Steinmann ME (2012) Structure, function, and modulation of GABA(A) receptors. J Biol Chem 287:40224–40231.

Skinner BF (n.d.) The Behavior of Organisms. B. F. Skinner Foundation.

Smiałowska M, Wierońska JM, Domin H, Zieba B (2007) The effect of intrahippocampal injection of group II and III metobotropic glutamate receptor agonists on anxiety; the role of neuropeptide Y. Neuropsychopharmacology 32:1242–1250.

Smith Y, Pare D (1994) Intra-amygdaloid projections of the lateral nucleus in the cat: PHA-L anterograde labeling combined with postembedding GABA and glutamate immunocytochemistry. J Comp Neurol 342:232–248.

Somogyi P, Klausberger T (2005) Defined types of cortical interneurone structure space and spike timing in the hippocampus. The Journal of Physiology 562:9–26.

Sosulina L, Schwesig G, Seifert G, Pape H-C (2008) Neuropeptide Y activates a G-protein-coupled inwardly rectifying potassium current and dampens excitability in

the lateral amygdala. Mol Cell Neurosci 39:491–498.

Stefanik MT, Kalivas PW (2013) Optogenetic dissection of basolateral amygdala projections during cue-induced reinstatement of cocaine seeking. Front Behav Neurosci 7:213.

Sun N, Cassell MD (1993) Intrinsic GABAergic neurons in the rat central extended amygdala. J Comp Neurol 330:381–404.

Szabadics J, Varga C, Molnár G, Oláh S, Barzó P, Tamás G (2006) Excitatory effect of GABAergic axo-axonic cells in cortical microcircuits. Science 311:233–235.

Sørensen G, Lindberg C, Wörtwein G, Bolwig TG, Woldbye DPD (2004) Differential roles for neuropeptide Y Y1 and Y5 receptors in anxiety and sedation. J Neurosci Res 77:723–729.

Tasan RO, Nguyen NK, Weger S, Sartori SB, Singewald N, Heilbronn R, Herzog H, Sperk G (2010) The Central and Basolateral Amygdala Are Critical Sites of Neuropeptide Y/Y2 Receptor-Mediated Regulation of Anxiety and Depression. Journal of Neuroscience 30:6282–6290.

Tatemoto K (1982) Neuropeptide Y: complete amino acid sequence of the brain peptide. Proc Natl Acad Sci USA 79:5485–5489.

Tatemoto K, Carlquist M, Mutt V (1982) Neuropeptide Y--a novel brain peptide with structural similarities to peptide YY and pancreatic polypeptide. Nature 296:659–660.

Thompson AJ, Lummis SCR (2006) 5-HT3 receptors. Curr Pharm Des 12:3615–3630.

Thorsell A, Michalkiewicz M, Dumont Y, Quirion R, Caberlotto L, Rimondini R, Mathé AA, Heilig M (2000) Behavioral insensitivity to restraint stress, absent fear suppression of behavior and impaired spatial learning in transgenic rats with hippocampal neuropeptide Y overexpression. Proc Natl Acad Sci USA 97:12852–12857.

Tye KM, Stuber GD, de Ridder B, Bonci A, Janak PH (2008) Rapid strengthening of thalamo-amygdala synapses mediates cue-reward learning. Nature 453:1253–1257.

Unal G, Paré J-F, Smith Y, Paré D (2014) Cortical inputs innervate calbindin-immunoreactive interneurons of the rat basolateral amygdaloid complex. J Comp Neurol 522:1915–1928.

van den Pol AN (2003) Weighing the role of hypothalamic feeding neurotransmitters. 40:1059–1061.

Verma D, Tasan RO, Herzog H, Sperk G (2012) NPY controls fear conditioning and fear extinction by combined action on Y_1 and Y_2 receptors. Br J Pharmacol 166:1461–

1473.

Vigot R, Barbieri S, Bräuner-Osborne H, Turecek R, Shigemoto R, Zhang Y-P, Luján R, Jacobson LH, Biermann B, Fritschy J-M, Vacher C-M, Müller M, Sansig G, Guetg N, Cryan JF, Kaupmann K, Gassmann M, Oertner TG, Bettler B (2006) Differential compartmentalization and distinct functions of GABAB receptor variants. Neuron 50:589–601.

Wahlestedt C, Håkanson R, Vaz CA, Zukowska-Grojec Z (1990) Norepinephrine and neuropeptide Y: vasoconstrictor cooperation in vivo and in vitro. Am J Physiol 258:R736–R742.

Wahlestedt C, Pich EM, Koob GF, Yee F, Heilig M (1993) Modulation of anxiety and neuropeptide Y-Y1 receptors by antisense oligodeoxynucleotides. Science 259:528–531.

Walf AA, Frye CA (2007) The use of the elevated plus maze as an assay of anxiety-related behavior in rodents. Nat Protoc 2:322–328.

Walker DL, Davis M (1997) Anxiogenic effects of high illumination levels assessed with the acoustic startle response in rats. Biol Psychiatry 42:461–471.

Walker DL, Miles LA, Davis M (2009) Selective participation of the bed nucleus of the stria terminalis and CRF in sustained anxiety-like versus phasic fear-like responses. Prog Neuropsychopharmacol Biol Psychiatry 33:1291–1308.

Walker DL, Ressler KJ, Lu K-T, Davis M (2002) Facilitation of conditioned fear extinction by systemic administration or intra-amygdala infusions of D-cycloserine as assessed with fear-potentiated startle in rats. J Neurosci 22:2343–2351.

Wallner M, Hanchar HJ, Olsen RW (2003) Ethanol enhances alpha 4 beta 3 delta and alpha 6 beta 3 delta gamma-aminobutyric acid type A receptors at low concentrations known to affect humans. Proc Natl Acad Sci USA 100:15218–15223.

Walther C, Mörl K, Beck-Sickinger AG (2011) Neuropeptide Y receptors: ligand binding and trafficking suggest novel approaches in drug development. J Pept Sci 17:233–246.

Washburn MS, Moises HC (1992a) Electrophysiological and morphological properties of rat basolateral amygdaloid neurons in vitro. Journal of Neuroscience 12:4066–4079.

Washburn MS, Moises HC (1992b) Inhibitory responses of rat basolateral amygdaloid neurons recorded in vitro. NSC 50:811–830.

Weisfeld GE, Goetz SMM (2013) Applying evolutionary thinking to the study of emotion. Behav Sci (Basel) 3:388–407.

WEISKRANTZ L (1956) Behavioral changes associated with ablation of the amygdaloid

complex in monkeys. J Comp Physiol Psychol 49:381–391.

Wessa M, Flor H (2007) Failure of extinction of fear responses in posttraumatic stress disorder: evidence from second-order conditioning. Am J Psychiatry 164:1684–1692.

Whissell PD, Lecker I, Wang D-S, Yu J, Orser BA (2015) Altered expression of δGABAA receptors in health and disease. Neuropharmacology 88:24–35.

Wickman K, Karschin C, Karschin A, Picciotto MR, Clapham DE (2000) Brain localization and behavioral impact of the G-protein-gated K+ channel subunit GIRK4. Journal of Neuroscience 20:5608–5615.

Wolak ML, DeJoseph MR, Cator AD, Mokashi AS, Brownfield MS, Urban JH (2003) Comparative distribution of neuropeptide Y Y1 and Y5 receptors in the rat brain by using immunohistochemistry. J Comp Neurol 464:285–311.

Wolff SBE, Gründemann J, Tovote P, Krabbe S, Jacobson GA, Müller C, Herry C, Ehrlich I, Friedrich RW, Letzkus JJ, LUthi A (2014) Amygdala interneuron subtypes control fear learning through disinhibition. Nature 509:453–458.

Woodruff AR, Monyer H, Sah P (2006) GABAergic excitation in the basolateral amygdala. J Neurosci 26:11881–11887.

Woodruff AR, Sah P (2007a) Networks of parvalbumin-positive interneurons in the basolateral amygdala. J Neurosci 27:553–563.

Woodruff AR, Sah P (2007b) Inhibition and synchronization of basal amygdala principal neuron spiking by parvalbumin-positive interneurons. Journal of Neurophysiology 98:2956–2961.

Yamada M, Inanobe A, Kurachi Y (1998) G protein regulation of potassium ion channels. Pharmacol Rev 50:723–760.

Yehuda R, Brand S, Yang R-K (2006) Plasma neuropeptide Y concentrations in combat exposed veterans: relationship to trauma exposure, recovery from PTSD, and coping. Biol Psychiatry 59:660–663.

Zhang H, He C, Yan X, Mirshahi T, Logothetis DE (1999) Activation of inwardly rectifying K+ channels by distinct PtdIns(4,5)P2 interactions. Nat Cell Biol 1:183–188.

Zhou Q, Homma KJ, Poo M-M (2004) Shrinkage of dendritic spines associated with long-term depression of hippocampal synapses. Neuron 44:749–757.

Zhou Z et al. (2008) Genetic variation in human NPY expression affects stress response and emotion. Nature 452:997–1001.

Zhu PJ, Stewart RR, McIntosh JM, Weight FF (2005) Activation of nicotinic

acetylcholine receptors increases the frequency of spontaneous GABAergic IPSCs in rat basolateral amygdala neurons. Journal of Neurophysiology 94:3081–3091.

Chapter 2

Y_2 Receptor Activation Modulates GABA-Mediated Inhibition of BLA Principal Neurons

2.1 INTRODUCTION

Fear and anxiety are adaptive and conserved emotions critical for appropriate defensive behaviors. These emotions are largely mediated by the amygdala, a collection of medial temporal lobe nuclei, which is required for the expression of fear-based behaviors. The basolateral amygdala (BLA) is an important group of cortical-like amygdala nuclei, heavily innervated by sensory-derived inputs (Pitkänen et al., 1997). When appropriate, the BLA coordinates fear or anxiety via excitatory projections to the central amygdala, the bed nucleus of the stria terminalis and other brain areas (Walker et al., 2009; Amano et al., 2010).

BLA output is mediated by glutamatergic principal neurons (PNs), which are its predominant neuron type (~85%) (McDonald, 1984; 1996). The output of these PNs is highly regulated by a diverse group of local GABA interneurons (Capogna, 2014). Thus, a balance of excitatory glutamatergic and inhibitory GABA transmission governs BLA output. In animal models, increases in BLA output are anxiogenic, while decreases are behaviorally anxiolytic (Sajdyk and Shekhar, 1997; Bueno et al., 2005). Although fear and anxiety are generally adaptive emotions, excessive and/or inappropriate anxiety is a hallmark of multiple potentially debilitating human anxiety disorders. Amygdala dysfunction, in turn, has been implicated in the etiology of many anxiety-related disorders (Shekhar et al., 1999; Phan et al., 2006; Prater et al., 2013).

Neuropeptide Y (NPY) is a 36 amino acid peptide highly expressed throughout the mammalian CNS. In humans, increased NPY expression is proposed to confer emotional resilience to traumatic stressors (Rasmusson et al., 2000; Sah et al., 2009); while local BLA infusions of NPY are potently anxiolytic in animal models (Sajdyk et

al., 1999). NPY receptors are G-protein- ($G_{i/o}$) coupled and Y_1, Y_2 and Y_5 receptor subtypes are expressed in the rodent BLA (Wolak et al., 2003; Stanić et al., 2006; Rostkowski et al., 2009). The acute anxiolytic effects of NPY are mediated largely via Y_1 receptors (Sajdyk et al., 1999). Our lab has previously shown that NPY inhibits half of all PNs in the basal lateral amygdala (BLA) and reduces a tonic H-current (I_h) via Y_1 receptors (Giesbrecht et al., 2010). Furthermore, Sosulina et al. (2008) showed that NPY inhibits half of all lateral amygdala (LA) PNs through Y_1 receptors; an effect mediated via activation of a G-protein coupled inwardly rectifying K^+ (GIRK) conductance (Sosulina et al., 2008). Interestingly, selective activation of BLA Y_2 receptors elicits increased anxiety, an opposite behavioral effect (Nakajima et al., 1998; Sajdyk et al., 2002b). The neuronal basis underlying the anxiogenic effects of selective Y_2 receptor activation is unclear. We have thus undertaken the present study to mechanistically dissect Y_2 receptor actions within the BLA.

NPY Y_2 receptors are typically expressed on presynaptic terminals where they act to inhibit neurotransmitter release (Colmers and Bleakman, 1994; Greber et al., 1994; Chen et al., 1997). Furthermore, BLA PNs show low *in vivo* and *in vitro* firing rates, in part, due to the strong inhibitory control of local GABA interneurons (Washburn and Moises, 1992a; Rosenkranz and Grace, 1999; Likhtik et al., 2006). We therefore hypothesized that a population of GABA interneurons, which target PNs, express Y_2 receptors on their synaptic terminals. We further hypothesized that activation of these presynaptic Y_2 receptors reduces GABA release and disinhibits PNs.

We now show that the Y_2 receptor selective agonist, [ahx$^{5-24}$]NPY, reduces the frequency of $GABA_A$-mediated miniature inhibitory post synaptic currents (mIPSCs) in

most PNs. However, in the absence of tetrodotoxin (TTX), effects of Y_2 receptor activation were more complex. Under these conditions, a subpopulation of PNs showed an increase in the frequency of larger amplitude spontaneous IPSCs (sIPSCs). Thus, Y_2 receptor activation appeared to increase the excitability of some interneurons, likely via disinhibition. Histological studies revealed that Y_2 receptors are expressed on interneurons that co-express NPY and the neuropeptide somatostatin (SOM). However, Y_2 receptors were not expressed by parvalbumin (PV) interneurons (the largest population of BLA interneurons). Disinhibition of PV interneurons by SOM/NPY cells would thus be consistent with our electrophysiological data.

Activation of Y_2 receptors, which are likely presynaptic, on SOM/NPY interneurons thus exerts complex actions on BA PNs. In the majority of cases, basal GABA-mediated inhibition of PNs was decreased, likely via direct actions on SOM/NPY interneurons. However, large amplitude IPSCs were increased in a subpopulation of PNs via Y_2 mediated disinhibition of another interneuron population. Ultimately these results enhance our understanding of the overall actions of NPY within the BLA, and provide further insight into how this important neuropeptide may modulate anxiety behavior.

2.2 MATERIALS AND METHODS

2.2a Animals

Electrophysiology experiments were performed using acute brain slices prepared from male Sprague Dawley rats between 6-16 weeks of age. Mice conditionally expressing the TdTomato fluorescent protein in neurons expressing cre-recombinase under control of the Y_2 receptor gene promoter (Y_2R-TdTomato) were used in a subset of electrophysiology experiments, and for immunohistochemistry. In these cases, male and female mice between 4-16 weeks of age were used. The care and use of animals was in accordance with standards set by the University of Alberta Care and Use Committee: Health Sciences, and were in compliance with regulations by the Canadian Council for Animal Care. Animals were group housed (2-3 per cage) with food and water supplied *ad libitum*.

2.2b Brain Slice Preparation

Rodents were decapitated, their brains rapidly removed and submerged in an icy slurry of artificial CSF (ACSF) optimized for slice preparation ("slicing solution"), containing (in mM): 118 NaCl, 3 KCl, 1.3 $MgSO_4$, 1.4 NaH_2PO_4, 5 $MgCl_2 \cdot 6H_2O$, 10 glucose, 26 $NaHCO_3$ and 1.5 $CaCl_2$. Slicing solution was continuously bubbled with carbogen (95% O_2, 5% CO_2) and was supplemented with kynurenic acid (1 mM) to prevent glutamate-mediated excitatory toxicity. Coronal brain slices containing BLA were cut with a vibrating slicer (Slicer HR2; Sigmann Elektronik) to a thickness of 300 μm for rats and 250 μm for mice. Slices were then transferred to a carbogenated ACSF ("Bath") solution, which contained the following (in mM); 124 NaCl, 3KCl, 1.3 $MgSO_4$, 1.4 NaH_2PO_4, 10 glucose 26 $NaHCO_3$, and 2.5 $CaCl_2$ (300 − 305 mOsm/L). Slices were

stored in room temperature (22 °C) carbogen-bubbled bath solution for at least 30 min following slicing. Mouse brain slices were protected from light to minimize fluorophore bleaching. Bath solution was used to perfuse slices for the remainder of all experiments. For electrophysiology, slices were placed into a recording chamber attached to a fixed stage of a movable upright microscope (Axioskop FS2; Carl Zeiss) and held submerged by a platinum and polyester fiber "harp". Slices were continuously perfused with warmed (34 ± 0.5 °C), carbogenated bath solution at a rate of 2-3 ml/min for at least 20 min prior to recording.

2.2c Electrophysiology

Patch pipettes were pulled from thin-walled, filamented borosilicate glass tubing (TW150F; WPI, Sarasota, FL) with a two-stage puller (PP-83; Narishige) to a tip resistance of 5-7 MΩ when back filled with internal solution. Either a K-gluconate or cesium methanesulphonate (126 mM) based internal solution were used for experiments. The K-gluconate solution contained in (mM): 126 K-gluconate, 10 HEPES, 4 KCl, 5 MgATP, 0.3 NaGTP, 1 EGTA and 0.3 CaCl$_2$. Neurobiotin (0.05 − 0.1%) was added and the pH adjusted to 7.27 − 7.30 with KOH, (275 − 285 mOsm/L). 126 mM cesium methanesulfonate was used in place of K-gluconate for the Cs$^+$ internal solution; in this case pH was adjusted with CsOH; otherwise constituents, concentrations and other properties were identical to K$^+$ internal solution. Recordings were made using a Multiclamp 700B amplifier and data were acquired at 20 kHz using pClamp (v 10.3 − 10.4) via a Digidata 1322 interface (all Molecular Devices, Sunnyvale, CA). Liquid junction potentials were calculated for K$^+$ and Cs$^+$ internal solutions as +14.4 mV and

+13.8 mV respectively; all voltage and current clamp data reported have been adjusted to reflect this.

The BA, which contains the basal and the basal medial amygdala nuclei, was identified in slices using criteria based on the Paxinos and Watson (1986) atlas. BA neurons were visually identified with infrared-differential contrast optics (ir-DIC) and PNs selected for recordings based on a large, pyramidal or stellate shaped soma and a prominent apical dendrite. Local circuit interneurons could generally be differentiated from PNs based on a smaller more spherical shaped soma. Once whole cell patch clamp configuration was established electrophysiological properties were used in conjunction with morphology to characterize neurons (Washburn and Moises, 1992b; Rainnie et al., 1993). In the case of K^+ intracellular recordings, neurons judged to be PNs exhibited: lower input resistance (30-100 MΩ), and longer duration action potentials compared to interneurons, with half widths greater than ≥ 1 ms (approximately twice as long as most interneurons) (Mahanty and Sah, 1998) and prominent accommodation of the action potential frequency when brought to threshold with 800 ms depolarizing current steps. The first spike of a PN action potential train also typically showed either a doublet spike burst or a prominent afterdepolarization.

For K^+ intracellular experiments, PNs were mainly held in voltage clamp at -75 mV for 5-10 min before the start of experiments and between experimental manipulations. In the case of Cs^+ intracellular recordings, PNs were held at -14 mV before and between measurements, but otherwise treated similarly. A series of experimental protocols were performed at 5 min intervals to establish the stability of baseline neuronal properties. For Cs^+ recordings, only neurons showing stable holding

current (measured in voltage clamp) and stable access resistance ($\pm$ 20 %) throughout an experiment were selected for analysis. For K^+ intracellular experiments, in addition to the above parameters, stability of neuronal resting membrane potential (RMP) was also established with short (30 s) passive current clamp recordings.

Miniature and spontaneous synaptic currents were measured with 2min long passive voltage clamp recordings, with PNs held at -55 mV or -14 mV in the case of K^+ or Cs^+ electrode recordings respectively. Holding PNs at -55 mV (K^+ electrode) allowed inhibitory $GABA_A$ currents to be visualized as outward events and differentiated from inward presumably glutametergic events. However, -55 mV was close to the Cl^- reversal potential ($\sim$ -70 mV) therefore in many cases $GABA_A$ IPSCs were of small amplitude and therefore difficult to quantify. Cs^+ electrodes allowed PNs to be held more depolarized (-14 mV), which substantially increased the Cl^- driving force and thus the amplitude of outward synaptic $GABA_A$ currents. Synaptic events were recorded under baseline conditions, in the presence of drugs and periodically during washout. Synaptic event inter-event intervals (IEI), amplitudes and the slope of the event rising phase were quantified with Mini Analysis (Synaptosoft). The full 2 min trace was generally analyzed in the case of K^+ electrode recordings while typically only the first 30-60 s of Cs^+ recordings were analyzed due to the high frequency of measurable $GABA_A$ events under this condition. In the case of Cs^+ recordings, a minimum of 500 events per PN per condition (control, drug and wash) were measured. Lower event numbers were used in K^+ recordings (200) due to the lower measurable event frequencies.

2.2d Immunohistochemistry

Y$_2$R-TdTomato mice were given a lethal dose of the anesthetics ketamine and xylazine by intra-peritoneal injection. Once mice were in surgical plane they were transcardially perfused with room temperature phosphate buffered saline (PBS) until their blood volume was visibly flushed. Mice were then perfused with 3% formalin fixative after which, their brains were carefully removed and stored overnight (protected from light) in 3% formalin fixative in the dark. Y$_2$R-TdTomato brains were then switched to PBS containing the preservative sodium azide (0.02 %) and sent to the laboratory of Dr. Janice Urban (Rosalind Franklin University, Chicago Medical School, North Chicago, Illinois) for sectioning and immunohistochemistry.

2.2e Materials

The Y$_2$ agonist [6-aminohexanoic$^{5-24}$]NPY ([ahx$^{5-24}$NPY]) was a gift from Dr. A. G. Beck-Sickinger (Leipzig, Germany). Kyneurenic acid was purchased from Abcam Biochemicals. GTP was purchased from Roche Diagnostics. CsCl, Cs$^+$-Methanesulphonate, K$^+$-Gluconate, EGTA, Mg•ATP, CsOH and formalin fixative were obtained from Sigma-Aldrich. TTX was purchased from Alomone Labs. Bicuculline was purchased from Tocris Bioscience. KOH was purchased from BDH Chemicals. All other chemicals were obtained from Thermo Fisher Scientific. [ahx$^{5-24}$]NPY and TTX were stored as concentrated stock solutions at -20 °C and diluted in ACSF bath solution immediately before application.

2.2f Data Analysis

Recordings were analyzed off-line with pClamp 10.3 (Molecular Devices). Figures were generated with GraphPad Prism, version 5.05. Statistical analyses were also

performed with GraphPad Prism. Data were expressed as mean ± SEM. Synaptic event cumulative probability histograms were constructed using the same number of events (500) per neuron per condition. Repeated-measures one-way ANOVA, with the Bonferroni post-test, was used to analyze the effects of drugs on mean synaptic event properties including inter-event intervals (IEI), amplitude, and the slope of the event rising phase (between 10-90% of peak amplitude). Synaptic event properties were compared under control conditions, during peak peptide effect and as possible after washout (10-20 min). Mean differences were considered significant at $p<0.05$, and significance levels are indicated in figures as follows: $*p<0.05$, $**p<0.01$, $***p<0.001$.

2.3 RESULTS

2.3a [ahx$^{5\text{-}24}$]NPY decreases the frequency of PN miniature IPSCs

Most BA PNs (in the case of Cs^+ recording) showed vigorous basal GABA mediated inhibition, which was seen in voltage-clamp as frequent spontaneous IPSCs (sIPSC). These sIPSCs appeared to be largely GABA$_A$-mediated as they reversed close to the Cl^- reversal potential (~ -70 mV) and were blocked by bath-applied bicuculline (10 µM). In recordings with intracellular Cs^+ (V_h= -14 mV), virtually every PN examined showed substantial spontaneous synaptic GABA$_A$ input, with a mean sIPSC frequency of 40.7 ± 0.3 Hz (n=25). As expected, TTX (500nM) decreased both unitary IPSC frequencies and amplitudes; however, neurons continued to receive mIPSC at a considerable rate (27.6 ± 0.3 Hz, n=11).

Bath application of the Y$_2$ receptor selective agonist [ahx$^{5\text{-}24}$]NPY (1µM), significantly and reversibly decreased the frequency of mIPSC in most PNs tested (Cs^+ electrode recordings) **(Figure 1A)**. Specifically, 9/12 PNs responded to [ahx$^{5\text{-}24}$]NPY with a reversible increase in the mean mIPSC IEI from 51.5 ± 4.8 ms to 66.5 ± 7.3 ms (p<0.001; n=9) **(Figure 1B)**. 1/12 neurons showed a pronounced frequency reduction that did not reverse on washout and 2/12 neurons showed no clear response to the agonist. mIPSC amplitude was unaffected by [ahx$^{5\text{-}24}$]NPY suggesting these actions were mediated by a presynaptic mechanism **(Figure 1C)**.

2.3b [ahx$^{5\text{-}24}$]NPY exerts complex effects on spontaneous PN IPSCs

Twelve out of 34 PNs, responded to [ahx$^{5\text{-}24}$]NPY with effects on sIPSC properties similar to those observed in the presence of TTX. In these PNs, [ahx$^{5\text{-}24}$]NPY

(1 μM) reversibly increased the mean sIPSC IEI from 59.4 ± 7.3 ms to 95.3 ± 9.9 ms (p<0.001; n=12), but had no effect on amplitude **(Figure 2A-C)**.

However in some PNs, [ahx$^{5-24}$]NPY elicited effects on sIPSCs that were not observed in the presence of TTX. Thus, 13/34 PNs responded to [ahx$^{5-24}$]NPY (1 μM) with a substantial and reversible increase in mean sIPSC amplitude from 25.8 ± 2.3pA to 34.4 ± 3.5pA (p<0.001; n=13) **(Figure 3C)**. Furthermore, 7 PNs showed reversible [ahx$^{5-24}$]NPY (1 μM)-mediated increases in event frequency. In these PNs the mean sIPSC IEI was decreased from 67.2 ± 10.0 pA to 46.7 ± 6.1 pA (p<0.01; n=7) **(Figure 3D)**. In most cases, when [ahx$^{5-24}$]NPY increased sIPSC frequency, event amplitude was also increased. However, several PNs responded to [ahx$^{5-24}$]NPY with reduced sIPSC frequency concurrent with increased event amplitude.

Drug-mediated effects on synaptic event amplitude are generally attributed to postsynaptic actions. However, it is unlikely that [ahx$^{5-24}$]NPY potentiated sIPSC amplitude via a postsynaptic mechanism as similar effects were absent in the presence of TTX.

2.3c [ahx$^{5-24}$]NPY likely acts on two distinct GABA interneuron populations

We then binned sIPSC amplitude data from these experiments into histograms. This approach allowed further investigation of the PNs in which [ahx$^{5-24}$]NPY increased sIPSC amplitude. If [ahx$^{5-24}$]NPY increased sIPSC amplitude via a postsynaptic mechanism, event amplitude distributions should be shifted evenly towards larger amplitudes. Instead, [ahx$^{5-24}$]NPY changed the shape of the amplitude distribution, selectively increasing the numbers of larger amplitude events **(Figure 3E)**.

We hypothesized that the above effects of [ahx$^{5-24}$]NPY on PN spontaneous and miniature IPSCs are best explained by Y_2 receptor actions on two distinct populations of GABAergic interneurons. We proposed that the first interneuron class termed (Y_2R-positive) expressed presynaptic inhibitory Y_2 receptors and selectively innervated PNs. Activation of these presynaptic Y_2 receptors reduces GABA release via an action potential-independent mechanism. We further proposed that these Y_2R-positive interneurons also innervated a second interneuron class, which do not express Y_2 receptors (Y_2R-negative) but also innervate PNs **(Figure 4)**. Thus in the presence of TTX, only actions of [ahx$^{5-24}$]NPY on Y_2R-positive interneurons would be evident. This would result in the observed uniform decrease in PN mIPSCs frequency. However we hypothesized that [ahx$^{5-24}$]NPY, via actions on presynaptic Y_2 receptors, also decreased GABA-mediated inhibition of Y_2R-negative interneurons. In the absence of TTX, such disinhibition would increase the firing rate of Y_2R-negative interneurons and result in the observed increase in large amplitude PN sIPSCs in some recordings.

The BLA contains multiple distinct interneuron subtypes. Of these interneuron types, those characterized by expression of the neuropeptide somatostatin (SOM) appeared to best meet our proposed Y_2R-positive interneuron criteria. Specifically, SOM interneurons predominately target PN distal dendrites and often co-express NPY (McDonald, 1989; Muller et al., 2006). Furthermore, histological data indicates SOM interneurons target BLA parvalbumin (PV) interneurons (Muller et al., 2006). PV interneurons, which predominantly innervate more proximal PNs domains (McDonald and Betette, 2001), could therefore be our proposed Y_2R-negative interneurons **(Figure 4)**.

Dendritic filtering causes synaptic events of more distal origin to appear slower and of lower amplitude (when measured with somatic recordings). Disinhibition of PV interneurons, which synapse more proximally on PNs, could thus explain the increase in large amplitude sIPSCs. If this were the case, these larger amplitude events should also display faster kinetics.

To quantify IPSC kinetics, we measured the slope of the unitary sIPSC rising phase (Methods), a parameter that does not vary with changes in event amplitude. An increase in this parameter indicates faster risetime kinetics in a population of events **(Figure 5B),** and would be consistent with a synaptic event occurring closer to the cell soma (Maccaferri et al., 2000).

10/34 PNs responded to [ahx$^{5-24}$]NPY (1 μM) application with a reversible increase in the mean sIPSC rise slope; from 15.1 ± 1.6 pA/ms to 20.4 ± 2.4 pA/ms (p<0.01; n=10) **(Figure 5C)**. Additionally, 2 PNs showed substantially increased rise kinetics, which did not reverse with washout. PNs responding to [ahx$^{5-24}$]NPY with increased sIPSC kinetics also virtually always also showed an increase in mean event amplitude. Interestingly, in the presence of TTX (500 nM), [ahx$^{5-24}$]NPY had no effects on mIPSC kinetics.

2.3d Y$_2$R-mediated increases in PN sIPSCs do not require glutamate transmission

BLA PNs are known to target PV interneurons with excitatory collateral projections (Smith et al., 2000). Experiments conducted in TTX suggested that [ahx$^{5-24}$]NPY disinhibits the majority of BLA PNs. This disinhibition could therefore increase excitatory drive from PNs onto PV interneurons and recruit feedback inhibition. Such feedback inhibition could underlie the [ahx$^{5-24}$]NPY-mediated increases in large

amplitude sIPSCs. We therefore conducted experiments in the presence of the non-selective glutamate receptor antagonist kyneurenic acid (1 mM) to determine if excitatory transmission is required for facilitation of large amplitude sIPSC by [ahx$^{5-24}$]NPY.

In the presence of kyneurenic acid PNs continued to respond to [ahx$^{5-24}$]NPY (1 µM) with increased sIPSCs amplitudes and frequencies, similar to effects observed in the absence of the glutamate blocker **(Figure 6)**. These results suggest that the Y_2 receptor-mediated increases in large amplitude sIPSC are not dependent on excitatory synaptic transmission, and would therefore be consistent with a mechanism mediated via disinhibition of PV interneurons.

2.3e Y_2 receptors are expressed by SOM/NPY interneurons in mice

Based on the above electrophysiological findings we predicted that SOM interneurons will express presynaptic Y_2 receptors. Activation of these SOM interneuron Y_2 receptors would result in the disinhibition of PN dendrites as well as disinhibition of another interneuron type. To test this hypothetical circuit we next sought to determine the BLA neuron types that express Y_2 receptors. Because receptors are relatively rare proteins and receptor antibodies are often unreliable, we instead took advantage of a mouse model in which animals expressed TdTomato conditionally in neurons that expressed cre recombinase under control of the Y_2 receptor gene promoter. This allowed for visual identification of Y_2 receptor expressing neurons based on TdTomato fluorescence.

We first verified that mouse BLA PNs responded to [ahx$^{5-24}$]NPY with similar effects on sIPSCs as seen in rat BLA. Similar to the rat data, bath application of [ahx$^{5-24}$]NPY (1 µM) reversibly increased the amplitude and/or frequency of sIPSC in a subset

of PNs in mouse BLA, while other PNs responded to $[ahx^{5-24}]$NPY with a reversible decrease in sIPSC frequency and no effect on amplitude. Interestingly a number of PNs clearly expressed TdTomato fluorescence, in addition to numerous interneurons. These Y_2 receptor-expressing PNs will be discussed in in Chapter 5.

To determine which BLA neuron types express Y_2 receptors, Dr. Urban's lab performed immunohistochemistry on BLA-containing brain sections from Y_2R-TdTomato mice. Based on double-label immunofluorescence, Dr. Urban's group observed that the great majority (95%) of BLA SOM interneurons also co-expressed NPY. Importantly TdTomato fluorescence was observed in all NPY/SOM neurons counted, but was not seen in interneurons expressing only SOM **(Figure 7B)**. These results suggest Y_2 receptors function as auto-receptors within the BLA interneuron population. With rare exceptions, TdTomato fluorescence was not observed in cells expressing the interneuron markers PV or calbindin. Staining for the PN marker calcium calmodulin dependent kinase type II (CaMKII) confirmed that many PNs also expressed TdTomato fluorescence.

2.4 DISCUSSION

Y_2 receptor activation has been reported to have a paradoxical effect on behavior relative to NPY itself. Specifically, selective Y_2 receptor activation mediates a behaviorally anxiogenic response, in contrast to the robustly anxiolytic actions of NPY (Sajdyk et al., 2002a). Here we show that the selective Y_2 receptor agonist, [ahx$^{5-24}$]NPY (1 μM) decreased the frequency of GABA$_A$-mediated mIPSCs in the majority of rat BA PNs tested, consistent with a presynaptic mechanism. Furthermore, since these effects were observed in the presence of TTX, they likely reflect direct actions on interneurons expressing presynaptic Y_2 receptors. This overall disinhibition of BLA output neurons likely results in the observed anxiogenic behavioral effects of Y_2 agonist application to the BLA.

In the absence of TTX, we observed in about 1/3 of BLA PNs what appeared to be an increase in the frequency of rapidly rising, large amplitude sIPSCs. Other PNs responded with a decrease in sIPSC frequency and no effect on amplitude, similar to the effects more uniformly observed in TTX.

This increase in rapidly-rising, large amplitude sIPSCs was likely due to the disinhibition of a class of interneurons, since it was never observed in the presence of TTX. Furthermore, this effect was not blocked by kyneurenic acid, indicating that [ahx$^{5-24}$]NPY could increase GABA events independently of glutamate-mediated excitation. Based on the large amplitude and fast kinetics of these [ahx$^{5-24}$]NPY enhanced events, we reasoned that they originate from more proximal GABA synapses such as those made by PV interneurons onto BLA PNs.

Thus, we have observed two distinct Y_2 receptor-mediated effects: direct disinhibition of PNs and disinhibition of another interneuron type, which likely innervates more proximal PN domains. We suspect that both of these actions are mediated via Y_2 receptor expressing SOM interneurons for the following reasons. Firstly, SOM interneurons send inhibitory projections to PNs as well as to PV interneurons (Muller et al., 2006). Secondly, Y_2 receptors often function as auto-receptors and, within the BLA, many SOM interneurons co-express NPY (McDonald, 1989). Third, we observed that nearly all of these SOM/NPY interneurons express TdTomato in the BLA of Y_2R-TdTomato mice. Finally, SOM interneurons primarily innervate PN distal dendrites (Muller et al., 2006). This is consistent with the [ahx$^{5-24}$]NPY mediated shift towards larger amplitude, faster spontaneous PN GABA events when interneurons, which presumably target more proximal PN domains, are disinhibited.

Immunohistochemical data from the Y_2R-TdTomato mouse are consistent with our rat electrophysiology findings. In mouse, most (if not all) NPY-SOM interneurons expressed Y_2 receptors. Also consistent with our model, PV type interneurons did not express Y_2 receptors and could thus underlie the [ahx$^{5-24}$]NPY mediated actions on fast, large amplitude GABA events. However, SOM interneurons also send inhibitory projections to another group of interneurons, characterized by expression of vasoactive intestinal peptide (VIP) (Muller et al., 2006). Direct recordings from PV interneurons will be necessary to clarify whether these cells are indeed disinhibited via Y_2 receptor activation.

2.5 FUNCTIONAL IMPLICATIONS

TTX experiments indicate that the majority of PNs (~85%) are disinhibited by [ahx$^{5-24}$]NPY, likely via direct actions on GABA terminals from NPY/SOM interneurons. PN dendrites are presumably disinhibited at a similar rate in the absence of TTX. However, due to the emergence of larger amplitude, action potential dependent GABA events in some neurons, this was not always apparent. PN excitability data (Chapter 3) suggest that distal inhibition is indeed reduced, even in those cells showing increases in larger amplitude IPSCs. Y$_2$ receptor-mediated disinhibition of PN dendrites thus provides a probable mechanism for the anxiogenic behavior effects of selective Y$_2$ receptor activation.

The [ahx$^{5-24}$]NPY-mediated increase in proximal inhibition seen in some but not all PNs has several possible implications. One possibility is that these large amplitude events lessen the anxiogenic output of BLA PNs, partly counteracting [ahx$^{5-24}$]NPY-mediated dendritic inhibition in a subpopulation of neurons. Alternatively, these events could synchronize PN output and contribute to the anxiogenic actions of selective Y$_2$ receptor activation.

Populations of PV interneurons are thought to synchronize BLA PN output. Furthermore, the anxiogenic neuropeptides corticotrophin releasing factor (CRF) and cholecystokinin (CCK) have been reported to facilitate synchronous large amplitude GABA$_A$ events, intermingled with excitatory events, termed compound postsynaptic potentials (CPSP) (Chung and Moore, 2009). However, CPSPs are inhibited by NPY (Chung and Moore, 2009). Furthermore CPSPs and other synchronizing GABA events have been shown to require excitatory transmission within the BLA (Chung and Moore,

2009; Popescu and Paré, 2011). By contrast [ahx$^{5-24}$]NPY continued to increase large amplitude sIPSCs even in the presence of kyneurenic acid.

Alternatively, these [ahx$^{5-24}$]NPY-mediated large amplitude GABA events may contribute to the overall anxiolytic effects of NPY by decreasing the excitability of some PNs. Indeed, it has been reported that Y_1 receptor activation also increases GABA inhibition of BLA PNs (Molosh et al., 2013). Thus Y_1 and Y_2 receptor actions may cooperate to facilitate GABA-mediated inhibition of subsets of BLA PNs.

It has become clear over the past decade that not all BLA PNs mediate fear and anxiety. Instead, specific PN populations also appear to decrease fear behaviors by facilitating extinction of conditioned fear (Herry et al., 2008; Senn et al., 2014). Since [ahx$^{5-24}$]NPY increased large amplitude IPSCs in only a subset of responsive PNs, it is possible that fear-coding PNs may selectively receive these large amplitude IPSCs. In the context of the anxiolytic full agonist NPY, these Y_2 receptor actions could facilitate selective inhibition of fear neurons. In contrast, Y_2 receptor effects would preferentially disinhibit extinction neurons. Fear and extinction neurons can be identified based on distinct patterns of afferent connectivity (Senn et al., 2014). Thus, future electrophysiology studies in conjunction with retrograde tracers could clarify whether fear neurons are the preferential targets of [ahx$^{5-24}$]NPY mediated proximal inhibition.

2.6 Y_2 RECEPTOR ACTIONS ON SOM INTERNEURONS – IMPLICATIONS FOR PLASTICITY

Our findings suggest that [ahx$^{5-24}$]NPY disinhibits PNs via Y_2 receptors expressed on SOM/NPY interneurons. Such Y_2 receptor actions provide a compelling mechanism for the reported anxiogenic behavioral effects of selective Y_2 receptor agonists (Sajdyk et al., 2002b). However, the question remains as to why NPY, which is itself anxiolytic, exerts these actions via its Y_2 receptors. The answer to this question may lie in part in the longer-term behavior effects elicited by NPY within the BLA. These actions suggest that NPY induces plastic changes in BLA circuitry (Gutman et al., 2008; Sajdyk et al., 2008)(Silveira et al (unpublished)).

Excitatory synaptic inputs reach PNs predominantly at spines on distal dendrites (Smith and Pare, 1994; Farb and LeDoux, 1999). These spines are, in turn, though to be principal sites of synaptic plasticity (Segal, 2005). Since SOM interneurons primarily innervate distal dendritic domains they are thought to regulate synaptic plasticity by dampening Ca^{2+} signaling (Chiu et al., 2013). In the context of NPY's global actions within the BLA, a Y_2R-mediated reduction in GABA inhibition from NPY/SOM interneurons may therefore facilitate anxiety-reducing plasticity. This hypothesis will be revisited in subsequent chapters.

2.7 FIGURES

Figure 1: [ahx$^{5-24}$]NPY Reduces mIPSC Frequency
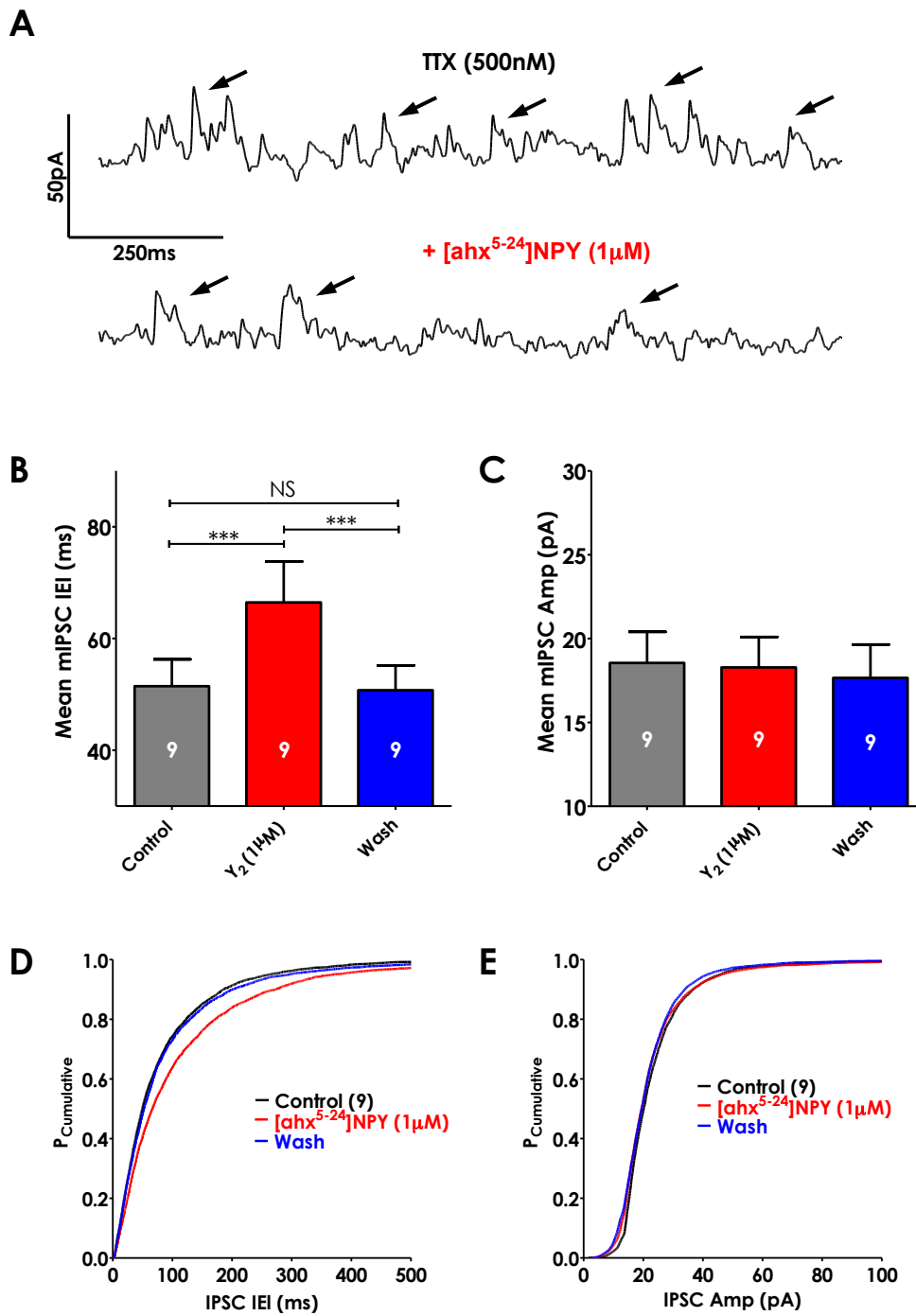
Figure 1: [ahx$^{5-24}$]NPY Reduces mIPSC Frequency

(A) Representative PN voltage clamp traces (-14 mV holding potential) in the presence of TTX (500 nM). Miniature inhibitory postsynaptic currents (mIPSC), seen as upward current deflections, occur frequently under control conditions (~20 Hz) (Top trace). Following bath application of [ahx$^{5-24}$]NPY (1 μM) fewer mIPSCs are observed (bottom trace).

(B) [ahx$^{5-24}$]NPY (1 μM) significantly and reversibly increased the mean PN mIPSC inter event interval (IEI) from 51.5 ± 4.8ms to 66.5 ± 7.3ms ($p<0.001$; n=9) in 9/12 PNs, indicating a reduction in mIPSC frequency.

(C) [ahx$^{5-24}$]NPY (1 μM) had no effect on mean PN mIPSC amplitude.

(D) PN mIPSC IEIs displayed in a cumulative probability histogram. The first 500 events detected per neuron under each condition were pooled (in control conditions, following bath application of [ahx$^{5-24}$]NPY (1 μM), and after prolonged (10-15 min) drug washout). [ahx$^{5-24}$]NPY reversibly decreased PN mIPSC frequency, seen here as a rightward shift in the cumulative probability curve.

(E) PN mIPSC amplitudes displayed in a cumulative probability histogram. The first 500 events detected per neuron were pooled and compared as above.

Figure 2: 1/3 of PNs Responded to [ahx$^{5-24}$]NPY With Reduced sIPSC Frequency (no Effect on Amplitude)
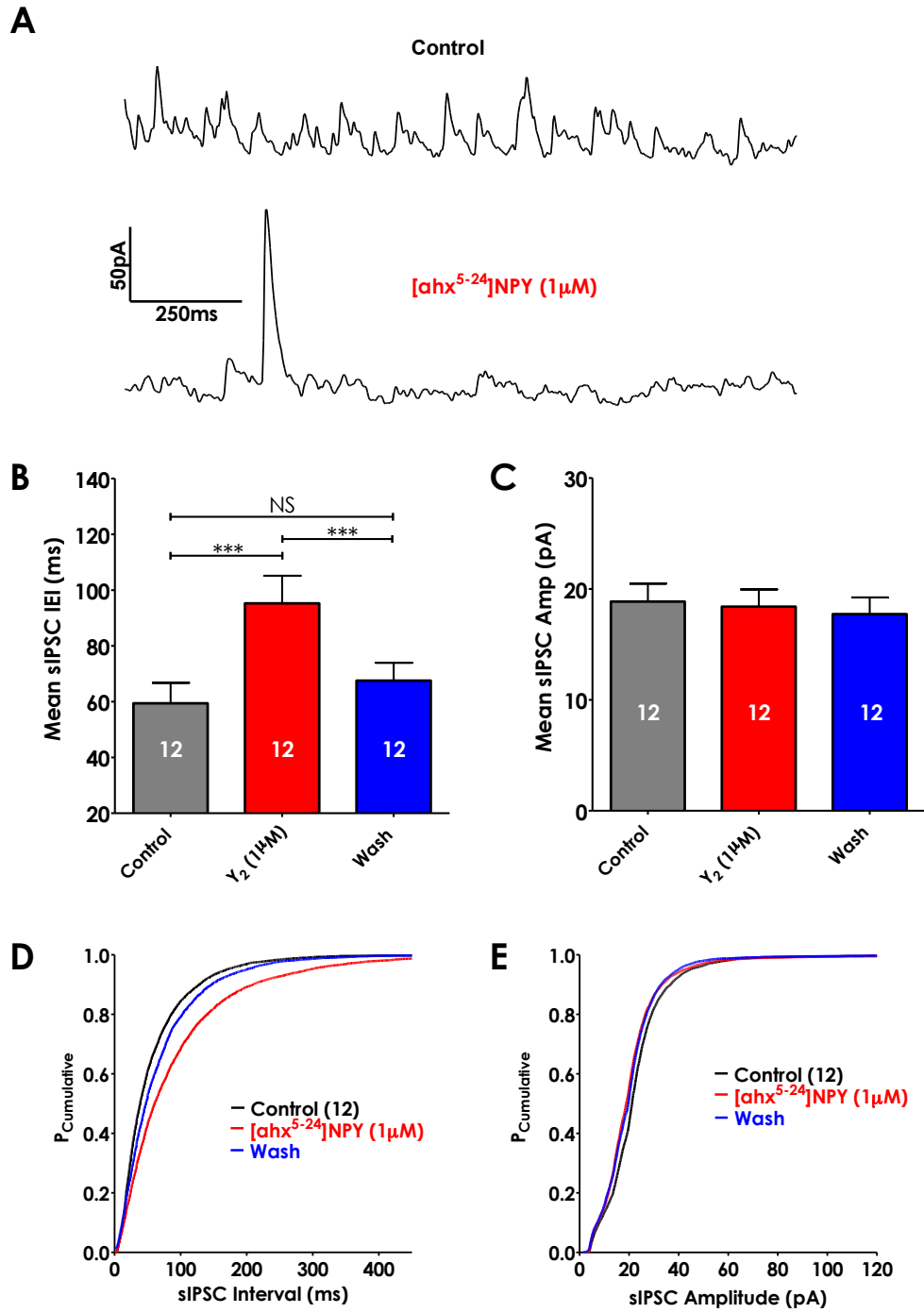
Figure 2: 1/3 of PNs Responded to [ahx$^{5\text{-}24}$]NPY With Reduced sIPSC Frequency (no Effect on Amplitude)

(A) Representative PN voltage clamp traces at a -14 mV holding potential, recorded using a Cs$^+$ pipette solution. Spontaneous inhibitory postsynaptic currents (sIPSC), seen as upward current deflections, are frequent under control conditions (~35 Hz) (Top trace). Following bath application of [ahx$^{5\text{-}24}$]NPY (1 μM) sIPSC frequency is substantially decreased (bottom trace), though occasional large amplitude events are observed.

(B) [ahx$^{5\text{-}24}$]NPY (1 μM) significantly and reversibly increased the mean PN sIPSC inter event interval (IEI) from 59.4 ± 7.3 ms to 95.3 ± 9.9 ms (p<0.001; n=12) in 12/34 PNs, indicating a reduction in sIPSC frequency.

(C) [ahx$^{5\text{-}24}$]NPY (1 μM) had no effect on mean sIPSC amplitude in these 12 PNs.

(D) sIPSC IEIs (from the 12 PNs) displayed in a cumulative probability histogram. The first 500 events detected per neuron were pooled under control conditions, following bath application of [ahx$^{5\text{-}24}$]NPY (1 μM), and after prolonged (10-15 min) drug washout. [ahx$^{5\text{-}24}$]NPY reversibly decreased sIPSC frequency, seen here as a rightward shift in the cumulative probability curve.

(E) sIPSC amplitudes (pooled as in Figure 1 from the 12 PNs) recorded under conditions indicated are displayed in a cumulative probability histogram.

Figure 3: [ahx⁵⁻²⁴]NPY Increased Large Amplitude PN sIPSCs

A
[ahx$^{5-24}$]NPY (1μM)
100pA
5min

B
Control

[ahx5-24]NPY (1μM)
100pA
250ms

C
Mean sIPSC Amp (pA)
NS
***   ***
13   13   13
Control   Y$_2$ (1μM)   Wash

D
Mean sIPSC IEI (ms)
NS
**   ***
7   7   7
Control   Y$_2$ (1μM)   Wash

E
Events
■ Control
■ [ahx$^{5-24}$]NPY (1μM)
■ Wash
sIPSC Amp (5pA Bins)
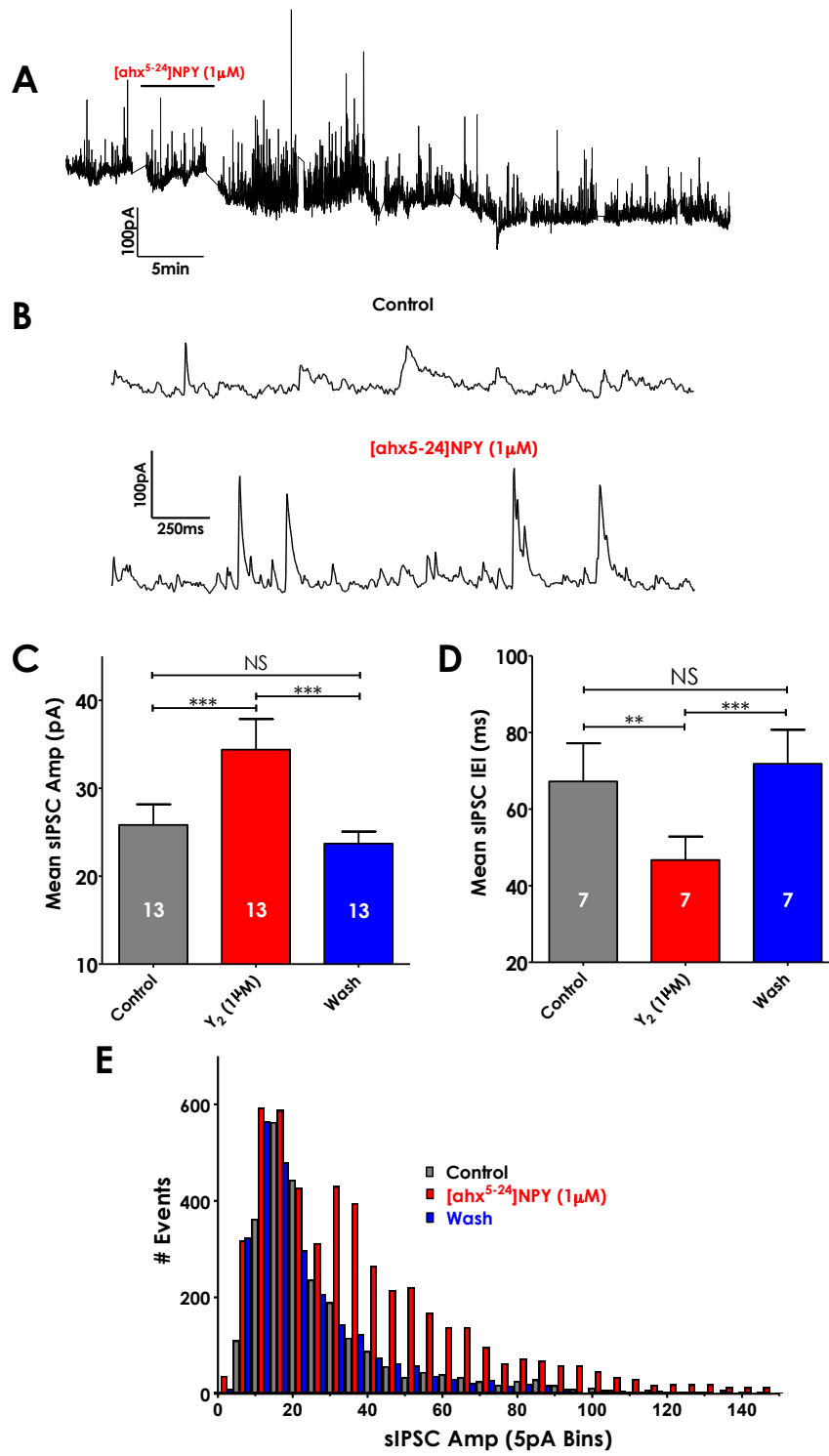
Figure 3: [ahx$^{5\text{-}24}$]NPY Increased Large Amplitude sIPSCs in 1/3 of PNs

(A) Representative voltage clamp traces (-14 mV holding potential, Cs$^+$ pipette) from a PN which responded to [ahx$^{5\text{-}24}$]NPY (1 μM) with a reversible increase in large amplitude sIPSCs. Over 40 minutes of recordings are displayed to illustrate the full time course of the response; intervening straight lines indicate times when other data was recorded.

(B) Representative PN voltage clamp traces (-14 mV holding potential, Cs$^+$ pipette). Spontaneous inhibitory postsynaptic currents (sIPSC) are seen as upward current deflections. Under control conditions (Top) sIPSC are of lower amplitude and less frequent than following bath application of [ahx$^{5\text{-}24}$]NPY (1 μM) (bottom).

(C) [ahx$^{5\text{-}24}$]NPY (1 μM) significantly and reversibly increased the mean PN sIPSC amplitude (p<0.001; n=13) in 13/34 PNs.

(D) [ahx$^{5\text{-}24}$]NPY (1 μM) significantly and reversibly decreased the mean PN sIPSC inter event interval (IEI) (p<0.01; n=7) in 7/34 PNs, indicating an increase in sIPSC frequency.

(E) Amplitude histogram from a representative PN in which [ahx$^{5\text{-}24}$]NPY (1 μM) substantially increased the frequency of large amplitude sIPSCs. sIPSCs, detected during 5 minutes of control recordings, 5 minutes during peak drug effects, and 5 minutes following prolonged drug washout were sorted into 5pA bins and displayed as bars representing the number of events detected in a given bin size.

Figure 4: Two Interneuron Circuit Model
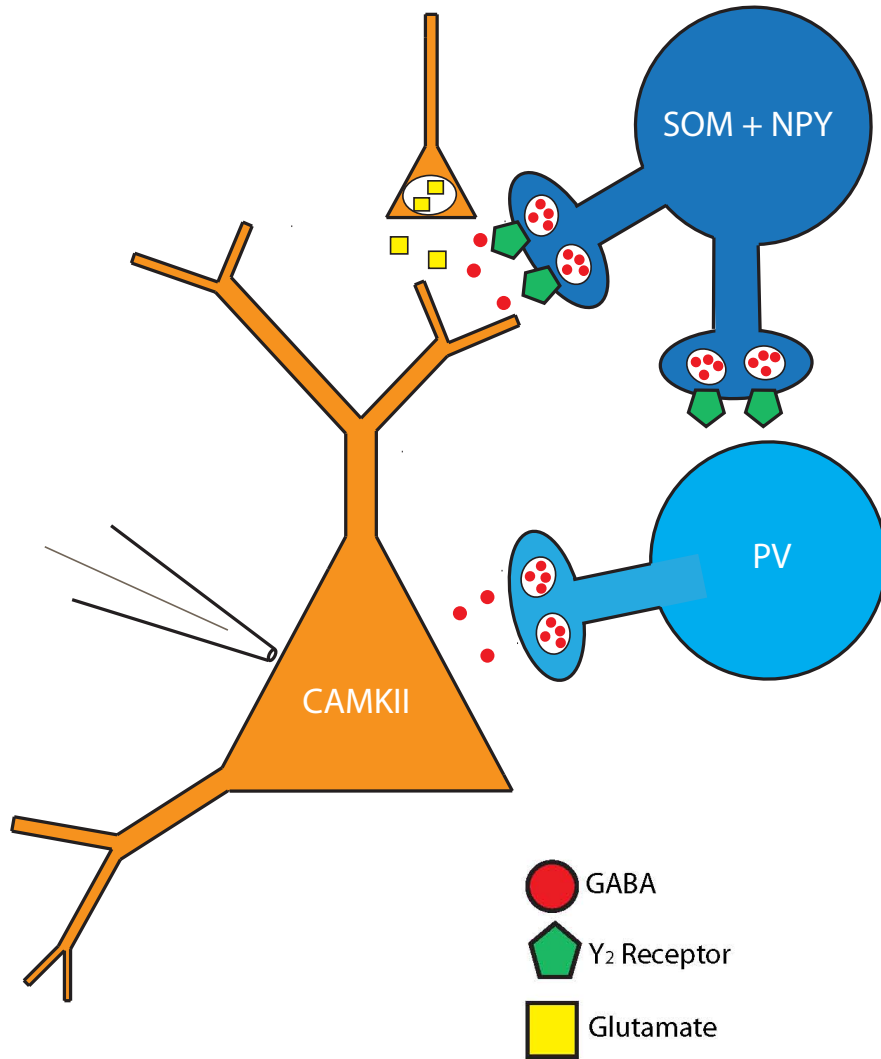
Figure 4: Two Interneuron Circuit Model

Circuit model proposed based on electrophysiology and imaging data. SOM/NPY interneurons, which express presynaptic Y_2 receptors, inhibit PN dendrites and PV interneurons. Activation of presynaptic Y_2 receptors decreases basal inhibition of both PN dendrites and PV interneurons. Disinhibition of PV increases proximal inhibition of PNs (this effect is not observed when Na^+ action potentials are blocked with TTX).

Figure 5: [ahx^{5-24}]NPY Increases sIPSC Kinetics
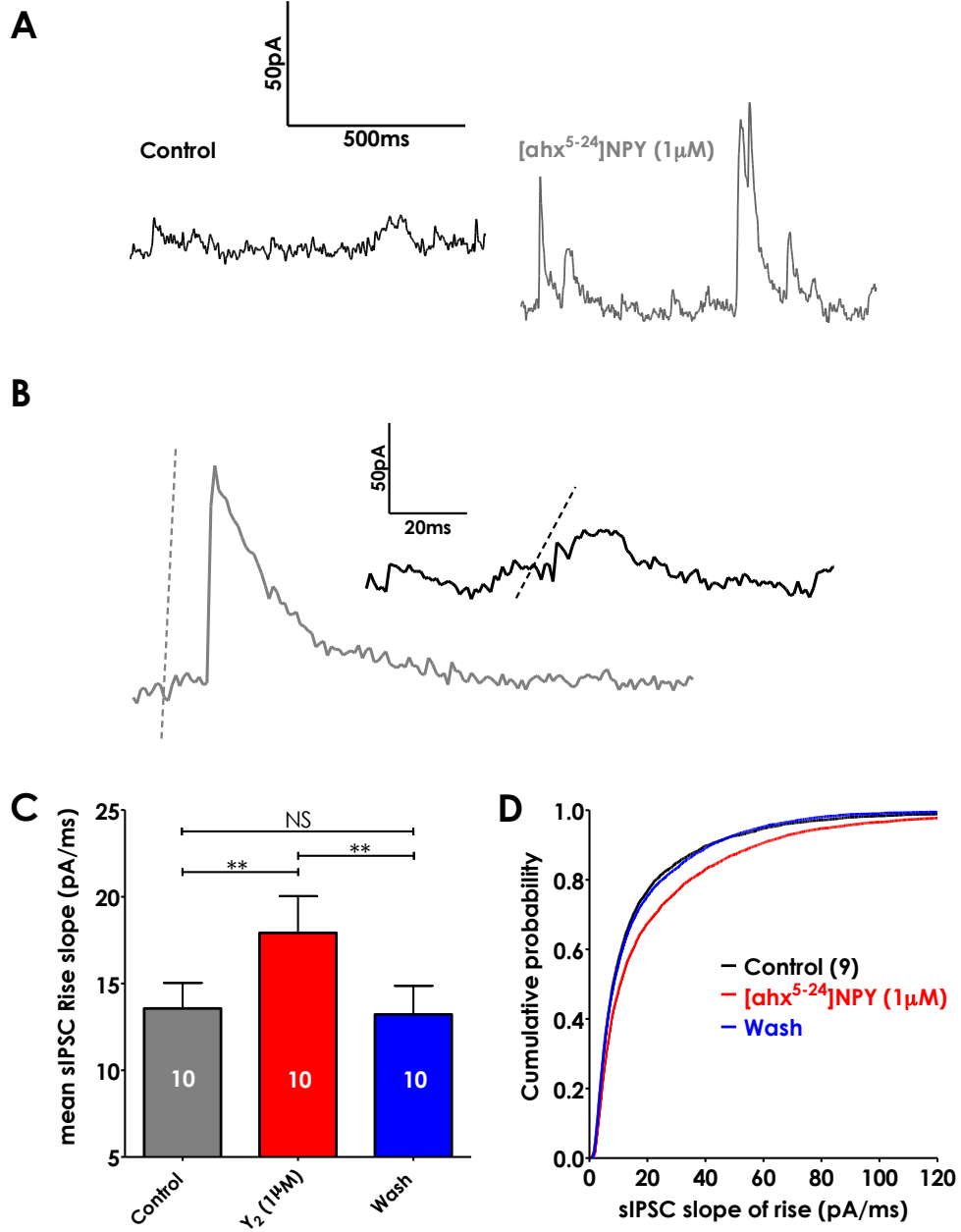
Figure 5: [ahx$^{5\text{-}24}$]NPY Increases sIPSC Kinetics

(A) Representative voltage-clamp traces from a PN (V_h = -14mV) in which [ahx$^{5\text{-}24}$]NPY (1 μM) increased the amplitude and rise time kinetics of sIPSCs.

(B) A larger amplitude, faster IPSC (Black) in comparison to a lower amplitude, slower kinetic event (Grey) (V_h = -14mV). The slope of sIPSC rising phase was measured.

(C) Bath application of [ahx$^{5\text{-}24}$]NPY (1 μM) significantly and reversibly increased the mean sIPSC rise slope (10-90%) from 15.1 ± 1.6 pA/ms to 20.4 ± 2.4 pA/ms ($p < 0.01$; n=10) in 10/34 PNs.

(D) Bath application of [ahx$^{5\text{-}24}$]NPY (1 μM) significantly and reversibly increased the mean sIPSC rise slope (10-90%) ($p < 0.01$; n=10) in 10/34 PNs. Larger values indicate faster risetimes.

Figure 6: Effects of [ahx$^{5-24}$]NPY on sIPSCs do Not Require Excitatory Transmission
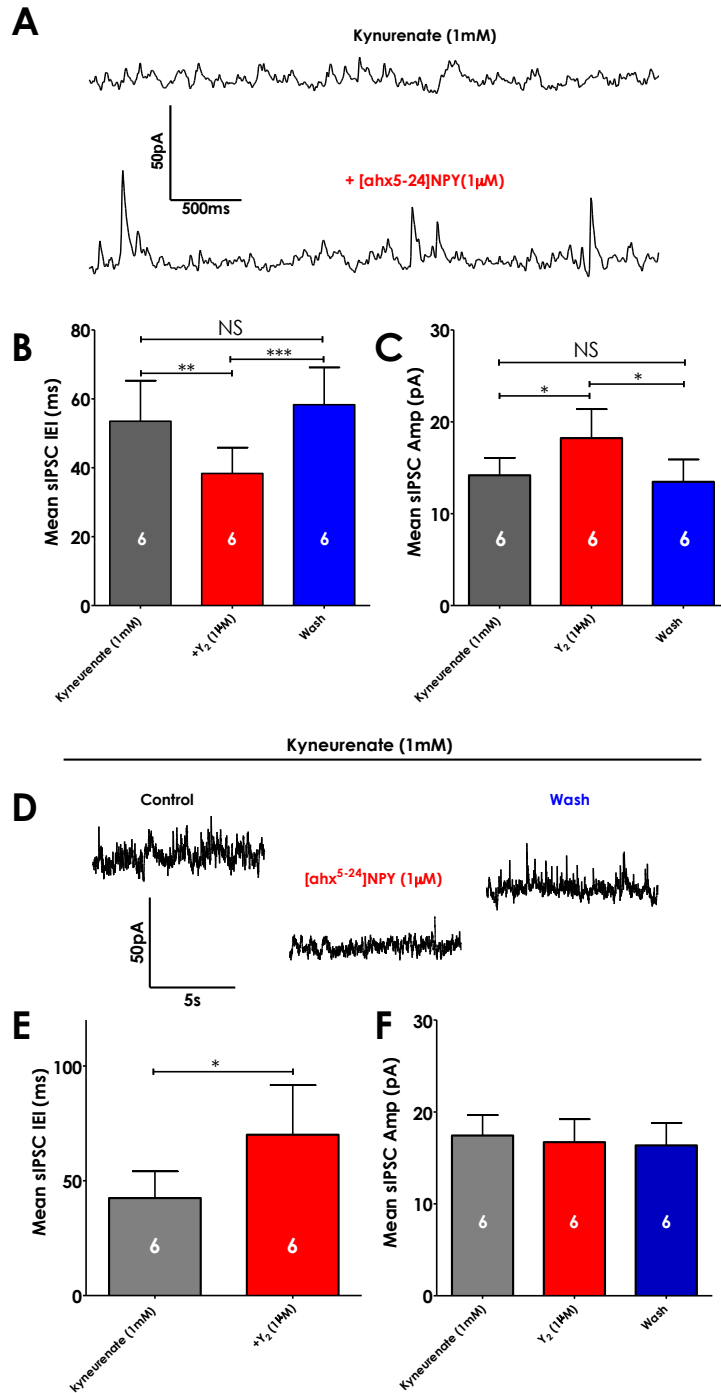
Figure 6: Effects of [ahx$^{5\text{-}24}$]NPY on sIPSCs do Not Require Excitatory Transmission

(A) Representative PN voltage clamp traces (-14 mV holding potential, Cs$^+$ pipette) in the presence of kyneurenic acid (1 mM). Spontaneous inhibitory postsynaptic currents (sIPSC) are seen as upward current deflections. Under control conditions (top trace) sIPSCs are of lower amplitude and less frequent than following bath application of [ahx$^{5\text{-}24}$]NPY (1 μM) (bottom trace).

(B) Bath application of [ahx$^{5\text{-}24}$]NPY (1 μM) (in the presence of kyneurenic acid (1mM)) significantly and reversibly decreased the mean sIPSC IEI (p<0.01; n=6) in 6/13 PNs.

(C) [ahx$^{5\text{-}24}$]NPY (1 μM) (in the presence of kyneurenic acid (1mM)) significantly and reversibly increased mean PN sIPSC amplitude from (p<0.05; n=6) in 6/13 PNs.

(D) Representative PN voltage clamp traces (-14 mV holding potential, Cs$^+$ pipette) in the presence of kyneurenic acid (1 mM). [ahx$^{5\text{-}24}$]NPY (1 μM) reversibly decreased the frequency of sIPSCs. Note change in holding current during Y$_2$ agonist application.

(E) In the presence of kyneurenic acid (1 mM) [ahx$^{5\text{-}24}$]NPY (1 μM) significantly decreased the mean PN sIPSC inter event interval (IEI) (p<0.05; n=6) in 6/13PNs, indicating an decrease in sIPSC frequency. This effect reversed in 3/6 PNs.

(F) In the presence of kyneurenic acid (1mM) [ahx$^{5\text{-}24}$]NPY (1 μM) had no effect on mean sIPSC amplitude in these 6/13 PNs.

Figure 7: Mouse NPY/SOM Interneurons Express Y$_2$ Receptors
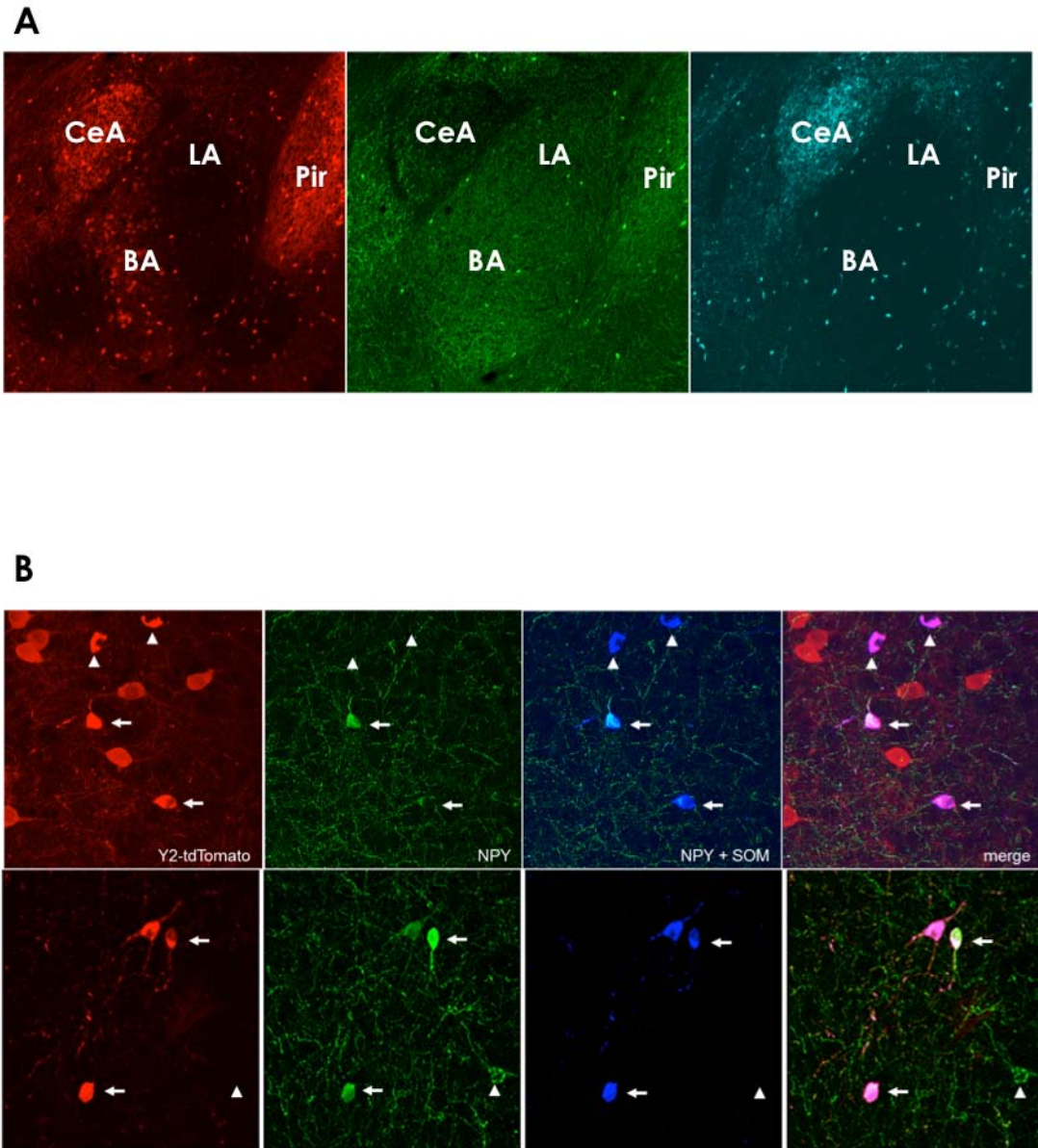
Figure 7: Mouse NPY/SOM Interneurons Express Y$_2$ Receptors

(A) BLA-containing Y$_2$R-TdTomato mouse brain slice. The right panel shows TdTomato fluorescence. The middle panel shows NPY immunofluorescence. The right panel shows SOM immunofluorescence.

(B) Illustrates co-localization of TdTomato fluorescence with SOM and NPY immunofluorescence in BLA interneurons. The far left panels show TdTomato fluorescence. The middle-left panels show NPY immunofluorescence. The middle-right panels show SOM immunofluorescence. Far right panels show merged images, indicating co-localization.

2.8 REFERENCES

Amano T, Unal CT, Paré D (2010) Synaptic correlates of fear extinction in the amygdala. Nat Neurosci 13:489–494.

Bueno CH, Zangrossi H, Viana MB (2005) The inactivation of the basolateral nucleus of the rat amygdala has an anxiolytic effect in the elevated T-maze and light/dark transition tests. Braz J Med Biol Res 38:1697–1701.

Capogna M (2014) GABAergic cell type diversity in the basolateral amygdala. Curr Opin Neurobiol 26:110–116.

Chen X, DiMaggio DA, Han SP, Westfall TC (1997) Autoreceptor-induced inhibition of neuropeptide Y release from PC-12 cells is mediated by Y2 receptors. Am J Physiol 273:H1737–H1744.

Chiu CQ, Lur G, Morse TM, Carnevale NT, Ellis-Davies GCR, Higley MJ (2013) Compartmentalization of GABAergic inhibition by dendritic spines. Science 340:759–762.

Chung L, Moore SD (2009) RAPID REPORTNEUROPEPTIDES MODULATE COMPOUND POSTSYNAPTIC POTENTIALS IN BASOLATERAL AMYGDALA. NSC 164:1389–1397.

Colmers WF, Bleakman D (1994) Effects of neuropeptide Y on the electrical properties of neurons. Trends Neurosci 17:373–379.

Farb CR, LeDoux JE (1999) Afferents from rat temporal cortex synapse on lateral amygdala neurons that express NMDA and AMPA receptors. Synapse 33:218–229.

Giesbrecht CJ, Mackay JP, Silveira HB, Urban JH, Colmers WF (2010) Countervailing Modulation of Ih by Neuropeptide Y and Corticotrophin-Releasing Factor in Basolateral Amygdala As a Possible Mechanism for Their Effects on Stress-Related Behaviors. Journal of Neuroscience 30:16970–16982.

Greber S, Schwarzer C, Sperk G (1994) Neuropeptide Y inhibits potassium-stimulated glutamate release through Y2 receptors in rat hippocampal slices in vitro. Br J Pharmacol 113:737–740.

Gutman AR, Yang Y, Ressler KJ, Davis M (2008) The Role of Neuropeptide Y in the Expression and Extinction of Fear-Potentiated Startle. Journal of Neuroscience 28:12682–12690.

Herry C, Ciocchi S, Senn V, Demmou L, Müller C, LUthi A (2008) Switching on and off fear by distinct neuronal circuits. Nature 454:600–606.

Likhtik E, Pelletier JG, Popescu AT, Paré D (2006) Identification of basolateral amygdala projection cells and interneurons using extracellular recordings. Journal of

Neurophysiology 96:3257–3265.

Maccaferri G, Roberts JD, Szucs P, Cottingham CA, Somogyi P (2000) Cell surface domain specific postsynaptic currents evoked by identified GABAergic neurones in rat hippocampus in vitro. The Journal of Physiology 524 Pt 1:91–116.

Mahanty NK, Sah P (1998) Calcium-permeable AMPA receptors mediate long-term potentiation in interneurons in the amygdala. Nature 394:683–687.

McDonald AJ (1984) Neuronal organization of the lateral and basolateral amygdaloid nuclei in the rat. J Comp Neurol 222:589–606.

McDonald AJ (1989) Coexistence of somatostatin with neuropeptide Y, but not with cholecystokinin or vasoactive intestinal peptide, in neurons of the rat amygdala. Brain Research 500:37–45.

McDonald AJ (1996) Glutamate and aspartate immunoreactive neurons of the rat basolateral amygdala: colocalization of excitatory amino acids and projections to the limbic circuit. J Comp Neurol 365:367–379.

McDonald AJ, Betette RL (2001) Parvalbumin-containing neurons in the rat basolateral amygdala: morphology and co-localization of Calbindin-D(28k). NSC 102:413–425.

Molosh AI, Sajdyk TJ, Truitt WA, Zhu W, Oxford GS, Shekhar A (2013) NPY Y1 receptors differentially modulate GABAA and NMDA receptors via divergent signal-transduction pathways to reduce excitability of amygdala neurons. Neuropsychopharmacology 38:1352–1364.

Muller JF, Mascagni F, McDonald AJ (2006) Postsynaptic targets of somatostatin-containing interneurons in the rat basolateral amygdala. J Comp Neurol 500:513–529.

Nakajima M, Inui A, Asakawa A, Momose K, Ueno N, Teranishi A, Baba S, Kasuga M (1998) Neuropeptide Y produces anxiety via Y2-type receptors. Peptides 19:359–363.

Phan KL, Fitzgerald DA, Nathan PJ, Tancer ME (2006) Association between amygdala hyperactivity to harsh faces and severity of social anxiety in generalized social phobia. Biol Psychiatry 59:424–429.

Pitkänen A, Savander V, LeDoux JE (1997) Organization of intra-amygdaloid circuitries in the rat: an emerging framework for understanding functions of the amygdala. Trends Neurosci 20:517–523.

Popescu AT, Paré D (2011) Synaptic interactions underlying synchronized inhibition in the basal amygdala: evidence for existence of two types of projection cells. Journal of Neurophysiology 105:687–696.

Prater KE, Hosanagar A, Klumpp H, Angstadt M, Phan KL (2013) Aberrant amygdala-frontal cortex connectivity during perception of fearful faces and at rest in generalized social anxiety disorder. 30:234–241.

Rainnie DG, Asprodini EK, Shinnick-Gallagher P (1993) Intracellular recordings from morphologically identified neurons of the basolateral amygdala. Journal of Neurophysiology 69:1350–1362.

Rasmusson AM, Hauger RL, Morgan CA, Bremner JD, Charney DS, Southwick SM (2000) Low baseline and yohimbine-stimulated plasma neuropeptide Y (NPY) levels in combat-related PTSD. Biol Psychiatry 47:526–539.

Rosenkranz JA, Grace AA (1999) Modulation of basolateral amygdala neuronal firing and afferent drive by dopamine receptor activation in vivo. J Neurosci 19:11027–11039.

Rostkowski AB, Teppen TL, Peterson DA, Urban JH (2009) Cell-specific expression of neuropeptide Y Y1 receptor immunoreactivity in the rat basolateral amygdala. J Comp Neurol 517:166–176.

Sah R, Ekhator NN, Strawn JR, Sallee FR, Baker DG, Horn PS, Geracioti TD (2009) Low cerebrospinal fluid neuropeptide Y concentrations in posttraumatic stress disorder. Biol Psychiatry 66:705–707.

Sajdyk TJ, Johnson PL, Leitermann RJ, Fitz SD, Dietrich A, Morin M, Gehlert DR, Urban JH, Shekhar A (2008) Neuropeptide Y in the Amygdala Induces Long-Term Resilience to Stress-Induced Reductions in Social Responses But Not Hypothalamic-Adrenal-Pituitary Axis Activity or Hyperthermia. Journal of Neuroscience 28:893–903.

Sajdyk TJ, Schober DA, Gehlert DR (2002a) Neuropeptide Y receptor subtypes in the basolateral nucleus of the amygdala modulate anxiogenic responses in rats. Neuropharmacology 43:1165–1172.

Sajdyk TJ, Schober DA, Smiley DL, Gehlert DR (2002b) Neuropeptide Y-Y2 receptors mediate anxiety in the amygdala. Pharmacol Biochem Behav 71:419–423.

Sajdyk TJ, Shekhar A (1997) Excitatory amino acid receptor antagonists block the cardiovascular and anxiety responses elicited by gamma-aminobutyric acidA receptor blockade in the basolateral amygdala of rats. J Pharmacol Exp Ther 283:969–977.

Sajdyk TJ, Vandergriff MG, Gehlert DR (1999) Amygdalar neuropeptide Y Y1 receptors mediate the anxiolytic-like actions of neuropeptide Y in the social interaction test. European Journal of Pharmacology 368:143–147.

Segal M (2005) Dendritic spines and long-term plasticity. Nat Rev Neurosci 6:277–284.

Senn V, Wolff SBE, Herry C, Grenier F, Ehrlich I, Gründemann J, Fadok JP, Müller C,

Letzkus JJ, LUthi A (2014) Long-range connectivity defines behavioral specificity of amygdala neurons. 81:428–437.

Shekhar A, Sajdyk TS, Keim SR, Yoder KK, Sanders SK (1999) Role of the basolateral amygdala in panic disorder. Ann N Y Acad Sci 877:747–750.

Smith Y, Pare D (1994) Intra-amygdaloid projections of the lateral nucleus in the cat: PHA-L anterograde labeling combined with postembedding GABA and glutamate immunocytochemistry. J Comp Neurol 342:232–248.

Smith Y, Paré JF, Pare D (2000) Differential innervation of parvalbumin-immunoreactive interneurons of the basolateral amygdaloid complex by cortical and intrinsic inputs. J Comp Neurol 416:496–508.

Sosulina L, Schwesig G, Seifert G, Pape H-C (2008) Neuropeptide Y activates a G-protein-coupled inwardly rectifying potassium current and dampens excitability in the lateral amygdala. Mol Cell Neurosci 39:491–498.

Stanić D, Brumovsky P, Fetissov S, Shuster S, Herzog H, Hökfelt T (2006) Characterization of neuropeptide Y2 receptor protein expression in the mouse brain. I. Distribution in cell bodies and nerve terminals. J Comp Neurol 499:357–390.

Walker DL, Miles LA, Davis M (2009) Selective participation of the bed nucleus of the stria terminalis and CRF in sustained anxiety-like versus phasic fear-like responses. Prog Neuropsychopharmacol Biol Psychiatry 33:1291–1308.

Washburn MS, Moises HC (1992a) Inhibitory responses of rat basolateral amygdaloid neurons recorded in vitro. NSC 50:811–830.

Washburn MS, Moises HC (1992b) Electrophysiological and morphological properties of rat basolateral amygdaloid neurons in vitro. Journal of Neuroscience 12:4066–4079.

Wolak ML, DeJoseph MR, Cator AD, Mokashi AS, Brownfield MS, Urban JH (2003) Comparative distribution of neuropeptide Y Y1 and Y5 receptors in the rat brain by using immunohistochemistry. J Comp Neurol 464:285–311.

Chapter 3

Selective NPY Y_2 Receptor Activation Excites BLA Principal Neurons By Reducing Tonic GABA Inhibition

3.1 INTRODUCTION

Fear and anxiety are adaptive emotions displayed by many animals, including humans. These emotions orchestrate behavioral and physiological responses to perceived threats and thereby generally facilitate survival. The basolateral amygdala (BLA) is a critical component of the conserved brain circuitry mediating these defensive emotions (Maren, 1999). The BLA integrates multimodal sensory information, based on which fear and anxiety responses may be coordinated via its afferent projections (Pitkänen et al., 1997; Rogan et al., 1997; LeDoux, 2000; Walker et al., 2009; Amano et al., 2010). BLA output, in turn, is mediated via complex glutamatergic principal neurons (PN) (McDonald, 1984; 1996), whose activity is normally highly constrained by a small but diverse group of local GABA interneurons (Capogna, 2014).

Inappropriately elevated amygdala activity has been linked to multiple human anxiety disorders (Shekhar et al., 1999; Phan et al., 2006; Prater et al., 2013). Much effort has therefore been directed towards understanding BLA circuitry, and in particular how endogenous neuromodulators shape its output. One such compound is neuropeptide Y (NPY), a 36 amino acid peptide highly expressed throughout the mammalian brain. Injection of NPY directly into the BLA is acutely anxiolytic (Sajdyk et al., 1999). Furthermore, NPY appears to induce longer-term, anxiety-reducing neural plastic changes within the BLA (Gutman et al., 2008; Sajdyk et al., 2008).

The NPY Y_1, Y_2 and Y_5 receptors are expressed in the BLA. All of these receptors are $G_{i/o}$ G-protein coupled but are likely expressed in distinct neuron types and cellular domains (Wolak et al., 2003; Rostkowski et al., 2009; Stanić et al., 2011). The acute anxiolytic effects of NPY appear to be largely mediated by BLA Y_1 receptors

(Sajdyk et al., 1999). In contrast selective activation of BLA Y_2 receptors increases anxiety-like behaviors (Sajdyk et al., 2002).

We have previously shown that selective activation of BLA Y_2 receptors directly decreases synaptic, $GABA_A$-mediated inhibition of PNs. This action likely involves NPY/somatostatin (SOM) interneurons, which express Y_2 receptors (Chapter 2) and target PN dendrites (Muller et al., 2006). However, additional effects were observed in a subpopulation of PNs. In these PNs, synaptic $GABA_A$ inhibition of more proximal cell domains was increased most likely via the disinhibition of another interneuronal subtype (Chapter 2).

However, it is unclear how these complex Y_2 receptor effects on GABA transmission affect BLA PN excitability. Here, we have determined how selective Y_2 receptor activation impacts PN excitability. Additionally, we aimed to gain further insights into how the actions of Y_2 receptors within the BLA contribute to NPY's overall anxiolytic actions.

We report here that the Y_2 receptor selective agonist [ahx$^{5-24}$]NPY increases PN excitability. Somewhat unexpectedly, these Y_2 receptor effects largely result from a reduction in a G-protein coupled, inwardly rectifying K^+ channel (GIRK) current, mediated in turn by a loss of tonic $GABA_B$-receptor activation. Because postsynaptic $GABA_B$ receptors are expressed on PN dendrites and $GABA_B$-GIRK currents suppress the NMDA receptor-mediated dendritic calcium signaling needed for synaptic plasticity (Morrisett et al., 1991; Otmakhova, 2004), this action may facilitate NPY-mediated plasticity.

3.2 MATERIALS AND METHODS

3.2a Animals

Male Sprague Dawley rats 6-16 weeks of age were used for experiments. The care and use of animals was in accordance with standards set by the University of Alberta Animal Care and Use Committee: Health Sciences, in compliance with regulations by the Canadian Council on Animal Care. Animals were group housed (2-3 per cage) with food and water supplied *ad libitum*.

3.2b Brain Slice Preparation

Rats were decapitated, their brains rapidly removed and submerged in an icy slurry of artificial CSF (ACSF) optimized for slice preparation, containing (in mM): 118 NaCl, 3 KCl, 1.3 $MgSO_4$, 1.4 NaH_2PO_4, 5 $MgCl_2 \cdot 6H_2O$, 10 glucose, 26 $NaHCO_3$ and 1.5 $CaCl_2$. "Slice solution" was continuously bubbled with carbogen (95 %O_2, 5% CO_2) and was supplemented with kynurenic acid (1 mM) to prevent glutamate-mediated excitatory toxicity. Coronal brain slices (300 μm) containing the BLA were prepared with a vibrating slicer (Slicer HR2; Sigmann Elektronik). Slices were then transferred to a carbogenated ACSF ("Bath") solution, which contained the following (in mM); 124 NaCl, 3KCl, 1.3 $MgSO_4$, 1.4 NaH_2PO_4, 10 glucose 26 $NaHCO_3$, and 2.5 $CaCl_2$ (300 – 305 mOsm/L). Slices were stored in room temperature (22 °C) carbogen-bubbled bath solution for at least 30min following slicing; bath solution was used to perfuse slices for the remainder of all experiments. For electrophysiology experiments, slices were placed into a recording chamber attached to a fixed stage of a movable upright microscope (Axioskop FS2; Carl Zeiss) and held submerged by a platinum and polyester fiber "harp".

Slices were continuously perfused with warmed (34 ± 0.5 °C), carbogenated bath solution at a rate of 2-3ml/min for at least 20min prior to recording.

3.2c Electrophysiology

Patch pipettes were pulled from thin-walled, filamented borosilicate glass (TW150F; WPI, Sarasota, FL) with a two-stage puller (PP-83; Narishige) to a tip resistance of 5-7 MΩ when back-filled with an internal solution containing in (mM): 126 K-gluconate, 10 HEPES, 4 KCl, 5 MgATP, 0.3 NaGTP, 1 EGTA, 0.3 CaCl$_2$. Neurobiotin (0.05 − 0.1%) was added and the pH adjusted to 7.27 − 7.30 with KOH, (275 − 285 mOsm/L). A modified internal solution containing 126 mM Cs-methanesulfonate in place of K-gluconate was used for several experiments; in this case pH was adjusted with CsOH; otherwise constituents, concentrations and other properties were identical to K$^+$ internal solution. Recordings were made using a Multiclamp 700B amplifier and data were acquired using pClamp (v 10.3 − 10.4) via a Digidata 1322 interface (all Molecular Devices, Sunnyvale, CA). Liquid junction potentials were calculated for K$^+$ and Cs$^+$ internal solutions as +14.4 mV and +13.8 mV respectively; all voltage and current clamp data reported have been adjusted to reflect this.

The BLA was identified in slices using criteria based on the Paxinos and Watson (1986) atlas. Here, we define the BLA as including both the basal and basal accessory nuclei, sometimes collectively referred to as the basal amygdala. Recordings were restricted to the BLA and avoided the LA.

BLA neurons were visually identified with infrared-differential contrast optics (DIC) and PNs selected for recordings based on a large, pyramidal- or stellate-shaped soma and a prominent apical dendrite. Local circuit interneurons could generally be

differentiated from PNs based on a smaller, more spherical soma. Once whole cell patch clamp configuration was established, electrophysiological properties were used in conjunction with morphology to characterize neurons (Washburn and Moises, 1992; Rainnie et al., 1993). Neurons judged to be PNs exhibited: low input resistance (30 – 100 MΩ), longer duration action potentials, with action potential half-width greater than 1 ms (approximately twice as long as most interneurons) (Mahanty and Sah, 1998) and prominent action potential spike frequency adaptation when brought above threshold with 800ms depolarizing current steps. PNs typically also typically demonstrated prominent action potential afterdepolarizations and initial doublet spike bursts.

In recordings using the K^+ internal solution, neurons were mainly held in voltage clamp at -75 mV for 5-10 min before start of experiments and between experimental manipulations. Recordings using the Cs^+ intracellular solution were treated similarly except neurons were held at -14 mV before and between measurements. A series of experimental protocols were performed at 5min intervals to establish the stability of baseline neuronal properties. Only neurons which showed stable resting membrane potentials (RMP) and holding currents (in voltage clamp) throughout a series of control measurements and which showed stable access resistance (± 20 %) during an experiment were selected for analysis.

During K^+ electrode recordings, RMP was measured periodically by averaging the potential during 30s long, passive current clamp recordings. Membrane potentials reported are all corrected for liquid junction potential.

3.2c(i) Current-clamp Experiments

Neuronal input resistance was measured in current clamp at the RMP with a series of 25 or 50 pA hyperpolarizing current steps and calculated using Ohms law (R = V/I). Current steps resulting in approximately 2-5 mV hyperpolarizations were chosen so as to minimally affect voltage-gated conductances. When drug applications changed RMP, direct current injection was used to return neurons to their control RMP for input resistance measurements.

Under our *in vitro* conditions using a K^+-gluconate pipette solution, PNs rarely if ever exhibited spontaneous action potentials. Therefore, to assess neuronal excitability in the absence or presence of drugs, we performed rheobase measurements. Rheobase was measured from the RMP in current clamp with a family of 800 ms depolarizing current ramps, of incrementally increasing amplitudes, as described previously (Giesbrecht et al., 2010). Typically a maximum of 8 ramps were used in each protocol. Rheobase current was defined as the depolarizing current magnitude at which the first action potential was elicited during a current ramp. Suites of ramps of the same depolarizing current magnitudes were used to compare rheobase in the absence or presence of test compounds unless dramatic changes in excitability occurred. Typically drug mediated changes in RMP were small; however, when large changes greater than ±5 mV occurred, rheobase measurements were taken both at the new RMP and with the neuron returned to control RMP via steady state current injection.

3.2c(ii) Voltage-clamp Experiments

Slow voltage clamp ramps were used to measure changes in steady state current-voltage (I-V) relationships. For recordings using the K^+ internal solution, neuron

membrane potential was ramped from the -75 mV holding potential to -135 mV over 2 seconds, held at -135 mV for 2 s, then slowly ramped (18 mV/ms) to -55 mV before returning it to the -75 mV.

In some recordings a Cs^+ methanesulphonate based intracellular solution was used to block K^+ channels, in this case an alternate voltage ramp protocol was used to reveal voltage-dependent Ca^{2+} currents in the PNs. Here, membrane potential was slowly (-50 mV/s) ramped from -14 mV to -124 mV, held at -124 mV for (1s), then ramped to +36 mV (300 mV/s) and returned to -14 mV.

Hyperpolarizing voltage steps were used to measure I_h in K^+ pipette recordings (Giesbrecht et al., 2010). As I_h activates slowly, these voltage steps were also used to differentiate drug effects on other membrane conductances from those on I_h. Families of 8 hyperpolarizing voltage steps were applied from a -55 mV holding potential, beginning with -10 mV and were successively increased by 10 mV to -135 mV; Steps also progressively decreased in length, the initial step lasted 1650 ms, with each successive step shortened by 100 ms. I_h magnitude at a given potential was determined as the difference between the peak current magnitude immediately after the voltage step and the steady state current at the end of the step. Analysis of I_h was restricted to PNs, which had initial I_h amplitudes of >150 pA at -135 mV. For each step, the step current immediately following the decay of the capacitative transient but preceding I_h activation was termed the instantaneous inward-rectifying current (I_{IR}). We have interpreted this I_{IR} as the membrane conductance in the absence of slowly activating I_h.

3.2d Materials

The Y_2 agonist [6-aminohexanoic[5-24]]NPY ([ahx[5-24]NPY]) was a gift from Dr. A. G. Beck-Sickinger (Leipzig, Germany). Baclofen was a gift from Ciba-Geigy. Kyneurenic acid was purchased from Abcam Biochemicals. GTP was purchased from Roche Diagnostics. CsCl, Cs^+-methanesulphonate, K^+-gluconate, EGTA, Mg•ATP, CsOH and ivabradine were obtained from Sigma-Aldrich. TTX was purchased from Alomone Labs. Bicuculline, SCH 23390, CGP 46381 and CGP 52432 were purchased from Tocris Bioscience. KOH was purchased from BDH Chemicals. All other chemicals were obtained from Thermo Fisher Scientific. All drugs were stored as concentrated stock solutions at -20 °C and diluted in ACSF bath solution immediately before application.

3.2e Data Analysis

Recordings were analyzed off-line with pClamp 10.3 (Molecular Devices). Statistical analyses were also performed with GraphPad Prism, which was also used to prepare figures. Data are expressed as mean ± SEM. A repeated-measures two-way ANOVA, with the Bonferroni post-test, was used to analyze effects of drugs on PN current-voltage (IV) plots and H-currents. A two way ANOVA (without repeated measures), followed by the Bonferroni post-test was used when control and drug measurements were not obtained from the same PN. For example when the current blocked by [ahx[5-24]]NPY was compared between two groups of PNs tested in the absence or presence of another drug, such as a $GABA_B$ antagonist. Effects of drugs on rheobase, input resistance and RMP were analyzed with the paired Students t-test, unless more than one drug was applied, in which case a repeated measures one way ANOVA with Bonferroni post-test was used. Mean differences were considered significant at $p < 0.05$,

and significance levels are indicated in figures as follows: *p<0.05, **p<0.01, ***p<0.001.

3.3 RESULTS

3.3a BLA principal neurons are highly inhibited *in vitro*

Using a K^+ internal solution, a representative sample of BLA PNs displayed a relatively hyperpolarized mean RMP (-81.3 ± 0.53 mV), (n=64), modestly more hyperpolarized than we reported previously in younger animals (Giesbrecht et al., 2010). PNs showed characteristically low input resistance under control conditions (59.5 ±2.5 MΩ), (n= 57) and virtually never fired spontaneous action potentials during passive current clamp recordings. Voltage-clamp ramps and steps were used to examine membrane conductance, and both approaches showed a prominent, inwardly-rectifying. current resembling a GIRK conductance. Hyperpolarizing voltage steps also showed prominent I_h in most cases **(Figure 2)**.

3.3b [ahx$^{5-24}$]NPY increases BLA principal Neuron excitability

With K^+-pipette solution, we compared the rheobase of BLA PNs under control conditions, in the presence of [ahx$^{5-24}$]NPY (1μM) and periodically during drug washout. In 25/30 neurons studied, this concentration of [ahx$^{5-24}$]NPY significantly decreased rheobase current from a mean control value of 387 ± 24 pA to 295 ± 19 pA, (p<0.001; n=25), a 24% reduction (**Figure 1A-B**). Effects of the peptide occurred rapidly (typically beginning during application), with effects peaking by 5 – 10 min wash, consistent with NPY actions reported in BLA and elsewhere) (Klapstein and Colmers, 1997; Giesbrecht et al., 2010). However, unlike the presynaptic Y_2 receptor effects, reported in Chapter 2, changes in neuronal excitability frequently (but not always) failed to reverse with drug washout.

Changes in PN excitability were mirrored by marked increases in neuronal input

resistance. 32/39 (82%) of PNs tested responded to [ahx$^{5-24}$]NPY (1 μM) with a substantial and sustained increase in input resistance from a mean control value of 59 ± 4.2 MΩ to 81 ± 5.40 MΩ (p<0.001; n=32), a 37 % increase **(Figure 1C)**.

Application of [ahx$^{5-24}$]NPY (1 μM) depolarized some PNs, this effect was typically modest and not as consistent as effects on excitability and input resistance. Application of [ahx$^{5-24}$]NPY (1 μM) to 45 PNs resulted in a significant mean depolarization of 2.7 ± 0.8 mV (p<0.01; n=45) from the control value of -80.9 ± 0.7 mV **(Figure D-E)**. However, 23/45 PNs showed no appreciable change in resting membrane potential (<2 mV change) and 2/45 PNs even hyperpolarized measurably (>2 mV). Excluding those not clearly depolarized by the Y$_2$ agonist, 20/45 BLA PNs responded to [ahx$^{5-24}$]NPY with an appreciable depolarization (>2 mV), on average, of 6.3 ± 1.1 mV (p<0.001; n=20).

3.3c [ahx$^{5-24}$]NPY Decreases Multiple Currents in BLA Principal Neurons (K$^+$ Internal)

The above observations indicated that [ahx$^{5-24}$]NPY significantly altered the postsynaptic membrane properties of BLA PNs. Therefore, we characterized these changes with voltage-clamp experiments.

Using the slow voltage ramp protocol [Section 3.2c(ii)], we observed that most PNs showed a pronounced steady-state inward rectification under control conditions. Application of [ahx$^{5-24}$]NPY (1 μM) typically reduced a markedly inward-rectifying current, suggesting inhibition of an inwardly rectifying K$^+$ conductance (IRK) **(Figure 2B-C)**. However, the reversal potential of the inhibited conductance varied considerably between PNs. This led us to hypothesize that [ahx$^{5-24}$]NPY inhibited more than one current in these cells **(Figure 3B-C)**.

143

Hyperpolarizing voltage steps, from a V_h of -55 mV, helped clarify [ahx$^{5-24}$]NPY's postsynaptic actions. Voltage steps revealed prominent H-currents (I_h) in the majority of PNs. As previously reported, I_h manifested as a slowly activating inward current whose magnitude and rate of activation increased with larger hyperpolarizing steps **(Figure 2D-E)**. We confirmed that this conductance was largely mediated via I_h by blocking it in a subset of PNs with the I_h blocker, ivabradine (30 μM) (n=5) (not illustrated). The voltage step protocol separated I_h from another, "instantaneously" activating membrane currents. This instantaneous membrane current was visible immediately following the decay of the capacitative transient and prior to I_h activation **(Figure 2E)**. The I-V relationship for this current also showed clear inward rectification, typically more pronounced than that seen with slow ramps from the same PN, so we refer to it as an instantaneous, inwardly-rectifying (I_{IR}) current. The I_{IR} reversed at -82.4 ± 1.0 mV (n=30), consistent with a largely K^+ conductance.

Application of [ahx$^{5-24}$]NPY (1 μM) significantly decreased the I_{IR} in the majority of PNs tested (21/25); the conductance inhibited by the Y_2R agonist reversed at -87.4 ± 3.0 mV (n=21) **(Figure 2F-G)**. Furthermore, in comparison with slow voltage ramp measurements, the variability in the apparent reversal potential of the Y_2R-sensitive I_{IR} was low, allowing data to be pooled between PNs. [ahx$^{5-24}$]NPY similarly decreased PN I_{IR} in the presence of TTX (500 nM) (6/8 neurons tested) **(Figure 3H-I)**. Interestingly, these [ahx$^{5-24}$]NPY effects typically did not readily reverse upon washout, either in the absence or presence of TTX.

In addition to the above effects, in many cases [ahx$^{5-24}$]NPY also clearly modulated I_h. Thus, in 11 of 21 PNs, [ahx$^{5-24}$]NPY significantly reduced the amplitude of

I_h measured at a step to -135 mV from 351 ± 51 pA to 234 ± 32 pA (p < 0.001, n=11), a 33% reduction. The I_{IR} current was always also reduced by [ahx$^{5-24}$]NPY in these PNs and as with the I_{IR}, the effects on I_h usually did not reverse with washout. The effects of [ahx$^{5-24}$]NPY on PN I_h will be discussed further in section 3.3g. Thus, inhibition of multiple currents in some but not all PNs may partly explain the great variability in the reversal potential of [ahx$^{5-24}$]NPY-sensitive currents measured with slow voltage ramps, (which cannot resolve I_h and early currents).

3.3d [ahx$^{5-24}$]NPY Inhibits a Principal Neuron GIRK

The above experiments suggested postsynaptic Y_2 receptor actions on PNs, in addition to the presynaptic actions documented in Chapter 2. Both presynaptic and postsynaptic actions could contribute to the observed enhanced PN excitability.

The Y_2-sensitive I_{IR} rectified inwardly and reversed close to the K$^+$ reversal potential, consistent with a GIRK K$^+$ conductance. Since GIRKs are common targets of neuromodulators, we hypothesized the above Y_2R-mediated effects result from the inhibition of these channels. SCH23390 a dopamine D_1 receptor antagonist which also directly blocks GIRK channels, was next used to test this hypothesis (Sosulina et al., 2008).

Bath application of SCH23390 (15 μM) caused a substantial loss of an inwardly-rectifying I_{IR} conductance in the majority of PNs tested (14/15) **(Figure 3A-B)**. The SCH23390-sensitive conductance contributed significantly to the voltage step I_{IR} and to the steady-state current, as measured with voltage ramps. In both cases, this SCH23390-sensitive I_{IR} resembled the current suppressed by [ahx$^{5-24}$]NPY and reversed at -94.2 ± 3.2 mV (n=14), (I_{IR}). Importantly, when [ahx$^{5-24}$]NPY (1 μM) was applied in the presence

of SCH 23390 (15 μM), effects of the Y_2 agonist were largely occluded **(Figure 3C-E)**. These results suggest that postsynaptic Y_2 receptor effects are mediated largely via GIRK current inhibition.

To further confirm that Y_2 receptor activation inhibits PN GIRK currents, we performed additional experiments with a Cs^+ pipette solution. Intracellular Cs^+ blocks outward but not inward GIRK currents (Sodickson and Bean, 1996). Therefore, if [ahx$^{5-24}$]NPY (1 μM) acts via GIRK inhibition, its effects on outward but not inward PN currents should be occluded in Cs^+ recordings. This effect was indeed observed (not illustrated). Similar effects were also observed in the presence of TTX (500 nM) **(Figure 3G-H)**.

3.3e [ahx$^{5-24}$]NPY reduces tonic GABA$_B$ inhibition of PNs

Although the above results suggest a Y_2 receptor-mediated inhibition of a GIRK current, NPY is more commonly seen to potentiate neuronal GIRK currents in other brain areas (Paredes et al., 2003; Sosulina et al., 2008; Melnick, 2012). Additionally, Y_2 receptors are typically presynaptic, and not postsynaptic (Colmers and Bleakman, 1994; Greber et al., 1994; Chen et al., 1997). We therefore, considered the possibility that these Y_2R-mediated effects are indirect.

[ahx$^{5-24}$]NPY inhibited GIRK currents in the presence of TTX, which is generally consistent with a postsynaptic mechanism. However, we previously reported that [ahx$^{5-24}$]NPY inhibits synaptic GABA inputs onto PNs even in the presence of TTX (Chapter 2). Since GABA$_B$ receptors commonly activate neuronal GIRK channels, we next considered the possibility that inhibition of Y_2R-sensitive miniature GABA events could also underlie the observed loss of tonic GIRK currents. If this were the case, Y_2 receptor-

sensitive GABA synapses must inhibit PNs via tonic $GABA_B$ receptor activation.

We tested this hypothesis with two well-characterized $GABA_B$ antagonists, CGP 46381 and the higher-affinity CGP 52432 (Olpe et al., 1993; Pozza et al., 1999). In K^+-gluconate pipette recordings, bath application of CGP 52432 (1 μM) alone resulted in a significant reduction in an inwardly-rectifying I_{IR} current in the majority of PNs tested (15/18) **(Figure 4C)**. As with SCH23390, the conductance blocked by CGP52432 was clearly visible both in voltage step and ramp measurements, and resembled the effects of [ahx$^{5-24}$]NPY. Importantly, in the presence of CGP 52432 (1 μM), effects of [ahx$^{5-24}$]NPY on tonic PN currents were largely but not entirely occluded **(Figure 4D-E)**. In the presence of CGP 52432 (1 μM), [ahx$^{5-25}$]NPY (1 μM) continued to significantly reduce PN I_{IR} conductance at -135 mV, but only by 59.0 ± 16.45 pA (n=12). By comparison, in the absence of CGP 52432 (at the same potential), [ahx$^{5-24}$]NPY inhibited 156.2 ± 26.24 pA (n=21) of current, a significant difference of 97.2 ± 37.1 pA (p<0.001) **(Figure 4F)**.

In experiments conducted with TTX (500 nM) present and using a Cs^+ intracellular solution, bath application of the $GABA_B$ antagonist CGP 463821 (100 μM) similarly caused the loss of an inwardly-rectifying current. This current, which was measured with a slow voltage-ramp (methods), was qualitatively similar to the conductance blocked by [ahx$^{5-24}$]NPY under identical conditions (not illustrated). Similar to above, addition of [ahx$^{5-24}$]NPY did not produce a significant additional effect on PN membrane currents in the presence of the $GABA_B$ antagonist.

If Y_2 receptor activation reduces GABA release, and this results in a loss of tonic $GABA_B$ receptor activation, then maximally activating $GABA_B$ receptors with an exogenous agonist should bypass Y_2R - effects. We therefore applied a near maximal

dose of the prototypic GABA$_B$ agonist, baclofen (30 µM) (Chen et al., 2005) to PNs in K$^+$ pipette recordings. Baclofen application resulted in a prominent increase in voltage step measured I$_{IR}$ conductance in all PNs tested (n=6) **(Figure 5D)**. Importantly, GIRK currents desensitized only minimally in 5 of the 6 PNs tested in the continued presence of baclofen. Addition of 1 µM [ahx$^{5-24}$]NPY in the presence of 30 µM baclofen resulted in minimal additional effects on the postsynaptic I$_{IR}$ currents (n=4) **(Figure 5E-F)**.

These results further suggest that in acute slices, BLA PNs are inhibited via tonically-active GABA$_B$ receptors, and that this occurs even without activity-dependent synaptic release of GABA. Additionally, our findings strongly suggest that the observed "postsynaptic" Y$_2$ receptor actions are due entirely to a Y$_2$-mediated reduction in tonic GABA release onto PNs. Actions of [ahx$^{5-24}$]NPY on PN excitability are thus better termed presynaptic.

3.3f [ahx$^{5-24}$]NPY's effects are partly mediated by loss of tonic GABA$_A$

In the presence of CGP 52432 (1 µM), [ahx$^{5-24}$]NPY continued to have small, but significant effects on PN conductance **(Figure 4E)**. Input resistance, measured in current clamp, was also increased by [ahx$^{5-24}$]NPY (1 µM) with GABA$_B$ receptors blocked, although to a lesser extent than in control **(Figure 4G)**. We therefore, hypothesized that [ahx$^{5-24}$]NPY acts in part by reducing tonic GABA$_A$-mediated inhibition. To test this, we next performed experiments in the presence of the GABA$_A$ antagonist, bicuculline methiodide. PNs held at – 55 mV with a K$^+$ pipette typically have a substantial outward current, as they normally rest 25 mV more negative and have relatively low input resistance. Bath application of bicuculline (10 µM) increased PN input resistance and substantially reduced the current required to hold PNs at -55 mV in voltage-clamp in all

cells tested **(Figure 6A-B)**. These results suggest considerable tonic $GABA_A$-mediated inhibition of PNs under *in vitro* conditions, consistent with the findings of Marowsky et al (2012).

When [ahx$^{5-24}$]NPY (1 μM) was applied in the presence of bicuculline (10μM), effects on the I_{IR} were partly occluded **(Figure 6C)**. However, several PNs continued to respond to [ahx$^{5-24}$]NPY with substantial reductions in an inwardly-rectifying I_{IR} conductance, **(Figure 6D)**. Interestingly, in the presence of bicuculline, the reversal potential for the Y_2R-sensitive I_{IR} was significantly more hyperpolarized than in its absence: -106.6 ± 7.1 mV (n=9) compared to -87.4 ± 3.02 mV in the earlier experiments (n=22) (unpaired t-test, p=0.0034). As was the case in the presence of CGP 52432, [ahx$^{5-24}$]NPY continued to significantly increase PN input resistance with bicuculline present, but again, less so than in its absence **(Figure 6H)**. Furthermore, [ahx$^{5-24}$]NPY (1 μM) continued to significantly increase PN excitability in bicuculline **(Figure 6F-G)**.

We therefore performed an additional experiment in the presence of both CGP 52432 and bicuculline to test whether the effects of [ahx$^{5-24}$]NPY on PN conductance and excitability are entirely due to reduced tonic activation of $GABA_A$ and $GABA_B$ receptors. Simultaneous bath application of CGP 52432 (1 μM) and bicuculline (10 μM) to BLA slices caused a substantial loss of conductance in all PNs tested. When [ahx$^{5-24}$]NPY (1 μM) was applied to PNs in the presence of both CGP 52432 (1 μM) and bicuculline (10 μM), effects on the I_{IR} were fully occluded **(Figure 7A-B)**. Furthermore, [ahx$^{5-24}$]NPY had no significant additional effects on PN rheobase or input resistance in the combined presence of bicuculline and CGP 52432 (1 μM) **(Figure 7C-E)**.

3.3g [ahx$^{5-24}$]NPY inhibits I$_h$ via loss of GABA$_B$

As reported above, bath application of [ahx$^{5-24}$]NPY (1 µM) significantly reduced I$_h$ in 11 out of 21 PNs tested **(Figure 8A-B)** and similar effects were observed in the presence of TTX (500nM) **(Figure 8C)**. Interestingly, a minority of PNs (6/20) responded to [ahx$^{5-24}$]NPY with an increase in I$_h$ although this was only significant at the -135 mV step (not illustrated). Although previous work indicated that the acute effects of NPY on I$_h$ were not blocked by a Y$_2$ receptor antagonist, the above results suggest that Y$_2$ receptors may play some role in the inhibition of I$_h$ by NPY.

Interestingly, bath application of CGP 52432 (1 µM) also modulated PN I$_h$. Thus, I$_h$ was significantly reduced by CGP 52432 in 5/11 PNs tested **(Figure 8D-E)**. Also similar to [ahx$^{5-24}$]NPY, I$_h$ was increased by CGP 52432 in some (4/11 PNs tested) cases. These results suggest that actions of [ahx$^{5-24}$]NPY on I$_h$ are likely mediated via inhibition of tonically active GABA$_B$ receptors rather than through direct postsynaptic actions. Furthermore, the GIRK channel blocker SCH 23390 (15 µM) also modulated I$_h$ in some PNs; significantly decreasing I$_h$ in 3/10 PNs tested and increasing I$_h$ in 4/10 cases. These results suggest that GABA$_B$ receptors may modulate I$_h$ indirectly via interactions with other channels, including GIRKs.

3.3h CRF inhibits an inward rectifying PN conductance

Like NPY, the anxiogenic neuropeptide corticotrophin releasing factor (CRF) elicits a longer-term emotional state when repeatedly injected into the BLA. However, in this case CRF evokes a longer-term increase in anxiety (Rainnie et al., 2004). NPY and CRF's opposing long-term emotional effects both require Ca^{2+}-dependent enzyme

complexes, specifically calcineurin and calcium calmodulin-dependent kinase type II (CaMKII) respectively (Rainnie et al., 2004; Sajdyk et al., 2008). Dendritic $GABA_B$ receptor activation damps Ca^{2+}-mediated plasticity (Leung and Peloquin, 2006). Therefore, we hypothesized that by removing the strong tonic $GABA_B$-mediated inhibition documented above, Y_2 receptor activation permits Ca^{2+}-dependent plasticity. Since CRF-mediated plasticity similarly requires elevations in dendritic Ca^{2+} levels, we hypothesized that this anxiogenic peptide will also remove tonic $GABA_B$-mediated inhibition of PNs to exert its long-term effects. We therefore next examined the effects of CRF on PN conductance.

We first examined the effects of CRF on PN excitability. Bath application of CRF (30 nM) significantly decreased rheobase current in 8/9 PNs from 364.7 ± 31.9 pA to 250.7 ± 21.8 pA ($p<0.01$; n=8) **(Figure 9A-B)**. Furthermore; CRF significantly increased input resistance in nearly all PNs tested (10/11) from 77.1 ± 10.4 to 107.1 ± 13.3 ($p<0.001$; n=10) **(Figure 9C)**.

Our lab previously found that CRF increased I_h in a subset of BLA PNs (Giesbrecht et al., 2010). However, it is unlikely that actions on I_h account for the increase in excitability observed here, since control and CRF rheobase measurements were conducted from the same membrane potential **(Figure 9A)**. Under such conditions, increased I_h would be expected to decrease neuronal resistance and produce the opposite effect. Furthermore, input resistance was increased by CRF in nearly all PNs tested, inconsistent with potentiation of I_h alone.

Measuring the I_{IR} in PNs with voltage steps revealed that CRF inhibits an inward-rectifying current, which reversed at -99.7 ± 6.5 mV (n=7). Future studies will be needed

to determine whether these actions of CRF are also mediated by reductions in tonic

$GABA_B$-mediated inhibition.

3.4 DISCUSSION

Here we provide compelling evidence that selective activation of BLA NPY Y_2 receptors reduces tonic $GABA_A$-$GABA_B$-mediated inhibition. This Y_2 receptor-sensitive tonic GABA release exerts profound and widespread inhibitory control over BLA PNs. Application of the Y_2 selective agonist $[ahx^{5-24}]$NPY relieved this tonic inhibition and increased the excitability of most BLA PNs. Despite the initial impression that the actions of the Y_2R agonist were postsynaptic, extensive evidence is consistent with an entirely presynaptic role for the Y_2R on GABA-releasing interneurons in the BLA. These actions would thus be expected to increase the anxiogenic output of BLA *in vivo,* and likely explain the acute anxiogenic effects of selective BLA Y_2 receptor action.

3.4a $[ahx^{5-24}]$NPY likely reduces extrasynaptic GABA inhibition

Earlier in this thesis (chapter 2), we demonstrated that $[ahx^{5-24}]$NPY reduces synaptic (phasic) GABA inhibition likely onto PN dendrites (Chapter 2). The effects described here indicate that $[ahx^{5-24}]$NPY also inhibits sustained GABA-mediated PN inhibition. This sustained GABA inhibition is likely mediated by extrasynaptic receptors, which are sensitive to low GABA concentrations and show minimal desensitization compared to synaptic receptors (Whissell et al., 2015). A large component of $[ahx^{5-24}]$NPY's effects were mediated via reduced tonic $GABA_B$ receptor activation, which further implicates extrasynaptic GABA, since $GABA_B$ receptors are predominately expressed at extrasynaptic sites (Scanziani, 2000; Kulik et al., 2003). We previously reported that NPY/SOM interneurons express Y_2 receptors (Chapter 2). These NPY/SOM interneurons also likely mediate actions of $[ahx^{5-24}]$NPY on tonic PN GABA inhibition,

since the effects of the Y_2 agonist on synaptic GABA events and tonic GABA-mediated currents both persisted in TTX indicating a monosynaptic mechanism **(Figure 10)**.

Y_2 receptor-mediated inhibition of GABA release via a presynaptic mechanism has been reported in other brain areas (Obrietan and van den Pol, 1996; Sun et al., 2001). The concurrent reduction in $GABA_B$-mediated GIRK responses is however unusual. Tonic, $GABA_B$-mediated inhibition of pyramidal cells has been reported *in vitro* in the rat prefrontal cortex. In this case however, Wang *et al.* (2010) reported only modest $GABA_B$ –mediated GIRK currents with physiological $[K^+]_o$ (Wang et al., 2010). In contrast, we observed robust $GABA_B$-dependent currents in most BLA PNs under physiological (3 mM) extracellular K^+ concentrations. Most surprising, tonic $GABA_B$-mediated inhibition in the BLA appeared to persist even in the presence of TTX; suggesting that substantial amounts of GABA are released extra-synaptically, independent of action potentials. Although surprising, this is consistent with the impressive GABA-mediated inhibition documented within the BLA. Furthermore, we have previously reported that this vigorous, basal GABA inhibition persists to a large degree in the presence of TTX (Chapter 2).

In many neuronal systems, multiple interneurons must fire closely together for sufficient GABA to escape reuptake and activate $GABA_B$ receptors (Scanziani, 2000). However, single action potentials in hippocampal neurogliaform interneurons are reported to activate pyramidal cell $GABA_B$ receptors (Tamás et al., 2003). Neurogliaform cells generally do not form distinct synaptic contacts with post synaptic neurons, and release GABA into the extra-synaptic space in a paracrine-like manner (Oláh et al., 2009). Neuroglaiform interneurons have also been described in the BLA and are

characterized by expression of NPY (Mańko et al., 2012). We reported earlier (Chapter 2) that in the mouse, virtually all NPY expressing interneurons also express Y_2 receptors (Chapter 2). Neurogliaform interneurons are thus likely candidates to mediate the Y_2 receptor-sensitive tonic $GABA_B$ currents we observed in the BLA.

The ability to sustain tonic $GABA_B$ receptor currents depends on the degree to which $GABA_B$-mediated currents desensitize in the continued presence of agonists. Great variability in rates of $GABA_B$ receptor desensitization have been reported throughout the CNS (Gassmann and Bettler, 2012). Here, application of baclofen to BLA PNs elicited substantial $GABA_B$-mediated outward currents that showed only minimal desensitization **(Fig 5A),** consistent with a tonic $GABA_B$-mediated inhibition in these neurons. To our knowledge, this is the first report of tonic activation of $GABA_B$ receptors via activity-independent GABA release. This action-potential independent tonic inhibition can furthermore be targeted for neuromodulation, via Y_2 receptors. Thus, the impact of tonic $GABA_B$ signaling on neuronal excitability may need to be re-evaluated in light of these findings.

3.4b Y_2 receptor effects on tonic GABA likely occur at principal neuron dendrites

$GABA_A$ receptors are expressed across the entire BLA PN somato-dendritic axis (Klenowski et al., 2015). However, anatomical and electrophysiology data suggest that $GABA_B$ receptors are expressed mainly on PN dendritic spines and shafts (Washburn and Moises, 1992; McDonald et al., 2004). Thus, inhibition of tonic $GABA_B$ currents by [ahx[5-24]]NPY suggests preferential Y_2R-mediated actions on PN dendrites. Furthermore, SOM interneurons, the predominant Y_2 receptor-expressing interneurons in the BLA (Chapter 2), primarily target PN dendrites (Muller et al., 2006) **(Figure 10)**.

Certain unusual aspects of our electrophysiological findings are also consistent with a primarily dendritic site of Y_2 receptor actions. Firstly, [ahx$^{5-24}$]NPY only modestly depolarized PNs, despite increasing input resistance and excitability via inhibition of GABA$_B$-mediated GIRK currents. This is very surprising since GIRK currents reverse at E_k. This is however, consistent with Y_2 receptor effects occurring at a distal, electrotonically-isolated site.

Another surprising observation was that [ahx$^{5-24}$]NPY significantly reduced I_h in half of all experiments, even in the presence of TTX. This effect was replicated by the GABA$_B$ antagonist CGP 52432, suggesting I_h was modulated via reduced tonic GABA inhibition. We anticipate that this effect is indirect, since blocking GIRK channels also affected I_h. HCN channels are preferentially localized to distal dendrites, in most pyramidal neuron types (Lörincz et al., 2002), as are GABA$_B$-activated GIRK channels. Thus, the Y_2-mediated reduction in tonic GABA$_B$-activated GIRK currents could result in dendritic depolarization, thereby deactivating tonic I_h in a voltage-dependent manner. Similar interactions between dendritic I_h and Kir2 inward rectifying K^+ channels were observed by Day et al. (2005) in Layer 5 pyramidal neurons (Day, 2005). Since we measured I_h in voltage clamp, indirect inhibition of this conductance via membrane depolarization could only be observed if it occurred at a distal site where voltage is not readily controlled.

Blocking GABA$_B$-GIRK currents should both increase the neuronal space constant (by increasing resistance) and depolarize dendrites. These actions should exert opposing effects on dendritic I_h when measured from the soma. Dendritic clamp will be improved by increasing the membrane space constant, while dendritic depolarization

must be counteracted with greater hyperpolarizing current to activate I_h. This may explain why [ahx$^{5\text{-}24}$]NPY, CGP 52432 and SCH 23390 all increased I_h in a subset of PNs.

3.4c Implications for NPY-mediated plasticity

Y_2 receptor activation likely disinhibits PN dendrites by removing tonic GABA$_B$-mediated inhibition. Dendritic GABA$_B$ receptors decrease Ca^{2+}-dependent plasticity by multiple mechanisms; firstly, activated GIRK currents damp NMDA currents and limiting action potential back-propagation (Morrisett et al., 1991). Secondly, dendritic GABA$_B$ receptors directly inhibit voltage gated Ca^{2+} channels (Greif et al., 2000; Vigot et al., 2006). This suggests that Y_2 receptor activation facilitates plasticity. We propose that the tonic GABA$_B$-mediated dendritic inhibition documented here, must be removed to permit long-term NPY-mediated plasticity, which requires calcineurin (Sajdyk et al., 2008). Coupling Y_2R effects with acute inhibitory effects of other NPY receptors should result in modest changes in dendritic Ca^{2+} levels, a condition favoring calcineurin activation.

This dendritic inhibition would also need to be lifted to permit CRF-mediated plasticity, which requires CaMKII (Rainnie et al., 2004). Consistent with this, CRF also inhibited a GIRK-like PN conductance. It remains to be seen however, whether these CRF actions are also mediated via reduced tonic GABA inhibition. If CRF and NPY both disinhibit BLA dendrites to permit plasticity, it will be important to determine what factors bias CRF towards CaMKII activity, and NPY towards calcineurin.

3.5 FIGURES

Figure 1: [ahx$^{5-24}$]NPY Increases PN Excitability
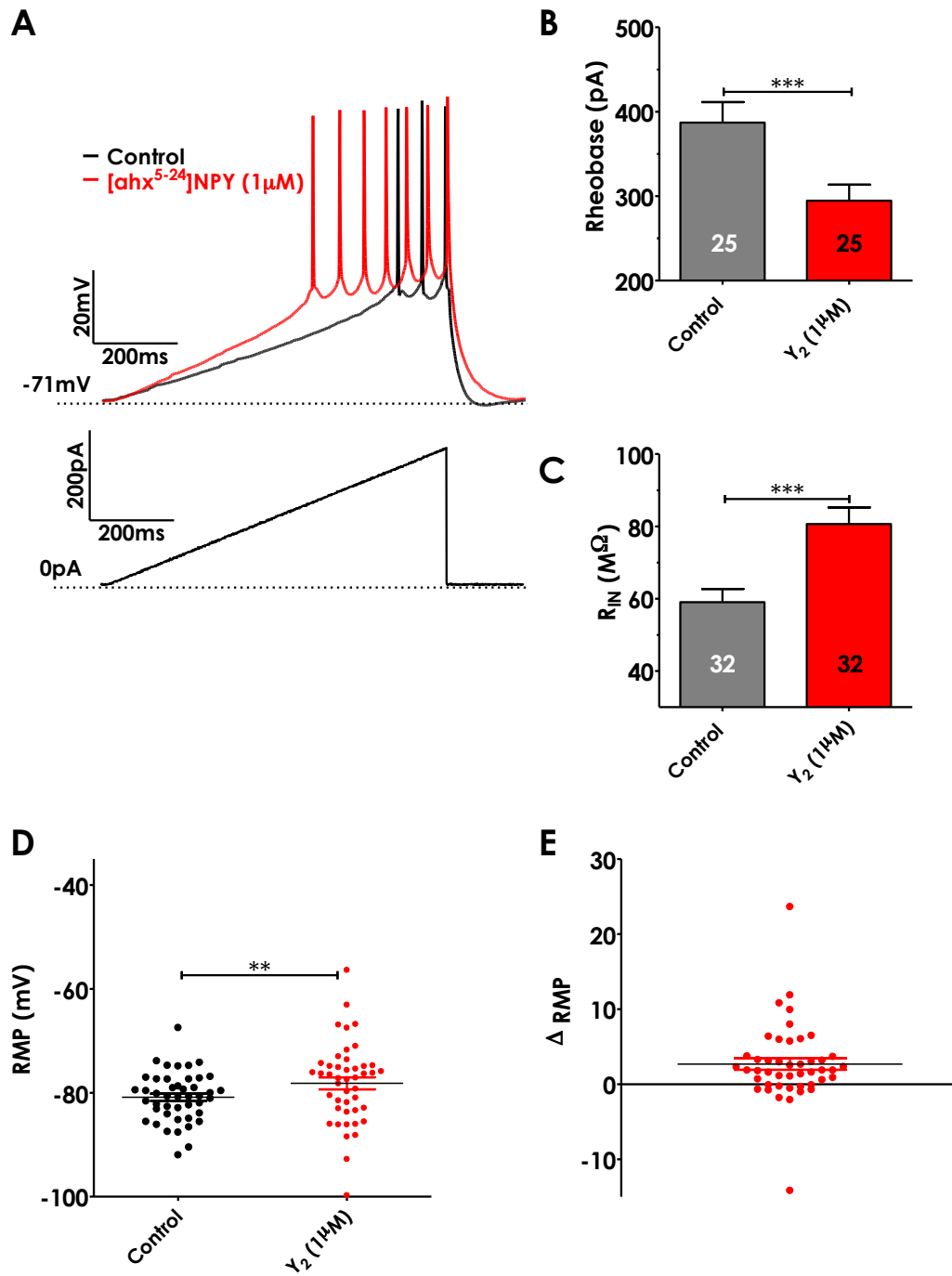
Figure 1: [ahx$^{5\text{-}24}$]NPY Increases PN Excitability

(A) Representative current clamp traces from a PN during a depolarizing current ramp. Following bath application of [ahx$^{5\text{-}24}$]NPY (1 µM), PN excitability is increased. This is seen as a substantial decrease in rheobase current, the amount of depolarizing current needed to elicit action potential firing.

(B) [ahx$^{5\text{-}24]}$NPY (1 µM) significantly decreased rheobase current from 387 ± 24 pA to 294 ± 18.8 pA, (p<0.001; n=25) in 25/30 PNs tested.

(C) [ahx$^{5\text{-}24}$]NPY (1 µM) significantly increased input resistance from 59.03 ± 4.17 MΩ to 80.63 ± 5.40 MΩ (p<0.001; n=32) in 32/39 PNs tested.

**(D)** Overall [ahx$^{5\text{-}24}$]NPY (1 µM) depolarized the mean PN RMP from -80.9 ± 0.7mV to -78.2 ± 0.8mV (p<0.01; n=45).

(E) [ahx$^{5\text{-}24}$]NPY- mediated effects on PN RMP. Overall [ahx$^{5\text{-}24}$]NPY significantly depolarized PNs 2.7 ± 0.8 mV (n=45). However, effects on RMP were heterogeneous with many PNs not responding appreciably and some even hyperpolarizing.

# Figure 2: [ahx$^{5-24}$]NPY Decreases an Inwardly-Rectifying Current
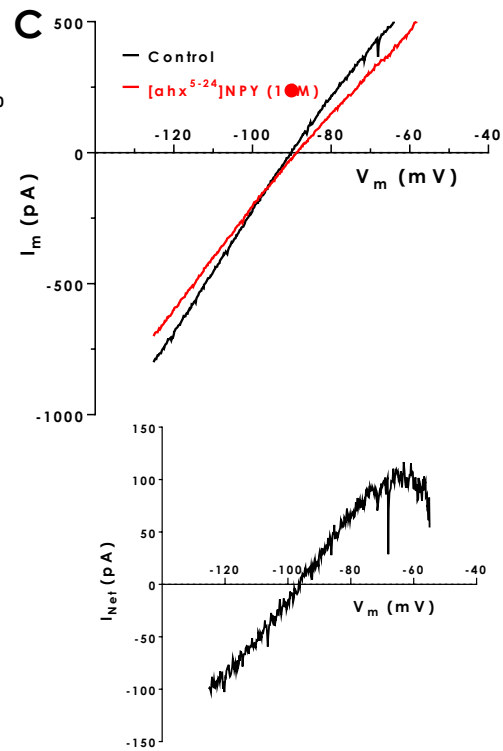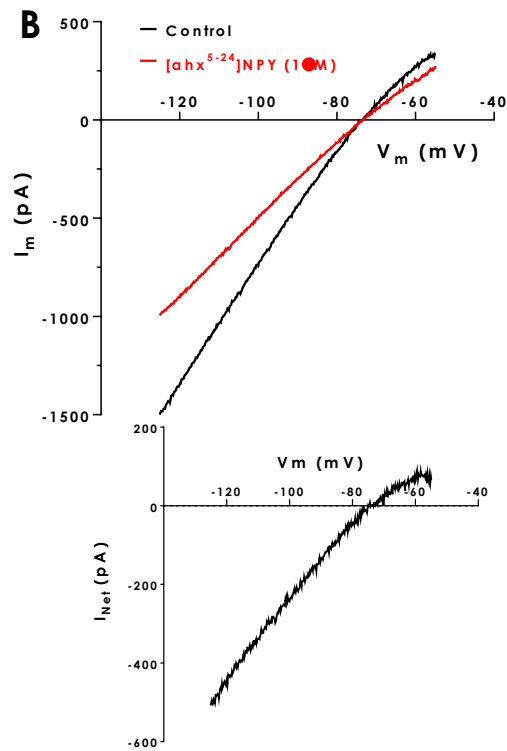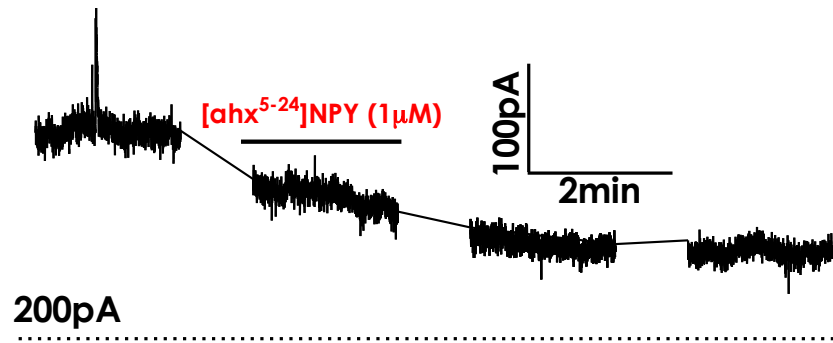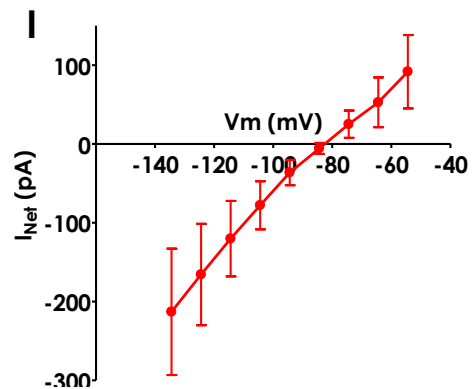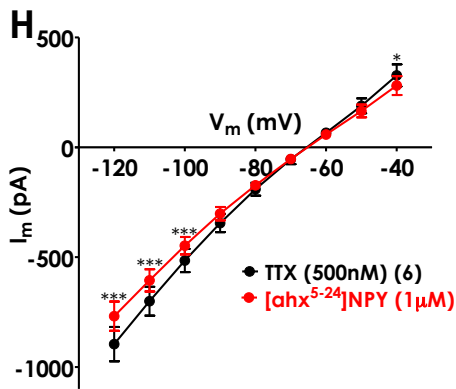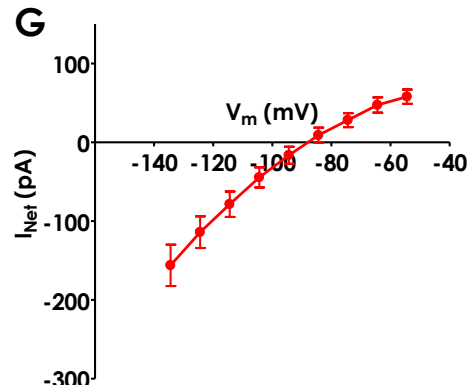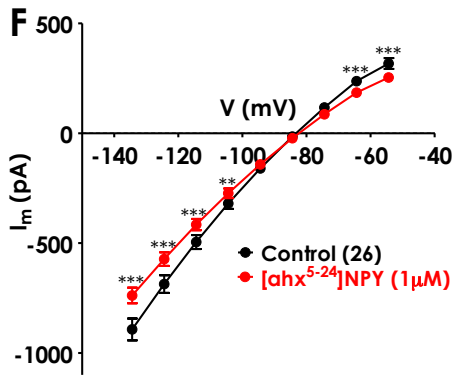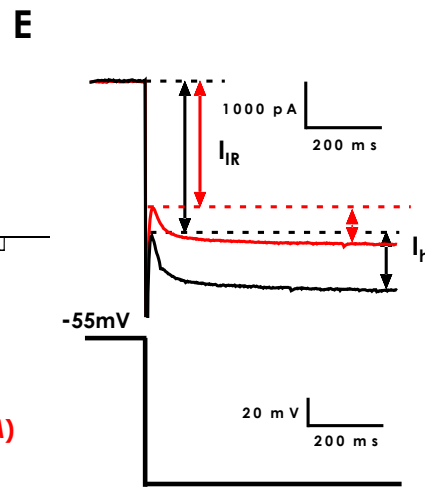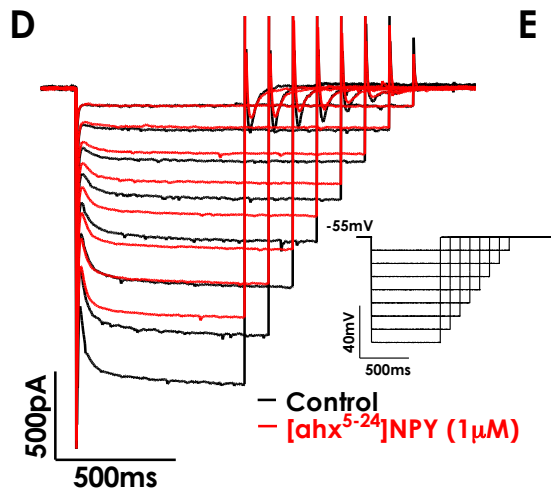
D Control
[ahx^{5-24}]NPY (1μM)

E

F

G

H

I

Figure 2: [ahx$^{5-24}$]NPY Decreases an Inwardly-Rectifying Current

(A) Representative PN voltage clamp traces at a -55 mV holding potential. Bath application of [ahx$^{5-24}$]NPY (1 μM) reduced the -55 mV holding current indicating actions on a steady state conductance.

(B) Representative PN voltage clamp ramp traces in which [ahx$^{5-24}$]NPY substantially decreased an inwardly-rectifying conductance with an apparent reversal potential of ~ -75 mV. The net current blocked by [ahx$^{5-24}$]NPY in this PN is shown in the bottom inset.

(C) Representative voltage clamp ramp traces of a PN in which [ahx$^{5-24}$]NPY substantially decreased an inwardly-rectifying conductance with an apparent reversal potential of ~ -95 mV. The net current blocked by [ahx$^{5-24}$]NPY in this PN is shown in the bottom inset. (Panels B-C) illustrate the variability in the apparent reversal potential of the [ahx$^{5-24}$]NPY sensitive current when measured with slow voltage ramps.

(D) Representative PN hyperpolarizing voltage steps from a -55 mV holding potential. Bath application of [ahx$^{5-24}$]NPY (1 μM) substantially decreased both the early current and I_h in this PN (traces from control and drug measurements were aligned at the -55 mV holding current in this and all similar figures).

(E) A -135 mV voltage step illustrating how the instantaneous inward rectifier (I_{IR}) and I_h are differentiated. The the I_{IR} is measured from the holding current as the current immediately following decay of the capacitive transient, but prior to I_h activation. I_h is measured as the difference between the I_{IR} and the steady-state current at the end of the step.

(F) I-V plots of I_{IR} current in BLA PNs in the absence and presence of the Y_2R agonist. [ahx$^{5-24}$]NPY (1 μM) significantly reduces an inward rectify conductance.

(G) Current-voltage relationship of the net PN I_{IR} inhibited by [ahx$^{5-24}$]NPY (1 μM). The [ahx$^{5-24}$]NPY-sensitive current appeared to reverse at -87.4 ± 3.02 mV (n=21) and showed clear inward rectification.

(H) [ahx$^{5-24}$]NPY (1 μM) continued to significantly reduce the PN I_{IR} conductance in the presence of TTX (500 nM).

(I) The net PN I_{IR} inhibited by [ahx$^{5-24}$]NPY (1 μM) in the presence of TTX (500nM) (n=6).

Figure 3: [ahx$^{5-24}$]NPY Inhibits a GIRK in BLA PNs
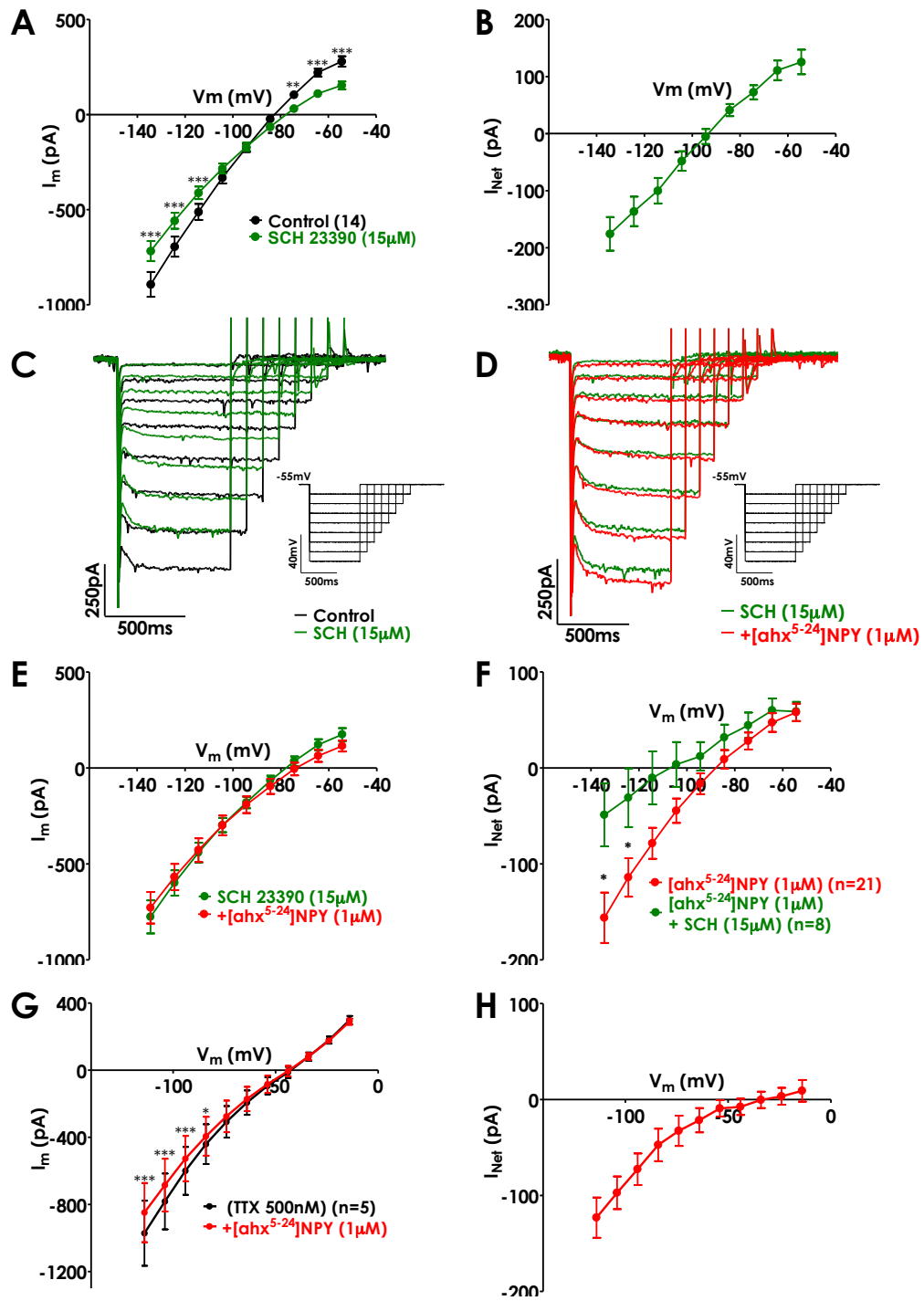
Figure 3: [ahx$^{5-24}$]NPY Inhibits a GIRK in BLA PNs

(A) PN voltage step I_{IR} I-V plots. The GIRK blocker SCH23390 (15 µM) significantly reduced an inwardly-rectifying conductance (n=14).

(B) Net PN I_{IR} blocked by SCH23390 (15 µM). The SCH23390 sensitive current appeared to reverse at -94.21 ± 3.15mV (n=14) and seemed qualitatively similar to the PN current blocked by [ahx$^{5-24}$]NPY (Fig 2G).

(C) Superimposed are membrane current responses in a PN to hyperpolarizing voltage steps from an I_h protocol (V_h = -55mV) in the absence and presence of SCH 23390. Bath application of SCH23390 (15 µM) substantially decreased I_{IR} in this PN.

(D) Superimposed are membrane current responses in a PN to hyperpolarizing voltage steps from an I_h protocol (V_h = -55mV) as in panel C. Application of [ahx$^{5-24}$]NPY (1 µM) in the presence of SCH23390 (15 µM) had little if any further effect on this PN's I_{IR} conductance.

(E) PN voltage step early current I-V plots. When [ahx$^{5-24}$]NPY was applied in presence SCH23390 (15 µM) its effects on PN I_{IR} conductance were largely occluded.

(F) Net PN I_{IR} conductance blocked by [ahx$^{5-24}$]NPY (1 µM) in the presence of SCH23390 (15 µM) (n=8), compared to the I_{IR} conductance blocked by [ahx$^{5-24}$]NPY (1 µM) in the absence of SCH23390 (n=21). Significantly less I_{IR} conductance was blocked by [ahx$^{5-24}$]NPY (1 µM) in the presence of SCH23390 (15 µM).

(G) PN I-V plots constructed from voltage ramps with intracellular Cs^+, in the presence of TTX (500 nM) containing bath solution. Under these conditions bath applied $[ahx^{5-24}]NPY$ (1 µM) significantly reduced inward PN current but had no effects on outward conductance.

(H) Net PN conductance blocked by $[ahx^{5-24}]NPY$ (1 µM) in the presence of intracellular Cs^+ and TTX (500 nM). $[ahx^{5-24}]NPY$ substantially decreased an inward current; however under these conditions $[ahx^{5-24}]NPY$'s effects on outward conductance were occluded.

Figure 4: [ahx$^{5-24}$]NPY Decreases Tonic GABA$_B$ Responses in BLA PNs
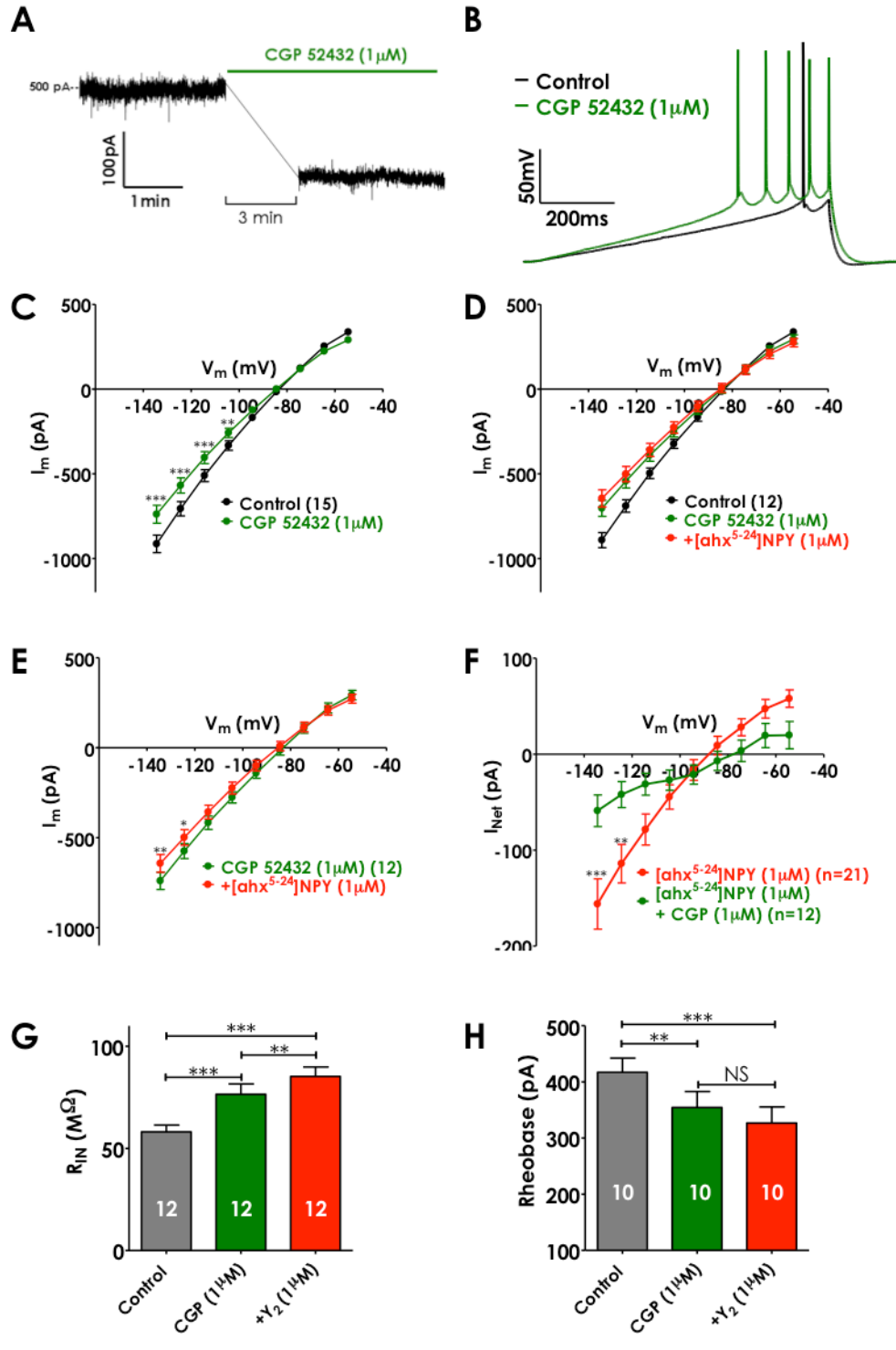
Figure 4: [ahx$^{5-24}$]NPY Decreases Tonic GABA$_B$ Responses in BLA PNs

(A) Representative PN voltage clamp membrane current traces at a -55 mV holding potential. Bath application of CGP 52432 (1 μM) reduced the -55 mV holding current indicating actions on a steady state conductance.

(B) Representative membrane potential traces from a PN during a depolarizing current ramp. Following bath application of CGP 52432 (1 μM), PN excitability was increased.

(C) Current-voltage responses of a PN I_{IR}. CGP 52432 (1 μM) significantly reduced an inwardly- rectifying conductance (n=15).

(D) Current-voltage responses of a PN I_{IR}. When [ahx$^{5-24}$]NPY was applied in presence CGP 52432 (1 μM) its effects on I_{IR} conductance were largely occluded (n=12).

(E) Net PN I_{IR} conductance blocked by [ahx$^{5-24}$]NPY (1 μM) in the presence of CGP 52432 (1 μM) (n=12), compared to the conductance blocked by [ahx$^{5-24}$]NPY (1 μM) in the absence of CGP 52432 (21). Significantly less I_{IR} conductance was blocked by [ahx$^{5-24}$]NPY (1 μM) in the presence of CGP 52432 (1 μM).

(F) Bath application of CGP 52432 (1 μM) significantly increased PN input resistance from 58.1 ± 3.3 MΩ to 76.5 ± 5.0 MΩ (p<0.001; n=12). Bath application of [ahx$^{5-24}$]NPY (1 μM) in the presence of CGP 52432 (1 μM) continued to significantly increase input resistance from 76.5 ± 5.0 MΩ to 85.2 ± 4.6 MΩ (p<0.01; n=12).

(G) Bath application of CGP 52432 (1 µM) significantly decreased PN rheobase from 417.1 ± 25.3 pA to 354.4 ± 28.5 pA (p<0.01; n=10). Subsequent bath application of [ahx$^{5-24}$]NPY (1 µM) in the presence of CGP 52432 (1 µM) did not significantly change PN rheobase.

Figure 5: Baclofen Blocks Effects of [ahx^{5-24}]NPY

171
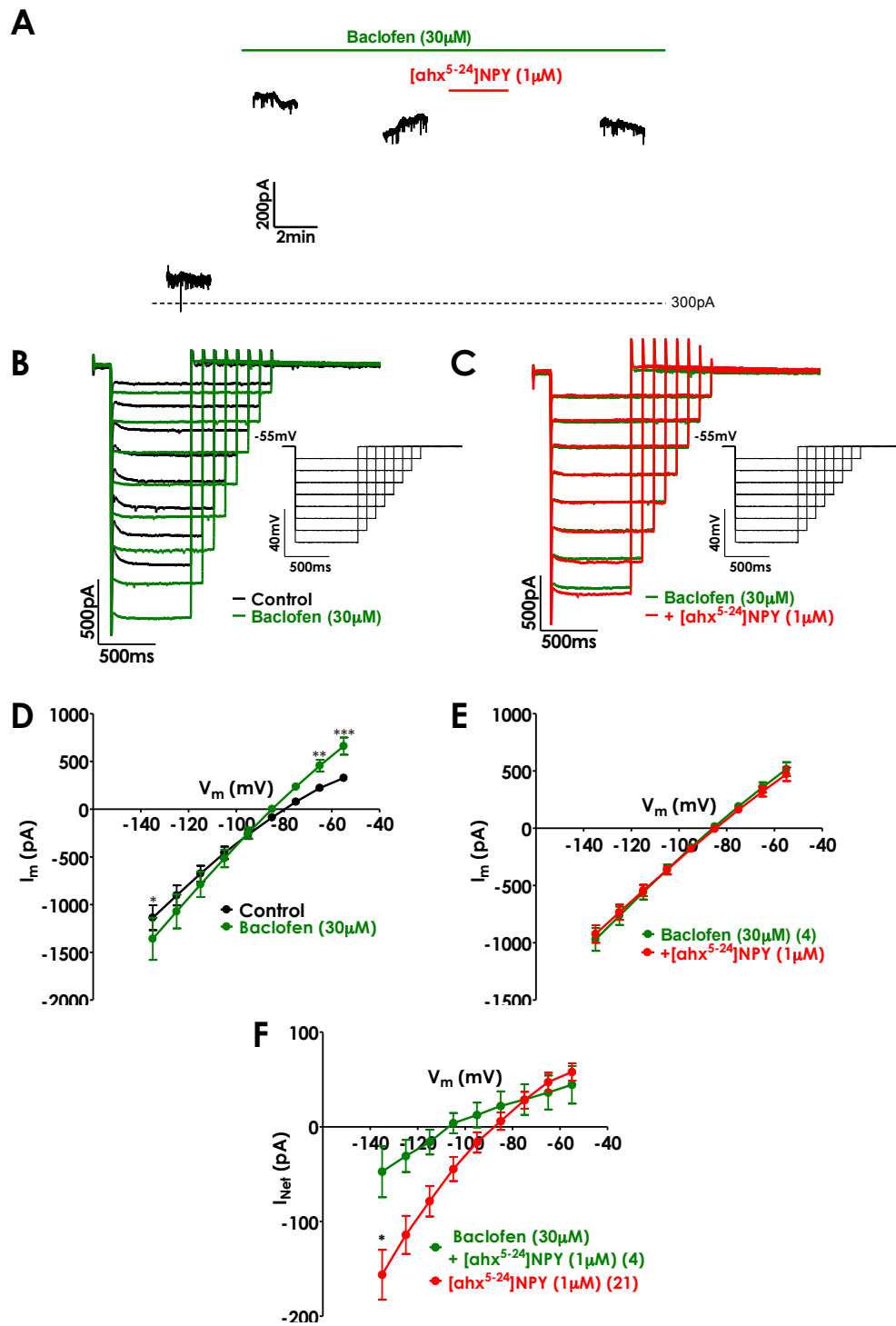
Figure 5: Baclofen Blocks Effects of [ahx$^{5-24}$]NPY

(A) Representative PN voltage clamp membrane current traces at a -55 mV holding potential. Bath application of baclofen (30 μM) substantially increased the -55 mV holding current. When [ahx$^{5-24}$]NPY (1 μM) was applied in the presence of baclofen (30 μM) it's effects on the holding current were largely blocked.

(B) Representative PN hyperpolarizing voltage steps from a -55mV holding potential. Bath application of baclofen (30 μM) substantially increased the I_{IR} in this PN and eliminated its I_h.

(C) Representative current traces from the same PN as (B). Application of [ahx$^{5-24}$]NPY (1 μM) in the presence of SCH23390 had little if any additional effects on this PN's conductance.

(D) PN voltage step I_{IR} I-V plots. Baclofen (30 μM) significantly increased PN conductance (n=6).

(E) PN voltage step I_{IR} I-V plots. When [ahx$^{5-24}$]NPY was applied in presence baclofen (30 μM) its effects on PN early current conductance were blocked.

(F) Net PN I_{IR} conductance blocked by [ahx$^{5-24}$]NPY (1 μM) in the presence of baclofen (30 μM) (n=4), compared to the conductance blocked by [ahx$^{5-24}$]NPY (1 μM) in the absence of baclofen (21). Significantly less PN I_{IR} conductance was blocked by [ahx$^{5-24}$]NPY (1 μM) in the presence of baclofen (30 μM).

Figure 6: [ahx$^{5-24}$]NPY Decreases Tonic GABA$_A$
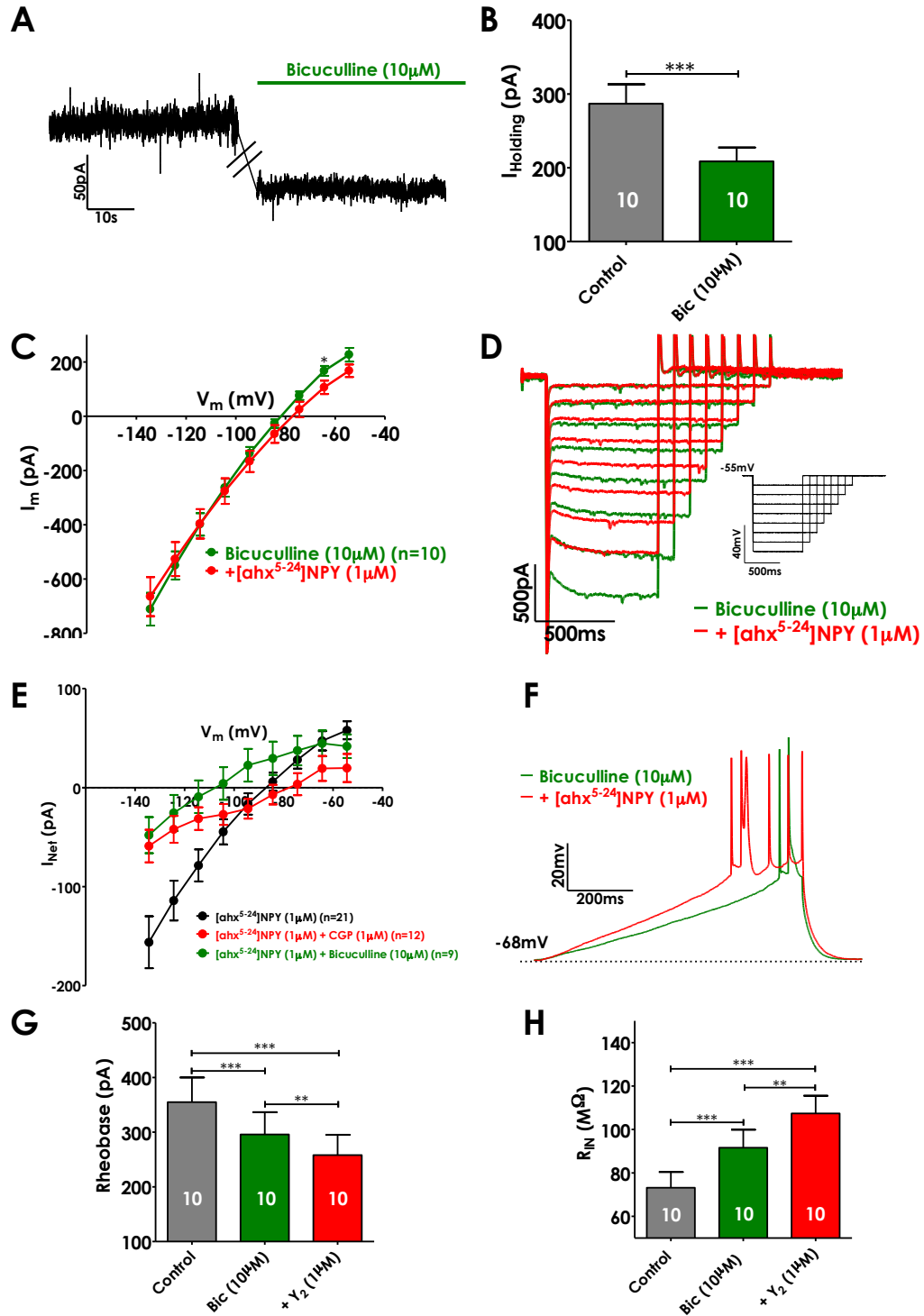
Figure 6: [ahx$^{5-24}$]NPY Decreases Tonic GABA$_A$

(A) Representative PN current traces at a -55 mV holding potential. Bath application of bicuculline (10 μM) reduced the -55 mV holding current indicating actions on a tonically active conductance.

(B) Bicuculline (10 μM) significantly decreased the -55 mV holding current in all PNs tested from 286 ± 26 pA to 208 ± 18 pA (p< 0.001; n=10).

(C) PN voltage step I$_{IR}$ I-V plots. When [ahx$^{5-24}$]NPY (1 μM) was applied in presence bicuculline (10 μM) its effects on PN early current conductance were partly occluded.

(D) PN I$_{IR}$ current-voltage (I-V) plots. When [ahx$^{5-24}$]NPY (1 μM) was applied in presence bicuculline (10 μM) its effects on PN I$_{IR}$ conductance were partly occluded.

(E) Representative PN current responses to hyperpolarizing voltage steps from a -55mV holding potential. In this PN, in the presence of bicuculline (10 μM), bath application of [ahx$^{5-24}$]NPY (1 μM) continued to substantially decrease an inwardly-rectifying I$_{IR}$ conductance.

(F) Representative mambrane potential traces from a PN during a depolarizing current ramp in the presence of bicuculline (10 μM). Following bath application of [ahx$^{5-24}$]NPY (1 μM), PN (rheobase measured) excitability was increased.

(G) Bath application of bicuculline (10 μM) significantly decreased PN rheobase from 354.9 ± 45.0 pA to 295.9 ± 40.7 pA (p<0.001; n=10). Bath application of [ahx$^{5-24}$]NPY (1

μM) in the presence of bicuculline (10 μM) continued to significantly decrease rheobase from 295.9 ± 40.7 pA to 258.1 ± 37.2 pA (p<0.01; n=10).

(H) Bath application of bicuculline (10 μM) significantly increased PN input resistance from 73.2 ± 7.2 MΩ to 91.6 ± 8.3 MΩ (p<0.001; n=10). Bath application of [ahx$^{5-24}$]NPY (1 μM) in the presence of bicuculline (10 μM) continued to significantly increase input resistance from 91.6 ± 8.3 MΩ to 107.4 ± 8.2 MΩ (p<0.01; n=10).

Figure 7: Blocking GABA$_A$ and GABA$_B$ Receptors Fully Occludes Effects of [ahx$^{5-24}$]NPY
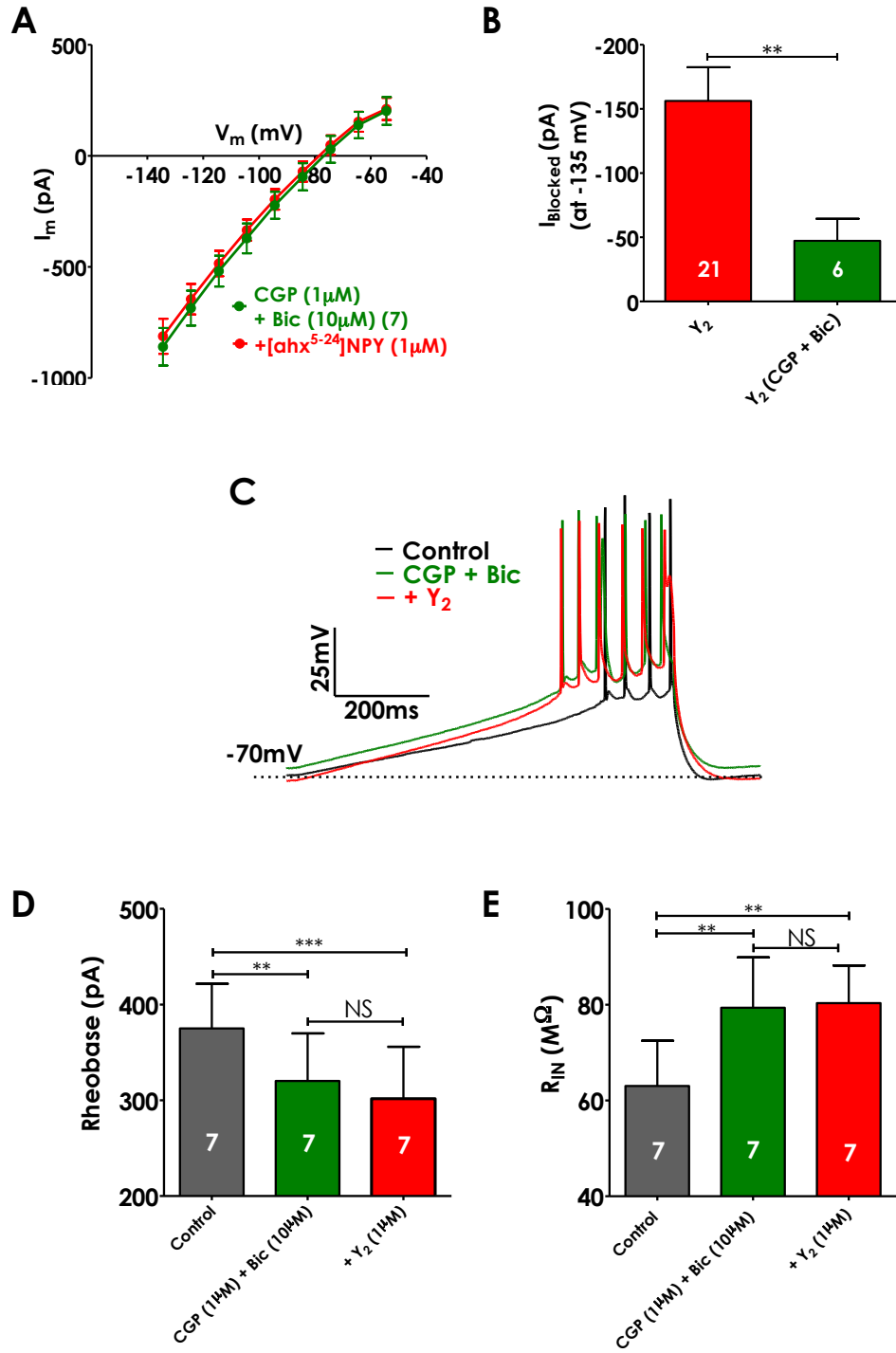
Figure 7: Blocking GABA$_A$ and GABA$_B$ Receptors Fully Occludes Effects of [ahx$^{5-24}$]NPY

(A) PN voltage step I_{IR} I-V plots. When [ahx$^{5-24}$]NPY (1 μM) was applied in presence bicuculline (10 μM) and CGP 52432 (1 μM) its effects on the PN I_{IR} conductance were completely occluded.

(B) Net PN I_{IR} conductance blocked by [ahx$^{5-24}$]NPY (1 μM) in the presence of CGP 52432 (1 μM) and bicuculline (10 μM) (n=7), compared to the conductance blocked by [ahx$^{5-24}$]NPY (1 μM) alone at -135 mV. Significantly less PN conductance was blocked by [ahx$^{5-24}$]NPY (1 μM) in the presence of CGP 52432 and bicuculline.

**(C)** Representative membrane potential traces from a PN during a depolarizing current ramp in the presence of CGP 52432 (1 μM) and bicuculline (10 μM). Following bath application of [ahx$^{5-24}$]NPY (1 μM), PN rheobase measured excitability was not changed.

(D) Bath application of bicuculline (10 μM) and CGP 52432 (1 μM) significantly decreased PN rheobase. Bath application of [ahx$^{5-24}$]NPY (1 μM) in the presence of bicuculline (10 μM) and 52432 (1 μM) did not significantly change PN rheobase.

(E) Bath application of CGP 52432 (1 μM) and bicuculline (10 μM) significantly increased PN input resistance. When [ahx$^{5-24}$]NPY (1 μM) was subsequently applied in the presence of CGP 52432 and bicuculline no further effect of input resistance were observed.

177

Figure 8: [ahx$^{5-24}$]NPY Modulates I$_h$ Via Suppression of Tonic GABA$_B$
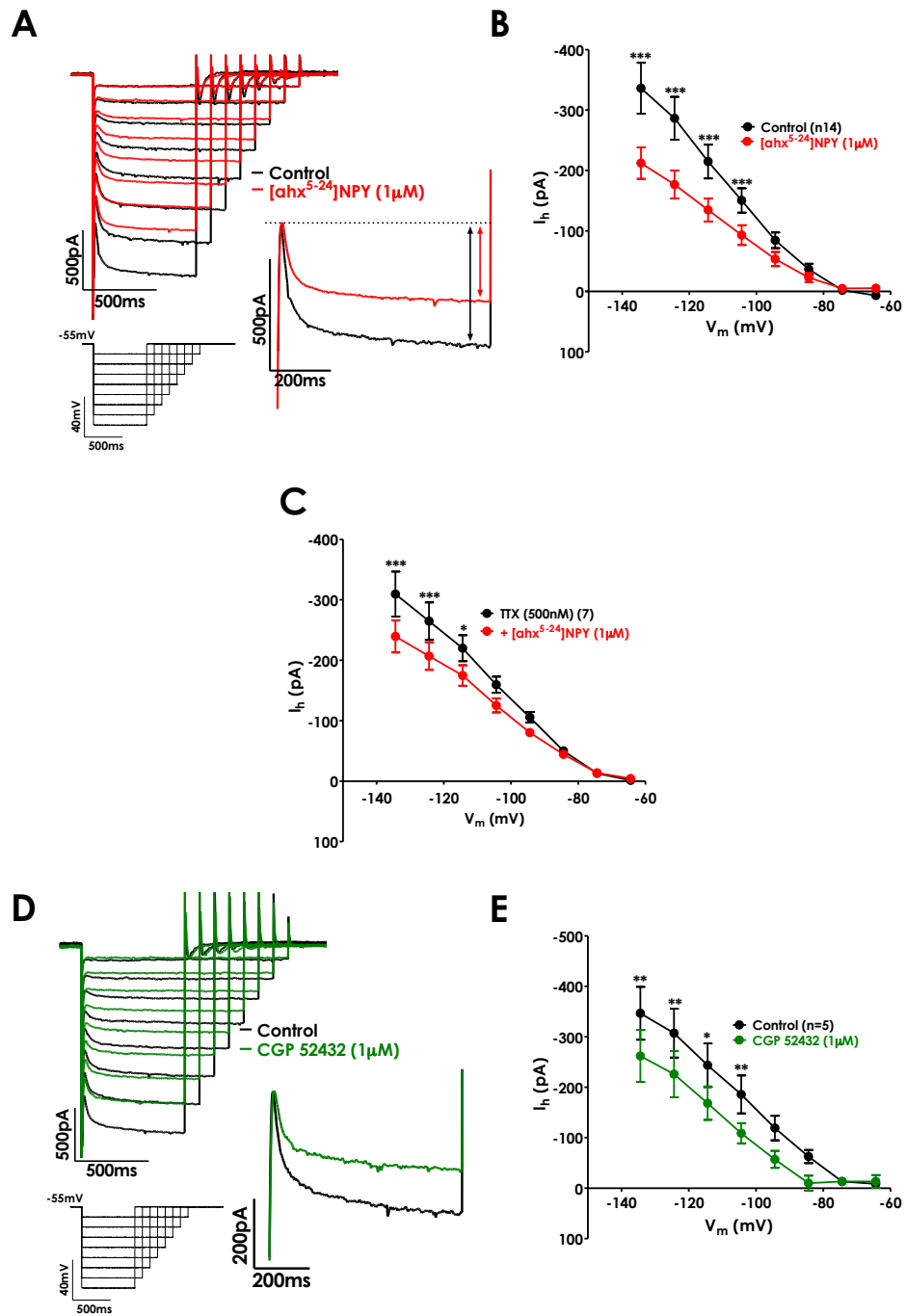
Figure 8: [ahx$^{5-24}$]NPY Modulates I$_h$ Via Suppression of Tonic GABA$_B$

(A) Representative PN current responses to hyperpolarizing voltage steps from a -55mV holding potential. Bath application of [ahx$^{5-24}$]NPY (1 µM) substantially decreased both the I$_{IR}$ and I$_h$ in this PN.

(B) [ahx$^{5-24}$]NPY (1 µM) significantly decreased PN I$_h$ (n=14).

(C) [ahx$^{5-24}$]NPY (1 µM) continued to decrease PN I$_h$ in the presence of TTX (500 nM).

(D) Representative PN hyperpolarizing voltage steps from a -55 mV holding potential. Bath application of CGP 52432 (1 µM) substantially decreased both the early current and I$_h$ in this PN.

(E) CGP 52432 (1 µM) significantly decreased PN I$_h$ (n=5).

Figure 9: CRF Excites PNs and Also Decreases an Inward Rectifying Current
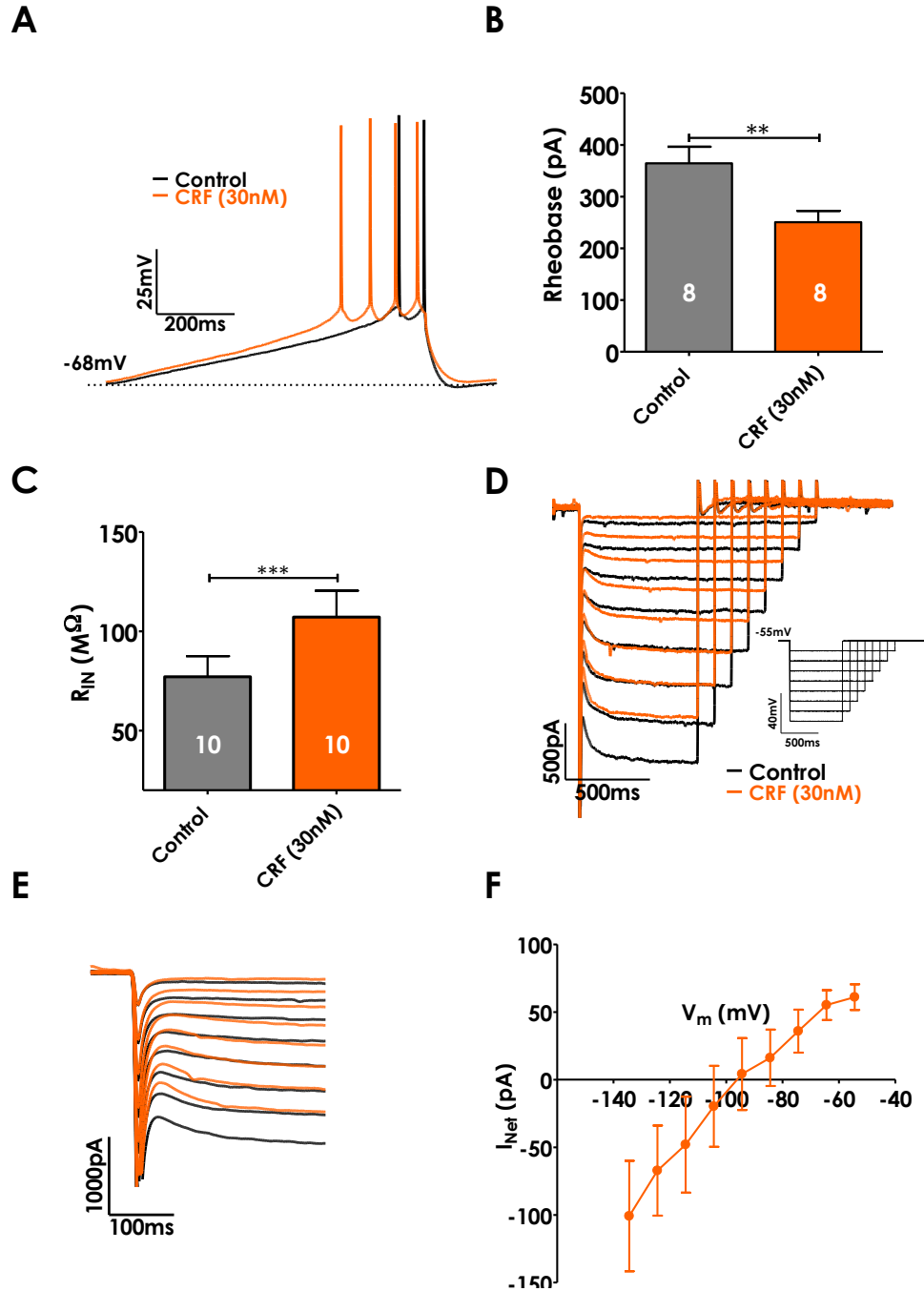
Figure 9: CRF Excites PNs and Also Decreases an Inward Rectifying Current

(A) Representative membrane potential traces from a PN during a depolarizing current ramp. Following bath application of CRF (30 nM), PN rheobase was decreased.

(B) CRF (30 nM) significantly decreased rheobase current from 364.7 ± 31.9 pA to 250.7 ± 21.8 pA ($p<0.01$; n=8) in 8/9 PNs tested.

(C) CRF (30 nM) significantly increased input resistance from 77.1 ± 10.4 to 107.1 ± 13.3 ($p<0.001$; n=10) in 10/11 PNs tested.

(D and E) Representative PN current responses to hyperpolarizing voltage steps from a -55mV holding potential. Bath application of CRF (30 nM) substantially decreased the I_{IR} in this PN.

(F) The net PN I_{IR} inhibited by CRF (30 nM). The CRF sensitive current reversed at -99.7 ± 6.5 (n=7) and showed clear inward rectification.

Figure 10: Model Summary
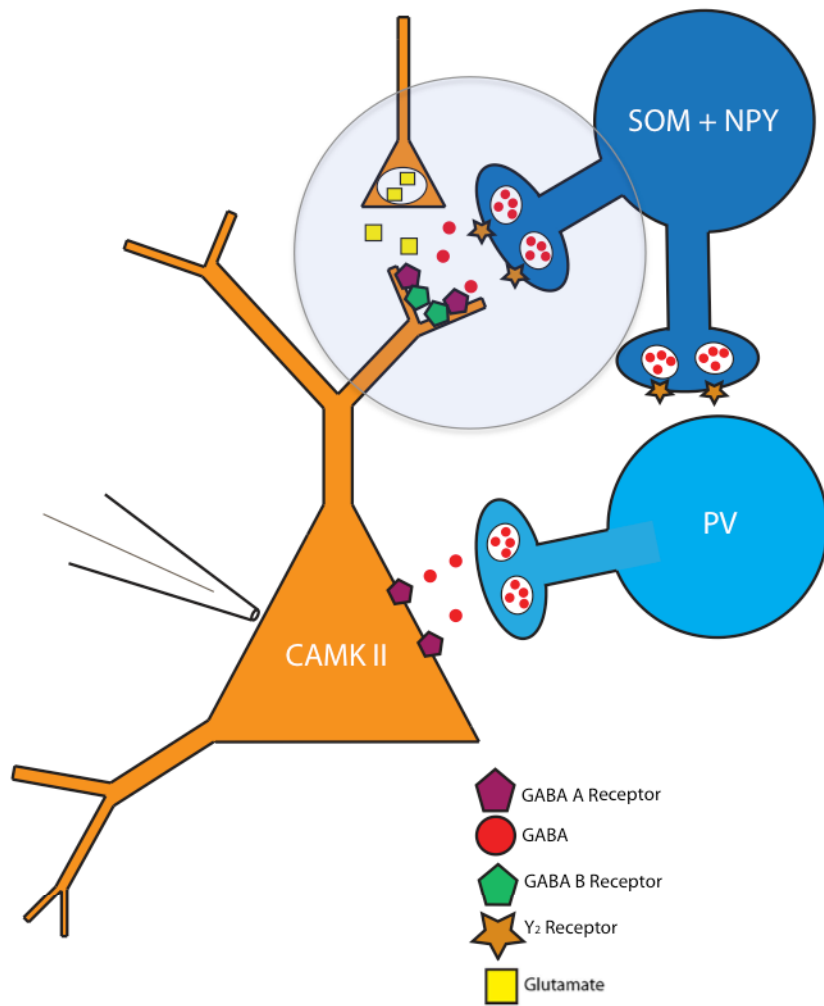
Figure 10: Model Summary

Activation of presynaptic Y_2 receptors decreases tonic GABA release from NPY-SOM interneurons. This activation relieves strong tonic $GABA_A$ and $GABA_B$-mediated inhibition of PN dendrites, which increases PN excitability. This action also puts PN dendrites into a state permissive for plasticity.

3.6 REFERENCES

Amano T, Unal CT, Paré D (2010) Synaptic correlates of fear extinction in the amygdala. Nat Neurosci 13:489–494.

Capogna M (2014) GABAergic cell type diversity in the basolateral amygdala. Curr Opin Neurobiol 26:110–116.

Chen X, DiMaggio DA, Han SP, Westfall TC (1997) Autoreceptor-induced inhibition of neuropeptide Y release from PC-12 cells is mediated by Y2 receptors. Am J Physiol 273:H1737–H1744.

Chen Y, Phillips K, Minton G, Sher E (2005) GABA(B) receptor modulators potentiate baclofen-induced depression of dopamine neuron activity in the rat ventral tegmental area. Br J Pharmacol 144:926–932.

Colmers WF, Bleakman D (1994) Effects of neuropeptide Y on the electrical properties of neurons. Trends Neurosci 17:373–379.

Day M (2005) Dendritic Excitability of Mouse Frontal Cortex Pyramidal Neurons Is Shaped by the Interaction among HCN, Kir2, and Kleak Channels. Journal of Neuroscience 25:8776–8787.

Gassmann M, Bettler B (2012) Regulation of neuronal GABA(B) receptor functions by subunit composition. Nat Rev Neurosci 13:380–394.

Giesbrecht CJ, Mackay JP, Silveira HB, Urban JH, Colmers WF (2010) Countervailing Modulation of Ih by Neuropeptide Y and Corticotrophin-Releasing Factor in Basolateral Amygdala As a Possible Mechanism for Their Effects on Stress-Related Behaviors. Journal of Neuroscience 30:16970–16982.

Greber S, Schwarzer C, Sperk G (1994) Neuropeptide Y inhibits potassium-stimulated glutamate release through Y2 receptors in rat hippocampal slices in vitro. Br J Pharmacol 113:737–740.

Greif GJ, Sodickson DL, Bean BP, Neer EJ, Mende U (2000) Altered regulation of potassium and calcium channels by GABA(B) and adenosine receptors in hippocampal neurons from mice lacking Galpha(o). Journal of Neurophysiology 83:1010–1018.

Gutman AR, Yang Y, Ressler KJ, Davis M (2008) The Role of Neuropeptide Y in the Expression and Extinction of Fear-Potentiated Startle. Journal of Neuroscience 28:12682–12690.

Klapstein GJ, Colmers WF (1997) Neuropeptide Y suppresses epileptiform activity in rat hippocampus in vitro. Journal of Neurophysiology 78:1651–1661.

Klenowski PM, Fogarty MJ, Belmer A, Noakes PG, Bellingham MC, Bartlett SE (2015) Structural and functional characterization of dendritic arbors and GABAergic synaptic inputs on interneurons and principal cells in the rat basolateral amygdala. Journal of Neurophysiology 114:942–957.

Kulik A, Vida I, Luján R, Haas CA, López-Bendito G, Shigemoto R, Frotscher M (2003) Subcellular localization of metabotropic GABA(B) receptor subunits GABA(B1a/b) and GABA(B2) in the rat hippocampus. J Neurosci 23:11026–11035.

LeDoux JE (2000) Emotion circuits in the brain. Annu Rev Neurosci 23:155–184.

Leung LS, Peloquin P (2006) GABA(B) receptors inhibit backpropagating dendritic spikes in hippocampal CA1 pyramidal cells in vivo. Hippocampus 16:388–407.

Lörincz A, Notomi T, Tamás G, Shigemoto R, Nusser Z (2002) Polarized and compartment-dependent distribution of HCN1 in pyramidal cell dendrites. Nat Neurosci 5:1185–1193.

Mahanty NK, Sah P (1998) Calcium-permeable AMPA receptors mediate long-term potentiation in interneurons in the amygdala. Nature 394:683–687.

Mańko M, Bienvenu TCM, Dalezios Y, Capogna M (2012) Neurogliaform cells of amygdala: a source of slow phasic inhibition in the basolateral complex. The Journal of Physiology 590:5611–5627.

Maren S (1999) Neurotoxic basolateral amygdala lesions impair learning and memory but not the performance of conditional fear in rats. J Neurosci 19:8696–8703.

McDonald AJ (1984) Neuronal organization of the lateral and basolateral amygdaloid nuclei in the rat. J Comp Neurol 222:589–606.

McDonald AJ (1996) Glutamate and aspartate immunoreactive neurons of the rat basolateral amygdala: colocalization of excitatory amino acids and projections to the limbic circuit. J Comp Neurol 365:367–379.

McDonald AJ, Mascagni F, Muller JF (2004) Immunocytochemical localization of GABABR1 receptor subunits in the basolateral amygdala. Brain Research 1018:147–158.

Melnick IV (2012) Cell type-specific postsynaptic effects of neuropeptide Y in substantia gelatinosa neurons of the rat spinal cord. Synapse 66:640–649.

Morrisett RA, Mott DD, Lewis DV, Swartzwelder HS, Wilson WA (1991) GABAB-receptor-mediated inhibition of the N-methyl-D-aspartate component of synaptic transmission in the rat hippocampus. Journal of Neuroscience 11:203–

209.

Muller JF, Mascagni F, McDonald AJ (2006) Postsynaptic targets of somatostatin-containing interneurons in the rat basolateral amygdala. J Comp Neurol 500:513–529.

Obrietan K, van den Pol AN (1996) Neuropeptide Y depresses GABA-mediated calcium transients in developing suprachiasmatic nucleus neurons: a novel form of calcium long-term depression. Journal of Neuroscience 16:3521–3533.

Oláh S, Füle M, Komlósi G, Varga C, Báldi R, Barzó P, Tamás G (2009) Regulation of cortical microcircuits by unitary GABA-mediated volume transmission. Nature 461:1278–1281.

Olpe HR, Steinmann MW, Ferrat T, Pozza MF, Greiner K, Brugger F, Froestl W, Mickel SJ, Bittiger H (1993) The actions of orally active GABAB receptor antagonists on GABAergic transmission in vivo and in vitro. European Journal of Pharmacology 233:179–186.

Otmakhova NA (2004) Contribution of Ih and GABAB to Synaptically Induced Afterhyperpolarizations in CA1: A Brake on the NMDA Response. Journal of Neurophysiology 92:2027–2039.

Paredes MF, Greenwood J, Baraban SC (2003) Neuropeptide Y modulates a G protein-coupled inwardly rectifying potassium current in the mouse hippocampus. Neurosci Lett 340:9–12.

Phan KL, Fitzgerald DA, Nathan PJ, Tancer ME (2006) Association between amygdala hyperactivity to harsh faces and severity of social anxiety in generalized social phobia. Biol Psychiatry 59:424–429.

Pitkänen A, Savander V, LeDoux JE (1997) Organization of intra-amygdaloid circuitries in the rat: an emerging framework for understanding functions of the amygdala. Trends Neurosci 20:517–523.

Pozza MF, Manuel NA, Steinmann M, Froestl W, Davies CH (1999) Comparison of antagonist potencies at pre- and post-synaptic GABA(B) receptors at inhibitory synapses in the CA1 region of the rat hippocampus. Br J Pharmacol 127:211–219.

Prater KE, Hosanagar A, Klumpp H, Angstadt M, Phan KL (2013) Aberrant amygdala-frontal cortex connectivity during perception of fearful faces and at rest in generalized social anxiety disorder. 30:234–241.

Rainnie DG, Asprodini EK, Shinnick-Gallagher P (1993) Intracellular recordings from morphologically identified neurons of the basolateral amygdala. Journal of Neurophysiology 69:1350–1362.

Rainnie DG, Bergeron R, Sajdyk TJ, Patil M, Gehlert DR, Shekhar A (2004) Corticotrophin releasing factor-induced synaptic plasticity in the amygdala translates stress into emotional disorders. J Neurosci 24:3471–3479.

Rogan MT, Stäubli UV, LeDoux JE (1997) Fear conditioning induces associative long-term potentiation in the amygdala. Nature 390:604–607.

Rostkowski AB, Teppen TL, Peterson DA, Urban JH (2009) Cell-specific expression of neuropeptide Y Y1 receptor immunoreactivity in the rat basolateral amygdala. J Comp Neurol 517:166–176.

Sajdyk TJ, Johnson PL, Leitermann RJ, Fitz SD, Dietrich A, Morin M, Gehlert DR, Urban JH, Shekhar A (2008) Neuropeptide Y in the Amygdala Induces Long-Term Resilience to Stress-Induced Reductions in Social Responses But Not Hypothalamic-Adrenal-Pituitary Axis Activity or Hyperthermia. Journal of Neuroscience 28:893–903.

Sajdyk TJ, Schober DA, Smiley DL, Gehlert DR (2002) Neuropeptide Y-Y2 receptors mediate anxiety in the amygdala. Pharmacol Biochem Behav 71:419–423.

Sajdyk TJ, Vandergriff MG, Gehlert DR (1999) Amygdalar neuropeptide Y Y1 receptors mediate the anxiolytic-like actions of neuropeptide Y in the social interaction test. European Journal of Pharmacology 368:143–147.

Scanziani M (2000) GABA spillover activates postsynaptic GABA(B) receptors to control rhythmic hippocampal activity. 25:673–681.

Shekhar A, Sajdyk TS, Keim SR, Yoder KK, Sanders SK (1999) Role of the basolateral amygdala in panic disorder. Ann N Y Acad Sci 877:747–750.

Sodickson DL, Bean BP (1996) GABAB receptor-activated inwardly rectifying potassium current in dissociated hippocampal CA3 neurons. Journal of Neuroscience 16:6374–6385.

Sosulina L, Schwesig G, Seifert G, Pape H-C (2008) Neuropeptide Y activates a G-protein-coupled inwardly rectifying potassium current and dampens excitability in the lateral amygdala. Mol Cell Neurosci 39:491–498.

Stanić D, Mulder J, Watanabe M, Hökfelt T (2011) Characterization of NPY Y2 receptor protein expression in the mouse brain. II. Coexistence with NPY, the Y1 receptor, and other neurotransmitter-related molecules. J Comp Neurol 519:1219–1257.

Sun QQ, Akk G, Huguenard JR, Prince DA (2001) Differential regulation of GABA release and neuronal excitability mediated by neuropeptide Y1 and Y2 receptors in rat thalamic neurons. The Journal of Physiology 531:81–94.

Tamás G, Lőrincz A, Simon A, Szabadics J (2003) Identified sources and targets of slow inhibition in the neocortex. Science 299:1902–1905.

Vigot R, Barbieri S, Bräuner-Osborne H, Turecek R, Shigemoto R, Zhang Y-P, Luján R, Jacobson LH, Biermann B, Fritschy J-M, Vacher C-M, Müller M, Sansig G, Guetg N, Cryan JF, Kaupmann K, Gassmann M, Oertner TG, Bettler B (2006) Differential compartmentalization and distinct functions of GABAB receptor variants. Neuron 50:589–601.

Walker DL, Miles LA, Davis M (2009) Selective participation of the bed nucleus of the stria terminalis and CRF in sustained anxiety-like versus phasic fear-like responses. Prog Neuropsychopharmacol Biol Psychiatry 33:1291–1308.

Wang Y, Neubauer FB, Lüscher H-R, Thurley K (2010) GABAB receptor-dependent modulation of network activity in the rat prefrontal cortex in vitro. Eur J Neurosci 31:1582–1594.

Washburn MS, Moises HC (1992) Electrophysiological and morphological properties of rat basolateral amygdaloid neurons in vitro. Journal of Neuroscience 12:4066–4079.

Whissell PD, Lecker I, Wang D-S, Yu J, Orser BA (2015) Altered expression of δGABAA receptors in health and disease. Neuropharmacology 88:24–35.

Wolak ML, DeJoseph MR, Cator AD, Mokashi AS, Brownfield MS, Urban JH (2003) Comparative distribution of neuropeptide Y Y1 and Y5 receptors in the rat brain by using immunohistochemistry. J Comp Neurol 464:285–311.

Chapter 4

NPY Y_1 and Y_2 Receptors Enhance The Slow After Hyperpolarizing Current In BLA Principal Neurons – A Potential Anxiety-Reducing Interaction

4.1 INTRODUCTION

We showed earlier (Chapter 3) that selective activation of NPY Y_2 receptors increases the excitability of BLA principal neurons (PN). This action, which occurs via a presynaptically-mediated reduction in tonic, $GABA_B$-mediated inhibition, likely underlies the acute anxiogenic behavioral effects of selective Y_2 receptor activation in the BLA (Sajdyk et al., 2002). Additionally, since these effects likely disinhibit PN dendrites, they may facilitate anxiety-reducing NPY-mediated plasticity (Sajdyk et al., 2008). However, NPY itself is acutely anxiolytic and reduces BLA PN excitability (Sajdyk et al., 1999; Giesbrecht et al., 2010). The question therefore arises as to how the actions of other NPY receptors interact with these acute excitatory Y_2 receptor-mediated effects so that NPY's acute anxiolytic actions predominate in the BLA?

An important clue came from voltage-clamp experiments showing that the selective Y_2 receptor agonist [ahx$^{5-24}$]NPY increased the Ca^{2+}-dependent, slow after-hyperpolarizing K^+ conductance (I_{sAHP}) in a subset of responsive PNs. Potentiation of the I_{sAHP} might be attributed to enhanced dendritic Ca^{2+} signaling, secondary to the loss of tonic $GABA_A$ and $GABA_B$-mediated inhibition (Chapter 3). Enhancement of the sI_{AHP} by [ahx$^{5-24}$]NPY limited the rate at which responsive PNs could discharge action potentials.

The acute anxiolytic effects of NPY are mediated largely via Y_1 receptors (Sajdyk et al., 1999). We therefore, next performed experiments with the Y_1 receptor selective agonist F^{7}P^{34}NPY to search for potential Y_1, Y_2 receptor interactions that might mitigate excitatory Y_2 receptor effects and recapitulate NPY's more inhibitory actions. Interestingly, the Y_1 agonist also potentiated the I_{sAHP}, likely via a different mechanism than [ahx$^{5-24}$]NPY. When both Y_1 and Y_2 receptors were co-activated greater potentiation

of the action potential after-hyperpolarization (AHP) occurred. Therefore, although Y_2 receptor activation appeared to increase PN Ca^{2+} influx, potentiation of the sI_{AHP} by Y_1 receptors may more effectively couple this Ca^{2+} to the inhibitory sI_{AHP} and limit PN discharge rates when Y_1 and Y_2 receptors are co-activated.

4.2 MATERIALS AND METHODS

4.2a Animals

Male Sprague Dawley rats 6-12 weeks of age were used for experiments (see section 3.2a for details).

4.2b Brain Slice Preparation

Acute BLA containing rate brain slices were prepared as described earlier in this thesis (see section 3.2b for details).

4.2c Electrophysiology

Electrophysiological experiments were performed essentially as described earlier in this thesis (Chapters 2, 3). Briefly, patch pipettes with a tip resistance of (5-7 MΩ) were filled with an internal solution containing in (mM): 126 K-gluconate, 10 HEPES, 4 KCl, 5 MgATP, 0.3 NaGTP, 1 EGTA, 0.3 CaCl$_2$. Neurobiotin (0.05 – 0.1%) was added and the pH adjusted to 7.27 – 7.30 with KOH, (275 – 285 mOsm/L). Recordings were made using a Multiclamp 700B amplifier and data were acquired using pClamp (v 10.3 – 10.4) via a Digidata 1322 interface (all Molecular Devices, Sunnyvale, CA). The liquid junction potential was calculated as +14.4 mV; all voltage and current clamp data reported have been adjusted to reflect this.

BLA PNs were selected for whole cell patch clamp recordings based on the criteria outlined in section 3.2c. PNs were mainly held in voltage clamp at -75 mV for 5-10 min before the start of experiments and between experimental manipulations. A series of experimental protocols were performed at 5min intervals to establish the stability of baseline neuronal properties. Only PNs, which showed stable resting membrane potential

(RMP) and holding current (in voltage clamp) in a series of control measurements and which showed stable access resistance (± 20%) throughout an experiment were selected for analysis.

4.2c(i) Current-clamp Experiments

Successive 800 ms depolarizing current-clamp steps of 50 pA or 100 pA increments were used to depolarize PNs and elicit action potential firing. The waveform of individual action potentials, and firing patterns of action potential trains were analyzed from steps in which 5-10 action potentials were fired. When analyzing effects of drugs on action potential properties, steps eliciting the same number of action potentials (±1) were compared for within-PN measurements. PNs in which recordings did meet the above criteria were excluded from analysis. Inter-spike spike intervals in action potential trains were measured and plotted as a function of their order in the train. Action potential after-hyperpolarizations (AHP) were also measured and plotted as a function of the action potential number in the train.

PNs display fast, medium and slow AHPs, which are mediated by voltage-gated K^+ (K_V) channels and Ca^{2+} dependent K^+ ($G_{K,Ca}$) channels (Sah, 1996). We have measured the slower AHP, which follows the fast AHP **(Figure 3A)**. This slower AHP can involve both medium and slow AHP currents (Sah and Faber, 2002). The medium AHP (mAHP) is mediated by apamin-sensitive SK $G_{K,Ca}$'s, and is evoked by single action potentials (Sah and Faber, 2002). The slow AHP (sAHP), is a $G_{K,Ca}$ carried by an unknown channel. Typically the sAHP is only recruited by trains of successive action potentials and leads to spike frequency adaptation (Sah and Bekkers, 1996; Power and Sah, 2008). The mAHP and sAHP are not readily separated in action potential trains

without pharmacological blockers. For clarity we will refer to the combined mAHP and sAHP as the AHP unless otherwise specified.

4.2c(ii) Voltage-clamp Experiments

Hyperpolarizing voltage steps were applied from a holding potential (V_h) of -55mV (as outlined in section 3.2c(ii)). In a subset of recordings, an I_{sAHP} was clearly activated following the termination of more hyperpolarized (>85 mV) voltage steps. This appeared as a slowly decaying outward current, often preceded by an inward tail current **(Figure 1A)**. [ahx$^{5-24}$]NPY often enhanced this current, sometimes substantially. The I_{sAHP} tail current was quantified by subtracting the mean steady-state holding current, at -55 mV, from the peak outward current, which was evoked by first hyperpolarizing neurons with a -135 mV voltage step, then stepping back to -55mV **(Figure 1B)**. In the case of large responses, this outward current did not fully decay during the interval between successive voltage steps (6 s) in which case the interval was increased to 10 s. The current-voltage (IV) relationship of the l$_{sAHP}$ tail current was analyzed with a version of this protocol in which a series of fast voltage steps were performed during the peak outward current.

4.2d Materials

The Y_2 agonist [6-aminohexanoic$^{5-24}$]NPY ([ahx$^{5-24}$NPY]) and the Y_1 agonist F^{7}P^{34}NPY ([Phe^7,Pro^{34}]NPY) were gifts from Dr. A. G. Beck-Sickinger (Leipzig, Germany). Kyneurenic acid was purchased from Abcam Biochemicals. GTP was purchased from Roche Diagnostics. K$^+$-Gluconate, EGTA, Mg•ATP, ivabradine, UCL 2077, CdCl$_2$, apamin and baclofen were obtained from Sigma-Aldrich. SCH 23390, and CGP 52432 were purchased from Tocris Bioscience. KOH was purchased from BDH

Chemicals. All other chemicals were obtained from Thermo Fisher Scientific. All drugs were stored as aliquots of concentrated stock solutions at -20 °C and diluted in ACSF bath solution immediately before application.

4.2e Data Analysis

Recordings were analyzed off-line with pClamp 10.3 (Molecular Devices). Figures were generated with GraphPad Prism, version 5.05. Statistical analyses were also performed with GraphPad Prism. Data are expressed as mean ± SEM. When effects of a drug on more than one action potential were compared, a repeated-measures two-way ANOVA, with the Bonferroni post-test, was used. Otherwise the paired Students t-test was used. The paired Students t-test was also used to test effects of drugs on the voltage-clamp measured I_{sAHP} tail current amplitude. Mean differences were considered significant at $p<0.05$, and significance levels are indicated in figures as follows: *$p<0.05$, **$p<0.01$, ***$p<0.001$.

4.3 RESULTS

4.3a Loss of Tonic GABA$_B$ Activation Potentiates The I$_{sAHP}$ In a Subset of Responsive Principal Neurons

When studying BLA PNs with voltage-clamp steps, we sometimes unexpectedly observed a slowly-decaying outward tail current. This current was seen when PNs were returned to -55 mV following larger hyperpolarizing steps. Although this outward tail current was generally small (or absent) under baseline conditions, it was often substantially enhanced in the presence of [ahx$^{5-24}$]NPY **(Figure 1A, B)**. Thus bath application of [ahx$^{5-24}$]NPY (1 μM) significantly increased this current from 61.6 ± 20.0 pA to 178.7 ± 34.8 pA (p<0.01; n=14) **(Figure 1C)** in 14/35 PNs tested. Using a brief hyperpolarizing step at the peak of this this outward current **(Figure 1D)**, we determined that it reversed near E$_K$ (~-80mV), consistent with a largely K$^+$ conductance, and showed clear outward rectification **(Figure 1D)**. Furthermore this current showed extremely slow decay kinetics with a single-exponential tau decay value >1s [1151 ± 145.1 ms (n=10)] **(Figure 1E).**

The GABA$_B$ receptor antagonist CGP 52432 (1 μM) also significantly potentiated a similar outward tail current with nearly identical kinetics [Tau decay = 1281 ± 121.2 ms (n=5)] at comparable rates to [ahx$^{5-24}$]NPY **(Figure 2A-B)**. These results suggest that the Y$_2$ receptor-mediated reduction in tonic GABA$_B$ activity (document in Chapter 3) also underlies this effect. Additionally, in all cases when the outward tail was potentiated by [ahx$^{5-24}$]NPY or CGP 52432 an instantaneous inwardly rectifying current (I$_{IR}$ − see Chapter 3) was concomitantly reduced **(Figure 1A)** and **(Figure 2A)**.

This slow kinetics of this outward tail current suggest it is mediated by the slow afterhyperpolarizing current (I$_{sAHP}$), a G$_{K,Ca}$ previously described in the BLA and

elsewhere (Sah and Bekkers, 1996; Power et al., 2011). Thus, we suspected that strong hyperpolarization of PNs removed inactivation of voltage-gated channels in addition to activating I_h. We hypothesized that this resulted in "anodal break" mediated recruitment of voltage gated Ca^{2+} channels (VGCC), when PN were returned to -55mV, and the elevated intracellular Ca^{2+} would activate the I_{sAHP}. Consistent with this mechanism, bath application of the non-specific VGCC blocker Cd^{2+} (100 – 200 μM) sharply reduced the amplitude of the outward tail current (p<0.01; n=10) **(Figure 2C-D)**. To confirm we were observing the I_{sAHP}, we next tested a relatively selective I_{sAHP} blocker, UCL 2077 (Shah et al., 2006). Application of UCL 2077 (10 μM) significantly reduced Y_2-facilitated outward tail currents by more than half (p<0.05; n=5), thus confirming they were mediated by the I_{sAHP} **(Figure 2E-F)**. Conversely, the SK channel blocker, apamin (1 μM) failed to block the outward tail current and in some cases actually enhanced it (not illustrated).

Both dendritic GIRK currents and I_h have both been shown to suppress dendritic excitability (Berger et al., 2003; Leung and Peloquin, 2006), which could explain sI_{AHP} enhancement by the Y_2 agonist and by the $GABA_B$ antagonist CGP 52432. However, the GIRK blocker SCH 23390 (15μM) did not fully replicate the effect of [ahx[5-24]]NPY or the CGP 52432. Only 3/16 (19%) PNs responded to SCH 23390 (15 μM) with a significant increase in the I_{sAHP} tail current from 194 ± 22 to 414 ± 62 (p<0.05; n=3) (not illustrated), compared to the ~40% response rate seen with [ahx[5-24]]NPY and CGP 52432. Additionally the I_{sAHP} was only potentiated by SCH 23390 in PNs, which already showed substantial current (>100 pA) prior to drug application (not illustrated). In comparison,

[ahx$^{5-24}$]NPY and CGP 52432 could unmask the I$_{sAHP}$ tail currents in PNs with no appreciable current under control conditions **(Figure 1A)** and **(Figure 2A)**.

4.3b Potentiation of the I$_{sAHP}$ by [ahx$^{5-24}$]NPY enhanced the PN action potential after-hyperpolarization

We previously documented that most BLA PNs (~85%) respond to [ahx$^{5-24}$]NPY (1 μM) with a reduction in tonic GABA-mediated inhibition, resulting in increased excitability (Chapter 3). However, we observed additional effects on the action potential waveform in the subset of PNs in which [ahx$^{5-24}$]NPY also potentiated the I$_{sAHP}$ tail current. In these PNs, the magnitude of the action potential after-hyperpolarization (AHP) was also (often dramatically) increased **(Figure 3A-B)**. 9/19 PNs tested, responded to [ahx$^{5-24}$]NPY (1 μM) with a greater than 30% increase in amplitude of the first AHP elicited by a depolarizing current step, which was increased from 6.21 ± 1.08 mV to 11.15 ± 1.13 mV (n=9, p<0.001) **(Figure 3E)**. All of these PNs also showed substantial Y$_2$R-mediated potentiation of the I$_{sAHP}$ tail current seen in voltage clamp, which was increased three-fold from 68.8 ± 27.8 pA to 221.6 ± 45.5 pA (p<0.01; n=9) **(Figure 3D)**. In most I$_{sAHP}$ responsive PNs, [ahx$^{5-24}$]NPY, significantly potentiated the AHP for all 5 of the first action potentials in a train **(Figure 3E)**. However, 3 PNs responded to [ahx$^{5-24}$]NPY (1 μM) with a substantial increase in the first AHP, then failed to fire any further action potentials for the remainder of the step **(Figure 3G)**.

In contrast, the I$_{sAHP}$ tail current was not significantly altered in those PNs in which [ahx$^{5-24}$]NPY (1 μM) inhibited the I$_{IR}$ current, but did not potentiate the AHP **(Figure 4)**. These results link potentiation of the I$_{sAHP}$ tail current seen in voltage-clamp steps with potentiation of the AHP.

4.3c Potentiation of the sI_{AHP} by [ahx$^{5-24}$]NPY reduces initial PN firing rates

The I_{sAHP}, which contributes to action potential spike frequency adaptation (Andrade et al., 2012) **(Figure 5A)**, is typically only recruited when BLA PNs fire trains of multiple action potentials. However, when enhanced by [ahx$^{5-24}$]NPY, the I_{sAHP} appeared to be elicited by the first action potential AHP of a train. This was seen as a substantial UCL 2077 (10 μM)-sensitive component of the first AHP, unmasked by exposure to [ahx$^{5-24}$]NPY **(Figure 5B)**.

We next investigated how these effects impacted PN firing rates. Surprisingly, in neurons where the Y_2 agonist also substantially (>10%) increased the I_{sAHP} tail current, action potential spike frequency adaptation was actually reduced **(Figures 5A and C)**. Inspection of action potential trains in this subset of PNs revealed that this effect was due to a substantial increase in the first inter-spike interval **(Figure 5C)**. In Y_2-I_{sAHP} responsive PNs this first inter-spike interval was more than doubled compared to control from 33.81 ± 9.47 ms to 80.05 ± 9.50 ms (p<0.001; n=9) **(Figure 5C)**. These results can be explained by examining the first after-hyperpolarization of a train, which was greatly exaggerated relative to control. Indeed, it appeared that the I_{sAHP} was near maximally recruited by the first action potential when unmasked by [ahx$^{5-24}$]NPY. This effect can therefore account for the reduced PN firing rates at the onset of spiking, and would prevent further slowing of the instantaneous firing rate with successive action potentials. In essence, potentiation of the I_{sAHP} by [ahx$^{5-24}$]NPY caused PN firing rates to be "pre-accommodated" at the onset of firing.

In Y_2 agonist-responsive PNs where the I_{sAHP} was not potentiated, we saw the opposite effect on the repetitive action potential discharge pattern. In these PNs, the

interval between the first two action potentials decreased significantly from 50.52 ± 7.11 ms to 29.33 ± 7.01 ms (p<0.01; n=10) **(Figure 5E-F)**. This was often due to the new onset of a first action potential doublet burst **(Figure 5F)**. Thus, increased spike frequency adaption was observed in PNs where [ahx$^{5-24}$]NPY reduced the I_{IR} but did not enhance the I_{sAHP}.

4.3d The selective Y_1 receptor agonist F^7P^{34}NPY also potentiates the I_{sAHP}

Interestingly, selective activation of Y_1 receptors also potentiated the PN I_{sAHP} **(Figure 6A-B)**. 7/15 PNs tested responded to bath application of the Y_1 selective agonist F^7P^{34}NPY (1 μM) with a significant increase in the voltage-clamp measured I_{sAHP} tail current from 107.8 ± 29.6 pA to 259.2 ± 72.2 pA (p<0.05; n=7).

All PNs in which either [ahx$^{5-24}$]NPY or CGP 52432 (1 μM) potentiated the I_{sAHP}, also showed a substantial reduction in a GIRK-like I_{IR} current. However in most cases F^7P^{34}NPY had little (if any) effects on the PN I_{IR} **(Figure 6A and D)**. These results suggest that Y_1 receptor-mediated potentiation of the I_{sAHP} was not due to reduced tonic GABA$_B$. However in many cases F^7P^{34}NPY reduced the PN I_h **(Figure 6A)**, consistent with previous findings (Giesbrecht et al., 2010).

In PNs that responded to F^7P^{34}NPY (1 μM) with increases in the I_{sAHP} tail current the AHP was also increased, although the magnitude of this effect was typically less than that observed with [ahx$^{5-24}$]NPY **(Figure 7A)**. However, when [ahx$^{5-24}$]NPY (1 μM) was subsequently applied to these F^7P^{34}NPY-responsive PNs, the first AHP in a train was further increased **(Figure 7B)**. Interestingly, in the majority (4/5) of such cases, following [ahx$^{5-24}$]NPY (1 μM) application only a single action potential could be elicited by

current steps. Although preliminary, these results suggest that in a subset of PNs, Y_1 and Y_2 receptor actions cooperate to enhance the action potential AHP and limit PN output.

4.4 DISCUSSION

In Chapter 3 we showed that the Y_2 agonist increased the excitability of most BLA PNs (~85%), via suppression of tonic $GABA_B$ receptor activation. Here we show that the Ca^{2+}-dependent I_{sAHP} is also potentiated by the Y_2 agonist in approximately half of Y_2-responsive PNs. The molecular identity of the channels underlying the I_{sAHP} is unknown. However, a biophysical study by Power et al (2011) suggested that I_{sAHP} channels are predominately expressed in PN dendrites (Power et al., 2011). Potentiation of the I_{sAHP} by [ahx$^{5-24}$]NPY is therefore consistent with the increased dendritic Ca^{2+} influx expected with the loss of $GABA_B$ tone.

Since the I_{sAHP} was similarly potentiated by the Y_2 agonist and the $GABA_B$ antagonist CGP 52432, the reduction in tonic $GABA_B$-mediated inhibition caused by [ahx$^{5-24}$]NPY (outlined in the previous chapter) likely unmasked this current. However, blocking PN GIRK channels with SCH 23390 did not fully replicate the effects of the Y_2 agonist on the I_{sAHP}. Therefore, removal of other tonic $GABA_B$ receptor actions, such as inhibition of dendritic VGCCs (Vigot et al., 2006), is likely also involved.

The I_{sAHP} is reportedly not recruited by single action potentials, but is instead activated when BLA PNs fire repeated action potential trains (Sah, 1996; Power and Sah, 2008; Andrade et al., 2012). This property underlies the prominent firing rate adaptation displayed by most PNs under basal conditions (Washburn and Moises, 1992; Rainnie et al., 1993; Power and Sah, 2008). However, when potentiated by the Y_2 agonist, the I_{sAHP}

was clearly and often massively recruited by a single PN action potential. This resulted in a prominent reduction in the initial firing rate, compared to controls in the same neurons. However, because of the [ahx$^{5-24}$]NPY-mediated reduction in tonic GABA inhibition (Chapter 3), less current was normally needed to elicit firing. Therefore selective Y_2R activation would be expected to have complex effects on the output of those PNs in which both effects occurred.

However, in approximately half of all [ahx$^{5-24}$]NPY responsive PNs, the I_{sAHP} was not potentiated, but only the reduction in the I_{IR} seen. In these neurons, the initial firing rate was significantly increased, largely due to the onset of a first action potential doublet burst. This effect is opposite to that observed in PNs where [ahx$^{5-24}$]NPY potentiated the I_{sAHP}. We hypothesize that this results from increased action potential back-propagation into disinhibited dendrites, but future experiments utilizing Ca^{2+} imaging will be required to clarify the mechanism via which these doublet bursts arise.

Changes in the ability of PNs to fire high-frequency bursts has great potential *in vivo* implications. Action potential bursts are preferentially integrated over single spikes in many central synapses (Lisman, 1997). Recently, Senn et al. (2014) demonstrated that fear conditioning increased doublet burst firing in BLA fear-coding PNs (fear neurons) and reduced doublet firing in BLA fear-extinction-coding PNs (extinction neurons). The opposite effect was observed following fear-extinction training (Senn et al., 2014). Since NPY is anxiolytic and facilitates extinction of conditioned fear (Sajdyk et al., 1999; Gutman et al., 2008), it is tempting to speculate that PNs in which [ahx$^{5-24}$]NPY potentiated the I_{sAHP} correspond to the fear neurons. Consequently, those PNs in which only the $GABA_B$-GIRK current was inhibited would be expected to correspond to

extinction neurons. This hypothesis can be tested in future studies combining *ex-vivo* electrophysiology with retrograde tracers to identify valence based PN subpopulations.

Interestingly, the selective Y_1 receptor agonist F^7P^{34}NPY also potentiated the I_{sAHP} in approximately half of all PNs tested. Potentiation of the I_{sAHP} by Y_1 receptors was unlikely caused by a loss of $GABA_B$-mediated inhibition, since F^7,P^{34} NPY did not reduce the I_{IR} current. However, NPY consistently affects BLA PNs by reducing I_h via activation of a Y_1 receptor-dependent mechanisms (Giesbrecht, 2010) and F^7,P^{34} NPY did reduce I_h in most PNs where it potentiated the I_{sAHP}. It is therefore possible that Y_1 receptor-mediated inhibition of dendritic I_h recruits the I_{sAHP} via increased dendritic Ca^{2+} entry in a subset of BLA PNs.

On the other hand, the I_{sAHP} is also a target of numerous other neuromodulators; indeed, CRF inhibits the I_{sAHP} in BLA PNs (Rainnie et al., 1992). Several other anxiogenic G_s –coupled receptors decrease PN I_{sAHP} by increasing intracellular cyclic AMP (cAMP) and recruiting protein kinase (A) (PKA) (Womble and Moises, 1993; Power and Sah, 2008). It is thus possible that the $G_{i/o}$-coupled Y_1 receptors might facilitate the I_{sAHP} via the inhibition of adenylyl cyclase. Our lab has previously documented countervailing modulation of I_h by Y_1 receptors and CRF (Giesbrecht et al., 2010). In any case, it appears that the I_{sAHP} of BLA PNs is under similar countervailing regulation by CRF and NPY.

Assuming that Y_1 and Y_2 receptors can potentiate the I_{sAHP} via different mechanisms, co-activation of both receptors should elicit greater effects than either alone. Preliminary evidence suggests that this is indeed the case and that greater potentiation of the action potential AHP is evoked when [ahx$^{5-24}$]NPY is applied to neurons whose I_{sAHP}

is responsive to F^7,P^{34} NPY. These results suggest a potential mechanism for transforming the excitatory actions of actions of [ahx$^{5-24}$]NPY to the inhibitory actions of the full agonist, by increasing coupling of Ca^{2+} to the inhibitory sI_{AHP}.

4.5 FIGURES

Figure 1: [ahx$^{5-24}$]NPY Increases An Outward-Rectifying K$^+$ Current in Some PNs
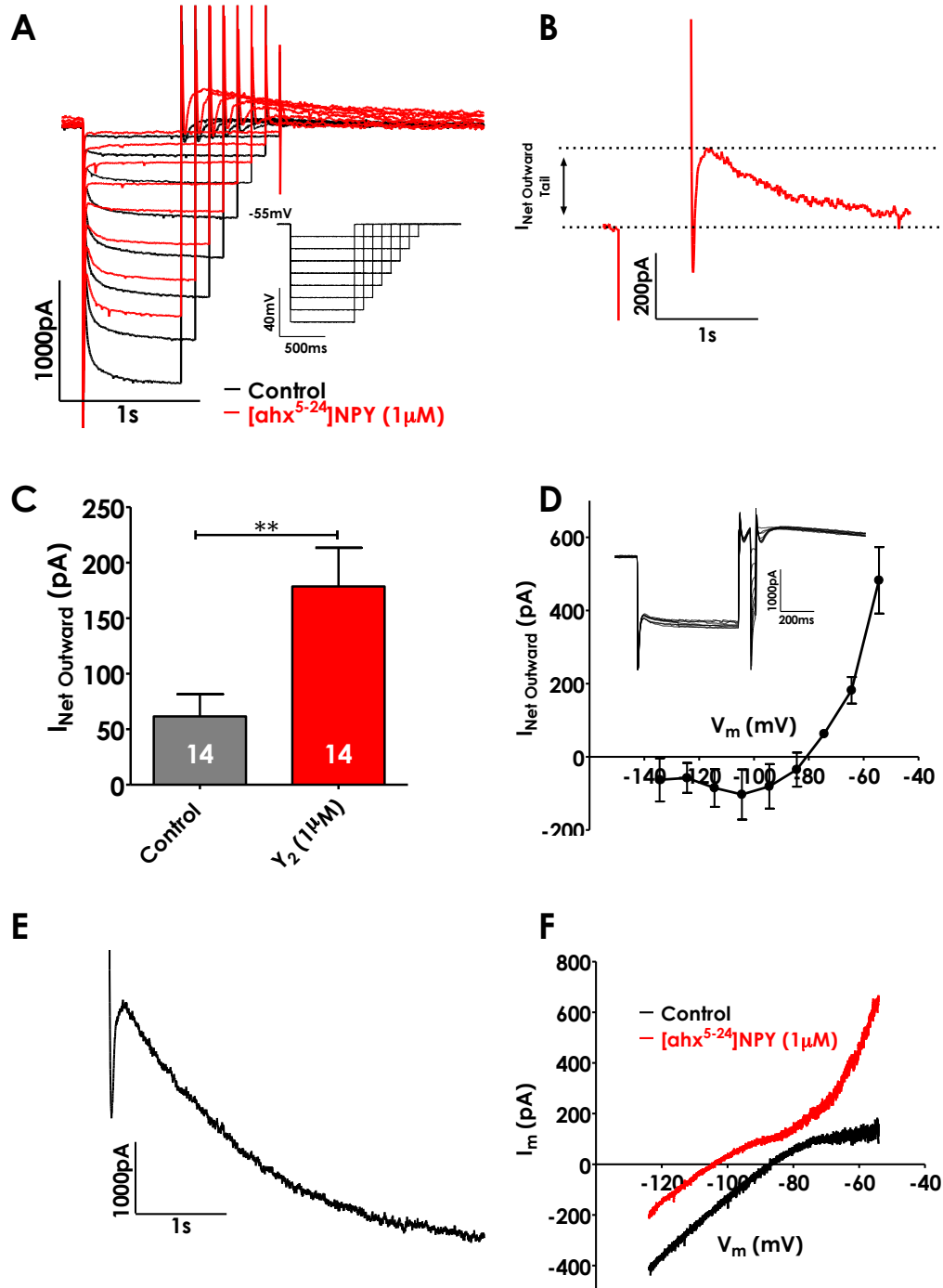
Figure 1: [ahx$^{5\text{-}24}$]NPY Increases An Outward-Rectifying K$^+$ Current in Some PNs

(A) Representative PN current responses to hyperpolarizing voltage steps from V_h = -55 mV. Bath application of [ahx$^{5\text{-}24}$]NPY (1 μM) substantially reduced both the instantaneous inward-rectifying current and I_h in this neuron. When this PN was returned to -55 mV following hyperpolarizations to -75 mV and greater, a slowly decaying outward current was elicited. An inward tail current preceded this slow outward current.

(B) Trace illustrating measurement of the slow AHP current (I_{sAHP}). The holding current at -55 mV was subtracted from the peak outward current seen following return to -55 mV from the most hyperpolarized (-135 mV) voltage step.

(C) Bath application of [ahx$^{5\text{-}24}$]NPY (1 μM) significantly increased the voltage step evoked outward tail current (illustrated in panel B) from 61.6 ± 20.0 pA to 178.7 ± 34.8 pA ($p<0.01$; n=14) in 14/34 PNs tested.

(D) The current-voltage (I-V) relationship of outward (I_{sAHP}) tail current measured with a series fast voltage steps, during peak voltage step-evoke outward current (n=3). The sI_{AHP} showed clear outward rectification and reversed at ~ -80 mV. Inset illustrates voltage steps used to measure this current.

(E) A large outward tail current elicited in the presence of the Y_1 receptor agonist F^7, P^{34} NPY (1 μM). This trace illustrates the markedly slow decay kinetics (>1 s) of the outward I_{sAHP} current.

(F) Voltage-clamp ramp traces from a representative PN in which [ahx$^{5-24}$]NPY (1 μM) substantially potentiated the I$_{sAHP}$ outward current. An [ahx$^{5-24}$]NPY-mediated reduction in conductance is seen in the voltage range below -80 mV. However, when the membrane is depolarized to ~ -70 mV, a substantial outward current which displays clear outward rectification emerges.

Figure 2: [ahx$^{5-24}$]NPY Increases the Ca^{2+}-Dependent I$_{sAHP}$
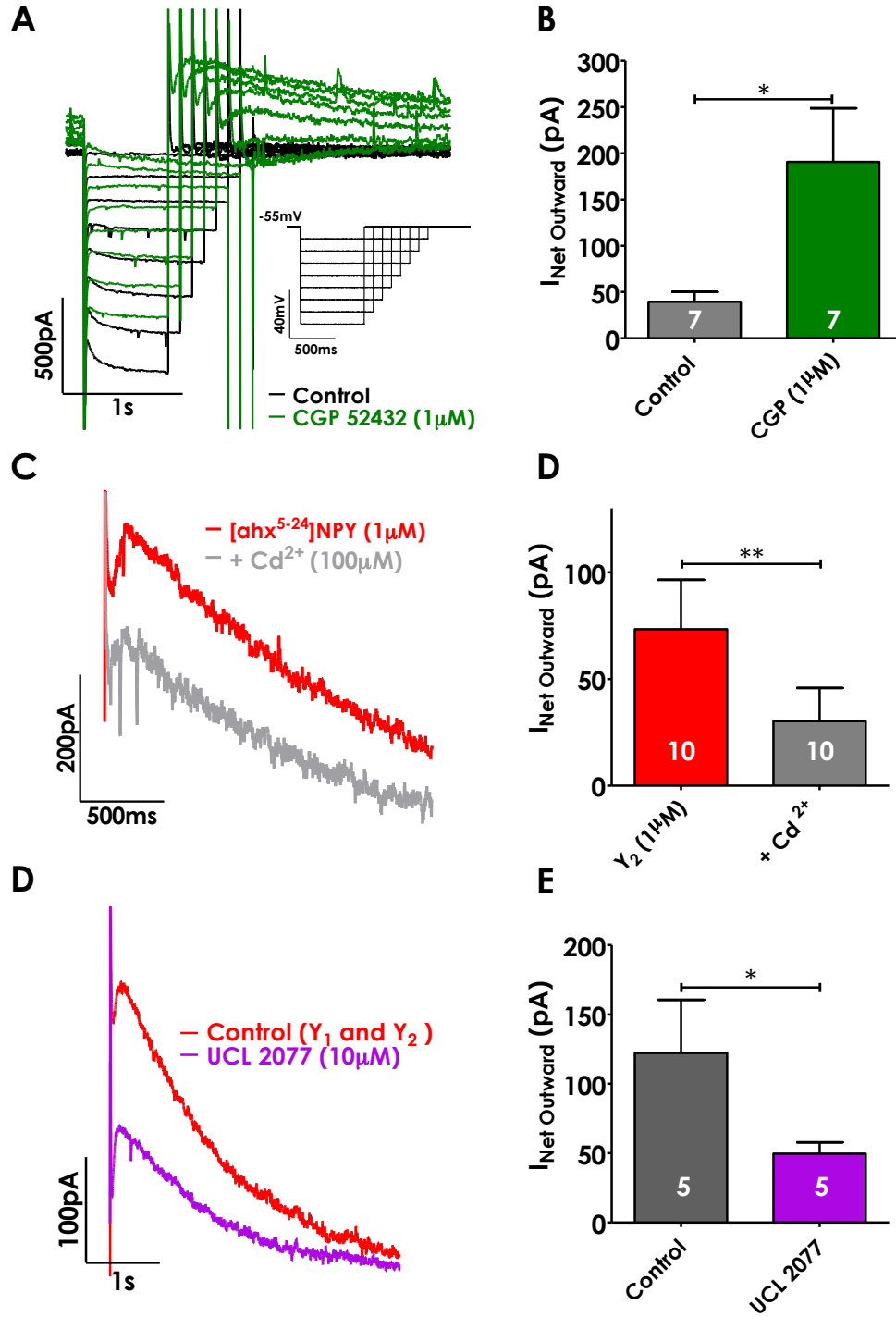
Figure 2: [ahx$^{5-24}$]NPY Increases the Ca^{2+}-Dependent I$_{sAHP}$

(A) Representative PN current responses to hyperpolarizing voltage steps from V$_h$ = -55mV. Bath application of the GABA$_B$ antagonist, CGP 52432 (1 μM) substantially reduced both the instantaneous inward-rectifying current and I$_h$ in this neuron. As in panel A, an inward tail current can be seen to precede the slow outward current.

(B) CGP 52432 application significantly increased the voltage step evoked outward tail current (panel E) from 39.5 ± 10.6 pA to 190.6 ± 58.1 pA (p<0.05; n=7) in 7/18 PNs tested.

(C) Representative PN voltage-clamp outward tail current induced by [ahx$^{5-24}$]NPY (1 μM), as shown in Figure 1. Bath application of Cd^{2+} (100 μM) substantially decreased the amplitude of the outward tail current, indicating its Ca^{2+} dependence.

(D) Bath application of Cd^{2+} (100 or 200 mM) significantly decreased the PN outward tail current, evoked with voltage-clamp steps (as before) by more than half (p<0.01; n=10).

(E) A large outward tail current elicited in the presence of both F^7, P^{34} NPY (1 μM) and [ahx$^{5-24}$]NPY (1 μM). Bath application of UCL 2077 (1 μM) decreased outward tail current amplitude by more than half, indicating it is mediated by the I$_{sAHP}$.

(F) Bath application of UCL 2077 (1 μM) significantly decreased the PN outward tail current, evoked with voltage-clamp steps (as before) by more than half (p<0.05; n=5).

Figure 3: PNs Whose I_{sAHP} is [ahx$^{5-24}$]NPY- Responsive Show Enhanced AHP amplitudes with the Y_2 agonist
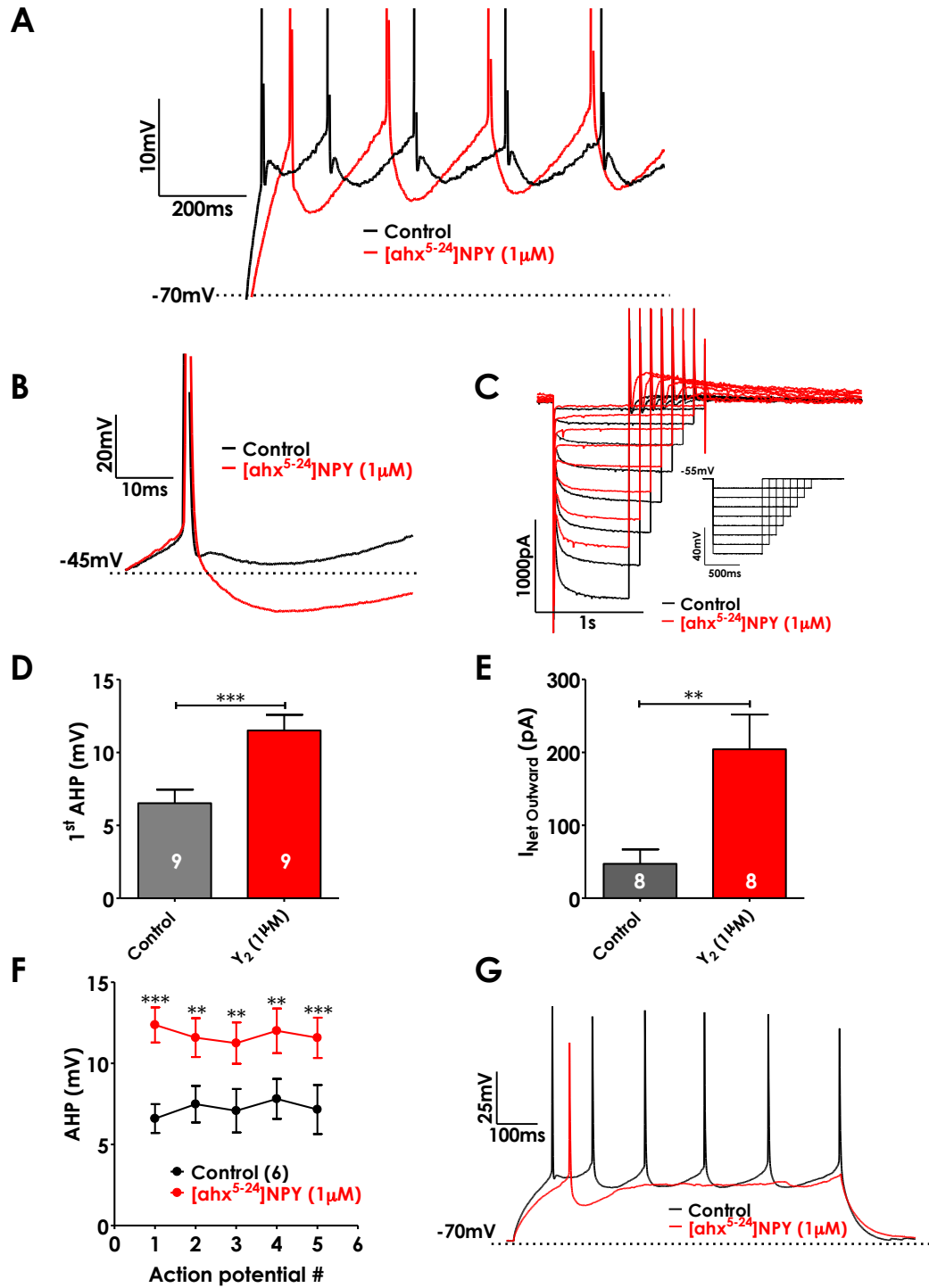
Figure 3: PNs whose I$_{sAHP}$ is [ahx$^{5-24}$]NPY- Responsive Show Enhanced AHP amplitudes with the Y$_2$ agonist

(A) Representative action potential trains evoked by depolarizing current steps in a PN where [ahx$^{5-24}$]NPY substantially enhanced the I$_{sAHP}$ tail current. In control conditions, action potentials are clearly followed by a fast AHP and a subsequent slower AHP. The slower AHP gradually increases in amplitude and duration with successive action potentials. Following bath application of [ahx$^{5-24}$]NPY (1 μM) the slower AHP is substantially increased as of the first action potential, and the fast AHP can no longer be distinguished. Furthermore, following the Y$_2$ agonist, the much larger slower AHP no longer increases in amplitude with successive action potentials.

(B) Superimposed initial action potentials and AHPs from the recordings in panel (A) highlighting the effect of the Y$_2$ agonist on the initial AHP in the train.

(C) Representative hyperpolarizing voltage-clamp steps as in (Figure 1 panel A). [ahx$^{5-24}$]NPY (1 μM) substantially increased the I$_{sAHP}$ tail current in this PN, which also showed a >30% increase in the amplitude of its first current-clamp evoked action potential AHP (as in panel B).

**(D)** [ahx$^{5-24}$]NPY (1 μM) significantly increased the amplitude of the first AHP in a train in 9/19 PNs tested from 6.21 ± 1.08 mV to 11.15 ± 1.13 mV (n=9, p<0.001).

(E) Outward tail currents from the 9 PNs in (D) whose AHPs were enhanced by [ahx$^{5-24}$]NPY (1 μM). In these cells, the Y$_2$ agonist also enhanced the outward current 3-fold from 68.8 ± 27.8 pA to 221.6 ± 45.5 pA (p<0.01; n=9).

(F) In 6 of the 9 PNs in which [ahx$^{5-24}$]NPY increased the first action potential AHP, the initial 5 AHPs in a train were all significantly increased in amplitude.

(G) Representative PN in which [ahx$^{5-24}$]NPY (1 μM) substantially enhanced the current step evoked action potential AHP. After [ahx$^{5-24}$]NPY (1 μM) application, this PN failed to fire successive action potentials. (3/9) AHP-responsive PNs showed a similar effect all 3 of which also showed substantial potentiation of the voltage-clamp measured I$_{sAHP}$ outward tail current.

Figure 4: The AHP In PNs That Do Not Show Y$_2$-dependent I$_{sAHP}$ Potentiation Is Unchanged by [ahx$^{5-24}$]NPY
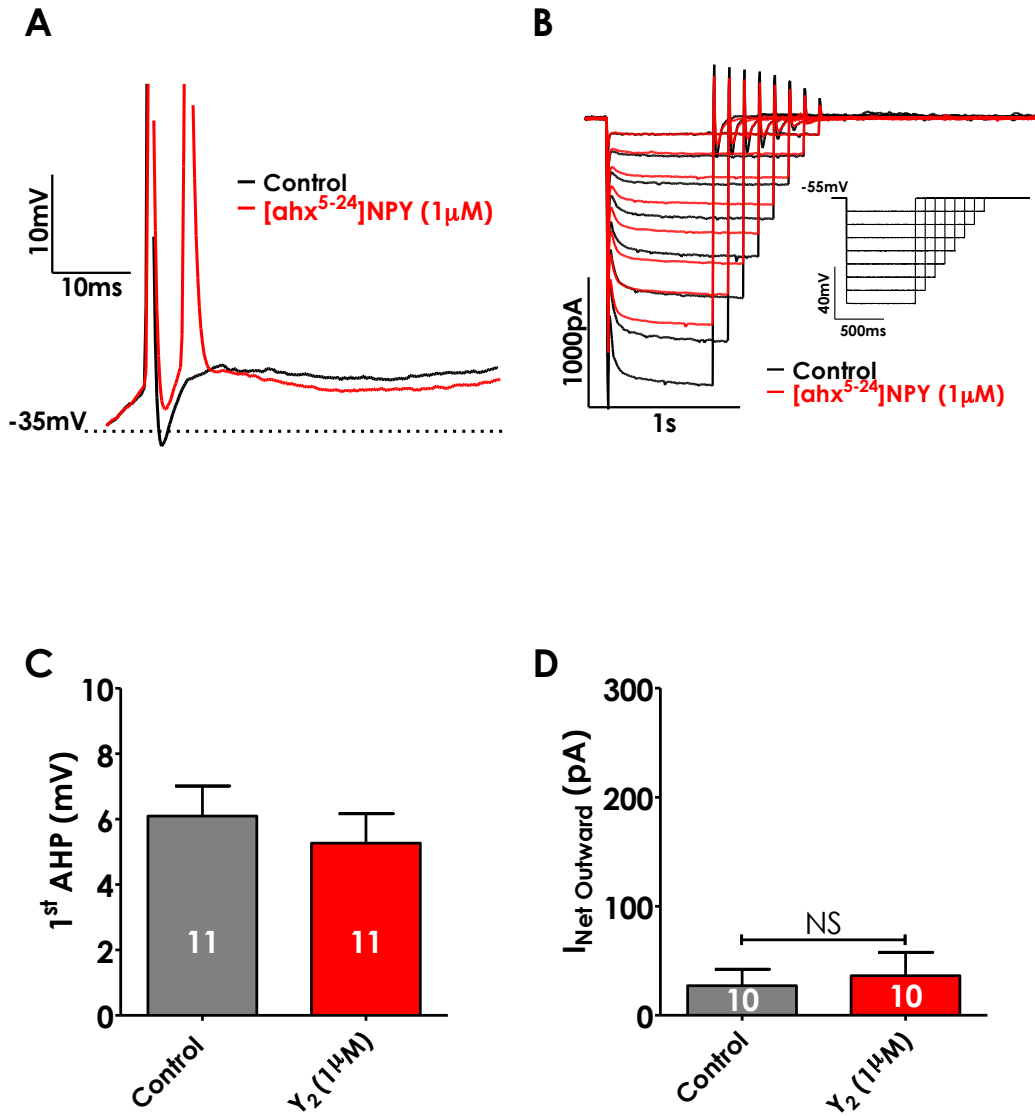
Figure 4: The AHP In PNs That Do Not Show Y_2-dependent I_{sAHP} Potentiation Is Unchanged by [ahx$^{5-24}$]NPY

(A) Initial action potential in a train from a representative PN in which [ahx$^{5-24}$]NPY (1 µM) had no effect on the I_{sAHP} tail current, although it significantly decreased the I_{IR} **(B)**. The slower AHP was not changed in this PN; however a doublet spike burst emerged following [ahx$^{5-24}$]NPY application.

(C) In 10/19 PNs tested [ahx$^{5-24}$]NPY (1 µM) had no effect on the first AHP amplitude. In these same neurons, I_{sAHP} was also unaffected by the Y_2 agonist **(D)**.

Figure 5: I$_{sAHP}$ Responsive/Non-Responsive PNs Show Opposite Effects On First Action Potential Interval
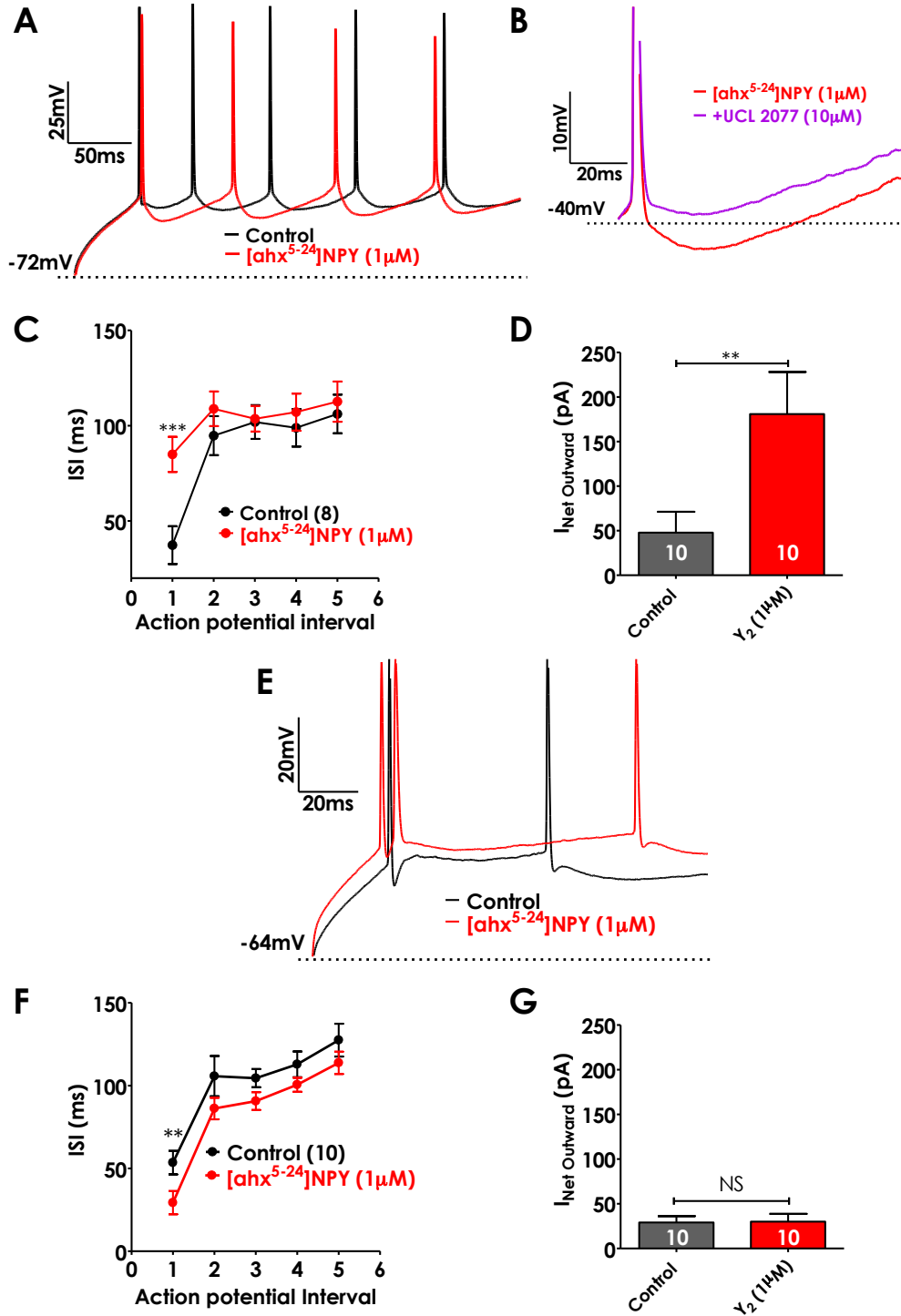
Figure 5: I_{sAHP} Responsive/Non-Responsive PNs Show Opposite Effects On First Action Potential Interval

(A) Representative action potential train from a PN with a Y_2-sensitive I_{sAHP}. Following [ahx$^{5-24}$]NPY (1 μM) application, the AHP was enhanced and the interval between the first 2 action potentials was substantially increased, such that this PN showed an apparent reduction in spike frequency adaptation. Current steps (800 ms) in which the same number of action potentials were fired under both conditions, were selected for comparison.

(B) Superimposed traces of first action potentials and AHPs from a PN with a Y_2-sensitive I_{sAHP} in the presences of [ahx$^{5-24}$]NPY (1 μM) and in the additional presence of UCL 2077 (1 μM) revealed that a substantial portion of this first action potential was I_{sAHP}-mediated.

(C) Inter-spike intervals from PNs in which the I_{sAHP} -tail current was substantially (>10%) enhanced by the Y_2 agonist. In these PNs the first inter-spike interval was more than doubled by [ahx$^{5-24}$]NPY (1 μM) from 33.81 ± 9.47 ms to 80.05 ± 9.50 ms (p<0.001; n=9).

(D) The Y_2 agonist significantly increased the voltage-clamp measured I_{sAHP} tail current in the PNs from panel C (p<0.01; n=10).

(E) Representative action potentials from an [ahx$^{5-24}$]NPY responsive PN in which the I_{sAHP} was not potentiated. Following [ahx$^{5-24}$]NPY (1 μM) application, a first action

potential doublet burst emerges. Current steps were selected from each neuron for comparison as in panel A.

(F) Inter-spike intervals from [ahx$^{5\text{-}24}$]NPY (1 μM) responsive PNs whose I$_{sAHP}$ was unaffected, as in E. In these PNs the first action potential inter-spike interval was significantly decreased by [ahx$^{5\text{-}24}$]NPY (1 μM) from 50.52 ± 7.11 ms to 29.33 ± 7.01 ms ($p<0.01$; $n=10$). In many cases this effect was due to the new onset of first action potential doublet bursts.

(G) I$_{sAHP}$ tail currents from neurons in panel F were not significantly potentiated by [ahx$^{5\text{-}24}$]NPY (1 μM).

Figure 6: Y$_1$ Receptor Activation Increases The sI$_{AHP}$
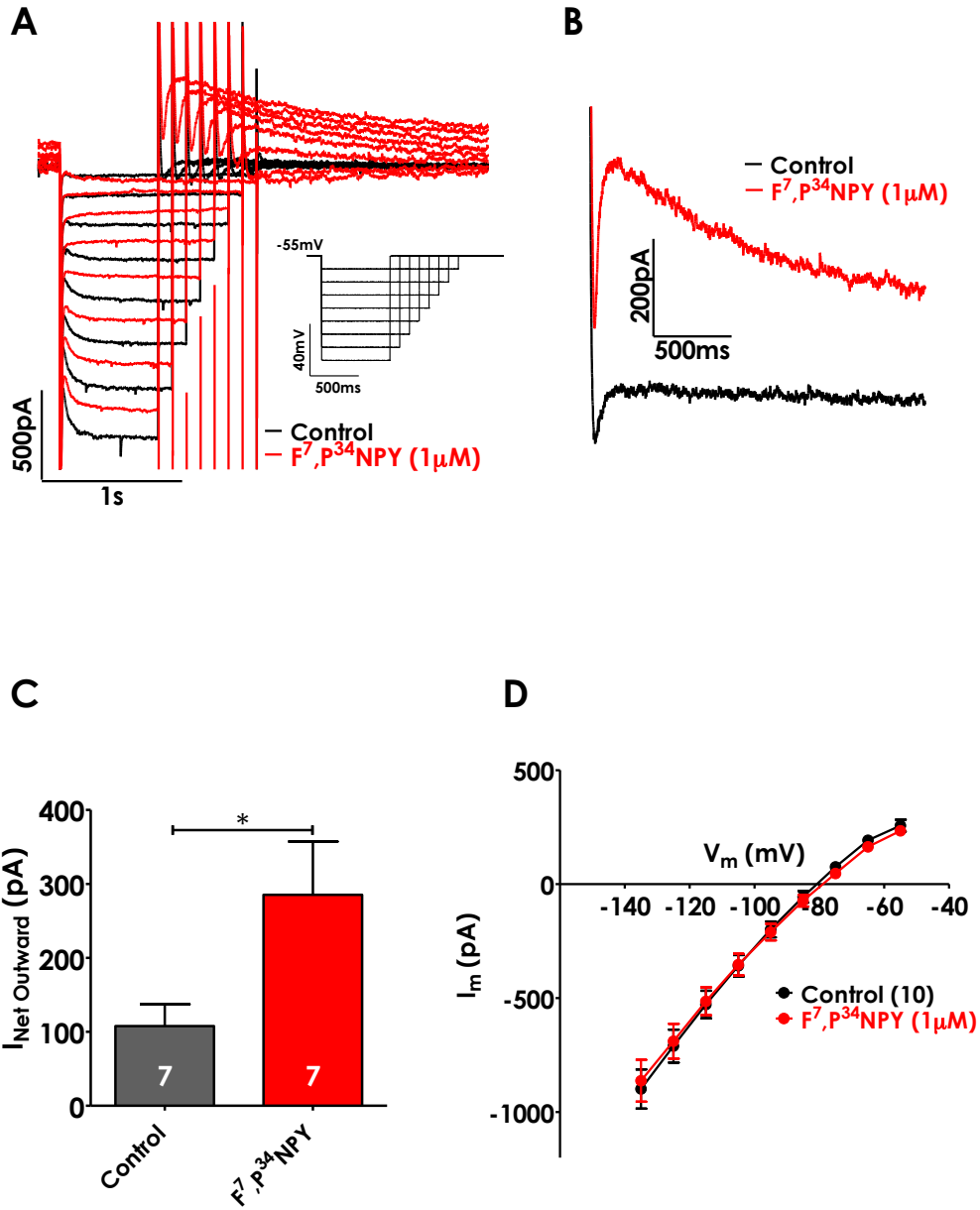
Figure 6: Y_1 Receptor Activation Increases The sI_{AHP}

(A) Representative PN current responses to hyperpolarizing voltage steps from $V_h = -55$ mV. Bath application of F^7, P^{34} NPY (1 μM) did not affect the instantaneous inward-rectifying current, but substantially reduced I_h. The Y_1 agonist also induced expression of a robust I_{sAHP} in this PN.

(B) Peak I_{sAHP} current from the end of step to -135 mV from cell in A, in the absence (black) and presence of the Y_1 agonist.

(C) Effect of F^7, P^{34}NPY (1 μM) to induce expression of the I_{sAHP} tail current from 107.8 ± 29.6 pA to 259.2 ± 72.2 pA (p<0.05; n=7) in 7/15 PNs tested.

(D) Bath application of F^7, P^{34}NPY (1 μM) had no effect on the PN (instantaneous inward-rectifying current (n=10).

Figure 7: The Y_1, Y_2 Receptor Interaction

A

10mV

20ms

— Control
— F^7,P^{34}NPY (1μM)

-65mV

B

5mV

20ms

-38mV

— F^7,P^{34}NPY (1μM)
— [ahx$^{5-24}$]NPY (1μM) + F^7,P^{34}NPY (1μM)
— + UCL 2077 (10μM)
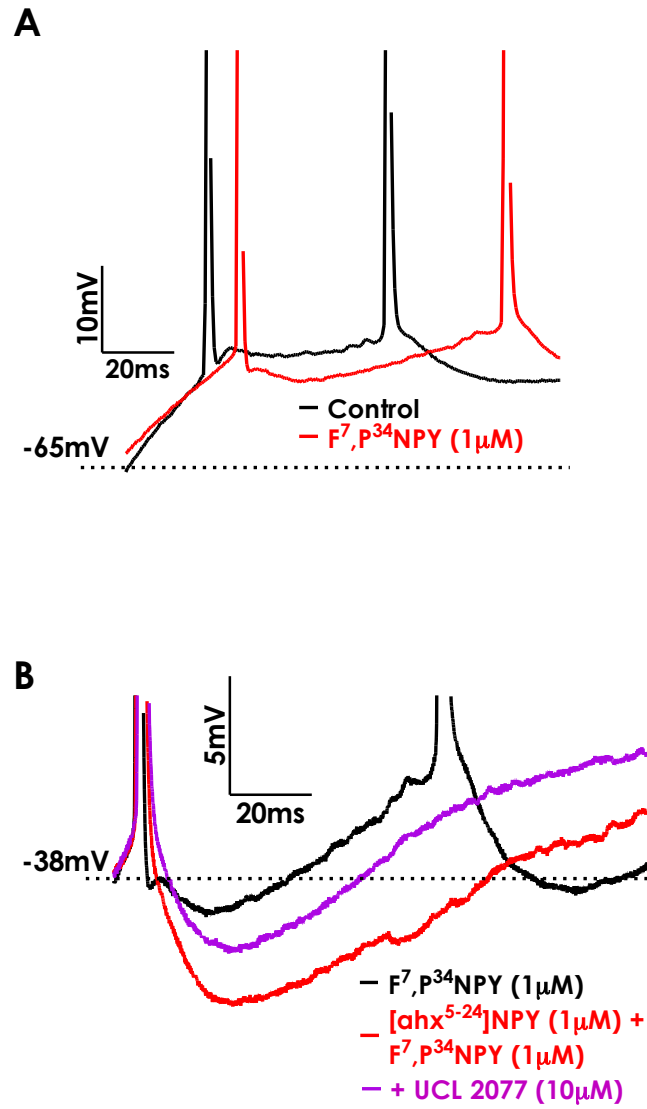
Figure 7: The Y$_1$, Y$_2$ Receptor Interaction

(A) Representative action potential traces from a PN with a Y$_1$-sensitive I$_{sAHP}$. Following F^7, P^{34}NPY (1 µM) application, the initial AHP was modestly enhanced.

(B) When [ahx$^{5-24}$]NPY (1 µM) and F^7, P^{34}NPY (1 µM) were subsequently co-applied to the PN from panel A, the first action potential AHP was substantially enhanced. This increase in the first action potential AHP was mediated by the I$_{sAHP}$ since it was largely reversed with UCL 2077 (1 µM).

4.6 REFERENCES

Andrade R, Foehring RC, Tzingounis AV (2012) The calcium-activated slow AHP: cutting through the Gordian knot. Front Cell Neurosci 6:47.

Berger T, Senn W, Lüscher H-R (2003) Hyperpolarization-activated current Ih disconnects somatic and dendritic spike initiation zones in layer V pyramidal neurons. Journal of Neurophysiology 90:2428–2437.

Giesbrecht CJ, Mackay JP, Silveira HB, Urban JH, Colmers WF (2010) Countervailing Modulation of Ih by Neuropeptide Y and Corticotrophin-Releasing Factor in Basolateral Amygdala As a Possible Mechanism for Their Effects on Stress-Related Behaviors. Journal of Neuroscience 30:16970–16982.

Gutman AR, Yang Y, Ressler KJ, Davis M (2008) The Role of Neuropeptide Y in the Expression and Extinction of Fear-Potentiated Startle. Journal of Neuroscience 28:12682–12690.

Leung LS, Peloquin P (2006) GABA(B) receptors inhibit backpropagating dendritic spikes in hippocampal CA1 pyramidal cells in vivo. Hippocampus 16:388–407.

Lisman JE (1997) Bursts as a unit of neural information: making unreliable synapses reliable. Trends Neurosci 20:38–43.

Power JM, Bocklisch C, Curby P, Sah P (2011) Location and Function of the Slow Afterhyperpolarization Channels in the Basolateral Amygdala. Journal of Neuroscience 31:526–537.

Power JM, Sah P (2008) Competition between calcium-activated K+ channels determines cholinergic action on firing properties of basolateral amygdala projection neurons. J Neurosci 28:3209–3220.

Rainnie DG, Asprodini EK, Shinnick-Gallagher P (1993) Intracellular recordings from morphologically identified neurons of the basolateral amygdala. Journal of Neurophysiology 69:1350–1362.

Rainnie DG, Fernhout BJ, Shinnick-Gallagher P (1992) Differential actions of corticotropin releasing factor on basolateral and central amygdaloid neurones, in vitro. J Pharmacol Exp Ther 263:846–858.

Sah P (1996) Ca(2+)-activated K+ currents in neurones: types, physiological roles and modulation. Trends Neurosci 19:150–154.

Sah P, Bekkers JM (1996) Apical dendritic location of slow afterhyperpolarization current in hippocampal pyramidal neurons: implications for the integration of long-term potentiation. Journal of Neuroscience 16:4537–4542.

Sah P, Faber ESL (2002) Channels underlying neuronal calcium-activated potassium

currents. Prog Neurobiol 66:345–353.

Sajdyk TJ, Johnson PL, Leitermann RJ, Fitz SD, Dietrich A, Morin M, Gehlert DR, Urban JH, Shekhar A (2008) Neuropeptide Y in the Amygdala Induces Long-Term Resilience to Stress-Induced Reductions in Social Responses But Not Hypothalamic-Adrenal-Pituitary Axis Activity or Hyperthermia. Journal of Neuroscience 28:893–903.

Sajdyk TJ, Schober DA, Smiley DL, Gehlert DR (2002) Neuropeptide Y-Y2 receptors mediate anxiety in the amygdala. Pharmacol Biochem Behav 71:419–423.

Sajdyk TJ, Vandergriff MG, Gehlert DR (1999) Amygdalar neuropeptide Y Y1 receptors mediate the anxiolytic-like actions of neuropeptide Y in the social interaction test. European Journal of Pharmacology 368:143–147.

Senn V, Wolff SBE, Herry C, Grenier F, Ehrlich I, Gründemann J, Fadok JP, Müller C, Letzkus JJ, LUthi A (2014) Long-range connectivity defines behavioral specificity of amygdala neurons. 81:428–437.

Shah MM, Javadzadeh-Tabatabaie M, Benton DCH, Ganellin CR, Haylett DG (2006) Enhancement of hippocampal pyramidal cell excitability by the novel selective slow-afterhyperpolarization channel blocker 3-(triphenylmethylaminomethyl)pyridine (UCL2077). Mol Pharmacol 70:1494–1502.

Vigot R, Barbieri S, Bräuner-Osborne H, Turecek R, Shigemoto R, Zhang Y-P, Luján R, Jacobson LH, Biermann B, Fritschy J-M, Vacher C-M, Müller M, Sansig G, Guetg N, Cryan JF, Kaupmann K, Gassmann M, Oertner TG, Bettler B (2006) Differential compartmentalization and distinct functions of GABAB receptor variants. Neuron 50:589–601.

Washburn MS, Moises HC (1992) Electrophysiological and morphological properties of rat basolateral amygdaloid neurons in vitro. Journal of Neuroscience 12:4066–4079.

Womble MD, Moises HC (1993) Muscarinic modulation of conductances underlying the afterhyperpolarization in neurons of the rat basolateral amygdala. Brain Research 621:87–96.

Chapter 5

Summary, General Discussion and Future Directions

5.1 SUMMARY

At the onset of this thesis work my primary aim was to investigate the impact of selective Y_2 receptor (Y_2R) activation on the electrophysiological properties of BLA PNs. This was undertaken in an attempt to elucidate potential cellular-circuit mechanism underlying the well-described acute anxiogenic behavioral effects resulting from selective activation of BLA Y_2Rs (Sajdyk et al., 2002). A secondary objective was to identify a mechanism by which Y_2Rs actions might interact with those of other NPY receptors and facilitate NPY's overall acute and long-term anxiolytic actions in the BLA (Sajdyk et al., 1999; 2008).

I have documented a number of Y_2R -mediated actions within the BLA. However, all of these effects appear to depend upon a common underlying mechanism. Specifically, Y_2Rs are expressed by a group of BLA NPY/SOM-expressing GABA interneurons (Chapter 2). These NPY-SOM interneurons exert strong, GABA-mediated inhibitory control over the BLA, while activation of their Y_2Rs decreases GABA release and disinhibits PNs.

5.1a Y_2R Activation Disinhibits The Majority of BLA PNs by Direct Actions On NPY/SOM Interneuron GABA terminals

Approximately 80% of BLA PNs responded to $[ahx^{5-24}]NPY$ with a substantial reduction in miniature (and spontaneous) $GABA_A$ unitary IPSC frequency. This suggests that even in acute slices, most BLA PNs are strongly inhibited by interneurons. Anatomical data in the mouse suggests that, by and large, NPY/SOM cells are the only BLA interneurons that express Y_2 receptors (Chapter 2). Therefore, disinhibition of PNs by $[ahx^{5-24}]NPY$ is likely mediated by Y_2 receptors expressed on the presynaptic terminals of these NPY/SOM interneurons. Furthermore, since SOM interneurons

primarily target BLA PN dendrites (Muller et al., 2006), Y_2 receptor activation likely disinhibits PN dendrites.

5.1b Y_2R Activation Increases Proximal GABA Mediated Inhibition in a Subset of PNs

In addition to simultaneously reducing a population of smaller events, [ahx$^{5-24}$]NPY increased the frequency of larger amplitude spontaneous GABA$_A$ IPSCs in a subset of PNs. These large amplitude [ahx$^{5-24}$]NPY-potentiated GABA events also showed relatively fast kinetics, which suggests facilitation of GABA release at more proximal synapses. Furthermore, these effects were likely action potential-dependent since [ahx$^{5-24}$]NPY did not increase the frequency of large amplitude IPSCs in the presence of TTX. Since SOM interneurons also target PV interneurons (Muller et al., 2006), I suggest that this less common effect of the Y_2 agonist results from the Y_2R-mediated inhibition of NPY-SOM interneurons and consequent disinhibition of PV interneurons. These results indicate that although [ahx$^{5-24}$]NPY predominately disinhibits PNs, via direct activations on interneuron Y_2 receptors disinhibition of another interneuron type also results in increased proximal GABA inhibition in a subset of PNs. Both of these effects were likely mediated by Y_2 receptor-expressing NPY/SOM interneurons. These results underlie a recurrent theme of my findings: uniform Y_2 receptor-mediated disinhibition of most PNs, whereby this disinhibition is mitigated in a subset of cells by an additional inhibitory effect.

5.1c Y_2R Activation Excites PNs by Decreasing Tonic GABA$_B$-Mediated Inhibition

In addition to decreasing synaptic GABA$_A$-mediated synaptic events, [ahx$^{5-24}$]NPY further disinhibited PNs by removing a strong tonic GABA$_B$ receptor-mediated

227

inhibition. This effect increased the initial excitability of most (~85%) BLA PNs. Since PNs primarily express $GABA_B$ receptors on their distal dendrites (McDonald et al., 2004), this action likely reflects disinhibition of dendrites. These observations are therefore also likely mediated by Y_2 receptor-expressing NPY/SOM interneurons (Chapter 2).

Surprisingly, this Y_2R-sensitive tonic inhibition persisted even in the presence of TTX. Thus in acute slices, BLA PNs are under a strong and largely action potential-independent form of tonic GABA inhibition. I suggest that removal of this tonic $GABA_B$-mediated inhibition is a prerequisite for Ca^{2+} dependent plasticity. Interestingly, preliminary evidence suggests that CRF similarly disinhibits PN dendrites. This may indicate that the plasticity induced by both anxiogenic and anxiolytic neuromodulators similarly requires disinhibition of PN dendrites.

5.1d Y_2R Activation Enhances The I_{sAHP} by Decreasing Tonic $GABA_BR$ Activation

Interestingly, in approximately half of all responsive PNs, $[ahx^{5-24}]NPY$ also enhanced the I_{sAHP}. This effect was due to loss of tonic $GABA_B$-mediated inhibition, which appears to result in increased dendritic Ca^{2+} influx during PN activity (Chapter 3). In such PNs, this effect limited their ability to repetitively fire action potentials at high frequencies, and most prominently affected the interval between the first two spikes.

Interestingly, in approximately half of PNs, $[ahx^{5-24}]NPY$ reduced a $GABA_B$-mediated GIRK current, but did not potentiate the I_{sAHP}. In this subpopulation, the interval between the first two action potentials was significantly reduced; often due to the emergence of a first action potential doublet burst. Thus $[ahx^{5-24}]NPY$ elicited opposite effects on repetitive action potential firing in the PNs in which it did not enhance the

228

I_{sAHP}. Action potential bursts from presynaptic neurons are thought to be preferentially integrated in many postsynaptic cells (Lisman, 1997). Therefore, these Y_2 receptor-mediated effects are of potentially great importance in determining how BLA output is integrated in afferent targets.

The selective Y_1 receptor agonist $F^7P^{34}NPY$ also potentiated the I_{sAHP} in half of all PNs tested. This however, was not due to reduced tonic $GABA_B$-mediated inhibition, since $F^7P^{34}NPY$ did not inhibit the GIRK I_{IR}. When $[ahx^{5-24}]NPY$ was subsequently applied to these Y_1-I_{sAHP} responsive PNs, an even greater enhancement of the action potential AHP ensued. I propose that Y_1 receptor-mediated facilitation of the I_{sAHP} offsets the excitatory effects of Y_2 receptor activation by more effectively coupling increased dendritic Ca^{2+} to the inhibitory sI_{AHP}. This could arise from a Y_1R-mediated reduction in dendritic I_h, which would result in increased dendritic input resistance, thereby enhancing synaptic and back propagation-mediated depolarizations.

5.2 GENERAL DISCUSSION

5.2a Dendritic Disinhibition Likely Mediates Acute Anxiogenic Effects of Selective Y_2R Activation

I have shown that $[ahx^{5-24}]$NPY increased the excitability of most BLA PNs by reducing a tonic $GABA_B$-mediated GIRK current. Although this action only minimally affected the somatic RMP, it did substantially increase neuronal input resistance and thus also decreased neuronal rheobase. Loss of tonic GIRK currents may indeed have depolarized PN dendrites, but this effect was not readily observed from the somatic recording site. I suggest that such dendritic depolarization underlies the inhibitory actions of $[ahx^{5-24}]$NPY on I_h observed in half of all PNs. Consistent with this, I_h was similarly modulated by blocking $GABA_B$ receptors. Loss of I_h may also have partially offset GIRK-mediated depolarization. Ultimately inhibition of I_h likely contributed to $[ahx^{5-24}]$NPY-mediated increases in input resistance.

Y_2R-mediated disinhibition of dendrites and loss of tonic $GABA_B$ activation would likely result in an increase in the (anxiogenic) output of BLA PNs. This Y_2R-mediated action is therefore a reasonable mechanism to explain the reported acutely anxiogenic effects of selective Y_2 receptor activation (Sajdyk et al., 2002).

5.2b Implications For Y_2R actions on BLA Plasticity:

$GABA_B$-coupled GIRK channels are abundant in dendritic spines where they reside in close proximity to NMDA receptors (Kulik et al., 2006; Vigot et al., 2006). GIRK-mediated membrane hyperpolarization facilitates the Mg^{2+} block of NMDA receptors and thus suppresses plasticity (Morrisett et al., 1991). It is also well established that dendritic $GABA_B$ receptors directly inhibit VGCCs (Pérez-Garci et al., 2013). For

these reasons, a Y_2R-mediated reduction in tonic $GABA_B$-mediated inhibition should facilitate Ca^{2+}-dependent synaptic plasticity.

I have not directly measured intra-dendritic Ca^{2+} levels in these studies. However, the enhancement of the Ca^{2+} dependent I_{sAHP} by both $[ahx^{5-24}]NPY$ and the $GABA_B$ antagonist CGP 52432 is entirely consistent with such a Y_2R-mediated potentiation of activity-dependent, PN Ca^{2+}-signaling.

Consistent with this, the pan-YR agonist NPY appears to engage Ca^{2+} dependent plasticity in the BLA. First, long-term NPY-mediated behavioral effects require the calcium dependent phosphatase calcineurin (Sajdyk et al., 2008). Secondly, NPY potentiates fear extinction, a learning process that requires both calcineurin and NMDA receptors (Gutman et al., 2008; Herry et al., 2008). For these reasons I propose that NPY's actions in the BLA cannot be purely inhibitory.

Some of the effects elicited by $[ahx^{5-24}]NPY$, such as potentiation of the I_{sAHP}, may inhibit BLA output, most markedly by reducing the firing rates of BLA PNs. However, Y_2 receptors appear to disproportionately mediate NPY's excitatory effects. Furthermore, I propose that these excitatory actions of NPY are necessary to allow Ca^{2+}-dependent plasticity in the face of normally high basal inhibition. However, when activated in isolation, Y_2 receptor activation enhances BLA output and is anxiogenic.

5.2c A Model For Y_2R Actions in the BLA

Based on the above hypotheses, I propose the model displayed in **(Figure 1)**. Here, I suggest that tonic $GABA_A$-$GABA_B$ mediated inhibition of dendrites gates PN plasticity. Removal of this tonic inhibition is a prerequisite for both anxiolytic and

anxiogenic plastic changes. This model makes several predictions, some supported by recent findings from our lab, and others yet to be tested.

5.2c(i) Prediction 1 - Commonalities between the actions of CRF and selective Y_2 receptor activation

The long-term anxiogenic actions of CRF require both CaMKII and NMDA receptors (Rainnie et al., 2004). Based on the above model, tonic $GABA_B$ receptor-mediated inhibition of PNs must also be lifted to permit CRF-mediated plasticity. Consistent with this, I have shown that CRF inhibits an inward-rectifying current and increases input resistance in most BLA PNs. This CRF sensitive current reversed close to the K^+ reversal potential ($\sim$ -100 mV). Furthermore, most ($\sim$90%) BLA PNs responded to CRF, similar to the response rate to [ahx$^{5-24}$]NPY. Although these effects are consistent with CRF-mediated reduced tonic $GABA_B$-mediated inhibition, this has yet to be explicitly tested. Future experiments will be required to determine whether blocking $GABA_B$ receptors occludes these specific actions of CRF.

Work in the Colmers lab by Dr. Sheldon Michaelson and others, using a BLA organotypic culture model, further supports commonalities in the actions of CRF and [ahx$^{5-24}$]NPY (unpublished data). These investigators found that similar hypertrophic changes to PN dendrites in culture were induced by the chronic application of either CRF or [ahx$^{5-24}$]NPY. Interestingly, NPY itself potently elicited structural plasticity in the opposite direction, specifically a marked dendritic hypotrophy. The hypothesis that structural plasticity mediated by NPY or CRF both require disinhibition of PN dendrites via the removal of tonic $GABA_B$-mediated inhibition could readily be tested by chronically applying a $GABA_B$ antagonist to the BLA OTC preparation. The model in

(Figure 1) predicts blocking $GABA_B$ receptors in this manner would mimic the effects of CRF and $[ahx^{5-24}]NPY$.

Although CRF and $[ahx^{5-24}]NPY$ appear to exert some overlapping actions within the BLA, there are clear differences in the actions of these peptides. CRF has been shown to inhibit the I_{sAHP} (Rainnie et al., 1992), however, I have shown that $[ahx^{5-24}]NPY$ enhances this current. It is likely that $[ahx^{5-24}]NPY$ potentiates the I_{sAHP} indirectly via increased activity-dependent dendritic Ca^{2+} entry. Recruitment of the I_{sAHP} in this manner may partly offset increased anxiogenic output. Since CRF inhibits the I_{sAHP}, this conductance would not dampen CRFs excitatory actions.

Furthermore, I have shown that selective Y_1R activation potentiates the I_{sAHP}. I have not determined the mechanism underlying this Y_1 receptor action. However, an attractive possibility is that by potentiating the I_{sAHP}, Y_1 receptor activation permits disinhibition of dendrites without increased excitatory output.

Moreover, CRF and $[ahx^{5-24}]NPY$ appear to exert opposing actions on I_h. Our lab has previously reported that CRF enhances PN I_h (Giesbrecht et al., 2010). In a minority of cases, I have observed enhancement of the PN I_h by $[ahx^{5-24}]NPY$. However, the predominant effect appears to be $[ahx^{5-24}]NPY$-mediated inhibition of this conductance, most likely indirectly via reduced tonic $GABA_B$ and consequent dendritic depolarization.

5.2c(ii) Prediction 2 – NPY and CRF both increase PN Ca^{2+} via dendritic inhibition; however CRF elicits greater effects.

Based on experiments reported in this thesis, I propose that NPY and CRF both reduce ongoing $GABA_B$-mediated dendritic inhibition. This action would facilitate NMDA receptor-mediated Ca^{2+} currents and remove tonic $GABA_B$-mediated inhibition of VGCCs. Calcineurin, which mediates NPY's long-term effects, has a higher affinity

for Ca^{2+} than does CaMKII and is therefore preferentially activated at relatively lower levels of elevated dendritic Ca^{2+} (Mansuy, 2003). Although NPY and CRF would both be predicted to increase dendritic Ca^{2+}, CRF should elicit the more pronounced increase. Based on the anxiogenic effects of selective Y_2 receptor activation, in conjunction with Dr. Michaelson's observations, I predict that [ahx$^{5-24}$]NPY will elicit greater Ca^{2+} influx than NPY in response to excitatory synaptic transmission and dendritic depolarization mediated by other events, such as action potential back-propagation.

The most direct way to test the above hypotheses would be to combine slice electrophysiology with two-photon dendritic Ca^{2+} imaging. This would most readily be accomplished by directly loading PNs with Ca^{2+} indicators via the patch pipette. Back propagating action potentials could then be evoked with somatic current injection and dendritic Ca^{2+} quantified. Localized application of agonists or antagonists in the absence or presence of the Y_2R agonist would help estimate the contributions of NMDA receptors to this increase, while application of L-, N- and T-type VDCC blockers would help define their roles in this action.

A fundamental prediction of the model outlined in **Figure 1** is that CRF and [ahx$^{5-24}$]NPY both elicit greater increases in dendritic Ca^{2+} flux than does NPY. I have therefore searched for postsynaptic mechanisms via which other NPY receptors might lessen Y_2 receptor-mediated dendritic Ca^{2+} influx to favor calcineurin-mediated plasticity. Molosh et al. (2013) have previously documented that Y_1 receptor activation decreases PN NMDA currents (Molosh et al., 2013). Y_1 receptor-mediated potentiation of the I_{sAHP} is another potential mechanism by which Y_1 receptors may mitigate Y_2 receptor-mediated Ca^{2+} influx.

Our lab has previously documented NPY-mediated inhibition of dendritic VGCCs in dentate granule cells (McQuiston et al., 1996; Hamilton et al., 2010; 2013). This would be a particularly attractive means of shifting levels of elevated intracellular Ca^{2+} from supporting CaMKII-mediated LTP-like plasticity to those preferentially supporting calcineurin-mediated, LTD-like plasticity. I therefore hypothesize that a similar mechanism may occur in BLA PNs.

Two lines of experimental evidence, although preliminary, suggest that NPY does indeed inhibit postsynaptic VGCCs in BLA PNs. The first experiment involved performing voltage-clamp ramps in the presence of intracellular Cs^+ (shown in Chapter 3). These experiments were conducted in the presence of TTX (500nM) to block voltage-gated Na^+ channels. When PN's were held at -114 mV and then quickly ramped to -14 mV [at a rate (300 mV/s)], prominent inward currents were observed during the depolarizing current ramp. Since these experiments were conducted in presence of TTX, these inward currents were likely VDCC-mediated. However this was not pharmacologically verified. In many PNs, bath application of NPY (1 µM) significantly decreased these presumed VGCC, Ca^{2+} currents **(Figure 2A, B)**.

The second line of evidence came from standard K^+ electrode experiments in which either the $GABA_B$ antagonist CGP 52432 (1µM) or [ahx$^{5-24}$]NPY (1 µM) enhanced the I_{sAHP} tail current measured in voltage clamp (Chapter 4). When the pan-agonist NPY (1 µM) was subsequently applied to these PNs, the I_{sAHP} tail current was reduced (**Figure 2C,D**). I hypothesized that this effect was not due to direct inhibition of the I_{sAHP}, but rather due to VGCC inhibition. I further hypothesized that, like in dentate granule cells, inhibition of PN VGCCs was Y_1 receptor-mediated. However, this hypothesis was

refuted by experiments in which the Y_1 receptor agonist F^7P^{34}NPY (1 μM) was applied to PNs. F^7P^{34}NPY (1 μM) also potentiated the I_{sAHP} tail current, often even more dramatically than $[ahx^{5-24}]$NPY (Chapter 4).

Since Y_1 receptor activation did not appear to inhibit Ca^{2+} currents, I next applied the Y_5 agonist CPP(1-7),NPY(19-23) (1 μM) to PN's in which previous F^7P^{34}NPY (1 μM) application had substantially potentiated the I_{sAHP} tail current. In 3/4 experiments, the Y_5 agonist substantially decreased this I_{sAHP} current (**Figure 4A**). Furthermore, in all cases the Y_5 agonist decreased the preceding inward tail current (**Figure 4B**), consistent with actions on a VGCC. Small numbers limit the conclusions that can be drawn from these experiments nor can the specific VGCC types involved be implicated.

I however strongly believe that these preliminary data merit further investigation. This is particularly true in light of recent findings from Ms. Ana Miranda Tapia in the Colmers labs, which suggest that BLA Y_5 receptors play a critical role in mediating the long-term anxiolytic effects of NPY (unpublished data). Furthermore, assuming that both CRF and NPY disinhibit PN dendrites, such actions may have great therapeutic potential. By decreasing postsynaptic Ca^{2+} influx, anxiogenic CaMKII-mediated plasticity could be shifted towards calcineurin and anxiolysis.

5.3 FROM BRAIN SLICES TO ANIMALS AND BACK AGAIN – FUTURE DIRECTIONS

It is clear that beyond its acute anxiety-reducing actions, NPY also elicits long-term plastic changes akin to learning. NPY clearly inhibits BLA PNs via multiple mechanisms. These inhibitory actions readily account for NPY's acute anxiolytic behavioral effects. However, I would argue that these inhibitory NPY actions are insufficient to explain longer-term plasticity, which is Ca^{2+} and NMDA receptor dependent. To this end I propose that removal of the tonic $GABA_B$ receptor-mediated inhibition of PNs (Chapter 3) is a prerequisite for both anxiogenic and anxiolytic plasticity. I have however only documented such tonic $GABA_B$-mediated inhibition in acute rat brain slices. An important next step will be to determine whether similar tonic $GABA_B$-mediated inhibition persists *in vivo*. If this is indeed the case, local BLA infusion of $GABA_B$ antagonists should elicit behavioral effects.

5.3a Interneuron recordings

A key finding of this thesis shows that activation of BLA Y_2 receptors reduces tonic $GABA_B$-mediated inhibition of BLA PNs. This likely occurs via Y_2 receptor actions on NPY/SOM interneurons. I have conducted several preliminary recordings from fluorescent interneurons in the Y_2 receptor tdTomato mouse; these are likely NPY/SOM interneurons (Chapter 2). These recordings suggest that [ahx$^{5-24}$]NPY does not inhibit these interneurons via postsynaptic actions. This is however consistent with NPY-SOM interneurons expressing Y_2 receptors largely on their synaptic terminals. The existence of such receptors could be directly demonstrated with paired (NPY/SOM)-PN recordings. This experiment would involve eliciting action potentials in the SOM/NPY cell and measuring evoked IPSCs in the postsynaptic PNs. Subsequently these evoked IPSCs

could be tested for sensitivity to [ahx$^{5\text{-}24}$]NPY. However, Y$_2$-fluorescent interneurons account for only a very small population of BLA neurons. In the Y$_2$ Tomato mouse many PNs are also fluorescent. It has thus proven to be extremely challenging to locate this small interneuron population in a figurative sea of fluorescent PNs.

A transgenic mouse expressing a reporter under control of the NPY gene promoter should selectively label NPY/SOM interneurons. Furthermore, targeting channelrhodopsin to this interneuron population would simplify electrophysiology by allowing IPSCs from NPY/SOM interneurons to be evoked with light.

An interesting question is whether NPY/SOM interneurons express other NPY receptors (Y$_1$ or Y$_5$). If so, this would imply that Y$_1$ or Y$_5$ receptors could inhibit these interneurons, and perhaps also disinhibit PN dendrites. Direct recordings from NPY/SOM interneurons could test whether postsynaptic Y$_1$ or Y$_5$ receptors inhibit these interneurons. Additionally, further anatomical studies could clarify whether NPY/SOM interneurons express other NPY receptors.

5.3b Fear and Extinction Neurons

As discussed previously (Chapter 1.4b), the output of BLA PNs does not uniformly signal fear and anxiety. Populations of PNs are involved in mediating reward-based behavior, and the extinction of conditioned fear. These distinct PN populations can be identified based on their afferent projections.

I have observed that [ahx$^{5\text{-}24}$]NPY disinhibits the majority of BLA PNs. Based on this high response rate, it is likely that Y$_2$ receptor activation affects both fear and extinction PN populations. Interestingly, although the majority of PNs tested responded to [ahx$^{5\text{-}24}$]NPY with the loss of a tonic GABA$_B$-mediated GIRK current (Chapter 3),

additional effects were observed in a subpopulation of PNs. Thus in approximately half of all responsive PNs, [ahx$^{5\text{-}24}$]NPY enhanced the I$_{sAHP}$ (Chapter 4). Furthermore, many PNs (~1/3) also respond to [ahx$^{5\text{-}24}$]NPY with an increase in large amplitude action potential-dependent IPSCs. These latter two effects might counteract increased excitability due to loss of the tonic GABA$_B$-GIRK. Furthermore, PNs in which [ahx$^{5\text{-}24}$]NPY substantially potentiated the I$_{sAHP}$, virtually always also showed an increase in large amplitude sIPSCs **(Figure 4)**.

Since NPY is overall anxiolytic when applied to the BLA, an intriguing possibility is that the potentiation of the I$_{sAHP}$ and sIPSCs occurs specifically in fear neurons. I hypothesize that the PNs in which Y$_2$ receptor activation reduced a GABA$_B$-GIRK current, without additional effects, correspond to extinction neurons. Such PNs would be preferentially excited by Y$_2$ receptor activation **(Figure 5)**. Preferentially increasing the excitability of extinction neurons is consistent both with NPY's anxiolytic actions and with its reported facilitation of conditioned fear extinction (Sajdyk et al., 1999; Gutman et al., 2008).

Fear neurons selectively project to the prelimbic medial prefrontal cortex while extinction neurons selectively innervate the infralimbic prefrontal cortex (Senn et al., 2014). Injecting retrograde tracing beads into these specific prefrontal cortex domains *in vivo* would allow fear and extinction neurons to be subsequently identified in slices and tested for these proposed differential Y$_2$ receptor effects.

5.3c Are Y$_2$R-Expressing PNs a Functionally Distinct Population?

As mentioned previously in Chapter 2, a number of BLA PNs in the Y$_2$R TdTomato mouse appear to express Y$_2$ receptors (indicated by expression of TdTomato

fluorescence). Like in the rat, most mouse PNs responded to [ahx$^{5-24}$]NPY with the loss of a GIRK-like I_{IR} conductance. However, both fluorescent and non-fluorescent PNs responded in this manner at similar rates. This suggests that (like in the rat) GIRK inhibition by [ahx$^{5-24}$]NPY is entirely due to loss of tonic GABA$_B$ even in those PNs that express Y$_2$ receptors. It is therefore likely that Tdtomato fluorescent PNs only express Y$_2$R on there synaptic terminals. However, immunohistochemistry staining will be necessary to determine the specific cellular domains where PNs express Y$_2$ receptors.

In addition to the differential expression of Y$_2$Rs, other differences between fluorescent and non-fluorescent PNs appear to exist. Fluorescent PNs have a more depolarized RMP and show a trend toward lower membrane capacitance, suggesting fluorescent PNs may be smaller. However in complex neurons where voltage-clamp is incomplete, capacitance can only roughly estimate membrane surface area. We are currently performing experiments to determine whether morphological differences exist between fluorescent and non-fluorescent PNs. Preliminary data, based on reconstructions of neuro-biotin labeled PNs, suggests that fluorescent PNs have greater total dendritic length than their non-fluorescent counterparts. This is the opposite result predicted by capacitance measurements, but it may be accounted for by morphological differences in the way this dendritic length in distributed **(Figure 6)**.

Y$_2$R-expressing terminals from the BLA innervate the central amygdala (CeA) (Tasan et al., 2010). Furthermore Senn et al. (2014) found that prelimbic projecting fear PNs send colateral projections to the CeA, while infralimbic projecting extinction PNs do not (Senn et al., 2014). I therefore hypothesize that in the BLA, fear neurons express Y$_2$ receptors while extinction neurons do not. A series of retrograde tracing imaging studies

in which fluorescent latex microspheres will be injected into appropriate medial prefrontal cortical domains will be employed to test this hypothesis. Labeled fear- or extinction- PNs will then be identified in BLA sections and tested for co-localization with TdTomato fluorescence.

5.3a Insights Into Behavior and Emotional Regulation

I now attempt to integrate the findings from my thesis research and work of many contemporary authors into a more refined learning-based model of NPY's actions in the BLA.

5.3a(ii) Hypothesis – NPY favors de-potentiation of sensory synapses carrying contextual cues

Activation of BLA NPY receptors facilitates calcineurin-dependent plasticity (Sajdyk et al., 2008). This implies a Ca^{2+}-dependent LTD-like process, which will culminate in synaptic de-potentiation (Mansuy, 2003). Ultimately, this suggests loss of information to some extent. But what information is lost and why would this decrease anxiety behavior?

I believe that this question is best answered by revisiting the classical fear-conditioning model (as outlined in Chapter 1.2b). During fear conditioning a subject learns to associate an intrinsically aversive shock (US) with an innocuous sensory cue (CS). When the subject conditions to this CS they show defensive behaviors in its presence alone. This process is thought to model fear (Maren, 2001). Importantly the CS is a distinct cue of little informational content.

During fear conditioning, a subject can also associate the experimental apparatus with the US shock; this is termed contextual conditioning. Contextual conditioning

results in a sustained state of heightened arousal (Maren, 2001; Laxmi et al., 2003). This is because unlike the CS, the experimental context cannot predict the US with any temporal certainty. Contextual conditioning is therefore considered to better model anxiety. Importantly, the sensory information describing the experimental context is vast in comparison to the discrete CS. Contextual conditioning would therefore be expected to recruit greater synaptic representation in the BLA than fear conditioning.

I propose that by recruiting calcineurin, NPY facilitates de-potentiation of BLA synapses carrying more contextual or generalized threat representations. In this model, during fear conditioning, UC-CS associations are formed and represented as potentiated sensory synapses in the BLA (Rogan et al., 1997). Contextual associations are similarly formed and likewise represented in the BLA.

Leitermann et al. (2016) recently suggested that NPY is released in the BLA following fear conditioning (Leitermann et al., 2016). I propose that this NPY could function to preferentially de-potentiate synapses which carry contextual information, while sparing the more CS- specific associations. This would prevent more generalized threat representations and reduce anxiety. Anxiety is adaptive when threats are vague and unpredictable (Barlow, 2000). Likewise, delivering un-signaled shocks to animals elicits greater contextual conditioning (Laxmi et al., 2003). Thus, I propose that less NPY will be released into the BLA under these conditions, which favor contextual associations and anxiety.

I have hypothesized that Y_2Rs facilitate recruitment of calcineurin by NPY. I thus further hypothesize that selectively agonizing or blocking BLA Y_2Rs will modulate

contextual fear conditioning. Consistent with this, knockout of BLA Y_2 receptors results in overgeneralization of conditioned fear (Tasan et al., 2010).

Contextual fear cues are mediated via hippocampal projections to the BLA (Anagnostaras et al., 2001). Therefore injecting anterograde tracers into the dorsal hippocampus may identify these projections within the BLA. This technique could also be used to target selective expression of optogenetic tools to these hippocampal BLA projections. I would hypothesize that injection of NPY (and perhaps receptor specific agonists) during or shortly after fear conditioning would de-potentiate these synapses. This should result in smaller excitatory events elicited in PNs when fibers of hippocampal origin are optically stimulated. I predict that blocking NPY receptors or infusing CRF would elicit the opposite effect.

5.4 CONCLUSION

In summary, the findings of this thesis present a probable mechanism by which selective activation of BLA Y_2Rs increases anxiety. Furthermore, based on my results, I have proposed testable mechanisms by which BLA Y_2Rs might interact with other NPY receptors. I propose that these interactions facilitate both short and long-term anxiolysis. Ultimately, this thesis presents numerous important new questions, which should be answered by further studies.

I believe that a key insight from these findings, in conjunction with those of others, is that simply inhibiting the BLA is not an effective long-term strategy for treating anxiety. I believe future therapeutics should facilitate anxiety-reducing plasticity within the BLA. To this end the NPY system provides several exciting potential targets.

5.5 FIGURES

Figure 1: Model
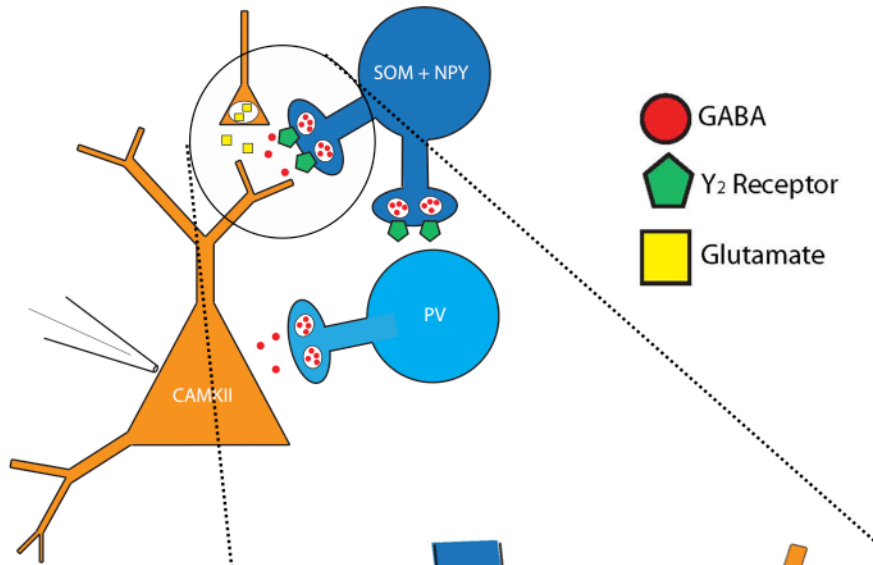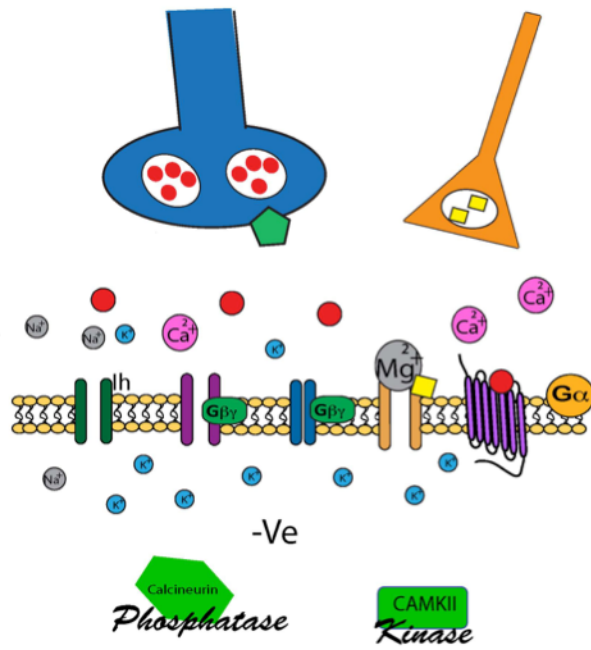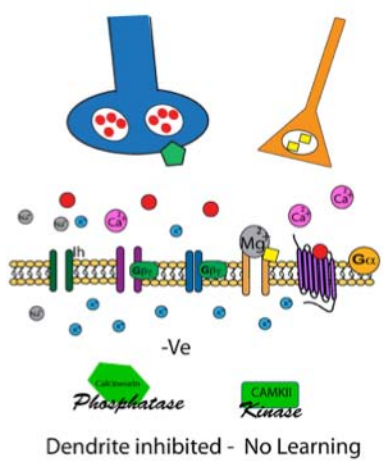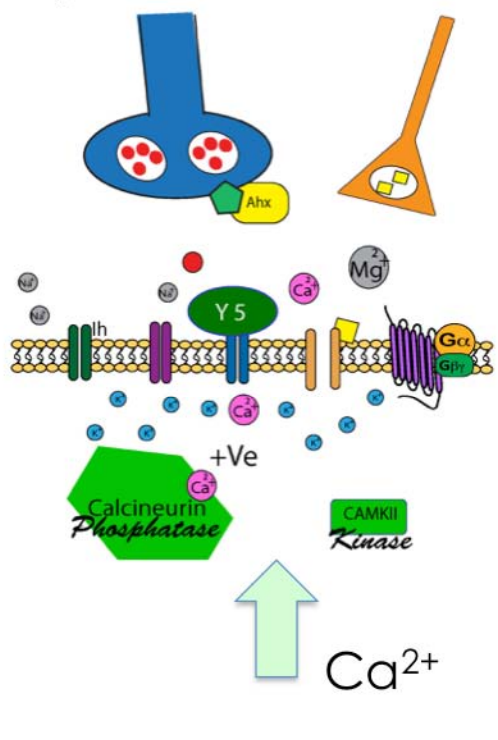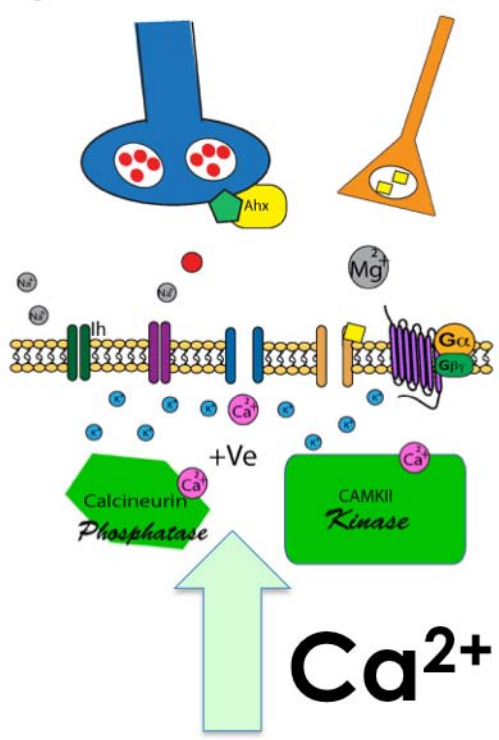
Figure 1: Model

**(A)** NPY-SOM interneurons, which express Y_2 receptors, release tonic GABA onto PN dendrites.

(B) This tonic GABA activates $GABA_B$ receptors on PN dendrites. $GABA_B$ mediated GIRK currents hyperpolarize dendrites, activate I_h, facilitate the Mg^{2+} block of synaptic NMDA receptors, and inhibit dendritic VGCCs. These actions profoundly inhibit dendrites and prevent synaptic plasticity.

(C) Selective activation of Y_2 receptors decreases tonic GABA release and consequently decreases tonic activation of dendritic $GABA_B$ receptors. Reduction of tonic $GABA_B$-GIRK currents will result in membrane depolarization, decrease dendritic I_h and reduce the Mg^{2+} block of the NMDA receptor. Tonic $GABA_B$-mediated inhibition of VGCCs is also reduced. These actions facilitate large increases in postsynaptic Ca^{2+} in response to appropriately timed excitatory input and/or back-propagating action potential activity. This favors recruitment of CaMKII and strengthening of excitatory synaptic connections. CRF similarly disinhibits dendrites and facilitates CaMKII mediated plasticity.

(D) When Y_2Rs are activated in concert with other NPY receptors, excitatory inputs recruit less postsynaptic Ca^{2+} than in the case of selective Y_2 receptor activation. This favors recruitment of calcineurin dependent plasticity.

Figure 2: NPY Inhibits a VGCC

A

B

C

CGP 52432 (1μM)
+ NPY (1μM)

500pA

500ms

D

Inward Tail current

— Control
— CGP 52432 (1μM)
— NPY (1μM)

200pA

500ms
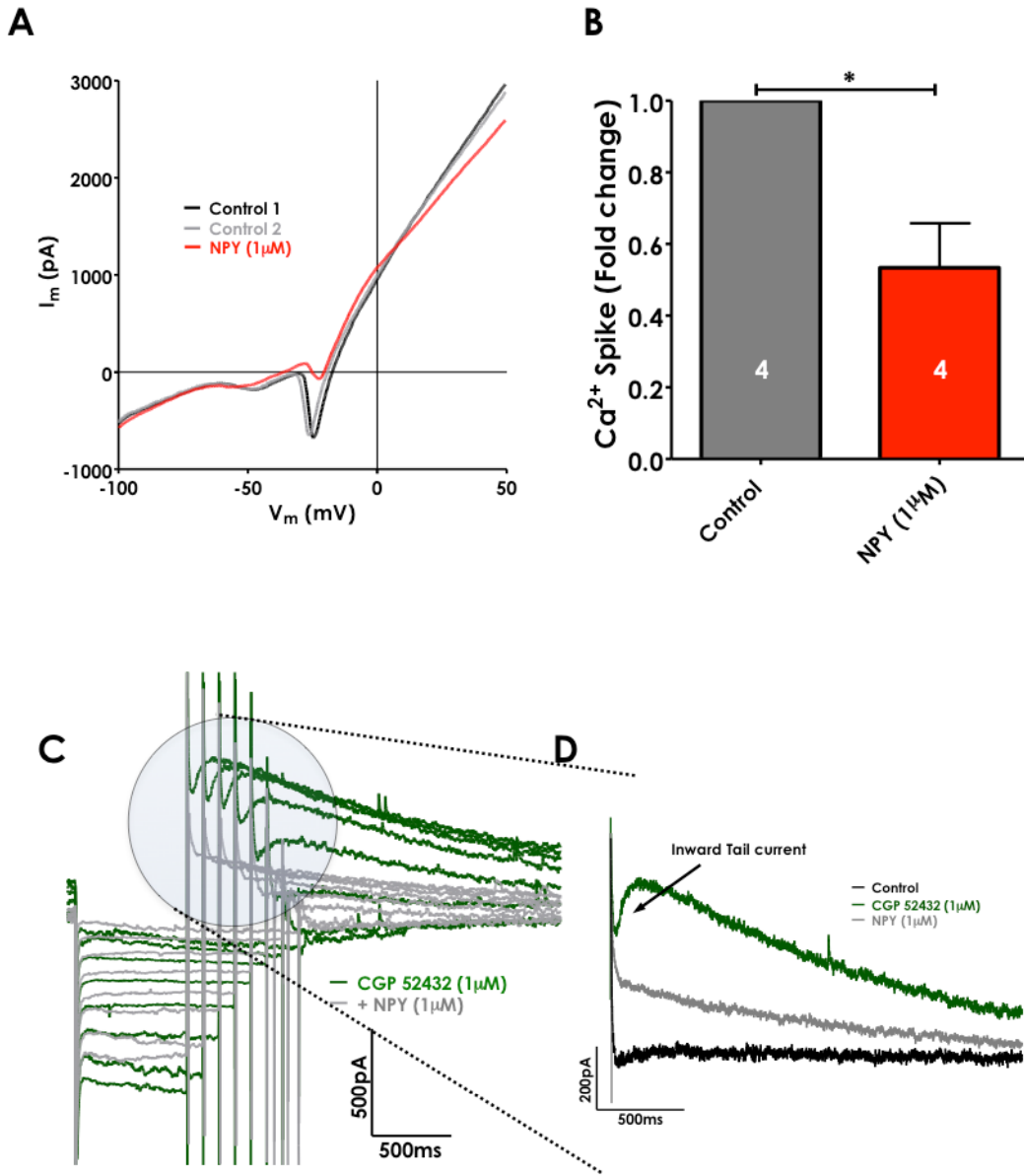
Figure 2: NPY Inhibits a VGCC

(A) Intracellular Cs^+ recording of a representative PN depolarizing voltage-clamp ramp in the presence of TTX (500 nM). The depolarizing ramp elicits an inward Ca^{2+} current. Bath application of NPY (1 µM) substantially decreased the amplitude of this inward Ca^{2+} current.

(B) NPY significantly decreased the amplitude of voltage-ramp elicited Ca^{2+} currents evoked under the conditions described in panel (A) ($p<0.05$; n=4). Ca^{2+} current amplitude is displayed as a fraction of control amplitude.

(C) Representative voltage-clamp traces at a -55 mV holding potential from a PN in which CGP 52432 (1 µM) substantially increased the amplitude of the I_{sAHP} outward tail current. Subsequent application of NPY (1 µM) sharply decreased the amplitude of this I_{sAHP} tail current.

(D) The I_{sAHP} tail current from the PN in panel C, which was elicited following termination of the most hyperpolarized (-135 mV) voltage step. Bath application of CGP 52432 (1 µM) elicited a substantial I_{sAHP} tail current and substantially increased the preceding inward tail current. Subsequent application of NPY (1 µM) decreased the I_{sAHP} tail current, but did not return it to control levels. The preceding inward tail current however, was eliminated following NPY (1 µM).

Figure 3: Y$_5$ receptors Inhibit A VGCC

A

1000pA

1s

— Y$_1$ (1μM)
— Y$_5$ (1μM)

B

100pA

100ms

— Y$_1$ + Y$_2$ (1μM)
— Y$_5$ (1μM)
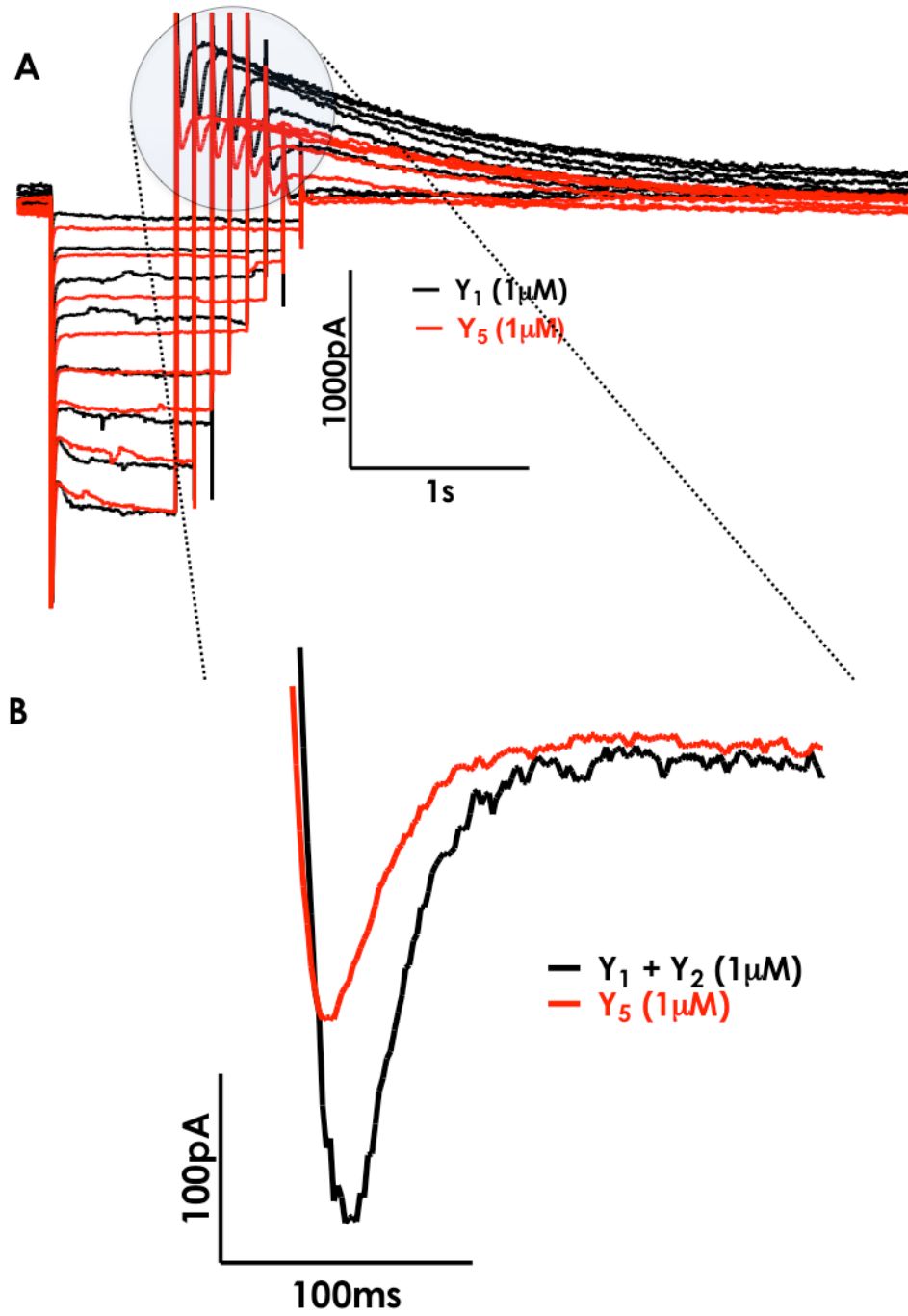
Figure 3: Y$_5$ Receptors Inhibit a VGCC

(A) Representative voltage-clamp traces at a -55 mV holding potential from a PN in which F^{7}P^{34}NPY (1 μM) substantially increased the amplitude of the I$_{sAHP}$ outward tail current. Subsequent application of the selective Y$_5$ agonist CPP(1-7),NPY(19-23) (1 μM) substantially decreased this I$_{sAHP}$ tail current. The Y$_5$ agonist also decreased the preceding inward tail current.

(B) Representative PN inward tail current evoked in voltage-clamp as in panel A, following termination of the most hyperpolarized (-135 mV). This inward tail current was substantially increased following application of F^{7}P^{34}NPY (1 μM), then [ahx$^{5-24}$]NPY (1 μM). Subsequent application of the Y$_5$ agonist substantially decreased the inward tail current.

Figure 4: Increased I$_{sAHP}$ and sIPSCs Often Occur in the Same PNs
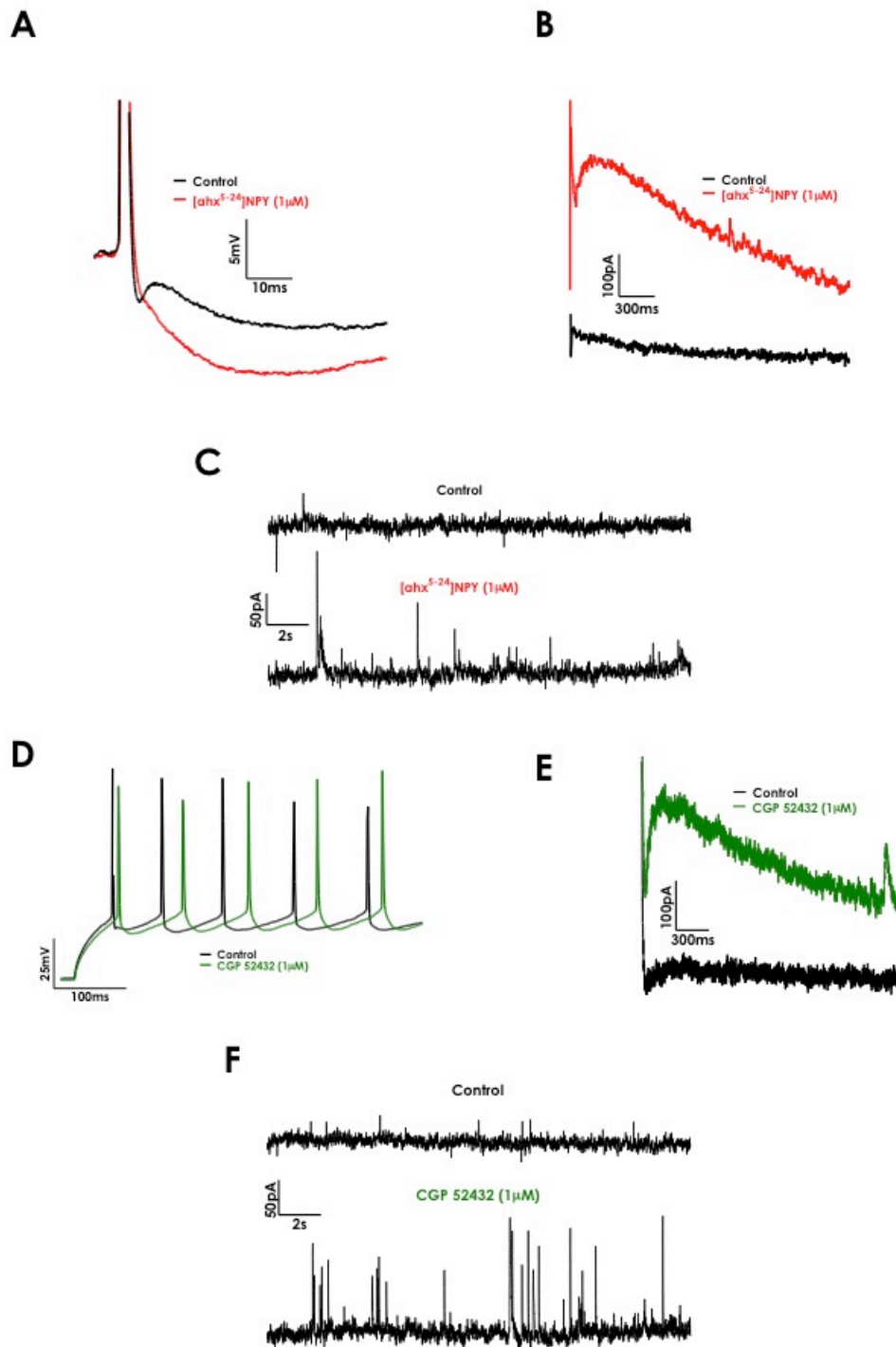
Figure 4: Increased I$_{sAHP}$ and sIPSCs Often Occur in the Same PNs

(A) Representative PN in which [ahx$^{5-24}$]NPY (1 µM) substantially increased the amplitude of the first evoked action potential AHP.

(B) [ahx$^{5-24}$]NPY substantially increased the voltage clamp evoked I$_{sAHP}$ tail current in the same PN as panel A.

(C) The same PN from panels (A and B) also showed a substantial increase in large amplitude sIPSCs with Y$_2$R agonist application. This was nearly always seen in PNs in which the I$_{sAHP}$ was substantially (>100 pA) increased.

(D) Representative PN in which CGP 52432 (1µM) substantially increased the amplitude of the first current step evoked action potential AHP and increased the interval between the first two step evoked action potentials.

(E) The same PN in panel (D) in which CGP 52432 (1µM) also substantially increased the voltage clamp evoked I$_{sAHP}$ tail current.

(F) The same PN from panels (D and E) also showed a substantial increase in large amplitude sIPSCs. This was also commonly seen in PNs in which CGP 52432 (1µM) substantially enhanced the voltage-clamp measured I$_{sAHP}$ (>100pA).

Figure 5: Hypothesis - Y_2 receptor Activation Differentially Effects Fear and Extinction Neurons

Y_2 Receptor Activation:

⬇ $GABA_B$-GIRK
⬆I_{sAHP}
⬆sIPSC

Y_2 Receptor Activation:
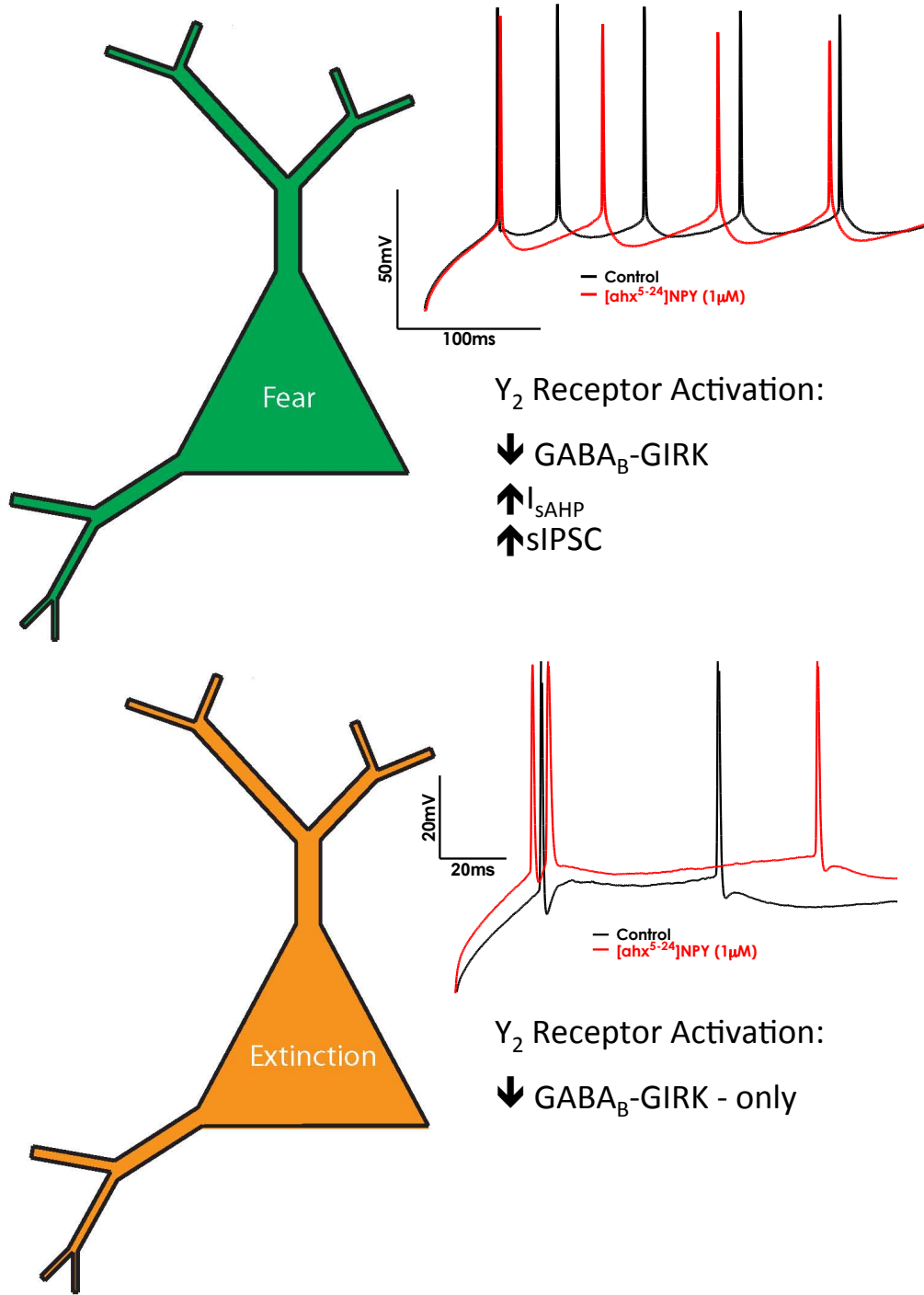
⬇ $GABA_B$-GIRK - only

Figure 5: Hypothesis - Y$_2$ receptor Activation Differentially Effects Fear and Extinction Neurons

In a subset of PNs, [ahx$^{5-24}$]NPY decreased a GABA$_B$-GIRK current but also increased the I$_{sAHP}$ and the frequency of large amplitude sIPSCs. I hypothesize that these are fear-coding PNs. In other PNs, [ahx$^{5-24}$]NPY only decreased a PN GABA$_B$-GIRK, these PNs are preferentially excited by [ahx$^{5-24}$]NPY. I hypothesize these are fear extinction-coding PNs.

Figure 6: Future Directions – Characterizing The Morphology of Y$_2$ Receptor Expressing PNs
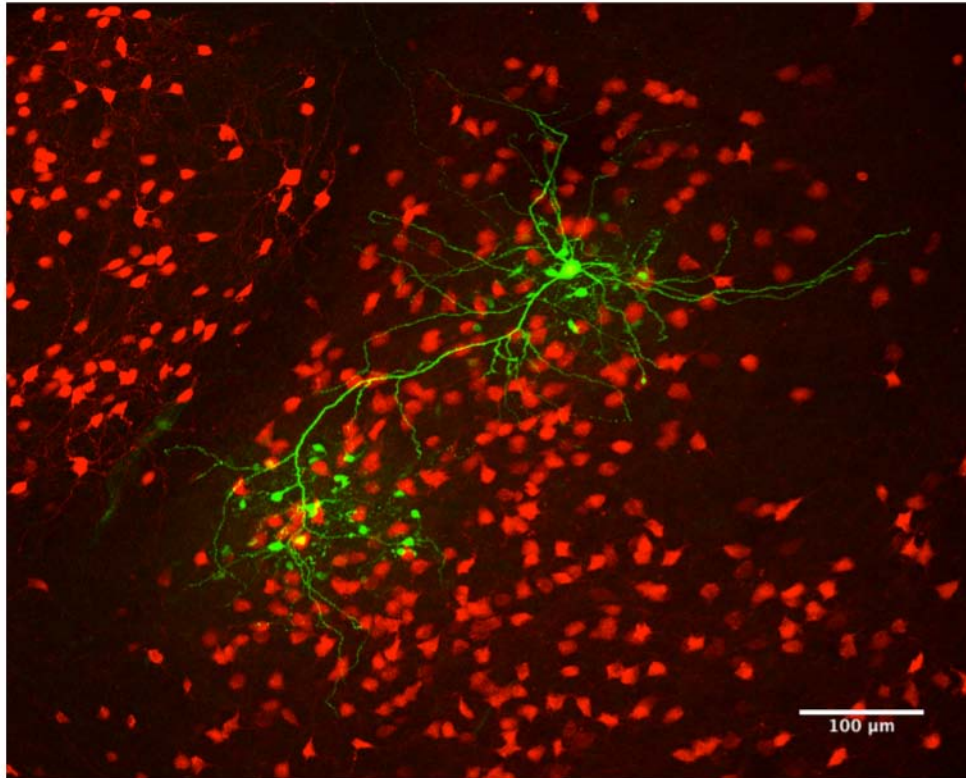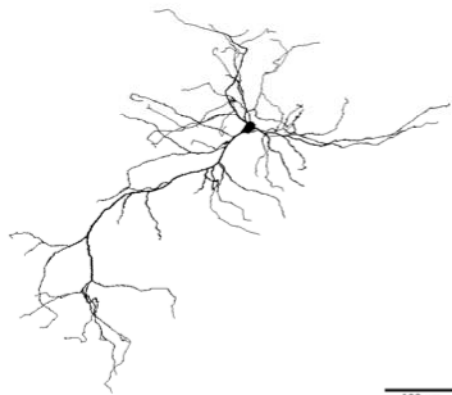
Figure 6: Future Directions – Characterizing The Morphology of Y_2 Receptor Expressing PNs

(A) Representative merged confocal Z-stack from a BLA slice from a Y_2 tdTomato mouse. A fluorescent PN (green), loaded with neurobiotin via a patch pipette, is labeled with streptavidin ALEXA-488. Other tdTomato-expressing neurons are shown in red

(B) Camera Lucida trace of the streptavidin ALEX-488 labeled Y_2 tdTomato fluorescent PN from panel A.

(C) Representative camera Lucida trace from a non-fluorescent PN from a Y_2 tdTomato mouse. Preliminary data suggest non-fluorescent PNs often show a more stellate morphology.

5.5 REFERENCES

Anagnostaras SG, Gale GD, Fanselow MS (2001) Hippocampus and contextual fear conditioning: recent controversies and advances. Hippocampus 11:8–17.

Barlow DH (2000) Unraveling the mysteries of anxiety and its disorders from the perspective of emotion theory. Am Psychol 55:1247–1263.

Giesbrecht CJ, Mackay JP, Silveira HB, Urban JH, Colmers WF (2010) Countervailing Modulation of Ih by Neuropeptide Y and Corticotrophin-Releasing Factor in Basolateral Amygdala As a Possible Mechanism for Their Effects on Stress-Related Behaviors. Journal of Neuroscience 30:16970–16982.

Gutman AR, Yang Y, Ressler KJ, Davis M (2008) The Role of Neuropeptide Y in the Expression and Extinction of Fear-Potentiated Startle. Journal of Neuroscience 28:12682–12690.

Hamilton TJ, Wheatley BM, Sinclair DB, Bachmann M, Larkum ME, Colmers WF (2010) Dopamine modulates synaptic plasticity in dendrites of rat and human dentate granule cells. Proc Natl Acad Sci USA 107:18185–18190.

Hamilton TJ, Xapelli S, Michaelson SD, Larkum ME, Colmers WF (2013) Modulation of distal calcium electrogenesis by neuropeptide Y_1 receptors inhibits neocortical long-term depression. J Neurosci 33:11184–11193.

Herry C, Ciocchi S, Senn V, Demmou L, Müller C, LUthi A (2008) Switching on and off fear by distinct neuronal circuits. Nature 454:600–606.

Kulik A, Vida I, Fukazawa Y, Guetg N, Kasugai Y, Marker CL, Rigato F, Bettler B, Wickman K, Frotscher M, Shigemoto R (2006) Compartment-dependent colocalization of Kir3.2-containing K+ channels and GABAB receptors in hippocampal pyramidal cells. J Neurosci 26:4289–4297.

Laxmi TR, Stork O, Pape H-C (2003) Generalisation of conditioned fear and its behavioural expression in mice. Behav Brain Res 145:89–98.

Leitermann RJ, Rostkowski AB, Urban JH (2016) Neuropeptide Y input to the rat basolateral amygdala complex and modulation by conditioned fear. J Comp Neurol:n/a–n/a.

Lisman JE (1997) Bursts as a unit of neural information: making unreliable synapses reliable. Trends Neurosci 20:38–43.

Mansuy IM (2003) Calcineurin in memory and bidirectional plasticity. Biochem Biophys Res Commun 311:1195–1208.

Maren S (2001) Neurobiology of Pavlovian fear conditioning. Annu Rev Neurosci

24:897–931.

McDonald AJ, Mascagni F, Muller JF (2004) Immunocytochemical localization of GABABR1 receptor subunits in the basolateral amygdala. Brain Research 1018:147–158.

McQuiston AR, Petrozzino JJ, Connor JA, Colmers WF (1996) Neuropeptide Y1 receptors inhibit N-type calcium currents and reduce transient calcium increases in rat dentate granule cells. Journal of Neuroscience 16:1422–1429.

Molosh AI, Sajdyk TJ, Truitt WA, Zhu W, Oxford GS, Shekhar A (2013) NPY Y1 receptors differentially modulate GABAA and NMDA receptors via divergent signal-transduction pathways to reduce excitability of amygdala neurons. Neuropsychopharmacology 38:1352–1364.

Morrisett RA, Mott DD, Lewis DV, Swartzwelder HS, Wilson WA (1991) GABAB-receptor-mediated inhibition of the N-methyl-D-aspartate component of synaptic transmission in the rat hippocampus. Journal of Neuroscience 11:203–209.

Muller JF, Mascagni F, McDonald AJ (2006) Postsynaptic targets of somatostatin-containing interneurons in the rat basolateral amygdala. J Comp Neurol 500:513–529.

Pérez-Garci E, Larkum ME, Nevian T (2013) Inhibition of dendritic Ca2+ spikes by GABAB receptors in cortical pyramidal neurons is mediated by a direct Gi/o-β-subunit interaction with Cav1 channels. The Journal of Physiology 591:1599–1612.

Rainnie DG, Bergeron R, Sajdyk TJ, Patil M, Gehlert DR, Shekhar A (2004) Corticotrophin releasing factor-induced synaptic plasticity in the amygdala translates stress into emotional disorders. J Neurosci 24:3471–3479.

Rainnie DG, Fernhout BJ, Shinnick-Gallagher P (1992) Differential actions of corticotropin releasing factor on basolateral and central amygdaloid neurones, in vitro. J Pharmacol Exp Ther 263:846–858.

Rogan MT, Stäubli UV, LeDoux JE (1997) Fear conditioning induces associative long-term potentiation in the amygdala. Nature 390:604–607.

Sajdyk TJ, Johnson PL, Leitermann RJ, Fitz SD, Dietrich A, Morin M, Gehlert DR, Urban JH, Shekhar A (2008) Neuropeptide Y in the Amygdala Induces Long-Term Resilience to Stress-Induced Reductions in Social Responses But Not Hypothalamic-Adrenal-Pituitary Axis Activity or Hyperthermia. Journal of Neuroscience 28:893–903.

Sajdyk TJ, Schober DA, Smiley DL, Gehlert DR (2002) Neuropeptide Y-Y2 receptors mediate anxiety in the amygdala. Pharmacol Biochem Behav 71:419–423.

Sajdyk TJ, Vandergriff MG, Gehlert DR (1999) Amygdalar neuropeptide Y Y1 receptors

mediate the anxiolytic-like actions of neuropeptide Y in the social interaction test. European Journal of Pharmacology 368:143–147.

Senn V, Wolff SBE, Herry C, Grenier F, Ehrlich I, Gründemann J, Fadok JP, Müller C, Letzkus JJ, LUthi A (2014) Long-range connectivity defines behavioral specificity of amygdala neurons. 81:428–437.

Tasan RO, Nguyen NK, Weger S, Sartori SB, Singewald N, Heilbronn R, Herzog H, Sperk G (2010) The Central and Basolateral Amygdala Are Critical Sites of Neuropeptide Y/Y2 Receptor-Mediated Regulation of Anxiety and Depression. Journal of Neuroscience 30:6282–6290.

Vigot R, Barbieri S, Bräuner-Osborne H, Turecek R, Shigemoto R, Zhang Y-P, Luján R, Jacobson LH, Biermann B, Fritschy J-M, Vacher C-M, Müller M, Sansig G, Guetg N, Cryan JF, Kaupmann K, Gassmann M, Oertner TG, Bettler B (2006) Differential compartmentalization and distinct functions of GABAB receptor variants. Neuron 50:589–601.